THE
PHYSICAL REVIEW
A Journal of Experimental and Theoretical Physics Established by E. L. Nichols in 1893

VOL. 50, NO. 4 AUGUST 15, 1936 SECOND SERIES

Cloud Chamber Observations of Cosmic Rays at 4300 Meters Elevation and Near Sea-Level

CARL D. ANDERSON AND SETH H. NEDDERMEYER, *Norman Bridge Laboratory of Physics, California Institute of Technology*
(Received June 9, 1936)

Cloud chamber photographs at 4300 meters elevation show positive and negative electron tracks similar to those observed at sea-level, but positive-negative electron showers occur more frequently and, in general, consist of more numerous tracks. Showers of 2–4 tracks, 5–10 tracks, and 11–100 tracks occur respectively, 8.6, 21 and 29 times as frequently per unit time at 4300 meters as they do near sea-level. Further measurements on the energy loss in lead of electrons up to 400 MEV, are given. They show that in this range of energies the energy loss in lead is roughly proportional to the incident energy. About one percent of the exposures on Pike's Peak reveal the presence of strongly ionizing particles which in most cases seem to be protons. The proportion of such tracks is considerably greater than at Pasadena. These heavy tracks in general bear only little relation in direction to that of the incoming beam, and usually arise from a type of nuclear disintegration not heretofore observed. The energies of these heavily ionizing particles may rise to values so high as 150 MEV, thus indicating that the source of the particle energies is in the cosmic rays.

THE magnet cloud chamber apparatus previously operated at Pasadena was used six weeks in the summer of 1935 to make about 10,000 counter-actuated exposures on the summit of Pike's Peak at an elevation of 4300 meters above sea-level.[1] A steady magnetic field of 7900 gauss was maintained with a solenoid current of 215 amperes at 110 volts obtained from a portable generator powered by an automobile engine.

Since the same apparatus was used both in Pasadena and on Pike's Peak, the screening material around the cloud chamber was sufficiently similar at both locations to permit reliable statistical comparisons on the occurrence of showers and heavy particles to be made.

I. Frequency of Occurrence of Electron[2] Showers and Their Distribution in Size at 4300 Meters and Near Sea-Level

Examples of electron showers photographed at 4300 meters are shown in Figs. 1–5. From a certain set of exposures made on Pike's Peak, counts were taken of the relative numbers of photographs showing respectively, a single track, two tracks, three tracks, etc. Throughout the set of exposures chosen for these statistics the chamber contained along its diameter a horizontal 0.35 cm lead plate; one Geiger counter was placed immediately above the chamber and one below. Similar counts were made on a number of photographs taken at Pasadena where the same lead plate was used, the counters were similarly

[1] C. D. Anderson, R. A. Millikan and S. H. Neddermeyer, Phys. Rev. **49**, 204, 415 (1936).

[2] The term "electron," when unmodified shall be taken to denote both positive and negative electrons.

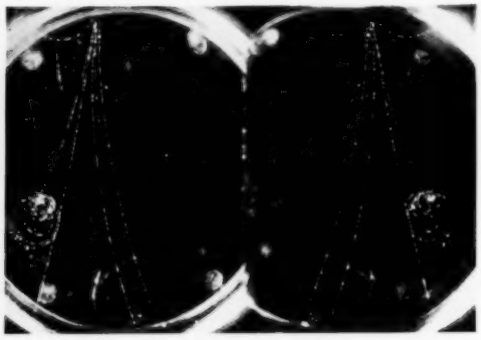

FIG. 1. Pike's Peak, 7900 gauss. An electron shower of three negatrons and three positrons of energies, respectively from left to right, 3.5, 55, 190, 78, 70, 90 MEV. The low energy electrons coincident in time with the shower represent the absorption of low energy photons accompanying the shower electrons. In all illustrations *the direct image is at the left.* The magnetic field is directed into the paper.

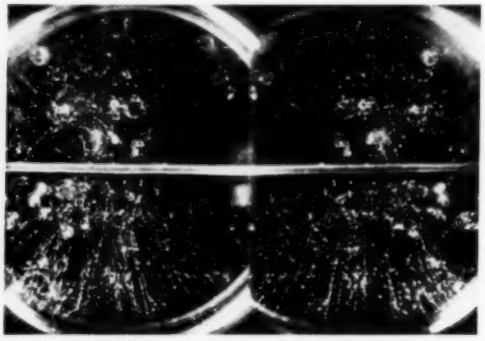

FIG. 2. Pike's Peak, 7900 gauss. A shower of numerous tracks showing several examples of low energy electrons resulting from photon absorption.

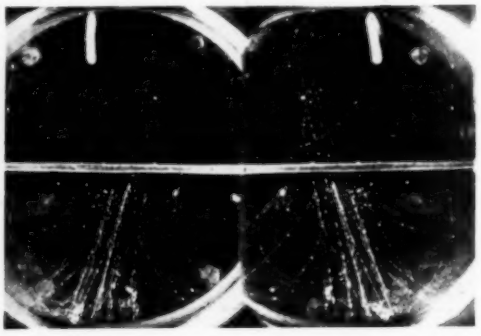

FIG. 3. Pike's Peak, 7900 gauss. A shower in which eight electrons (+ and −) strike the upper surface of the 0.35 cm lead plate. More than twenty-four electrons emerge from the lower face of the lead plate. This photograph is an example of the multiplication of shower tracks in a thin piece of absorbing material. Observation of many cases of this type shows that most of the additional tracks arise from the absorption of photons which accompany the electrons, but occasionally an electron itself may produce several positron-negatron secondaries.

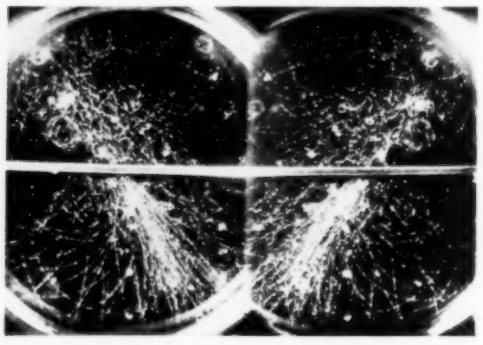

FIG. 4. Pike's Peak, 7900 gauss. A shower of more than 100 electrons. The summed energy represented by this shower probably exceeds 10,000 MEV. A shower such as this might result from one elementary process, but it is more likely due to a multiplication of tracks through photon intermediaries as in Fig. 3.

arranged, and the magnetic field strengths were comparable in the two instances, so that a comparison of the two sets of data may be made. It should be remembered that the counter-controlled cloud chamber, in responding to single particles selects only those within the small solid angle defined by the counters, whereas it records a relatively large proportion of the total number of showers which occur. The result is that the ratio of the number of photographs showing showers, to the number showing single tracks is enormously greater when counter control is used, than it is with the random method; the latter represents the showers in their true relation to the single particles. In a preceding publication[3] the single tracks were shown to constitute about 88 percent of the successful exposures made at Pasadena by the random method. In Table I a summary of the new results is given. The examples of multiple tracks listed here include not only those cases where all the tracks seem to diverge from a single point, but all cases of "time associated" tracks. Tracks not coincident in time with those tripping the counters are omitted. With an increase in elevation the rate of occurrence of showers determined in this way increases more rapidly than does that of the single tracks.

The number of coincidences recorded per hour on Pike's Peak was approximately 92 as com-

[3] C. D. Anderson, Phys. Rev. **44**, 415 (1933).

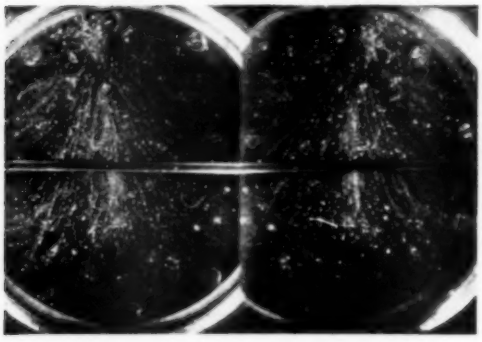

FIG. 5. Pike's Peak, 7900 gauss. A shower of a large number of electrons. The electrons in this shower were not counted, but estimates show that more than 300 are probably present. The summed energy probably exceeds 15,000 MEV.

pared with 33 at Pasadena for the same arrangement of the counters. Correcting for accidental coincidences, and for the resetting time of the cloud chamber (15 seconds) during which time the counters were inoperative, we find the true counting rates of 120 per hour on Pike's Peak and 34 per hour at Pasadena. This corresponds to a counting rate 3.5 times as fast on Pike's Peak as at Pasadena.

Using the data in Table I, which gives the relative frequency of occurrence of showers *per single track* at the two locations, we can compute the relative frequency of occurrence of showers *per unit time*, as a function of the number of rays which they contain, at the two locations. The results are given in the upper section of Table II.

To minimize the effects of statistical fluctuations we may collect the showers into three groups of respectively, 2–4 tracks, 5–10 tracks, and 11–100 tracks. The data so grouped are given in the lower section of Table II.

The numerical values here obtained are to be expected to depend to a considerable degree upon the distribution of matter about the cloud chamber and upon the position of the counters, thus making difficult a close comparison of these results with those of other observers who have used different experimental methods.

A rough comparison, however, can be made with those experiments in which counters arranged out of line are used to record showers, and with experiments in which electroscopes or ion-chambers are used to record bursts of ionization.

All the experiments[4] with the exception of the counter experiments of Gilbert[5] seem to agree that the numbers of showers and bursts increase with increasing altitude more rapidly than does the total ionization measured. For example Johnson[6] and Woodward,[7] who have made observations at an altitude comparable with that of

[4] B. Rossi and S. de Benedetti, Ricerca Scient. **511**, 119 (1934); T. H. Johnson, Phys. Rev. **47**, 318 (1935); R. D. Bennett, G. S. Brown and H. A. Rahmel, Phys. Rev. **47**, 437 (1935); J. C. Street and R. T. Young, Phys. Rev. **46**, 823 (1934); **47**, 572 (1935); C. G. and D. D. Montgomery, Phys. Rev. **47**, 429 (1935); W. H. Pickering, Phys. Rev. **47**, 423 (1935).

[5] C. W. Gilbert, Proc. Roy. Soc. **A144**, 559 (1934).

[6] T. H. Johnson, Phys. Rev. **47**, 318 (1935). (Reference is made only to those experiments carried out at altitudes comparable with 4300 meters.)

[7] R. H. Woodward, Phys. Rev. **49**, 638 (1936).

TABLE I. *Summary of data.*

n = Number of tracks appearing on photograph	1	2	3	4	5	6–10	11–20	21–100	>100
Total number of cases observed in group indicated:									
Pasadena	2301	168	95	31	16	41	14	18	0
Pike's Peak	1023	210	110	90	65	125	76	72	4
Frequency of occurrence of photographs, normalized to unit interval, that show n tracks per 1000 that show single tracks:									
N_1 Pasadena	1000	73	41.3	13.5	7.0	3.6	0.6	0.1	—
N_2 Pike's Peak	1000	205	108.0	88.0	64.0	24.4	7.4	0.9	—
N_2/N_1	1	2.8	2.6	6.5	9.1	6.8	12.3	9.0	—

n	1	2–4 tracks	5–10 tracks	11–100 tracks
N_2/N_1	1	3.2	7.7	10.6

TABLE II. *Ratio of the frequency of occurrence per unit time of single tracks and showers of n electron tracks on Pike's Peak to the frequency at Pasadena.*

n	single tracks	2	3	4	5	6–10	11–20	21–100
ratio	2.7	7.5	6.9	17	24	18	33	24

n	single tracks	2–4 tracks	5–10 tracks	11–100 tracks
ratio	2.7	8.6	21	29

the present experiments, find for particular arrangements of counters surmounted by a lead sheet, counting rates respectively 6.8 and 8.5 times greater at 4300 meters than near sea-level. Their values may be compared with the value found here, *viz.* 8.6 for showers of 2–4 tracks, although in their experiments the average number of rays in the recorded showers is somewhat uncertain.

Experiments have been made on the frequency of bursts of ionization at various altitudes, for example by Montgomery and Montgomery[8] and by Young,[9] who find an increase between near sea-level and 4300 meters by factors of 26.6 and 22 respectively, for the discharges corresponding to from 30 to 300 rays. These values may be compared with the ones given in Table II, *viz.*, 21 and 29, respectively, for the factor of increase in frequency of showers of 5–10 and 11–100 rays. Too much weight should not be attached to these rather close numerical agreements in view of the differences in experimental method, though the fact that the showers and bursts increase more rapidly with elevation than does the total radiation seems to be well established.

Experiments by Montgomery and Montgomery[10] have furnished evidence that the smaller discharges recorded in their ion-chamber may be explained as showers of electrons. From the proof given by the cloud chamber results here reported that electron showers of so many as 300 particles do occur, it appears quite certain that their interpretation is correct. In the Montgomerys' ion-chamber a shower of 300 tracks should correspond to about 6×10^6 ion-pairs. It is quite possible that the very large discharges from a hundred to a thousand times this value are produced by showers of many thousand electrons, but this has not yet been fully demonstrated.

The experiments discussed above show that the shower phenomena are more frequently associated with the soft component of the cosmic rays than with the penetrating components.

II. Further Data on the Absorption of Electrons

Until the absorption laws of high energy electrons and photons are known the above effects cannot be understood in detail nor can the soft component of the primary cosmic rays be definitely identified. Our direct measurements on the energy loss of electrons passing through fairly thick lead plates (0.6 – 1.0 cm) have shown the occurrence of nuclear radiative impacts in which a considerable fraction of the total energy of the electron is sometimes removed, the measured values of the energy loss being much greater than that due only to ionization along the path and to the production of electron secondaries.[11] These data, however, as stated at the time, were not adequate to give a reliable value of the average specific energy loss of fast electrons in lead.

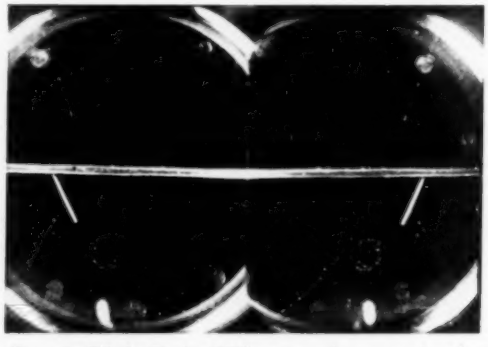

FIG. 6. Pike's Peak, 7900 gauss. An example of an electron losing a large amount of energy in a lead plate. In this case, a positron of ~480 MEV energy strikes a 0.35 cm lead plate. Below the plate three electrons appear of energies respectively: positron, 45 MEV; negatron 45 MEV; and positron 31 MEV. One of the tracks below the plate presumably represents the incident positron after passage through the plate, and the other two tracks a pair generated by the absorption of a photon produced in the plate. The energy lost in the plate by the incident positron is at least 435 MEV, which corresponds to a specific energy loss of ~1150 MEV/cm of lead since the distance traversed is 0.38 cm. The short heavy track may represent an alpha-particle arising from contamination in the plate.

[8] C. G. and D. D. Montgomery, Phys. Rev. **47**, 429 (1935).
[9] R. T. Young, Phys. Rev. **49**, 638 (1936).
[10] C. G. and D. D. Montgomery, Phys. Rev. **48**, 786 (1935). See also recent paper by H. Carmichael, Proc. Roy. Soc. **A154**, 223 (1936).
[11] C. D. Anderson and S. H. Neddermeyer, Int. Conf. on Physics, London, 171 (1934).

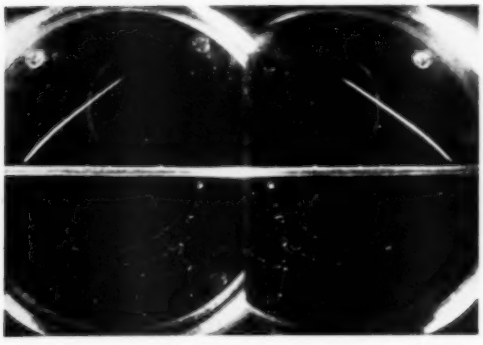

FIG. 7. Pike's Peak, 7900 gauss. A dense track whose range exceeds 6.3 cm measured in the chamber, which contained argon at 1.8 atmospheres pressure. This corresponds to a range greater than 11.5 cm in standard air. This track, coincident in time with the electron shower which also appears on the photograph, is probably due to a proton of low energy which resulted from a nuclear disintegration in the material of the cloud chamber. The scattering which this track exhibits makes impossible a reliable determination of its curvature.

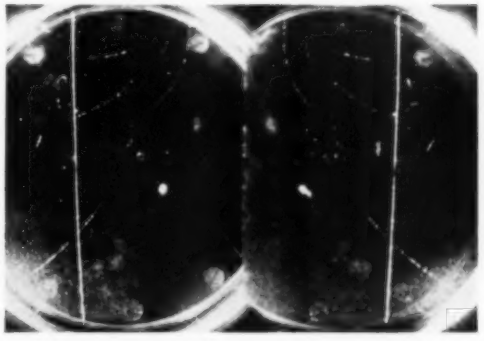

FIG. 8. Pike's Peak, 7900 gauss. A strongly ionizing particle traversing nearly vertically the full diameter of the chamber. It is probably coincident in time with the electron shower which also appears. If traveling downward it has a positive charge and an $H\rho = 1.8 \times 10^6$ gauss cm. If it is assumed to be a proton its energy is 150 MEV and its velocity 0.5 c. The density of ionization exhibited by this track is therefore not inconsistent with the view that it represents a proton. Only a very few examples of strongly ionizing particles traversing the chamber vertically are observed.

Further measurements of energy loss in a plate of more suitable thickness (0.35 cm) showed the specific energy loss to increase with the energy of the incident electron.[12] Recently we have extended these data to include measurements on tracks corresponding to electron energies up to about 300 MEV. To avoid any selective action of the counters controlling the chamber, in this group are included only those photographs where a particle, other than the one measured, appeared, which could have set off the lower counter. These data, given separately in Table III, include two groups of measurements, one taken in a field of 4500 gauss and the other in 7900 gauss. The average initial energy of the electrons (+ and −) in each group is designated by $\overline{E}_1$ and the average energy loss by $\overline{\Delta E/d}$, obs., where d is the thickness of material traversed, and ΔE the difference between the initial and final energy. The total average specific energy loss ($\overline{\Delta E/d}$, theor.) to be expected from radiative and ionizing collisions in a lead plate of the particular thickness used (0.35 cm), calculated from the theory of Bethe and Heitler[13] is given also in Table III.

Within the accuracy of the measurements the experimental energy losses and those calculated from the theory are in agreement up to electron energies of ~300 MEV. The total number of positron-negatron pairs produced in the plate (13 pairs) by the passage of the 227 electrons is approximately the number to be expected if they are produced by the absorption in the plate of the photons originating in the radiative impacts. No reliable average values of energy loss for higher energy electrons (>300 MEV) have been obtained; however, the several individual particles that have been measured, some of which showed energy losses greater than 1000 MEV/cm of lead, do not so far indicate a breakdown of the theoretical formula at somewhat higher energies (see Fig. 6). A more complete discussion of the energy loss of electrons with special reference to the distribution of the observed losses, including also measurements on absorption in substances other than lead will be given later.

The direct energy loss measurements on electrons, so far, furnish no evidence that the theory

TABLE III. *Energy loss of electrons in Pb. (MEV/cm).*

7900 gauss	0.35 cm Pb plate			(Pike's Peak)	
Energy interval in MEV	<50	50–100	100–150	150–200	200–400
No. of tracks	29	65	18	13	21
$\overline{E}_1$	31	75	123	177	272
$\overline{\Delta E/d}$ obs.	42	82	178	191	358
$\overline{\Delta E/d}$ theo.	50	110	175	248	378
4500 gauss	0.35 cm Pb plate			(Pasadena)	
Energy interval in MEV	<50	50–100	100–150	150–200	
No. of tracks	22	28	15	16	
$\overline{E}_1$	26	71	117	170	
$\overline{\Delta E/d}$ obs.	37	84	124	207	
$\overline{\Delta E/d}$ theo.	43	105	167	240	

[12] S. H. Neddermeyer and C. D. Anderson, Phys. Rev. **48**, 486 (1935).

[13] H. Bethe and W. Heitler, Proc. Roy. Soc. **A146**, 83 (1934).

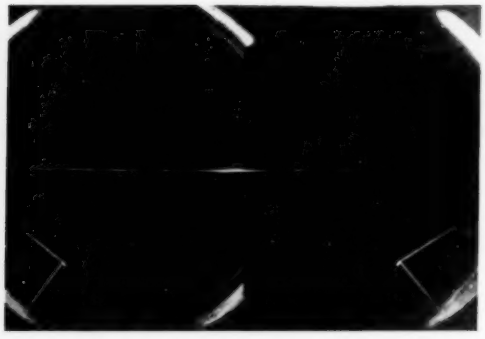

FIG. 9. Pike's Peak, 7900 gauss. A disintegration occurring in the gas (argon) of the chamber. An electron shower occurring apparently simultaneously with this disintegration is only barely visible due to the poor development of the negative on the mountain in a too cool solution. The three heavy particles all diverge within a hemisphere, so that it is impossible for the three particles among themselves to conserve momentum. Momentum might have been supplied by an incoming neutron producing the disintegration. It is possible also that in the disintegration one or more neutrons were ejected. These neutrons would produce no tracks, but can be called upon to conserve momentum in the disintegration. Stereoscopic examination shows that neither of the two longer tracks ends in the gas. It is not possible definitely to identify the particles; the two longer ones may be either protons or alpha-particles and the shorter one the remainder of the argon nucleus.

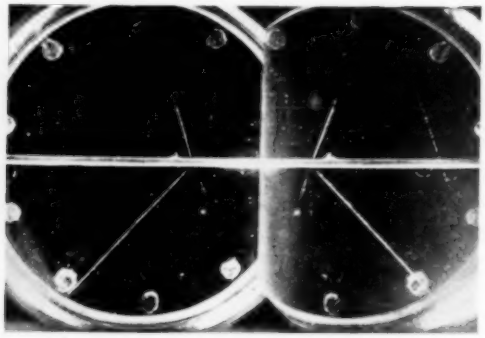

FIG. 10. Pasadena, 4500 gauss. Five shower particles appear, diverging from a region above the chamber. One of these shower particles, probably an electron, in passing through the 0.35 cm lead plate produces a disintegration which results in the ejection of two strongly ionizing particles, one downward to the left and another upward to the left; a third particle which produces a short track in the chamber (downward to the right), shows a lower specific ionization than the others and may be either an electron or a fast proton. The two particles which show a specific ionization too great to be electrons are probably protons. The one ejected downward is positively charged and has an energy of 40 MEV ($H\rho = 9\times10^5$ gauss cm) if it is a proton. The sign of charge of the one ejected upward is not determined; its energy if it is a proton is greater than 20 MEV ($H\rho > 6.5\times10^5$ gauss cm). Stereoscopic examination shows these tracks to intersect very accurately in the plate at a point on the path of the shower particle.

of absorption through radiative losses is not valid at high energies. Nevertheless our observations of many thousand traversals of high energy particles through lead plates (detailed data have been given on 2400 of these[11]) show an observed number of electron secondaries fewer in order of magnitude than that to be expected theoretically through the production of secondary photons and their absorption in the plate itself, provided that these particles are all electrons. The experiments of Rossi,[14] Street, Woodward and Stevenson[15] also have shown the presence of particles too penetrating to permit identifying them with electrons if the Bethe-Heitler theory is assumed to be even approximately valid at high energies. It is obvious that either the theory of absorption breaks down for energies greater than about 1000 MEV, or else that these high energy particles are not electrons.

If one assumes that these penetrating particles are not electrons and that the theory of absorption of photons and electrons remains approximately valid up to very high energies some well known cosmic-ray phenomena, e.g., the production of large electron showers; the transition effects; the variation in counting rate of tube-counters arranged out of line to record showers, as a function of the kind and thickness of material above them, etc., find a qualitative explanation in terms of the production of photons through radiative impacts, and their absorption through pair-production. On the other hand, their interpretation presents some difficulty if one assumes that the theory of absorption of electrons breaks down at high energies to an extent such that the penetrating particles referred to above, can be interpreted as electrons. In particular, the rapid increase in the number of showers with increasing altitude indicates that the photons and electrons producing the showers are highly absorbable and have a high probability of secondary electron production. This large absorbability of electrons and photons is difficult to reconcile with the highly penetrating character of a large fraction of the sea-level particles on the view that the latter are electrons.[16]

[14] B. Rossi, Zeits. f. Physik **82**, 151 (1933), and Int. Conf. on Physics, London (1934).

[15] J. C. Street, R. H. Woodward and E. C. Stevenson, Phys. Rev. **47**, 891 (1935). See also two recent papers by P. Ehrenfest and P. Auger and L. Leprince-Ringuet, J. de phys. et rad. **7**, 65 and 67 (1936).

[16] Reference 11. Footnote p. 182.

It is therefore important to identify the penetrating particles. Some difficulties with identifying a large fraction of them with protons have already been discussed by Bowen, Millikan and Neher,[17] and by ourselves.[11] Furthermore, experiments that we have carried out at Pasadena, designed to bring into evidence high energy primary particles of protonic mass, should they exist in appreciable numbers, have so far given negative results. Since the energy loss by ionizing collisions to be expected of a proton traversing the earth's atmosphere vertically to sea-level is only about 2000 MEV, and since the earth's magnetic field will not permit the entry at this latitude of protons of energy less than 5000 MEV, the chance is especially small of observing a primary proton sufficiently near the end of its range so that it can be readily distinguished from an electron when counters are used to select only the nearly vertical tracks as is normally done. Therefore, photographs were taken with a 0.35 cm lead plate placed across the chamber at 45° with the vertical, and with the two counters placed above and to one side of the chamber so as to permit the entry of particles up to 70° with the vertical, which particles could have traversed up to three times the vertical thickness of the atmosphere; and other photographs in which a meter of lead was placed above the counters for the particles to traverse before entering the chamber. Although the total number of exposures (1500) taken under these conditions is not large, they have so far revealed no tracks which could be ascribed to primary protons near the ends of their ranges. These experiments are being continued.

III. Occurrence of Strongly Ionizing Particles at 4300 Meters and Near Sea-Level, and the Disintegrations Giving Rise to Them

Out of a set of 9188 exposures taken on Pike's Peak 113 showed 123 strongly ionizing particles associated with the cosmic radiation,[18] most of which seem to be protons. Such particles occur very rarely at sea-level, only a few scattered observations having been previously published.[20] The particles reported here are clearly differentiated from alpha-particles arising from radioactive contamination, since, first, their range is in some cases much greater than that of the alpha-particles from any radioactive substance (see Figs. 7, 8) and, second, in other cases they arise from disintegrations which occur in the gas of the chamber itself, or in a plate placed across its center (see Figs. 9, 10, 11, 12, 14).

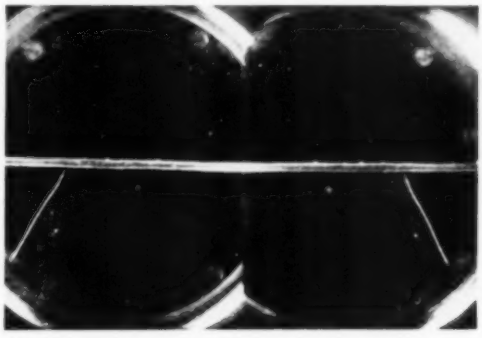

Fig. 11. Pike's Peak, 7900 gauss. A proton and an electron ejected from a point in the lead plate by a nonionizing ray. One of our early photographs at Pasadena indicated that such a process could occur and was so interpreted at that time.[19] The distortion of the low energy proton track due to scattering in the argon and to a motion of the gas, which seems to have occurred in this case, does not permit a measurement of its curvature; the electron's energy exceeds 240 MEV ($H\rho > 8\times10^5$ gauss cm). The nonionizing particle producing the disintegration may be either a photon or a neutron, but the fact that the electron receives most of the energy tends to favor the photon.

Table IV. *Space distribution of the dense tracks occurring on Pike's Peak.*

Angle with vertical (degrees)	0–30	31–60	61–90
Number	55	41	27

The spatial distribution of the dense tracks occurring on these exposures is shown in Table IV, in which is given the number of heavy particles occurring in 30° intervals of the angle with

[17] I. S. Bowen, R. A. Millikan and H. V. Neher, Int. Conf. on Physics, London (1934), p. 206.

[18] F. Rieder and V. F. Hess, Nature **134**, 772 (1935) report the observation of several heavily ionizing particles at 2300 meters. G. Herzog and P. Scherrer, J. de phys. et rad. **6**, 489 (1936) report one heavily ionizing track at 3500 m.

[19] C. D. Anderson and R. A. Millikan, Phys. Rev. **40**, 325 (1932); C. D. Anderson, Phys. Rev. **41**, 408 (1932), Fig. 5.

[20] C. D. Anderson, Phys. Rev. **41**, 405 (1932); **44**, 406 (1933); C. D. Anderson and S. H. Neddermeyer, London Conf. (1934); P. M. S. Blackett and G. P. Occhialini, Proc. Roy. Soc. **A139**, 699 (1933); J. C. Street, E. G. Schneider and E. C. Stevenson, Phys. Rev. **48**, 463 (1935). G. L. Locher, Phys. Rev. **44**, 779 (1933), has interpreted short diffuse heavy tracks as representing cosmic-ray effects, but many of these tracks are doubtless due to alpha-particles arising from contamination in the chamber.

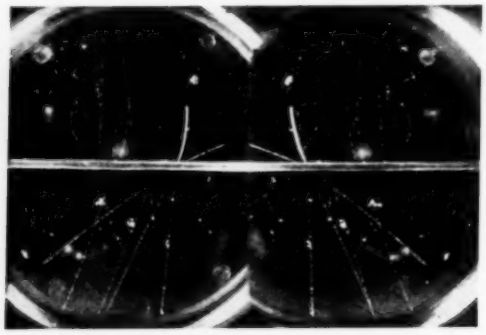

FIG. 12. Pike's Peak, 7900 gauss. A disintegration produced by a nonionizing ray occurs at a point in the 0.35 cm lead plate, from which six particles are ejected. One of the particles (strongly ionizing) ejected nearly vertically upward has the range of a 1.5 MEV proton. Its energy (given by its range) corresponds to an $H\rho = 1.7 \times 10^6$, or a radius of 20 cm, which is three times the observed value. If the observed curvature were produced entirely by magnetic deflection it would be necessary to conclude that this track represents a massive particle with an e/m much greater than that of a proton or any other known nucleus. As there are no experimental data available on the multiple scattering of low energy protons in argon it is difficult to estimate to what extent scattering may have modified the curvature in this case. The particle is therefore tentatively interpreted as a proton. The other particle ejected upward to the right may be either an electron or a fast proton. The four particles ejected downward are positively charged and do not ionize sufficiently strongly to represent protons of the curvatures shown. If they are positrons their energies are respectively 105, 250, ~500 and 60 MEV. The summed energies of the six particles produced in this disintegration must exceed 1000 MEV. Since an electron shower, coming in from above the chamber, occurs on this exposure coincident in time with the disintegration in the plate, the latter probably resulted from an encounter by a photon or neutron which was produced along with the electrons in the shower. The fact that light particles receive so much energy would tend to favor the photon view. This disintegration in which all the ejected particles are probably positively charged represents a process fundamentally different from the usual electron shower; *it shows that charge has been removed from the nucleus and made to appear in the form of light particles.*

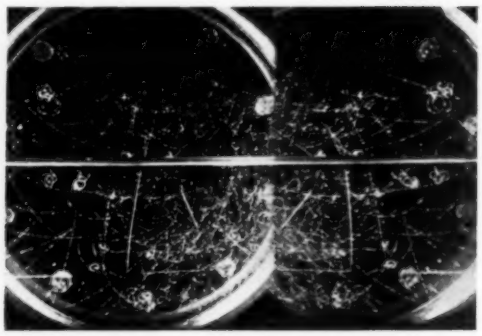

FIG. 13. Pasadena, 4500 gauss. A complex electron shower not clearly defined in direction, and three heavy particles with specific ionizations definitely greater than that of electrons. The sign of charge of two of these heavy particles represented by short tracks cannot be determined, but the assumption that they represent protons is consistent with the information supplied by the photograph. The third heavy track appears above the 0.35 cm lead plate where it has a specific ionization not noticeably different from that of an electron. It penetrates the lead plate and appears in the lower half of the chamber as a nearly vertical track near the middle. Below the plate it shows a greater ionization than an electron, and is deviated in the magnetic field to indicate a positively charged particle. Its $H\rho$ is apparently at most 1.4×10^5 gauss cm, which corresponds to a proton energy of 1 MEV and a range of only 2 cm in the chamber, whereas the observed range is greater than 5 cm. A difficulty of the same nature was discussed in the description of the previous photograph.

the vertical as measured in the plane of the chamber. Whereas the high energy electrons favor the vertical direction very strongly, a large percentage of the heavy particles are nearly horizontal, and in several instances they are clearly seen to be projected upward (see Figs. 9, 10, 12), indicating that in general they represent secondaries resulting from nuclear disintegration.

Wherever the direction of the particles is definitely known (as for particles produced by a disintegration occurring inside the chamber), the sense of curvature in the magnetic field is such as to indicate particles of positive charge. In the cases where the direction of travel is not known, but the assumption made that the particle travels downward, there occur 33 tracks representing positively charged particles, and 5 representing negative particles; the latter 5 tracks, however, may well represent positive particles thrown backward.

For comparison with the Pike's Peak data a set of 10,543 exposures made at Pasadena under

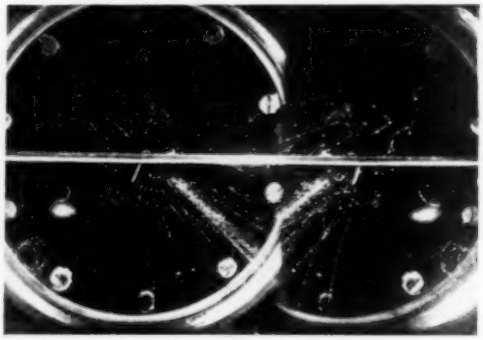

FIG. 14. Pasadena, 4500 gauss. A short dense track shows the ejection of a strongly ionizing particle from the lead plate, apparently coincident in time with the electron shower. This particle may be a proton although it is not possible to determine its energy.

similar conditions was studied, 11 of which showed unambiguous cases of strongly ionizing cosmic-ray particles. Dense tracks are found, therefore, 11.8 times as frequently per exposure on Pike's Peak as at Pasadena. The frequency of occurrence *per exposure* of the larger electron showers with 11–100 tracks increases between the two locations by a factor 8.4, which agrees within a probable fluctuation, with the factor for heavy tracks. This observation, together with the fact that of the 113 Pike's Peak photographs showing heavily ionizing particles, 30 also show time-associated electron showers, suggests that the strongly ionizing particles in most instances result from disintegrations produced by photons and electrons, and in some instances by neutrons which arise in the electron showers. The number of strongly ionizing particles given here represents a lower limit to the true number occurring, as all cases of dense tracks which could possibly arise from radioactive contamination are excluded. It is probable that a certain number of these excluded cases result from cosmic ray effects.

The photographs reveal distinctly new types of nuclear disintegrations, heretofore unreported. Our earlier photographs have shown the presence in the cosmic rays of photons of energies ranging from below 10 MEV up to above 3000 MEV. Many of these photons—those of smaller energy—clearly arise as secondaries in the electron showers.[21] The new photographs present evidence of disintegration of a heavy element, *viz.* lead, by photons (Figs. 11 and 12). The probability of this type of nuclear photo-absorption, although apparently much smaller than the probability of producing the positive-negative electron pairs and showers, seems to be large enough to account for many of the strongly ionizing particles observed. Evidence is here found for the first time that electrons also can occasionally disintegrate nuclei and eject from them massive particles. In Fig. 10 an electron apparently disintegrates a lead nucleus, ejecting protons from it. Some evidence is found of disintegrations which seem to be produced by neutrons occurring as secondaries in the cosmic rays (Fig. 9). Figs. 7–14 all show examples of heavily ionizing particles and the types of disintegrations giving rise to them. Descriptions of the individual photographs are given in the captions.

The foregoing data show that (1) the majority of the heavy tracks seem to represent protons. (2) They appear to be ejected in all directions and to have little relation to the direction of the incoming beam. (3) In several cases electrons and protons originate in the same center. (4) The proton tracks appear as the result of disintegrations produced by both ionizing and nonionizing rays. (5) Practically all the heavy particles can be interpreted only as secondaries produced within the atmosphere or material surrounding the cloud chamber. (6) Certain types of disintegrations, heretofore unobserved, in which the summed energies of the ejected particles exceeds 1000 MEV show that at these high energies the ejection of several particles is common. In these high energy disintegrations the particles ejected show a greater divergence from the direction of the incoming ray than do the electrons produced in the usual high energy electron showers. (7) Whereas many of the disintegrations produced by nonionizing rays seem to result from photon encounters, certain types of disintegrations heretofore unobserved, seem to indicate the presence of neutrons.

We wish to express our sincere gratitude to Professor R. A. Millikan for his unfailing support and interest in the work, and for his continual assistance in the planning of it, and the analysis of the results. Our thanks are due also to Dr. John Strong for aluminizing the mirrors used for the stereoscopic photography, and to Messrs. Lewis Browder and Thomas Harper for their able assistance in preparing the apparatus for use on Pike's Peak, and in gathering data from the photographs. It is a pleasure to thank Mr. E. E. Ewing and Mr. B. Stewart for their courtesies extended to us on Pike's Peak. We are also much indebted to the Union Oil Company of California for their kind gift of the fuel used to operate the power plant on the summit, and to the Carnegie Corporation of New York and the Carnegie Institution of Washington for allotting to Professor Millikan the major part of the funds which have made these researches possible.

[21] C. D. Anderson and S. H. Neddermeyer, Phys. Rev. **45**, 295 (1934); C. D. Anderson, R. A. Millikan, S. H. Neddermeyer and W. H. Pickering, Phys. Rev. **45**, 352 (1934).

On the Continuous γ-Radiation Accompanying the β-Decay

F. BLOCH, *Stanford University*

(Received May 22, 1936)

Combining Fermi's theory of the β-decay with the ordinary principles of quantum electrodynamics one can treat the continuous radiation, to be expected from the acceleration of charges during the nuclear decay. Formulae for its spectral distribution and its total intensity are developed, applicable to light elements, where the effect of the nuclear Coulomb-field on the electrons can be neglected. The relative amount of energy, liberated in the form of radiation, increases monotonously with increasing total energy; in the case of radioactive boron it amounts to about 0.6 percent.

1. INTRODUCTION

IN his theory of the β-decay Fermi[1] has introduced elementary processes where a neutron in the nucleus is transformed into a proton simultaneously with the creation of a neutrino and an electron. The total energy D liberated by the nuclear transformation in such a process reappears in the sum of the energies of the two created particles. One may think, however, that the transformation could also occur in such a way that besides the two particles a light quantum will be emitted. This idea, that part of the energy D can appear in form of radiation, immediately suggests itself, if, for a moment, one considers the β-decay from a classical point of view: Of the two opposite charges originally neutralizing each other in the nucleus the positive one will remain there (and, since attached to a heavy particle, practically stay at rest) while the negative charge will be set into motion and appear as β-ray. Wherever charges are accelerated, according to classical electrodynamics, radiation will be emitted; although the very process of the creation of an electron is entirely beyond the possibility of a classical description one should expect a corresponding radiation in quantum theory.

In fact it is included in Fermi's theory if only the interaction between the electron and the electromagnetic field is taken into account. Of course the most important part of this interaction is already anticipated in the normal β-decay by the fact that the electron is surrounded by a Coulomb-field and has a mass, part of which must be of electromagnetic origin. The well-known difficulties of relativistic quantum mechanics do not allow at present a consistent account of this aspect and thus a rigorous description of electromagnetic effects must be abandoned off-hand. Nevertheless one can obtain unambiguous and reliable information about the radiation effects to be expected, by restricting the theory to the same approximation in which also atomic radiation processes appear. The total process here to be considered can then be regarded as to happen in two stages:[2]

(1) The nuclear transformation, accompanied by the creation of a neutrino in a state σ and an electron in an "intermediate" state s'.

(2) The transition of the electron from the state s' into a final state s by simultaneous emission of a light quantum.

It shall be the purpose of the next sections to develop a quantitative study of the radiation, thus to be expected, particularly for light nuclei.

It will be found that it forms a continuum, extending from zero to a maximum circular frequency

$$\omega_{max} = (D - mc^2)/\hbar$$

(mc^2 = rest-energy of the electron, $2\pi\hbar$ = Planck's quantum of action). For $D - mc^2$ of the order of magnitude mc^2 the intensity is such that the ratio of the probabilities of radiative and normal β-decay will be given approximately by the value of Sommerfeld's fine structure constant $e^2/\hbar c = 1/137$; i.e., roughly one percent of the energy of a β-active substance will appear in form of radiation.

Of course it is always possible that after the

[1] E. Fermi, Zeits. f. Physik **88**, 161 (1934).

[2] Similar to the radiation of particles, penetrating a potential barrier, investigated by Heisenberg, Pauli and Oppenheimer. W. Heisenberg and W. Pauli, Zeits. f. Physik **56**, 1 (1929); J. R. Oppenheimer, Phys. Rev. **35**, 939 (1930).

β-decay, the nucleus will be found in an excited state and then emit another quantum. This ordinary γ-radiation is very different in character and intensity from the radiation here discussed and shall not be considered further.

2. Probability of Radiative β-Decay

We consider a nucleus which in its initial state contains a neutron in a state with eigenfunction u_m and energy E_m.[2] After the decay we will have instead of the neutron a proton in a state with eigenfunction v_n and energy E_n. This transformation shall be considered under the action of two perturbing energies H and K, the former being the one introduced by Fermi in his theory of the β-decay, the latter being the interaction energy between electron and radiation field.

We will have to consider three specified states of the unperturbed system:

(I) The nucleus in its initial state and no neutrino, electron, or light quantum present.

(II) The nucleus in its final state, together with a neutrino in a state σ with energy E_σ and an electron in the "intermediate" state s' with energy $E_{s'}$ but still without light quantum.

(III) The nucleus in its final state, together with a neutrino in the state σ, the electron in its "final" state s with energy E_s and a light quantum with circular frequency ω, emitted in the positive z-direction and polarized in the x-direction. (The last two restrictions about the light quantum are obviously made without any loss of generality.)

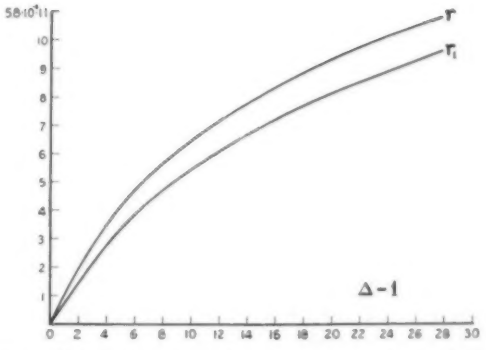

Fig. 1. Values of r and r_1 as functions of $\Delta-1$, the maximum kinetic energy of the electrons divided by mc^2.

The amplitudes of probability of these three states shall be designated by α, $\beta(s', \sigma)$, $\gamma(s, \sigma, \omega)$. They are functions of the time and have to satisfy the initial condition, that for $t=0$:

$$\alpha=1; \qquad \beta(s', \sigma)=\gamma(s, \sigma, \omega)=0.$$

Taking only the terms of lowest order in the perturbation energies H and K, the variation of constants gives for the change of β and γ in course of the time:

$$-(\hbar/i)\dot{\beta}(s', \sigma)=H^{m}{}_{n;\ s'\sigma}e^{(i/\hbar)(E_{s'}+E_\sigma-D)t}, \tag{1a}$$

$$-(\hbar/i)\dot{\gamma}(s, \sigma, \omega)=\sum_{s'}K_s{}^{s'}(\omega)\beta(s', \sigma)e^{(i/\hbar)(\hbar\omega+E_s-E_{s'})t}, \tag{1b}$$

and therefore after a time t with the initial condition mentioned before

$$\beta(s'\sigma)=H^{m}{}_{n;\ s'\sigma}\frac{e^{(i/\hbar)(E_{s'}+E_\sigma-D)t}-1}{D-E_{s'}-E_\sigma}, \tag{2a}$$

$$\gamma(s'\sigma\omega)=\sum_{s'}\frac{H^{m}{}_{n;\ s'\sigma}K_s{}^{s'}(\omega)}{E_{s'}+E_\sigma-D}\left[\frac{e^{(i/\hbar)(E_s+E_\sigma+\hbar\omega-D)}-1}{E_s+E_\sigma+\hbar\omega-D}-\frac{e^{(i/\hbar)(E_s+\hbar\omega-E_{s'})t}-1}{E_s+\hbar\omega-E_{s'}}\right]. \tag{2b}$$

In (1) and (2)

$$D=E_m-E_n \tag{3}$$

stands for the total energy, liberated in the transformation, $2\pi\hbar=h$ is Planck's quantum of action and $H^{m}{}_{n,\ s'\sigma}$, $K_s{}^{s'}(\omega)$ are the matrix-elements of the perturbation energies H and K, which account for the transitions from the states I to II and II to III respectively. They obtain a simple form if

[2] We consider here only the case of negative electron emission. By interchanging the words "neutron" and "proton" and writing "positron" instead of "electron" our considerations as well as the final results apply immediately also to the case of positron emission.

we neglect from now on the influence of the nuclear charge on the electron; for usual values of the decay-energy we commit thus only an error of the relative order of magnitude $Ze^2/\hbar c$; i.e., for light elements of a few percents. The eigenfunctions of the states s, s' of the electron and σ of the neutrino are then solutions of Dirac's wave equation for free particles, namely plane waves with amplitudes having four components according to the four values of the spin variable. We obtain thus

$$H^m_{n;\,s'\sigma} = (gI/V) a_{s'}{}^* \eta b_\sigma{}^*, \tag{4}$$

$$K_s{}^{s'}(\omega) = e\hbar (2\pi c/Vp)^{\frac{1}{2}} a_s{}^* \alpha_x a_{s'}, \tag{5}$$

$g = 4 \cdot 10^{-50}$ cm^3 erg is the constant, appearing in Fermi's theory,

$I = \int v_n{}^* u_m d\tau$ the overlapping-integral of the eigenfunctions of neutron and proton.[4]

$a_{s'}$, α_s and b_σ are the amplitudes of the plane waves, representing the states s, s', and σ of the electron and the neutrino with momenta $\mathbf{p}_{s'}$, $\mathbf{p}_s$, $\mathbf{p}_\sigma$, respectively. $p = \hbar\omega/c$ is the absolute value of the momentum $\mathbf{p}$ of the light quantum with components $p_x = p_y = 0$; $p_z = \hbar\omega/c$. It is connected with $\mathbf{p}_s$ and $\mathbf{p}_{s'}$ by the equation

$$\mathbf{p}_{s'} = \mathbf{p} + \mathbf{p}_s. \tag{6}$$

η is the matrix $\begin{pmatrix} 0 & -1 & 0 & 0 \\ 1 & 0 & 0 & 0 \\ 0 & 0 & 0 & 1 \\ 0 & 0 & -1 & 0 \end{pmatrix}$ introduced by Fermi.[5] $\alpha_x = \begin{pmatrix} 0 & 0 & 0 & 1 \\ 0 & 0 & 1 & 0 \\ 0 & 1 & 0 & 0 \\ 1 & 0 & 0 & 0 \end{pmatrix}$ is one of Dirac's matrices, which appears in the interaction energy between the electron and a light quantum, polarized in the x-direction. e is the elementary charge, c the velocity of light and V is a large volume within which the states of electron, neutrino, and light quantum are quantized and normalized. Furthermore, as in Fermi's theory, it is assumed that the wave-lengths p_s/h, $p_{s'}/h$, p_σ/h of electron and neutrino are large compared to nuclear dimensions.

From (2b) we find now in the usual way that the number of transitions per unit time, which lead to the final state III, is given by

$$\frac{dP}{dt} = \frac{2\pi}{\hbar} \delta(\hbar\omega + E_s + E_\sigma - D) \left| \sum_{s'} \frac{H^m_{n;\,s'\sigma} K_s{}^{s'}(\omega)}{E_{s'} - E_s - \hbar\omega} \right|^2, \tag{7}$$

where δ is Dirac's singular δ-function.[6] The summation over s' has to be performed over all intermediate states s' of the electron; since for given values $\mathbf{p}$ and $\mathbf{p}_s$ the matrix element $K_s{}^{s'}(\omega)$ is only different from zero if the momentum $\mathbf{p}_{s'}$ has the value given by (6), this summation extends only over the four states, which, according to Dirac's equation, belong to the momentum $\mathbf{p}_{s'}$. We designate these four states by an index λ and obtain thus from (4) and (7)

$$\frac{dP}{dt} = \delta(\hbar\omega + E_s + E_\sigma - D) \frac{4\pi^2 g^2 |I|^2 e^2 \hbar c}{V^3 p} \left| \sum_{\lambda=1}^{4} \frac{a_s{}^* \alpha_x a_{\lambda s'} a_{\lambda s'}{}^* \eta b_\sigma{}^*}{E_{\lambda s'} - \hbar\omega - E_s} \right|^2 \tag{8}$$

with

$$\begin{aligned} E(p_s) = E_s &= +c(p_s{}^2 + m^2c^2)^{\frac{1}{2}}, \qquad E(p_\sigma) = E_\sigma = +cp_\sigma,{}^{7} \\ E_{1s'} = E_{2s'} &= +c(p_{s'}{}^2 + m^2c^2)^{\frac{1}{2}}, \qquad E_{3s'} = E_{4s'} = -c(p_{s'}{}^2 + m^2c^2)^{\frac{1}{2}}.{}^{8} \end{aligned} \tag{9}$$

[4] We assume this integral to be different from zero; the changes that have to be made otherwise are quite analogous to the corresponding ones in Fermi's theory and do not essentially alter our considerations.

[5] Fermi uses δ instead of η.

[6] Defined by

$$\int_a^b \delta(x)dx = \begin{cases} 1 & \text{for } a < 0 < b, \\ 0 & \text{otherwise.} \end{cases}$$

[7] We assume the mass of the neutrino to be zero.

[8] Obviously, in this scheme both "positive" and "negative" intermediate states have to be taken into account. If, instead, one assumes (with Dirac) all negative states to be filled, due to the exclusion principle only positive intermediate

The summation over λ in (8) can easily be carried out if one takes into account the relation of completeness of the amplitudes $a_{\lambda s'}$ with respect to the spin-variable, and leads to

$$\frac{dP}{dt}=\delta(\hbar\omega+E_s+E_\sigma-D)\frac{4\pi^2g^2|I|^2e^2\hbar c}{V^3p[E_{s'}^2-(\hbar\omega+E_s)^2]^2}|a_s^*\alpha_x\Gamma\eta b_\sigma^*|^2 \tag{10}$$

with
$$\Gamma=\hbar\omega+E_s+c(\boldsymbol{\alpha}\mathbf{p}_{s'})+\beta mc^2 \tag{11}$$

and
$$E_{s'}^2=c^2p_{s'}^2+m^2c^4,$$

the vector matrix $\boldsymbol{\alpha}$ and the matrix β being the same as in Dirac's relativistic theory of the electron. In formula (10) not only the momenta $\mathbf{p}_s$ and $\mathbf{p}_\sigma$ of electron and neutrino but also their spin-directions are supposed to be given. For the total transition probability we have to sum over these spin directions. Indicating this summation by $\sum_{s.\,d.}$ we obtain

$$\sum_{s.\,d.}\frac{dP}{dt}=\delta(\hbar\omega+E_s+E_\sigma-D)\frac{4\pi^2g^2|I|^2e^2\hbar c}{V^3p[E_{s'}^2-(\hbar\omega+E_s)^2]^2}\overline{(M\alpha_x\Gamma N\Gamma\alpha_x)}. \tag{12}$$

M and N are the two matrices

$$M=1+[c(\boldsymbol{\alpha}\mathbf{p}_s)+\beta mc^2]/E_s, \qquad N=1+c(\boldsymbol{\alpha}\mathbf{p}_\sigma)/E_\sigma. \tag{13}$$

The bar over the last matrix product in (12) indicates the average value, i.e., one-fourth of the sum of its diagonal elements. It is

$$\overline{(M\alpha_x\Gamma N\Gamma\alpha_x)}=f(\mathbf{p}_s,\boldsymbol{\pi}_\sigma,\boldsymbol{\pi}_{s'})=c^2(\pi_{s'}^2+m^2c^2)+2(\hbar\omega+E_s)\left(\frac{c^2(\boldsymbol{\pi}_\sigma\boldsymbol{\pi}_{s'})}{E_\sigma}+\frac{c^2(\mathbf{p}_s\boldsymbol{\pi}_{s'})-m^2c^4}{E_s}\right)$$

$$+(\hbar\omega+E_s)^2\left(1+\frac{c^2(\mathbf{p}_s\boldsymbol{\pi}_\sigma)}{E_sE_\sigma}\right)+\frac{c^4}{E_sE_\sigma}\left(2(\boldsymbol{\pi}_\sigma\boldsymbol{\pi}_{s'})[(\mathbf{p}_s\boldsymbol{\pi}_{s'})-m^2c^2]-(\mathbf{p}_s\boldsymbol{\pi}_\sigma)[\pi_{s'}^2-m^2c^2]\right), \tag{14}$$

where $\boldsymbol{\pi}_\sigma$ and $\boldsymbol{\pi}_{s'}$ are vectors with components $p_{\sigma x}$, $-p_{\sigma y}$, $-p_{\sigma z}$ and $p_{s'x}$, $-p_{s'y}$, $-p_{s'z}$, respectively. Integrating (12) over the momentum-space of the neutrino and over the directions of the emitted electron, we finally obtain the rate of transition (probability per unit time) of a process, in which an electron is emitted with an energy between E and $E+dE$ [9] simultaneously with a light quantum of circular frequency between ω and $\omega+d\omega$. The light quantum shall be emitted within an angle between θ and $\theta+d\theta$ against the direction of the electron and be polarized in the plane, connecting the momenta of electron and light quantum.[10]

With (6), (9), (12), and (14) this rate of transitions becomes:

$$dR_x=A(E+\hbar\omega-D)^2\frac{u}{(1-u\cos\theta)^2}\left[\frac{h^2\omega^2}{2}(1-u\cos\theta)+E(E+\hbar\omega)u^2\sin^2\theta\right]\frac{d\omega}{\omega}dE\sin\theta d\theta, \tag{15}$$

where
$$A=g^2|I|^2e^2/4\pi^4\hbar^8c^7 \tag{16}$$

and $u=v/c=(1/E)(E^2-m^2c^4)^{\frac{1}{2}}$ is the velocity of the electron in units of the velocity of light. If on

---

states of the electron have to be taken into account. In this case, however, one has to consider that the final state III can also be reached by a double process, in which first an electron makes a transition from a negative state s' into the positive state s by emission of a light quantum and where afterwards by the nuclear transition another electron is created in such a way that it fills the hole in the negative states, left by the transition of the first electron. It is easy to show that the net result will be the same as given by (8).

[9] We now omit the index s.

[10] We have thus chosen here this plane to be the $x-z$-plane of our coordinate system.

the other hand the light quantum is polarized perpendicularly to the direction of electron, we obtain similarly

$$dR_y = A(E+\hbar\omega-D)^2 \frac{u}{(1-u\cos\theta)^2}\left[\frac{\hbar^2\omega^2}{2}(1-u\cos\theta)\right]\frac{d\omega}{\omega}dE\sin\theta d\theta, \tag{17}$$

and thus for the rate of transition without specifying the polarization

$$\begin{aligned} dR &= dR_x + dR_y \\ &= A(E+\hbar\omega-D)^2 \frac{u}{(1-u\cos\theta)^2}\left[\hbar^2\omega^2(1-u\cos\theta)+E(E+\hbar\omega)u^2\sin^2\theta\right]\frac{d\omega}{\omega}dE\sin\theta d\theta. \end{aligned} \tag{18}$$

This result has been obtained by assuming Fermi's form for the interaction between nucleus and electron-neutrino field. Konopinski and Uhlenbeck[11] have proposed another form, which contains as a factor the energy of the neutrino. With the exception of a few minor changes the calculation remains practically the same, if we accept this second form of the interaction; we shall briefly indicate these changes:

Instead of (4), one has to take

$$H^{m}_{n;\,s\sigma} = \frac{gI}{V}\frac{E_\sigma}{mc^2}a_{s'}{}^{*}\eta\beta b_\sigma{}^{*} \tag{4a}$$

and thus finds instead of (12)

$$\sum_{s,\mathrm{d.}}\frac{dP}{dt} = \delta(\hbar\omega+E_s+E_\sigma-D)\frac{4\pi^2g^2|I|^2c^2\hbar c}{V^3p[E_{s'}{}^2-(E_s+\hbar\omega)^2]^2}\left(\frac{E_\sigma}{mc^2}\right)^2\overline{(M\alpha_x\Gamma N_1\Gamma\alpha_x)} \tag{12a}$$

with $N_1 = 1-c(\mathfrak{a}\mathfrak{p}_\sigma)/E_\sigma$. Instead of (14) it is

$$\overline{(M\alpha_x\Gamma N_1\Gamma\alpha_x)} = f(p_s,\ -\pi_\sigma,\ \pi_{s'}), \tag{14a}$$

where f is the same function as in (14). Finally instead of (18) one obtains for the rate of transition

$$dR_1 = A\frac{(E+\hbar\omega-D)^4}{m^2c^4}\frac{u}{(1-u\cos\theta)^2}\left[\hbar^2\omega^2(1-u\cos\theta)+E(E+\hbar\omega)u^2\sin^2\theta\right]\frac{d\omega}{\omega}dE\sin\theta d\theta. \tag{18a}$$

3. Discussion: Spectral Distribution and Total Amount of Radiated Energy

Formulae (18) and (18a) show that there is to be expected an anisotropy of the intensity of radiation with respect to the direction of the emitted electron very similar to that of the continuous radiation, caused by the impact of electrons. In the non-relativistic case, i.e., if

$$\hbar\omega/mc^2 \ll u \ll 1,$$

the intensity per unit solid angle will be proportional to $\sin^2\theta$ as one should expect it classically from a dipole radiation. In the highly relativistic case, however, i.e., for $u \leqq 1$ the anisotropy will be essentially determined by the denominator $(1-u\cos\theta)^2$ which then becomes very small for small angles θ. In this case, therefore, most of the radiation will be emitted nearly parallel to the direction of the electron.

While (18) and (18a) are valid for all velocities of the electron[12] they obviously break down for very small values of the frequency ω. This can be seen from the fact that the frequency appears once in the denominator so that by integrating over the frequency from zero to its maximum value $(D-E)/\hbar$ one would get an infinite result for the probability of radiative β-decay. The same situation is found wherever not only the radiationless process is possible but also the same process, simul-

[11] E. J. Konopinski and G. E. Uhlenbeck, Phys. Rev. **47**, 202 (1935).
[12] Except for the fact that for very small velocities the Coulomb-field of the nucleus becomes important.

taneous with the emission of an arbitrarily soft light quantum,[13] and has its origin in the treatment of the electromagnetic field as a small perturbation. It is due to this treatment that there appears (as in formula (7)) the denominator $E_{\varepsilon'}-E_{\varepsilon}-\hbar\omega$, which for sufficiently small values of ω becomes arbitrarily small and ultimately leads to a divergent result for the probability of the radiative process. Although strictly speaking incorrect, when applied to transition probabilities, our formulae (18) and (18a) seem to give trustworthy results for the average energy of the radiation. In this case indeed we have to multiply them by another factor $\hbar\omega$, thus avoiding the divergence, mentioned before.

Integrating (18) over the angle θ from 0 to π and over the energy of the electron E from mc^2 to $D-\hbar\omega$ we obtain

$$\hbar\omega\int_{\theta}\int_{E} dR = i(\omega)d\omega$$

as the radiation energy emitted into the frequency range $d\omega$ per unit time. It is

$$i(\omega) = A\hbar(mc^2)^5 F((D-\hbar\omega)/mc^2) \tag{19}$$

with

$$F(x)=\left[\Delta^2\left(\frac{2}{3}x^3+x\right)-\Delta\left(x^4+x^2-\frac{1}{8}\right)+\frac{7}{15}x^3-\frac{3}{8}x\right]\lg\,(x+(x^2-1)^{\frac{1}{2}})$$
$$-\left[\Delta^2\left(\frac{11}{9}x^2+\frac{4}{9}\right)-\Delta\left(\frac{7}{4}x^3+\frac{1}{8}x\right)+\frac{689}{900}x^4-\frac{1021}{1800}x^2-\frac{8}{75}\right](x^2-1)^{\frac{1}{2}}$$

and $\Delta = D/mc^2$. Similarly from (18a)

$$i_1(\omega) = A\hbar(mc^2)^5 F_1((D-\hbar\omega)/mc^2) \tag{19a}$$

with

$$F_1(x)=\left[\Delta^2\left(\frac{2}{5}x^5+2x^3+\frac{3}{4}x\right)-\Delta\left(\frac{2}{3}x^6+3x^4+\frac{3}{4}x^2-\frac{1}{24}\right)+\frac{32}{105}x^7+x^5-\frac{1}{2}x^3-\frac{5}{24}x\right]\log\,(x+(x^2-1)^{\frac{1}{2}})$$
$$-\left[\Delta^2\left(\frac{137}{150}x^4+\frac{607}{300}x^2+\frac{16}{75}\right)-\Delta\left(\frac{3}{2}x^5+\frac{17}{6}x^3+\frac{1}{24}x\right)+\frac{2449}{3675}x^6+\frac{9413}{14700}x^4-\frac{19603}{29400}x^2-\frac{32}{735}\right](x^2-1)^{\frac{1}{2}}.$$

The intensity distribution of the emitted radiation, as given by (19) and (19a), shows a rather rapid decrease from its maximum at $\omega=0$ to the zero value at the high frequency limit $\omega_{max}=(D-mc^2)/\hbar$. In the limiting case $\Delta\gg mc^2$ about 50 percent of the total radiation according to (19), 60 percent according to (19a) will be found at a frequency less than one-fourth of the high frequency limit.

Finally, we find for the total intensity of the radiation from (19)

$$I_{tot}=\int_0^{\omega_{max}} i(\omega)d\omega=\frac{A}{2}(mc^2)^6\phi(\Delta) \tag{20}$$

with $$\phi(\Delta)=\left[\frac{4}{45}\Delta^6+\frac{1}{3}\Delta^4-\frac{1}{72}\right]\log\,(\Delta+(\Delta^2-1)^{\frac{1}{2}})-\left[\frac{44}{225}\Delta^5+\frac{27}{100}\Delta^3-\frac{103}{1800}\Delta\right](\Delta^2-1)^{\frac{1}{2}}$$

and from (19a)

$$(I_{tot})_1=\int_0^{\omega_{max}} i_1(\omega)d\omega=(A/2)(mc^2)^6\phi_1(\Delta) \tag{20a}$$

[13] It also appears for example in the theory of radiative impacts. (Bethe and Heitler.)

with

$$\phi_1(\Delta)=\left[\frac{2}{105}\Delta^8+\frac{2}{15}\Delta^6-\frac{1}{12}\Delta^2-\frac{1}{192}\right]\log\left(\Delta+(\Delta^2-1)^{\frac{1}{2}}\right)$$
$$-\left[\frac{691}{14700}\Delta^7+\frac{171}{1176}\Delta^5-\frac{9589}{117600}\Delta^3-\frac{11063}{235200}\Delta\right](\Delta^2-1)^{\frac{1}{2}}.$$

In order to get a convenient measure for the total intensity, we will divide (20) and (20a) by the average kinetic energy $\bar{E}_{\text{kin}}=\overline{(E-mc^2)}$ given to the electrons per unit time. According to Fermi's theory this is[14]

$$\bar{E}_{\text{kin}}=A(mc^2)^6(hc/e^2)\psi(\Delta) \tag{21}$$

with $\psi(\Delta)=\left[\frac{1}{60}\Delta^5-\frac{1}{30}\Delta^4-\frac{1}{30}\Delta^3+\frac{3}{20}\Delta^2+\frac{49}{240}\Delta+\frac{2}{15}\right](\Delta^2-1)^{\frac{1}{2}}-\left[\frac{1}{8}\Delta^2+\frac{1}{4}\Delta+\frac{1}{16}\right]\log\left(\Delta+(\Delta^2-1)^{\frac{1}{2}}\right)$,

according to Uhlenbeck and Konopinski

$$\bar{E}_{\text{kin}}=A(mc^2)^6(hc/e^2)\psi_1(\Delta) \tag{21a}$$

with

$$\psi_1(\Delta)=\left[\frac{1}{280}\Delta^7-\frac{1}{105}\Delta^6-\frac{5}{336}\Delta^5+\frac{2}{21}\Delta^4+\frac{1913}{6720}\Delta^3+\frac{247}{420}\Delta^2+\frac{3571}{13440}\Delta+\frac{8}{105}\right](\Delta^2-1)^{\frac{1}{2}}$$
$$-\left[\frac{1}{8}\Delta^4+\frac{1}{2}\Delta^3+\frac{3}{8}\Delta^2+\frac{1}{4}\Delta+\frac{5}{128}\right]\lg\left(\Delta+(\Delta^2-1)^{\frac{1}{2}}\right).$$

Dividing (20) by (21) and (20a) by (21a) we find now the percentage of energy liberated in form of γ-radiation by the β-decay in the form

$$r(\Delta)=I_{\text{tot}}/\bar{E}_{\text{kin}}=(e^2/2hc)(\phi(\Delta)/\psi(\Delta))=5.81\cdot10^{-4}\chi(\Delta) \tag{22}$$

with $$\chi(\Delta)=\phi(\Delta)/\psi(\Delta)$$

and $$r_1(\Delta)=5.82\cdot10^{-4}\chi_1(\Delta) \quad \text{with} \quad \chi_1(\Delta)=\phi_1(\Delta)/\psi_1(\Delta), \quad \text{respectively.} \tag{22a}$$

In the nonrelativistic case, i.e., for $\Delta=1+\epsilon$ with $\epsilon\ll1$, we have $\chi(\Delta)=(32/33)\epsilon$ and $\chi_1(\Delta)=(32/45)\epsilon$. On the other hand for $\Delta\gg1$, we obtain the asymptotic formulae

$$\chi(\Delta)=\frac{16}{3}\left(\log 2\Delta-\frac{11}{5}\right) \quad \text{and} \quad \chi_1(\Delta)=\frac{16}{3}\left(\log 2\Delta-\frac{691}{280}\right).$$

The two values r and r_1 are plotted in Fig. 1 as functions of $\Delta-1$, i.e., of the maximum kinetic energy of the electrons, divided by mc^2.[15]

While for example for radiophosphorus ($\Delta=5$) the radiation contains only about 0.17 percent of the total average energy, liberated in the decay, it amounts to about 0.6 percent in the case of the radioactive boron isotope B^{12} ($\Delta=26$).

Note added in proof: While this paper was in press an article on the same problem has appeared in Physica **3**, 425 (1936). J. K. Knipp and G. E. Uhlenbeck reach essentially the same conclusions as obtained in this paper.

[14] Neglecting again the Coulomb-field around the nucleus.
[15] I am indebted to Mr. R. D. Gordon for valuable help in computation.

Pressure Effect in the HCN Bands in the Near Infrared

S. D. CORNELL AND WILLIAM W. WATSON, *Sloane Physics Laboratory, Yale University*

(Received June 10, 1936)

Contrary to the observations of Herzberg and Spinks it is found that all the lines of the HCN absorption band at 1.04μ are broadened equally by increase in HCN gas pressure. The half-widths increase linearly with pressure at the rate of 0.56 cm^{-1} per atmosphere. This value is slightly less than that found by H. Becker for the first harmonic band of HCl, as is to be expected from the relative polarizabilities of the two molecules. The results indicate dispersion forces to be the predominant broadening influence.

INVESTIGATIONS of the absorption spectrum of HCN in the photographic infrared have been made by Badger and Binder[1] and by Herzberg and Spinks.[2] Both of these comment on the considerable breadth of the rotational lines when saturated vapor pressures of HCN are used in the absorption tube. Herzberg and Spinks photographed the intense (0, 0, 3, 0) band[3] at 1.04μ, which has a simple P, R branch structure due to the linear nature of the HCN molecule, at several vapor pressures from 130 mm to 650 mm. They observed that whereas at the lower pressure the absorption lines were as sharp as could be expected from the slit width used, at the highest pressure all the lines became very broad. The broadening effect of a partial pressure of air was noted to be very much smaller than the influence of the HCN molecules on each other. Additional observations were that these lines are considerably more broadened by increase in the HCN pressure than are the lines of the second overtone HCl band at corresponding pressures of HCl, and that the broadening decreases with increasing molecular rotation.

It was concluded by Herzberg and Spinks that this pressure broadening could not be pure Lorentz collision broadening, and that an apparently necessary condition for the effect is that the molecule be rather easily deformable as shown by one small vibration frequency. Their observations of this pressure broadening seem to have been only qualitative, however. And since a reconciliation of these facts with other pressure broadening effects appeared to be very difficult, quantitative measurements on the variation of the half-widths of these lines with density of absorbing vapor and with rotational quantum number J were to be desired. Such measurements do not reveal any unusual pressure broadening effect and are susceptible to simple theoretical interpretation.

Experimental Procedure

The HCN was generated by dropping a concentrated solution of sodium cyanide into sulphuric acid, dried with calcium chloride and introduced into the previously evacuated absorption cell. This cell was made from a Pyrex tube 200 cm long and 4 cm diameter with flat Pyrex windows fused on to each end. A heating coil was provided to raise the temperature of the cell somewhat above the boiling point (26°C) of HCN when necessary. The light source was either a 150 c.p. Point-o-lite lamp or a 32 c.p. double filament automobile headlight lamp run on 16 volts with the two filaments in series. After passing through the absorption cell twice the light was focused on the slit of the 21-foot concave grating in a stigmatic mounting.

All spectrograms of the 1.04μ absorption band were taken in the first order of this grating, the dispersion being 4.72A/mm. Using a slit 0.04 mm in width the exposure times with Eastman I–Z plates ranged from 8 to 24 hours. Fe lines in the second order served as a comparison spectrum. HCN vapor pressures used were 131, 230, 265 and 525 mm at the room temperature of 21°C and 820 mm at 40°C. This highest pressure reduced to 21°C for pressure effect comparison with the others is 770 mm. A number of lines of both low and high J values in the P branch of the band as

[1] R. M. Badger and J. L. Binder, Phys. Rev. **37**, 800 (1931).

[2] G. Herzberg and J. W. T. Spinks, Proc. Roy. Soc. **A147**, 434 (1934).

[3] The vibrational energy level assignments for the infrared HCN bands have been made by A. Adel and E. F. Barker, Phys. Rev. **45**, 277 (1934).

TABLE I. *Half-value widths $\nu_{\frac{1}{2}}$ in cm^{-1} for P branch lines of the 1.04μ HCN absorption band.*

J	$P=131$ mm	$P=230$ mm	$P=265$ mm	$P=525$ mm	$P=770$ mm
1				1.08	
2				1.19	
3				1.19	1.26
4	0.87	0.92	0.98	1.10	1.20
5				1.14	1.34
6				1.21	
7					1.18
8					1.40
9					1.51
10					1.26
11	0.91		1.05		1.62
12	0.84	0.92	1.03		1.73
13	0.94	0.89	0.89	1.27	1.18
14	0.82	0.99	1.08	1.23	1.38
15	0.97	0.98	0.94	1.36	1.08
16	0.80	1.04	0.86	1.26	1.20
17	0.89	0.93	0.98	1.26	1.52
18				1.19	
19				1.06	1.40
20				0.86	
Ave.	0.88	0.95	0.98	1.17	1.35

produced at each of these pressures were photometered with the 40 : 1 magnification of a Koch-Goos registering microphotometer. The dispersion for these photometer traces is 0.108 cm^{-1}/mm.

LINE WIDTHS

The measurements of the half-value widths $\nu_{\frac{1}{2}}$ of all the lines we have photometered are collected in Table I. In Fig. 1 is displayed the distribution of these line widths about their mean values for two of the pressures. Inspection of the table and the graph shows a random variation of the widths with rotational quantum number J about the mean values at each pressure. There is certainly no decrease in line width with increasing molecular rotation. It is true that at a first glance at a spectrogram such as the one reproduced in Fig. 2 for a fairly high vapor pressure the lines near the band origin do look definitely broader. But the maximum of the rotational energy distribution comes at a rather low quantum number ($J=7$) the greater resulting intensity for these lines thus giving the false impression that they are broader than the weaker high J lines. Such an error of judgment is one commonly made. It should be emphasized that the relative breadths of absorption lines of unequal intensity may only be learned from measurements of their half-value widths from photometer traces with any necessary correction for plate characteristic.

Fig. 3 is a plot of the mean values of the half-widths as a function of the pressure of the absorbing HCN vapor. The vertical dashed double-headed arrows indicate by their length the average numerical deviation of the individual widths from their mean. These deviations would naturally be expected to increase with increasing line breadth. The mean values show the usual strictly linear increase with pressure, the change being 0.56 cm^{-1} per atmosphere. This is only slightly larger than the pressure broadening produced by foreign gases both for atomic and molecular spectral lines.[4, 5]

DISCUSSION

The magnitude of this pressure broadening, its linear increase with pressure and its independence of the rotational energy of the absorbing molecule all indicate that dispersion forces are the predominant broadening influence. This is in agreement with London's[6] work on the attractive force between rotating dipoles in which it is shown that even for a strong dipole gas such as HCl the dispersion effect is considerably larger than the Debye induction effect and the direction effect. Furthermore, the expression for the

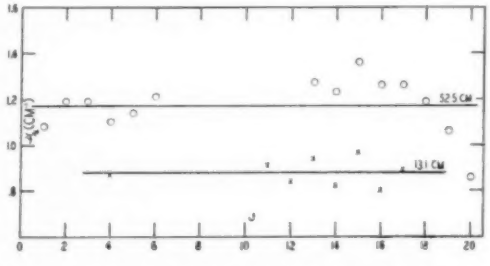

FIG. 1. Half-value widths of $P(J)$ lines of the 1.04μ absorption band of HCN at pressures of 131 mm and 525 mm. Note the random distribution about the mean values (horizontal lines).

[4] H. Margenau and W. W. Watson, Rev. Mod. Phys. **8**, 22 (1936).
[5] W. W. Watson and G. F. Hull, Jr., Phys. Rev. **49**, 592 (1936).
[6] F. London, Zeits. f. Physik **63**, 245 (1930).

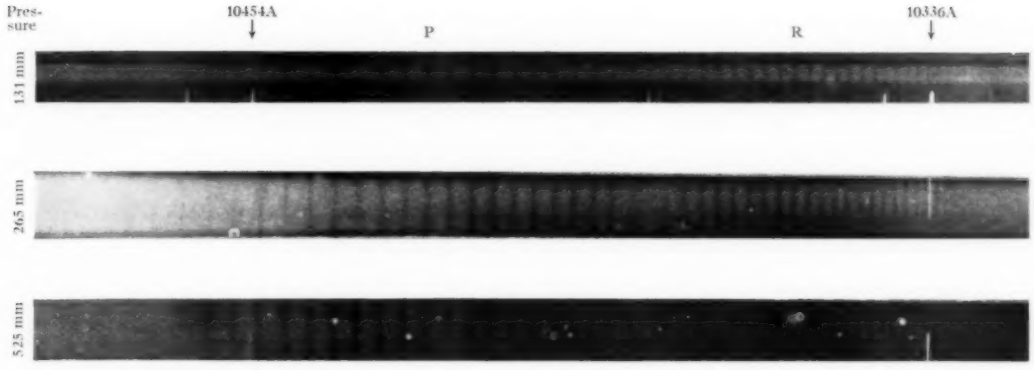

FIG. 2. 1.04μ HCN band with HCN pressures of 131, 265 and 525 mm.

interaction energy between a molecule of polarizability α and a rigid rotator of dipole moment μ developed recently by Margenau[7] indicates an insignificant dependence on the rotational quantum number J.

Using the Lorentz-Lorenz relation with the known index of refraction for HCN, one computes the polarizability α to be 2.58×10^{-24}. Since for HCl $\alpha=2.71\times10^{-24}$ it is to be expected that the HCl band lines should actually show a somewhat greater pressure broadening than do these HCN lines. Becker[8] has measured the half-width of a line of the first harmonic band of HCl at 1.74μ at pressures of 3, 5, 7, 9 and 11 atmospheres as 8.65, 14.0, 17.1, 21.75 and 25.1A respectively. The rate of increase of this width with pressure is about 0.7 cm^{-1} per atmosphere, a value in good agreement with our expectations. The same broadening influence, dispersion forces, is undoubtedly in large part responsible for the pressure broadening in both cases, and there is no evidence for molecular association.

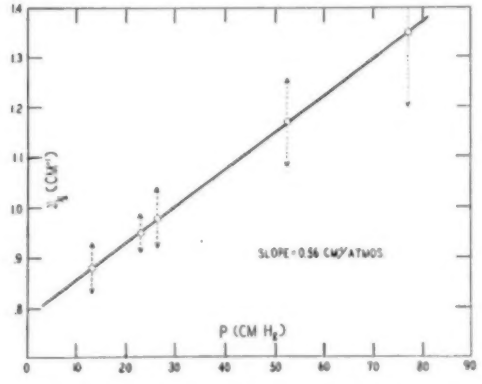

FIG. 3. Mean value of line half-widths *vs.* HCN vapor pressure.

It has been reported by Mecke that the H_2O band lines are relatively quite sharp. Now H_2O does have a polarizability but little more than half that of HCN. If vapor pressures comparable to those used in the present work were employed, however, one would certainly expect to observe the H_2O lines to be broadened to almost the same extent as these HCN lines.

We wish to thank Professor H. Margenau for helpful discussion.

[7] H. Margenau, Phys. Rev. **49**, 596 (1936).

[8] H. Becker, Zeits. f. Physik **59**, 583 (1930).

Mass Spectrum Analysis

1. The Mass Spectrograph. 2. The Existence of Isobars of Adjacent Elements*

KENNETH T. BAINBRIDGE† AND EDWARD B. JORDAN,‡ *Harvard University*

(Received June 12, 1936)

(1) The simultaneous fulfillment of the conditions for high resolving power, sensitivity and dispersion have been obtained in an instrument for the investigation of isotopes. Important features of the design are the linearity of the mass scale over a broad region of the recording plate, the elimination of the troublesome effects of surface charges on the electric deflection plates, and the use of relatively wide collimating slits at small separation. The ions diverging from the second collimating slit S_2 are deflected through $\pi/\sqrt{2}$ radians, using the radial field method of electrostatic focusing introduced by Hughes and Rojansky, which produces an energy spectrum in front of the third slit S_3. Beams of ions of all m/e values comprising up to 3 percent of this energy spectrum, traversing S_3, are further deflected through a mean angle of $\pi/3$ radians by a magnetic field which focuses the ions and produces a mass spectrum on the recording plate. The mean dispersion is 5 mm for one percent mass difference, the mean radius in the electric and magnetic fields is 25.4 cm, and a resolving power $M/\Delta M$ of *ca.* 10,000 is attained in routine work. Over 140 mm on the plate, the maximum divergences from linearity are $\pm 1/7000$. (2) Mattauch and Sitte have suggested that isobars differing by one unit in atomic number are unstable or do not exist at all. To test for the existence of isobars of this class, singly and in some cases doubly ionized germanium, cadmium, indium, tin, tellurium, mercury, lead and bismuth were examined, using hydrogen free ion sources. Definite proof was obtained for the existence of three isobaric pairs $Cd^{113}In^{113}$, $In^{115}Sn^{115}$ and $Sb^{123}Te^{123}$, which apparently are stable. The isotopes Cd^{116}, Sn^{121}, Hg^{197}, Pb^{209}, which have been reported as members of isobaric pairs, cannot be present to greater than 1/8, 1/60, 1/2, 1/10, respectively, of the amounts published by Aston. The existence of Pb^{205} is also doubtful. In accordance with Beck's suggestion, developed by Bethe, and by Yukawa and Sakata, both members of these isobaric pairs could be stable for a neutrino mass $m_n > 0$. This hypothesis would necessitate modifications in the theory of the emission of β-rays. Alternatively, a difference in the nuclear spins of the members of the isobaric pairs might result in a condition of effective stability for these nuclei.

1. THE MASS SPECTROGRAPH

VARIOUS combinations of electric and magnetic fields, which act to separate out beams of ions of the same m/e values, are used for the photographic recording of mass spectra. By these methods different degrees of velocity and direction focusing are attained, depending on the ability of the instrument to focus on the recording plate ion beams which are heterogeneous in energy or which diverge from the source. No review of the subject will be undertaken here, as there is an excellent discussion and comparison of mass spectrographs of various types in a recent work by Brueche and Scherzer.[1]

In practice no one instrument has been able to attain simultaneous fulfillment of the conditions for velocity and direction focusing, together with a linear mass scale, one or another having been sacrificed to obtain high resolving power, freedom from "polarization" phenomena or other undesirable effects. The first part of this paper is a brief description of a mass spectrograph of high resolving power, high sensitivity and high dispersion which has been constructed for the study of the masses and the relative abundance of atomic species. The instrument conforms to a new design in which velocity and direction focusing have been secured to a useful extent, and at the same time the undesirable effects of surface charges on the deflecting plates which occasionally might act to change the shape and position of the lines on the recording plate, have been eliminated. An important feature of the design and one which is useful in the comparison of the masses of isotopes to the highest degree of accuracy, is the linearity of the mass scale over a broad region of the recording plate.

The second part of the paper reports the results of the analyses of certain elements, undertaken to secure experimental evidence concerning the

* Presented at the St. Louis meeting of the Am. Phys. Soc., January 2, 1936.

† Sometime Fellow of the John Simon Guggenheim Memorial Foundation. The mass spectrograph was designed during the tenure of this Fellowship.

‡ National Research Fellow.

[1] E. Brueche and O. Scherzer, *Geometrische Elektronenoptik* (J. Springer, 1934).

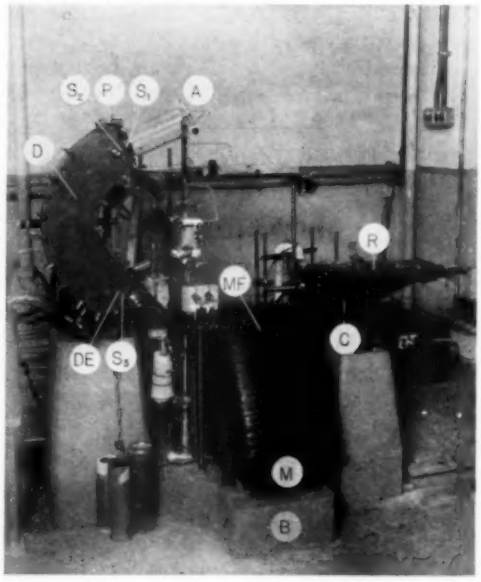

FIG. 1. The mass spectrograph. *A*, the discharge tube. S_1, adjustable steel slit under the cathode. *P*, port for adjusting S_2, the second slit. *D*, deflection chamber containing radial electrostatic field deflecting plates. *DE*, adjustable diaphragm in front of the third slit S_3. *MF*, the magnetic field. *M*, the magnet yoke. *B*, reinforced concrete base. *C*, camera chamber. *R*, cover of the plate-holder compartment.

existence of isobars of elements differing by one unit in atomic number. Mattauch[2] has suggested that isobars of this class either are unstable or do not exist at all and a similar conclusion follows from Heisenberg's discussion of nuclear stability.[3]

[2] J. Mattauch. Zeits. f. Physik **91**, 361 (1934).

The mass spectrograph

Fig. 1 is a photograph and Fig. 2 is a scale drawing of the mass spectrograph. The ions from the discharge tube *A* are collimated by slits S_1 and S_2. They are then deflected through $\pi/\sqrt{2}$ radians, using the radial field method of electrostatic focusing introduced by Hughes and Rojansky[4] to produce an energy spectrum in front of the third slit S_3. Beams of ions of all m/e values comprising up to 3 percent of this energy spectrum, diverging from the focal plane of the electrical deflector, are further deflected through a mean angle of $\pi/3$ radians by the magnetic field, *MF*, which forms a mass spectrum of focused ion beams on the recording plate.

Velocity focusing of the ions

The focusing of ions of different velocities is obtained as a result of the geometrical arrangement of the electric and magnetic deflecting fields which are so placed that the dispersion of the ions produced by one field is cancelled by the dispersion produced by the other field for a given velocity difference. Under these conditions ions of the same m/e values having all velocities within a certain range are focused on the recording plate.

[3] W. Heisenberg. Zeits. f. Physik **78**, 156 (1932).
[4] A. L. Hughes and V. Rojansky, Phys. Rev. **34**, 284 (1929).

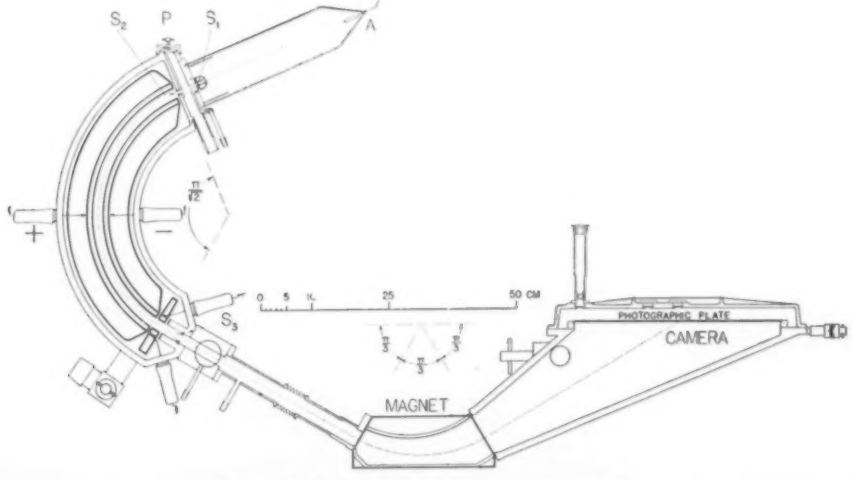

FIG. 2. Scale drawing of the mass spectrograph.

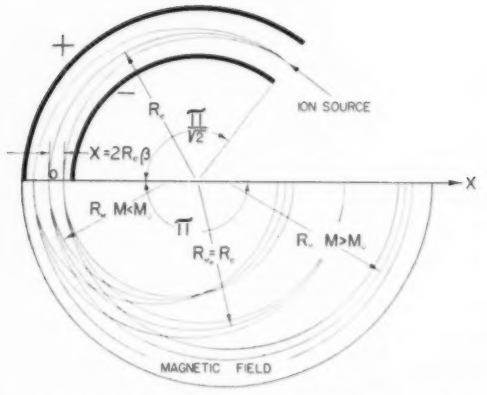

FIG. 3. $\pi/\sqrt{2}$ electric and π magnetic deflections combined. Not to scale.

The principle of the method used to secure magnetic focusing of ions which differ in velocity may be explained by considering first the elementary special case of 180° magnetic deflection applied to ions which enter the field with the dispersion in velocities produced by the Hughes and Rojansky electrostatic analyzer. For the purpose of this illustration the electric and magnetic fields are assumed to terminate at the x axis.

The expression for the displacement of ions of different velocities which have emerged from the inverse first power electrostatic field between the plates in Fig. 3 is given by $x=\Delta Re=2R_e(\beta-\beta^2)$ where $\beta=\Delta V/V_0=(V_0-V)/V_0$, V is the ion velocity and V_0 is the velocity of the ions in the central path of radius R_e. $\Delta R_e=2R_e\beta$ to a sufficient approximation. In the magnetic field $\Delta R=-R\beta$ as β is negative for $V>V_0$.

Ions of masses M greater or less than that, M_0, of the central beam for which $R_{\text{mag}}=R_{M_0}=R_e$ have radii of curvature $R_M=R_{M_0}(M/M_0)^{\frac{1}{2}}$.[5]

The condition for optimum focus of ions of mass M of different velocities is $R_{M_0}=R_e$. In this case the trajectories of all the ions in the magnetic field intercept the x axis at the same point after a deflection of 180°. The general expression for the distance from the origin to the point of intersection with the x axis is given by $x=2R_{M_0}(M/M_0)^{\frac{1}{2}}(1-\beta)+2R_e\beta$, and if $R_{M_0}=R_e$ and $M=M_0$, x is the same for all values of β which may extend over a range of 2 percent, corresponding to a 4 percent energy band in a practical apparatus.

For ions of mass differing from M_0 the breadth of focus increases on each side of the position $x=2R_{M_0}$. The width of the traces, considering velocity focusing only, is given by $4\beta R_{M_0}((M/M_0)^{\frac{1}{2}}-1)$.

In Table I the width of the traces which is due to imperfect velocity focusing is listed for line positions corresponding to masses of values from $0.6M_0$ to $1.4M_0$, somewhat more than an octave of mass. In the case of 180° magnetic focusing the closest approximation to a linear mass scale over the recording plate is secured if M_0 is at the center of the plate at a distance from the origin $x=2R_{M_0}$. Table I was compiled on this basis.

Various alternative arrangements of the electric and magnetic fields were considered to improve the velocity focusing, to obtain a closer approximation to a linear scale, to avoid the overlapping of stray fields and to obviate the necessity of using a magnet with large pole area to obtain spectra of high dispersion.[6]

The geometry of the fields shown in Figs. 2 and 4 was finally selected as a satisfactory arrangement because it allowed the conditions for velocity and angle focusing to be simultaneously satisfied. With this disposition of the fields, an electric deflection of $\pi/\sqrt{2}$ and a mean magnetic deflection of $\pi/3$ radians, a good approximation to a linear mass scale is secured over the whole of the plate. Over a region 14 cm long the maximum divergences from linearity as determined experimentally are $\pm 1/5000$ to $1/7000$ depending on the particular slit arrangements used and the position of the recording plate.

It was not found possible to obtain simple equations to express the dispersion and trace

[5] The Hughes and Rojansky focusing method produces an energy spectrum of focused ions of all m/e values after a deflection of $\pi/\sqrt{2}$ radians in the radial electric field. Any ion of mass M which followed the central path in the electric field, $R=R_e$, describes in the magnetic field a path with a radius of curvature $R_M=R_{M_0}(M/M_0)^{\frac{1}{2}}$, where $R_{M_0}=R_e$, and M_0 is the mass of the ions which are incident on the center of the recording plate. The trajectories in the electric and magnetic fields of ions of different energies can be more simply expressed as a function of $\beta=\Delta V/V_0$, the fractional deviation in velocity, than as a function of their fractional energy difference.

[6] The interesting papers of R. Herzog, and J. Mattauch and R. Herzog, Zeits. f. Physik **89**, 447, 786 (1934), in which entirely different field arrangements are discussed were not published until some months after the present design had been completed and construction of the instrument had been started in the Harvard University instrument shops.

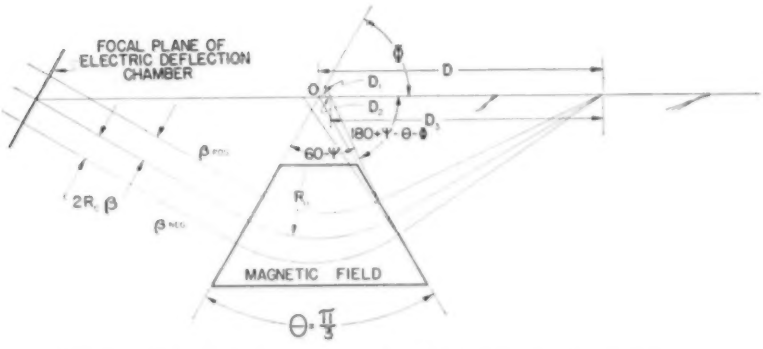

FIG. 4. $\pi/\sqrt{2}$ electric and $\pi/3$ magnetic deflections combined. Not to scale.

width to the desired accuracy. An exact expression for these quantities, however, is easily written down. Using the designations given in Fig. 4 the distance D from the origin O to the point of intersection on the recording plate has been calculated for ions of different masses using values of β equal to $+0.005$, 0, and -0.005 corresponding to a 2 percent range in energy of the focused ions.

$$D=D_1+D_2+D_3=R_0\{(M/M_0)^{\frac{1}{2}}(1-\beta)-1+2\beta\}\times\cos\Phi+\frac{R_0\{(M/M_0)^{\frac{1}{2}}(1-\beta)-1+2\beta\}\sin\Phi}{\tan(180^\circ+\psi-\theta-\Phi)}+\frac{R_0}{\cos(180^\circ+\psi-\theta-\Phi)}\left[(M/M_0)^{\frac{1}{2}}(1-\beta)-\frac{\frac{1}{2}(M/M_0)^{\frac{1}{2}}(1-\beta)-1+2\beta\}\sin\Phi}{\sin(180^\circ+\psi-\theta-\Phi)}\right] \quad (1)$$

and

$$\sin\psi=\frac{\frac{1}{2}(M/M_0)^{\frac{1}{2}}(1-\beta)-1+2\beta\}\sin\theta}{(M/M_0)^{\frac{1}{2}}(1-\beta)}. \quad (2)$$

These equations are for the general case and reduce to those already given for the restricted 180° case when the appropriate values of Φ and θ are substituted.

Table I gives the values of D when the appropriate values $\beta=\pm0.005$, $\Phi=\theta=60°$, and $M=0.6$ to $1.4M_0$ are substituted in Eqs. (1) and (2). When the degree of velocity focusing and linearity of scale attained are compared with those obtainable for 180° magnetic deflection, the immediate advantages of a magnetic deflection of less than π radians are apparent. Also, if the ions are deflected through a mean angle of only $\pi/3$ radians, the radius of curvature for a given dispersion is only one-half that for 180° focusing and a magnet of very much smaller dimensions can be used.

TABLE I. *Trace widths and line positions for 180° and 60° magnetic deflection compared for equal mass dispersion at the center of the recording plate. Energy band width 2 percent.*

		180° Magnetic Focusing		60° Magnetic Focusing			
					Position		
Mass	Position on Linear Mass Scale	Position $\beta=0$	Total Trace Width $\beta(\pm0.005)$	Total Trace Width $\pm\beta$	$V>V_0$ $\beta=-0.005$	$V=V_0$ $\beta=0$	$V<V_0$ $\beta=0.005$
$0.6M_0$	$1.2R_0$	$1.0984R_0$	$0.009R_0$	$0.0019R_0$	$1.1876R_0$	$1.1885R_0$	$1.1895R_0$
0.65	1.3	1.2249	.0078	.0012	1.2934	1.2939	1.2946
0.7	1.4	1.3466	.0065	.0008	1.3970	1.3974	1.3978
0.8	1.6	1.5777	.0042	.00026	1.6005	1.6003	1.6003
0.9	1.8	1.7947	.0021	.00006	1.8004	1.8004	1.8004
1.0	2.0	2.0000	.0000	.0007	2.0007	2.0000	2.0007
1.1	2.2	2.1952	.0019	.0004	2.2008	2.2009	2.2012
1.2	2.4	2.3818	.0038	.0012	2.4039	2.4043	2.4050
1.3	2.6	2.5607	.0056	.0023	2.6106	2.6116	2.6129
1.35	2.7	2.6476	.0064	.0028	2.7157	2.7169	2.7185
1.4	2.8	2.7329	.0073	.0038	2.8219	2.8236	2.8257

Magnetic focusing of divergent beams

The ions entering the electric deflection chamber from S_2 as a divergent beam are brought to convergence at the focal plane after a deflection through $\pi/\sqrt{2}$ radians. The width of the image of S_2 in the focal plane, considering solely the breadth produced by the divergence of the ions, is equal to $4/3\alpha^2 R_c$. α is the half-angle of divergence equal to the sum of the widths of slits S_1 and S_2 divided by twice their separation.

The ions leaving the focal plane of the first section of the spectrograph again diverge and enter the region of uniform magnetic field intensity between the pole pieces of the magnet. Barber[7] has shown that if the central beam of a divergent bundle of ions enters and leaves the field normal to the edges of the poles, the ions are brought to a focus on the line extended from the source through the center of curvature of the central beam. In the mass spectrograph one beam of ions fulfills this condition exactly, that for which $R_{M_0}=R_{\text{mag}}=R_c$. The width of the trace is $\alpha^2 R_{M_0}=2.5\times10^{-4}$ cm where $\alpha=1/360$ for slits of width $S_1=0.13$ mm and $S_2=0.1$ mm separated 4.2 cm. If the divergent ions were not focused at the recording plate the width of the trace would be 1.1 cm $=2\alpha L/\sin\nu$, where L is the path length of the ions from their point of divergence and ν is the angle between the plate and the direction of motion of the incident ions. Figs. 5, 6 and 7 illustrate spectra taken using slits of the width given above. The center of the recording plate is tangent to the locus of the foci of ions of mass greater and less than M_0, the locus lying below the plate.

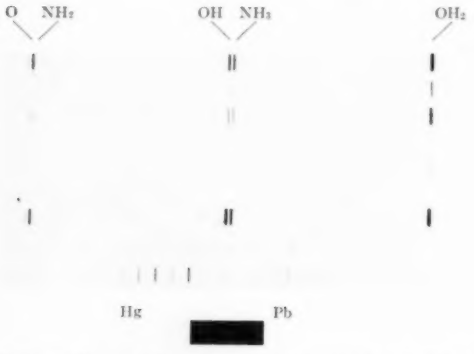

FIG. 5. Natural size. Spectra of matched OH−NH₂ doublets and the isotopes of mercury and lead, $S_1=0.13$ mm, $S_2=0.1$ mm, $S_3=5$ mm. The black rectangle represents the width of a single trace for the same slit dimensions but without magnetic refocusing of divergent beams of ions.

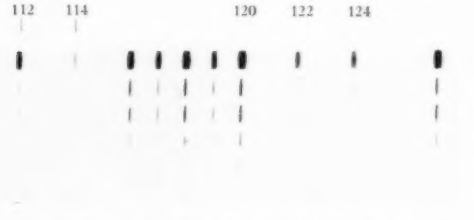

FIG. 6. Natural size. Doubly ionized tin. The magnetic field changed while the top spectrum was being photographed giving the effect of double width lines. On the original plate Sn^{115} appears on the first four spectra but the reported Sn^{121} is not present at all.

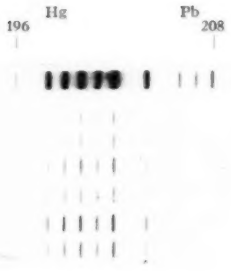

FIG. 7. Natural size. An overexposed spectrum of mercury, and lead, showing the mercury 196 line and comparison spectra from the same plate. An abundance range of 60,000/1 can be recorded and measured.

Good focusing of divergent ion beams is secured over the center of the plate for the high intensity spectra (wide slits close together) used in the analysis of the isotopic constitution of elements and in the search for rare isotopes, Figs. 5, 6, 7. The magnitude of α in the present instrument may appear small, but it is about 5 to 30 times greater than that which has been used in the earlier types of precision photorecording mass spectrographs not utilizing angle focusing.[8, 9, 10] The slit widths are 2 to 5 times greater and the distance between slits has been reduced by one-third to one-tenth. The resolving power $M/\Delta M$ achieved for wide slits is between 1500 and 2000 representing an increase of 3 to 10 times.

[7] N. F. Barber, Proc. Leeds Phil. Soc. **2**, 427 (1933); W. E. Stephens and A. L. Hughes, Phys. Rev. **45**, 123 (1934); W. E. Stephens, Phys. Rev. **45**, 513 (1934).

[8] J. Costa, Ann. d. Physik **4**, 425 (1925).
[9] F. W. Aston, Proc. Roy. Soc. **A115**, 487 (1927).
[10] K. T. Bainbridge, Phys. Rev. **40**, 132 (1932).

FIG. 8. $O-CH_4$, $D^2-H^1_2$ doublets, and D^2H lines, natural size, for slit widths $S_1=0.06$, $S_2=0.02$, $S_3=1.25$ mm.

As the trace width for magnetic focusing varies as α^2 a reduction of the collimating slit width to values comparable to past usage aids in making the attainment of exceptionally high resolving power entirely practicable.[11]

Resolving power

The factor responsible for a large part of the width of a trace at the recording plate is the non-homogeneity in energy of the ions which pass through each point along the focal plane of the electric deflection chamber. In the focal plane an energy spectrum of ions of all m/e values is formed of overlapping images of the slit S_2. The width of an image $=S_2+4/3\alpha^2R_e=S_2$, as the second term is negligible in comparison to the slit width. At any point in the focal plane the maximum spread in the velocity of ions of all m/e values passing through the same point is given in terms of $\beta=(V_0-V)/V_0=S_2/2R_e$. When the values of S_2 and R_e are substituted, 0.1 mm and 25.4 cm respectively, the maximum value of β is 1/5000. Consequently ions leaving a single point along the focal plane have all radii of curvature between R and $R(1+\beta)$, so the maximum resolving power $R/\Delta R=M/\Delta M=V/\Delta V=5000$ under the geometrical conditions defined above. When the trace width assignable to imperfect velocity and direction focusing is considered,

[11] The resolving power is defined as the ratio $M/\Delta M$ for *complete* separation of two lines and so is more stringent than the optical definition. A standard value for the density of the traces on Q plates should be included in the definition. The value 0.3 is suggested.

FIG. 9. A portion of Fig. 8 enlarged 5×. $O-CH_4$ and $D^2-H^1_2$ doublets.

FIG. 10. Some $D^2-H^1_2$ doublets enlarged 5×. $S_1=0.03$, $S_2=0.017$, $S_3=1.0$ mm. Resolving power 10,000 to 15,000.

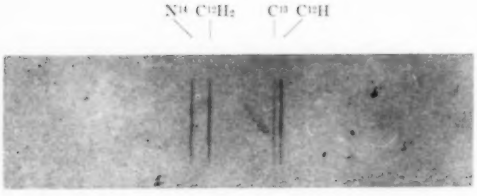

FIG. 11. $N-CH_2$, $C^{13}-C^{12}H$, doublets. Enlarged 5×.

FIG. 12. $CO-N_2$ doublets taken without a diaphragm in front of the recording plate. Enlarged 5×. The ions differ in mass by 1/2500. $S_1=0.04$ mm, $S_2=0.017$ mm, $S_3=1$ mm.

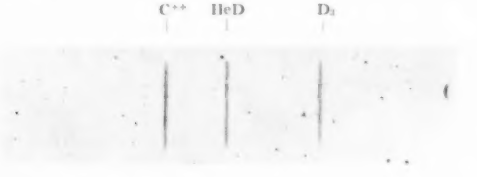

FIG. 13. $C^{++}-HeD^2-D^2_2$ matched triplet. Enlarged 5×.

the maximum realizable resolving power = 1850 for values $S_1=0.13$ mm, $S_2=0.1$ mm, $S_3=5$ mm. The spectra reproduced in Figs. 5, 6, 7 show that the resolving power deduced from simple theoretical considerations has been attained in the completed instrument. Experimentally it was found that for the optimum focus the photographic plate must be approximately 0.68 cm above the plane indicated by theory. A practical advantage of great value results when the plate is in this position as experimentally one finds that the traces are symmetrical and that the position of the traces is nearly independent of the density. Both of these features are an aid to accurate mass measurements, the primary aim in the construction of this mass spectrograph.

Once the spectrograph had been satisfactorily aligned and adjusted using wide slits and the analysis of a series of elements had been secured,[12] experiments were undertaken with the object of obtaining a resolving power greater than 10,000. The spectra shown in Figs. 8, 9 were taken with $S_1 \leq 0.06$, $S_2=0.02$, $S_3=1.25$ mm yielding a resolving power of 6000 to 8000. The $D^2-H_2^1$ doublets which had never been resolved completely before are well separated even at high trace densities. The duration of the exposures varied from 1 to 5 seconds for the hydrogen spectra. The oxygen-methane doublets are 20 second exposures.

The final slit adjustments now used for routine mass measurements are $S_1=0.03$, $S_2=0.017$, $S_3=1.0$ mm, permitting a resolving power of 10,000 to 15,000 and exposure times of from 2 or 3 seconds for the hydrogen deuterium doublet and 60–180 seconds for the $C^{13}-C^{12}H^1$ doublet. The rare carbon isotope, for several spectra, has been matched in intensity with $C^{12}H^1$ by running a discharge in CO with a trace of methane. Enlarged spectra of various doublets are shown in Figs. 10, 11, 12, 13. Fig. 14 is a densitometer record of a $D^2-H_2^1$ doublet. The mass separation of $D^2-H_2^1$ is approximately equal to $2\frac{1}{2}$ times the electronic mass and the width of the traces is only 0.00015 mass unit.

The ion source

The ions are produced in the low pressure discharge tube *A* which is usually run at 20,000 volts. The power for the discharge tube is furnished by a full wave rectifier set, generally operated without smoothing condensers. On those occasions when a filtered source of high potential is desired two 0.5 mfd 25 kv condensers in series may be connected. Steadier accelerating potentials for special work are available from the laboratory 100 kv storage battery.

Gas is admitted to the discharge tube under the cathode as shown in Fig. 2. The iron base of the tube supports an aluminum cathode of the Thomson type. This base has been so machined that a spherical discharge tube with a narrow neck which just clears the cathode may also be used.

[12] Described in the second part of this paper.

Ions of metallic elements are obtained in general by introducing a quantity of the element to be investigated, or a halide salt, into the cathode and running a discharge in neon. Under these conditions a copious supply of singly and doubly ionized metallic ions is formed.[13] In the case of tellurium and indium small beads of these elements were placed in a circular array of holes drilled in an aluminum cathode. Iodides of germanium and tin were used in the same type of cathode. A bismuth cathode was used directly, and lead and cadmium cathodes containing their respective iodides furnished ions of these metals. Zinc, selenium, beryllium, aluminum, and iron have yielded ions by the same general method.[14, 15] Shielding the side of the discharge tube with a glass cylinder as indicated in Fig. 2 is advantageous in preventing the formation of arcs between the cathode and the tube walls.

Experience with another type of mass spectrograph showed that a discharge operated at approximately 15 kilovolts gave a nice balance between high ion current density and the high energy useful in securing satisfactory photographic records.[16] At the same time a discharge at 10–20 kilovolts can be operated at pressures which permit a high concentration of the vapor under investigation in the tube, with a low partial pressure of undesirable contaminating gases.

In the low pressure discharge run at 15–20,000 volts used with the mass spectrograph, the cathode fall space extends for 15 to 25 cm and the positive column is absent or localized just at the anode. The position of the metal or salt which is used to furnish ions is not critical. Substances of high vapor pressure ($P > 10^{-3}$ mm at 200°C) may be placed on the iron base of the discharge tube, as has been done successfully for selenium, beryllium chloride, and the bromide and iodide of cadmium. Tin iodide works well if it is evaporated into the discharge from a side tube. The ions actually recorded on the plate have originated not in the immediate region of the cathode but in the vicinity of the negative glow and along the axis of the tube where the electron density is greatest.

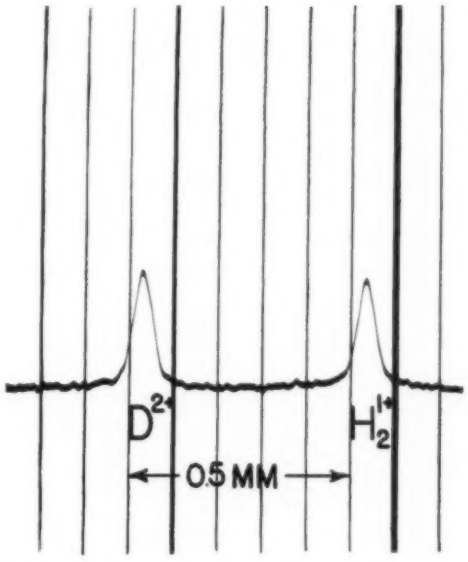

FIG. 14. A matched $D^2 - H^1_2$ doublet. Microphotometer slit width 0.025–0.030 mm.

The addition of neon serves to stabilize the discharge and to produce a controlled evaporation of the substance struck by the neon ions. The energy of the incident ions has been sufficient to melt a bismuth cathode and a sheet of cerium placed in poor thermal contact with an aluminum cathode. After a zinc or cadmium cathode has been used for some time the crystalline structure of the metals is brought out as if local evaporation and sputtering had etched the surface in the area of maximum intensity of the incident ions.

The dissociation and ionization of the heterogeneous vapor of the substance evaporated from the cathode probably result from the action of the high speed electrons which have their maximum density along the axis of the tube. The intensity of the central electron beam is so great that unless special care is taken the wall of the pyrex discharge tube may be punctured by local overheating. (A hole one or two millimeters in diameter can be neatly drilled in the end wall by the electrons.) As the ions proceed towards the cathode against this stream of electrons, it is probable that the multiply charged ions are formed in greatest abundance along the axis of

[13] K. T. Bainbridge, Phys. Rev. **39**, 847, 1021 (1932).
[14] K. T. Bainbridge, Phys. Rev. **43**, 1056 (1933).
[15] H. Lukanow and W. Schutze, Zeits. f. Physik **82**, 610 (1933).
[16] K. T. Bainbridge, J. Frank. Inst. **215**, 509 (1933).

the tube, although some may result from collisions of the second kind with neon ions.

The collimating slits

The ions from the discharge tube are collimated by the slits S_1 and S_2 and enter the chamber D, Fig. 1. The slits, which are 0.1 to 0.15 mm in width for work at high intensities, are separated 4.2 cm. By this arrangement they subtend a larger solid angle than is usual in the collimating system of a photo-recording mass spectrograph, with a corresponding gain in the sensitivity of the instrument.

The first slit, S_1 is formed by a pair of adjustable iron jaws placed in a slot in the discharge tube base directly under the aluminum cathode. S_2 is made of strips of hardened steel screwed to a supporting brass cylinder. The adjustment or removal of the second slit is accomplished through the port, P, Figs. 1 and 2.

The region between the slits is evacuated to isolate the low pressure deflection chamber from the higher pressure region in the discharge tube.

The energy selector

The diverging beam of ions, heterogeneous in energy and m/e values, leaves S_2 and enters the region between two accurately figured cast bronze deflecting plates. The 1.9 cm separation of the plates permits ions differing by 4 percent in energy, diverging in an angle of 1/50, to be focused in front of S_3, after deflection through $\pi/\sqrt{2}$ radians. This wide separation also helps to eliminate the effects of possible surface charges on the plates.

The radius of the central ion path is 25.4 cm. The magnitude of the deflecting voltage V_d, is given in terms of the accelerating voltage V_a by the equation $V_d = 0.16 V_a$, as $mv^2/R = 2V_a e/R = V_d e/R \log b/a$ and the radii of the deflecting plates a and b are 24.45 cm and 26.35 cm respectively. Ions of 15,000 electron-volts energy are deflected by the required amount in the energy selector when the circular plates are connected 1200 volts above and below ground. The auxiliary deflecting plates illustrated in Fig. 2 are used to secure small angle adjustments of the deflected ion beams. It was found experimentally that these plates had to be at three-fourths of the potential of the main deflecting plates in order to have the central beam of ions proceed exactly along the center of the tube connecting the energy selector and the magnet.

Fifty-four large capacity 45-volt radio batteries furnish the potential for the deflecting plates.

The slit S_3 is a brass plate with a 10 mm slot cut in it. In practice 7.5 mm was found to be the maximum useful width of S_3, since any increase beyond 7.5 mm adds little to the intensity and brings about an objectionable decrease in the resolving power.[17] For adjusting S_3, two tapered ground joints which hold thin brass flags, Fig. 2, either of which may be turned to cover the slit completely, have been added since the photograph Fig. 1 was taken. By adjusting both of the flags it is possible without breaking the vacuum to select ions of a band of energies of any width up to the maximum spread of 4 percent incident on S_3.

Since the photograph Fig. 1 was taken a window has been provided at DE, Fig. 1, so that S_3 may be inspected visually. The plate in the vicinity of the slit has been coated with willemite, which fluoresces brightly under the impact of the incident positive ions and provides a convenient check on the proper adjustment of the discharge tube.

Freedom from surface charge effects

A definite practical advantage results from the use of deflector plates which are relatively far apart and are maintained at high potentials compared to those of the deflecting plates in other types of mass spectrographs.

Under intense ion bombardment surface films attaining a potential of 1 volt on the deflecting plates have been reported. With small separations the charging of surface films on these plates acts to distort the shape and alter the positions of the traces of the ion beams which are incident on the recording plate.[18, 19] The presence of such effects not only decreases the theoretically attainable resolving power of an instrument, but also makes it difficult to compare accurately the relative positions of the lines. It was partly to overcome these difficulties that the present instrument was designed with deflector plates separated by 1.9

[17] The cadmium spectra, one of which was used for Fig. 16, were taken with $S_1 = S_2 = 0.25$ mm, $S_3 = 10$ mm.

[18] F. W. Aston, Proc. Roy. Soc. **A115**, 495 (1927).

[19] A. J. Dempster, Proc. Am. Phil. Soc. **75**, 764 (1935).

cm, to be maintained at a high difference of potential.

With the resolving power adjusted to 2000, observations were made through a 10 power microscope of the fluorescence produced by the ion beams, H, H_2, CH_4, on a willemite screen placed in the same position as the usual recording plate. Under these conditions fluctuations of one part in 2000 in the positions of the lines, caused by changes in the magnetic or electric fields, would have appeared in the microscope as a 2.5 mm shift of the ion beam. No motion of the ion beam could be detected. Spectra taken under different conditions with varying lengths of exposure at resolving powers from 400 to 12,000 show definite sharp edges to the traces.

The potential of semiconducting surface films can be lowered if the charging current per unit area is reduced. One reason for the freedom from surface charges on the deflector plates of this mass spectrograph is that with the large separation and area of the plates, even though the beam issuing from S_2 is very intense, the density of the ions striking the deflector plates is low.

The excellent vacuum conditions in the spectrograph also hinder the formation of surface films on the deflector plates. The gas pressure during a series of exposures is 10^{-6} mm, as measured by an ionization gauge. The sharpness of the lines formed on the recording plate by ions which have traveled more than a meter and a half through the mass spectrograph demonstrates the high vacuum maintained for routine work.

If 0.1 volt surface potentials should appear on the plates a shift in the positions of the recorded lines of only one part in 25,000 would result. No distortion of the shape of the lines can occur when the slits S_1, S_2 and S_3 are adjusted for high resolving power, as the field distribution in the central region between the deflector plates remains uniform even if the area struck by ions incident on the plates becomes charged.

The magnet

The magnet is constructed of two quadrants and a straight section of Armco iron which after machining were properly annealed to insure high permeability at high flux densities. The magnet is wound with approximately 5000 turns of number 12 B. & S. D.C.C. enameled wire, the resistance of the winding being 24 ohms. The heaviest ions examined are brought to the center of the plate with an expenditure of only six watts in the coils. Four 90 ampere-hour six volt automobile batteries connected in series-parallel supply the exciting current for the magnet.

The pole pieces are separated by 0.32 cm brass strips shown in Fig. 2. The top area of the pole faces is open to a depth of 3.5 cm for convenience in measuring the field with a search coil and Grassot fluxmeter.

Allowance for the deflection of the ions in the stray field of the magnet was made from calculations of the integrated effect of the field.[20] The edges of the poles were cut back approximately $1\frac{1}{2}$ gap widths. A still higher order correction can be obtained by a small angular rotation of the electric deflection chamber and the recording plate, but the excellent performance of the mass spectrograph does not require it at this time.

The recording plates and camera

All of the mass spectra secured have been recorded on "*Q*" plates which were developed by the Ilford Laboratories.[21, 22] Two types of the *Q* emulsion have been used.[23] There is available one of exceptionally high sensitivity to positive rays which is particularly suited for the detection of isotopes of low abundance and for the photometry of mass spectra. Isotopes with an abundance ratio of 60,000/1 can be recorded without any indication of solarization of the denser trace. Fig. 15 shows a graph of the density-abundance

[20] The senior author is indebted to Dr. L. H. Rumbaugh of the Bartol Research Foundation for helpful suggestions concerning the stray magnetic field correction.

[21] F. W. Aston, Proc. Roy. Soc. **A132**, 487 (1931).

[22] Ilford Ltd., J. Sci. Inst. **12**, 333 (1935).

[23] An investigation was made of the sensitivity of various plates by means of a parabola apparatus (J. J. Thomson, Phil. Mag. **13**, 561 (1907); R. Conrad, Physik. Zeits. **31**, 888 (1930)) in which five plates mounted on a hexagon could be brought rapidly into the correct position for exposure so that each plate might receive the same total exposure and fluctuations in the discharge would cancel out. Exposures were for twenty periods of 15 seconds each taken in rotation. Plates sensitized to the infrared by dyes did not respond to positive ions. The Eastman Kodak Process and ultraviolet sensitized plates were more sensitive than the Paget halftone plates previously favored for recording positive rays. None of these plates, however, could compare with the *Q* plates in sensitivity. Samples of these plates have been tested in the far ultraviolet at this laboratory by Dr. H. M. O'Bryan and at the M. I. T. spectroscopy laboratory by Professor J. C. Boyce. The plates are sensitive over the whole of the region tested from 140A to 3000A.

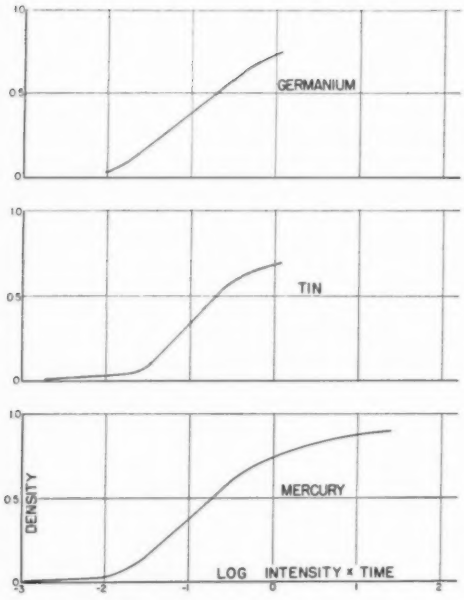

FIG. 15. Characteristic curves of *Q* plates for germanium, tin and mercury ions.

characteristic of the emulsion for 20,000 electron volt tin ions incident on the plate, and 10,000 electron volt germanium and mercury ions. With Paget halftone plates the density at the peak of the linear position of the curve seldom exceeds the value 0.2. With Schumann plates values up to 3.0 are easily attained but the slope of the density intensity graph is very steep.

An exceptionally fine grain *Q* emulsion of good sensitivity is also available which is particularly suited for the mass spectra including close doublets. Figs. 8, 9, 10, 11, are reproductions of spectra taken with this type of emulsion and Fig. 14 is a densitometer record of a $D^2-H_2^1$ doublet. The $CO-N_2$ doublets, Fig. 12, were recorded on the more sensitive larger grained *Q* plates.

The *Q* plates are particularly pleasing to work with because of their uniformity, and they are free from chemical fog even when developed two or three times the normal period in a hydroquinone-caustic soda developer (E. K. Co., D–9).

In the mass spectrograph the recording plate, 2 inches wide and 16 inches long, is supported on a cast bronze carriage. Contact with a lapped plane surface is made over the entire length of the ends and edges of the plate, which is held in position by eight springs. The carriage may be moved parallel to itself by a rack and pinion arrangement, permitting twelve exposures of spectral lines about 3 mm in height. The position of the plate relative to the mass spectrograph is marked by projecting the reduced image of a slit on the plate as illustrated in Fig. 2. The fiducial marker returns to the same position after a new plate is inserted in the spectrograph, as the cover supporting it is accurately aligned by two hardened steel pins.

The large brass stopcocks illustrated in Fig. 2 permit plates to be changed without letting air into the electric deflection chamber and discharge tube or into the mercury diffusion pump which evacuates the camera chamber.

2. The Existence of Isobars of Adjacent Elements

Of the 250 known nuclear species[24] there are some of the same mass number but different atomic number which are called isobars.[25]

The members of one class of these isobaric pairs differ by two units in nuclear charge. Heisenberg,[26] Gamow,[27] and Goeppert-Mayer[28] have presented theoretical arguments which support the experimentally observed fact that both members of some 40 of these pairs are stable or, in other words, that no capture or loss of two electrons occurs which would reduce the pairs to a single isotope.

There is a second important class of isobars, those pairs of the same mass number which differ by one unit in nuclear charge. Approximately 16 pairs of this class have been reported, some of which have one member which is definitely known to be unstable. For example K^{40} and Rb^{87} which are paired with Ca^{40} and Sr^{87} respectively, transmute into the latter elements by the emission of beta-rays.[29] One of the isotopes of

[24] O. Hahn, Ber. d. D. Chem. Ges. **A69**, 5 (1936).

[25] The term *isobar* originally suggested by Stewart (Phil. Mag. **36**, 326 (1918)) was altered to *isobare* to avoid confusion with the metereological term!

[26] W. Heisenberg, Zeits. f. Physik **78**, 156 (1932) and Scott Lectures, Cambridge Univ. 1934.

[27] G. Gamow, 1934 Int. Conf. Physics, **1**, 60 (1935).

[28] M. Goeppert-Mayer, Phys. Rev. **48**, 512 (1935).

[29] G. von Hevesy and W. Dullenkopf, Zeits. f. anorg. Chemie **221**, 167 (1934); G. P. Baxter and C. M. Alter,

neodymium may also belong in this category.[30] Mattauch[31] and Sitte[32] concluded from a study of the known atomic species that for adjacent elements there are no isobaric pairs of which both members are stable. This conclusion is in agreement with the results of Heisenberg's discussion of the stability of nuclei with respect to beta-ray emission.

The work described below was undertaken to determine experimentally whether stable isobaric pairs do exist for elements differing by one unit in atomic number. The type of ion-source previously described permitted the use of hydrogen-free compounds of the elements under investigation. In this way successful analyses were made of elements which previously had been introduced into the discharge tube only in chemical combination with methyl and ethyl radicals.

The elimination of hydrides in the discharge tube does away with two types of error in isotopic analysis. The addition of hydrogen to an isotope results in another line in the mass spectrum which may be mistaken for an isotope, and the measurement of the relative abundance of actual isotopes may be invalidated by superimposed hydrides.

Isotopic analysis

The first element investigated was tellurium ($z=52$). First and second order spectra gave further proof of the existence of Te^{123} which is isobaric with $Sb^{123}(z=51)$.[33] No Te^{127}, isobaric with $I^{127}(z=53)$, was present to more than 0.8 percent of the total. Tellurium was analyzed before any iodides had been introduced into the discharge tube so that a test could be made for the presence of Te^{127} without the danger of confusion with I^{127}.[33]

Indium ($z=49$) gave two isotopes of mass number 115 and 113 in agreement with the results of Wehrli and Miescher,[34] and Aston.[35] In^{115} is a member of the isobaric triplet reported by Aston[18, 36, 37] in which he includes the isotopes $_{48}Cd^{115}$ and $_{50}Sn^{115}$. In^{113} is isobaric with Cd^{113} which is one of the more abundant isotopes of this element.

Cadmium was analyzed to test the reality of the $In^{115}-Cd^{115}$ and $In^{113}-Cd^{113}$ isobaric pairs. A microphotometer record of cadmium is shown in Fig. 16 where the black line above the figure 115 illustrates the amount of Cd^{115} reported by Aston.[36] No evidence was found for its existence to $\frac{1}{8}$ of this amount. Dempster[18] has also reported an analysis of cadmium in which Cd^{115} does not appear, without giving an upper limit for the abundance. Cd^{118}, found from band spectrum analysis[38] to be more abundant than Cd^{106} and Cd^{108}, does not appear.

Tin was examined for the purpose of investigating the isobaric pairs $_{50}Sn^{115}-_{49}In^{115}$ and $_{50}Sn^{121}-_{51}Sb^{121}$. Fig. 6 shows a series of four spectra of doubly ionized tin which with some of singly ionized tin gave proof of the existence of Sn^{115}, which appeared on all of the spectra, but failed to show Sn^{121}, although from the photometric records of these spectra 1/60 of the amount reported by Aston[18, 36] would be easily detectable. The appearance of a line of mass 121 which accompanied the tin isotopes in Aston's spectra is difficult to explain. If this line were a hydride of the most abundant isotope Sn^{120} it would indicate 11 percent hydride contamination and the corresponding hydrides of Sn^{122} and Sn^{124} should have been easily detected as their abundance would exceed that of the real isotope Sn^{115}. If the line of mass 121 was not a hydride but a fortuitously occurring molecular ion there arises the difficulty of accounting for the consistency in the measurements of its apparent abundance on successive spectra taken under different conditions.

Mercury was investigated for the purpose of examining Hg^{197} and Hg^{203} to which values have been assigned by their discoverer[39] of *ca.* 0.01 and 0.006 percent abundance. $_{80}Hg^{197}$ would be isobaric with $_{79}Au^{197}$ and $_{80}Hg^{203}$ forms a pair

J. Am. Chem. Soc. **55**, 3270 (1933); O. Klemperer, Proc. Roy. Soc. **A148**, 638 (1935); A. O. Nier, Phys. Rev. **48**, 283 (1935).

[30] W. F. Libby, Phys. Rev. **45**, 845 (1934).

[31] J. Mattauch, Zeits. f. Physik **91**, 361 (1934).

[32] K. Sitte, Zeits. f. Physik **96**, 512 (1935).

[33] K. T. Bainbridge, Phys. Rev. **39**, 1021 (1932). Te^{127} was previously reported as a doubtful isotope.

[34] M. Wehrli, Naturwiss. **22**, 289 (1934); M. Wehrli and E. Miescher, Helv. Phys. Acta **7**, 298 (1934).

[35] F. W. Aston, Proc. Roy. Soc. **A149**, 396 (1935).

[36] F. W. Aston, Proc. Roy. Soc. **A130**, 302 (1931).

[37] F. W. Aston, Phil. Mag. **49**, 1191 (1925).

[38] E. Svensson, Nature **131**, 28 (1933); G. Stenvinkel and E. Svensson, Nature **135**, 955 (1935).

[39] F. W. Aston, Nature **130**, 847 (1932).

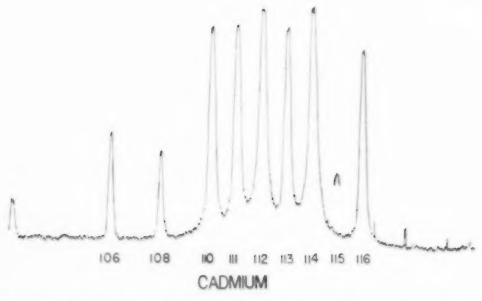

FIG. 16. Densitometer record of a spectrum of cadmium taken with $S_1=0.25$ mm, $S_2=0.25$ mm, $S_3=10$ mm.

with the $_{81}Tl^{203}$ isotope.[40, 41, 42] No Hg^{197} was found to $\frac{1}{2}$ of the abundance reported although this amount could easily have been detected. The presence of the line of mass 197 previously reported cannot be attributed to a hydride of Hg^{196} as the low abundance of this isotope, 0.1 percent, would require a 10 percent hydride effect which was not apparent for the Hg^{202} or Hg^{204} isotopes. Sitte's[32] suggestion that Hg^{201} does not exist has absolutely no foundation in fact. A definite answer concerning Hg^{203} is not possible at this time as second order spectra of mercury of sufficient intensity to record a line of abundance 1/20,000 or less were not taken and in the first order a hydride $Hg^{202}H^1$, present to even 1/5000 of the abundance of Hg^{202}, invalidates any attempts to examine Hg^{203}. Hydrides of mercury do form and appear to be dependent more on the concentration of water vapor in the discharge tube than upon the partial pressure of any hydrogen which may be present. Fig. 17 shows a series of four spectra of mercury taken with a new discharge tube in which water vapor was freely given off from the glass walls when the tube was first used. The decrease in the intensity of the hydride lines at 197, 203 and 205 corresponding to lower water vapor concentration in the discharge is apparent for successive spectra. The addition of molecular hydrogen directly to a discharge in mercury vapor does not produce hydrides of the same high intensity.

In addition to the most abundant isotopes of lead Pb^{206}, Pb^{207}, and Pb^{208} found by mass

[40] A. J. Dempster, Nature **136**, 65 (1935).
[41] S. Imanishi, Inst. Phys. and Chem. Res., Tokyo, Sci. Papers **28**, 129 (1935).
[42] H. Schüler and J. E. Keyston, Naturwiss. **19**, 320 (1931).

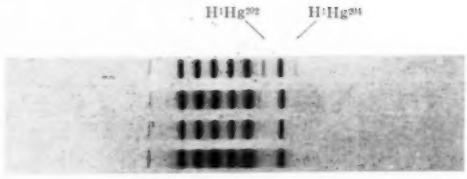

FIG. 17. Spectra of mercury showing hydrides of Hg^{202} and Hg^{204}. Successive spectra were taken with decreasing amounts of water vapor in the discharge tube.

spectrum analysis,[43] and Pb^{204} from work on hyperfine structure,[44] Aston[45] has reported small amounts of Pb^{203}, Pb^{205}, Pb^{209} and Pb^{210}. $_{82}Pb^{209}$ which is isobaric with $_{83}Bi^{209}$ is the most abundant of these new isotopes and was reported present to 0.85 percent. No line of mass 209 appeared on our spectra, although 1/10 of the abundance previously reported could easily have been detected. Fig. 7 shows one of the spectra of lead, and another taken with phosphine in the discharge tube is shown in Fig. 5. Aston's figures for the abundance of Pb^{205} and Pb^{209} were obtained from spectra definitely contaminated by lead hydride which by his measurement was present to 2.3 percent. As we could find no line of mass 209 our results indicate that the actual abundance of lead hydride was probably 4 percent (an increase of 1.7 percent) and the lines of mass 205 and 209 present to 0.02 of 204 and 0.017 of 208 on Aston's spectra were hydrides of Pb^{204} and Pb^{208}.

Bismuth was analyzed and appears to consist of a single isotope 209 with no other present to more than 2 percent. This result is in agreement with the value for the chemical atomic weight.

The superior qualities of *Q* plates for photometric work made it advisable to repeat the examination of germanium which had been made with another instrument using Schumann plates. The new spectra confirmed the previous results,[46] showing five isotopes 70, 72, 73, 74 and 76.

Photometric measurements

Upper limits were set for the abundance of the rare or non-existent isobars by photometric analysis of the mass spectra.

[43] F. W. Aston, Nature **120**, 224 (1927).
[44] H. Schüler and E. G. Jones, Naturwiss. **20**, 171 (1932). Zeits. f. Physik **75**, 563 (1932).
[45] F. W. Aston, Proc. Roy. Soc. **A140**, 535 (1933). Nature **129**, 649 (1932).
[46] K. T. Bainbridge, Phys. Rev. **43**, 1056 (1933); J. Frank. Inst. **215**, 509 (1933).

The plates were first calibrated by making a series of exposures of different duration while the discharge tube conditions were maintained as constant as possible, and the plate calibration secured in this way was checked against Aston's photometric measurements of the relative abundance of the definitely attested isotopes of the elements investigated. The agreement was satisfactory for the purpose.

The density-log abundance curve was then extended as far as possible taking care that for the longer exposures the density of the traces of the low abundance isotopes should be at least as great as the density of the traces secured at shorter exposures for the isotopes of higher abundance. In a series of exposures of decreasing duration finally there is a point where only a fraction of the isotopes are recorded, the less abundant ones failing to appear against the background. From the photometric curve and the relative abundance of the isotopes determined initially by the method of exposures of different duration, a limit may be found in this way for the minimum detectable amount of an isotope.

The upper limits given in this report for the abundance of apparently nonexistent isotopes were *three times* the "minimum detectable amount" as found from the calibration curves and photometric analyses of the most intense spectra of the elements in the appropriate region for Sn^{121}, Pb^{209} and other isobars under investigation. The upper limits published are considered amounts which could be detected with certainty were the isobars present to these values.

Discussion of results

Six isotopes were found definitely to constitute isobaric pairs: $Cd^{113}In^{113}$, $In^{115}Sn^{115}$, and $Te^{123}Sb^{123}$. The apparent stability of isobars of this class[47] may be accounted for on the neutrino hypothesis introduced by Pauli and Fermi,[48] if the neutrino mass μ is greater than zero as Beck and Bethe have suggested.[49, 50] Yukawa and Sakata have developed a general theory of the stability of adjacent isobars of atomic numbers z and $z-1$.[51] If the difference in the proper energy ΔW of the isobars, $(M_z-M_{z-1})c^2$, is larger than $(m_\beta+\mu)c^2$ the emission of a positron can take place from the nucleus of charge z. If ΔW is smaller than $-(m_\beta+\mu)c^2$ then the isobar $z-1$ can disintegrate with the emission of an electron. In the region of ΔW between $+(m_\beta+\mu)c^2$ and $-(m_\beta+\mu)c^2$, both nuclei could be stable were it not that the isobar of higher atomic number can change by capture of a K electron if ΔW is larger than $-m_\beta c^2(1-\alpha^2z^2)^{\frac{1}{2}}+\mu c^2$, where α is the fine structure constant. The condition for stability is that ΔW must be less than $-(m_\beta+\mu)c^2$ and greater than $-(m_\beta-\mu)c^2$, considering the energy of orbital electrons as simply $m_\beta c^2$. This condition can be satisfied if the mass of the neutrino is greater than zero. In addition ΔW should be small, which is not impossible as the isotopic weight defect curve has a minimum in the region $z=50$,[52] and the masses of isobars could be nearly equal.

Assuming zero neutrino mass, Yukawa and Sakata have calculated the probability of occurrence of the three modes of transmutation for different values of z and of ΔW, for $\Delta W \gtrless +m_\beta c^2$ or $\lessgtr -(1-\alpha^2z^2)^{\frac{1}{2}}m_\beta c^2$. The values obtained for the mean lifetimes of the nuclei, assuming the same spin values for the isobars of a pair, are extraordinarily short, of the order of several hours to a few days for elements in the region $z=50$. But if the members of the isobaric pairs have different spins in every case, the result is a condition of practical stability for the isobaric nuclear species of a pair. It is significant in this connection that there are large variations in spin magnitudes in the region $z=50$,[53] and that the magnetic moment is negative for the odd mass number isotopes Cd^{111}, Cd^{113}, Sn^{117}, Sn^{119}. No measurements have been made of the spins of both members of an isobaric pair of the class considered, owing to the low abundance of Sn^{115}

[47] Libby, Phys. Rev. **46**, 196 (1934), reports that tin is not β radioactive. Mattauch, reference 2, refers to some unpublished work of G. Kirsch, Rieder and Kara-Michailowa in which antimony failed to show any β activity. Weak α radioactivity from Te has been looked for by Kirsch (ibid.), and indium was examined by J. Schintlmeister, Akad. Wiss. Wien Ber. **144**, 475 (1935), but it is not known if these experiments could have detected a weak β-radiation. We have compared the activity of indium with that of lead free tin by means of a Geiger-Müller screen counter. There is no indication of any radiation from indium.

[48] E. Fermi, Zeits. f. Physik **88**, 161 (1934).

[49] G. Beck, Zeits. f. Physik **91**, 370 (1934); Phys. Rev. **47**, 202 (1935).

[50] H. Bethe, Rev. Mod. Phys. **8**, 198 (1936).

[51] H. Yukawa and S. Sakata, Proc. Phys. Math. Soc. Japan, **17**, 467 (1935).

[52] F. W. Aston, *Mass Spectra and Isotopes*, p. 167.

[53] S. Tolansky, Proc. Roy. Soc. **A144**, 574 (1934).

and Te^{123}. It is hoped that the examination of In^{113} may be possible as this isotope is present to approximately 5 percent of In^{115} and so is a nucleus more amenable to analysis than Sn^{115} or Te^{123}.

The construction of the mass spectrograph was made possible by a grant to Professor Theodore Lyman and the senior author from the Milton Fund. The authors take great pleasure in acknowledging the interest and encouragement of Professor Lyman, the assistance of Professors H. R. Mimno and J. C. Street, the suggestions and aid of Mr. David Mann, who was responsible for the construction of the instrument, and Mr. Leighton's assistance with the glass parts.

We are indebted to Professor H. Bethe for valuable discussions and to Professor W. A. Noyes, Jr. and Dr. E. A. Flood of Brown University, to Professor A. V. Grosse of the University of Chicago, and to Professor G. P. Baxter and Dr. J. H. Faull of Harvard University for their generous assistance in providing the chemical compounds which were used in the analyses.

AUGUST 15, 1936 PHYSICAL REVIEW VOLUME 50

The Transmutation of Sulphur by Th C′ Alpha-Particles

CHARLES J. BRASEFIELD AND ERNEST POLLARD,* *Sloane Physics Laboratory, Yale University*

(Received May 12, 1936)

The protons emitted from sulphur under bombardment of Th C′ alpha-particles have been resolved into three groups corresponding to nuclear energy changes -2.4 ± 0.3, -2.85 ± 0.3 and -3.6 ± 0.3 MEV. The first of these values, together with Bainbridge's value for the mass of Cl^{35}, has been used to deduce a value for the mass of S^{32}, namely 31.9812 ± 0.0016. An excitation curve for the emission of protons has been plotted which obeys the Gamow penetration formula within the limits of error: from this formula the nuclear radius of S^{32} has been derived and has the value $5.4\pm0.3\times10^{-13}$ cm.

THE determination of the energy levels of as many nuclei as possible is an essential preliminary to the foundation of a satisfactory nuclear theory. In particular, the binding energy of a nucleus, which depends on its mass defect, is of great importance and the present knowledge of nuclear masses as far as neon has already been used to test various suggested intranuclear forces and constitutions. Beyond neon the information is unsatisfactory and there is clearly need for an experimental determination of as many nuclear masses as possible in this region of heavier nuclei. The element sulphur offers an opportunity for investigation since the isotopic mass of its neighbor chlorine is known and a transmutation to chlorine, with a determination of the energy change involved, would enable the isotopic mass of sulphur to be found. Such a transmutation is feasible according to the reaction:

$$_{16}S^{32}+{}_{2}He^{4}\rightarrow{}_{17}Cl^{35}+{}_{1}H^{1},$$

in which the only unknown mass is that of sulphur.

The fact that sulphur has the relatively high nuclear charge of 16 means that its potential barrier is high and therefore that the proposed transmutation will not take place unless very energetic particles are used to bombard it. The alpha-particles emitted by Th C′ are the most energetic available, having an energy of nine million electron volts, and are therefore the most likely to effect the required change. We therefore bombarded a sulphur target with Th C′ alpha-particles with intent to detect emitted protons and measure their maximum energy. This has enabled the mass of sulphur to be derived. At the same time transmutations leaving a chlorine nucleus in an excited state occur, giving groups of shorter range protons, and measurement of the ranges of these groups has enabled the values of the excited energy levels to be found.

It is further possible to derive information

* Sterling Fellow.

about the potential barrier of the sulphur nucleus by determining the variation of proton yield with alpha-particle energy and so to make an estimate of the nuclear radius.

The transmutation of sulphur by alpha-particles was first reported by Rutherford and Chadwick[1] who did not, however, measure the energy of the emitted protons. In a recent account Haxel[2] describes experiments on the three elements Mg, Si and S showing that the protons from each element are emitted in three groups and that the interval between corresponding values of the nuclear energy change appears to be the same for each element.

Experimental Procedure

The technique for observing protons in the presence of ionizing radiations has been described by Wynn-Williams and Ward[3] and elaborated by Dunning, Haxel and Duncanson and Miller.[4] As detection apparatus we used a proportional counter following the design of Geiger and Zahn[5] consisting of a fine axial wire in a cylindrical case at a high negative voltage. The case, which was maintained at -3600 volts was filled with air at 25 cm pressure: the axial wire was of nichrome, one-half millimeter diameter. The wire was connected to the grid of an amplifier, the output from which actuated both a thyratron relay-Cenco counter system and a cathode-ray oscillograph. The grid leak on the first stage of the amplifier was small (one megohm), thus favoring the sharp proton deflections rather than the irregular wobble due to the gamma-ray background and a "tone control" device set to pass only frequencies above roughly a thousand was included to accentuate the shortening of the time for an impulse to record. The deflections were watched on the oscillograph and the thyratron bias set at the minimum value which did not respond to gamma-ray background fluctuations. We were unable to count the fastest protons in this way because of their low specific ionization, but for the separation of groups this is no great disadvantage. (It must, however, be remembered, in considering the absorption curves given later, that a rise in the numbers counted at any absorption means only a rise in the number of *detected* particles.) We estimated from trial experiments that our counting level was such as to record all protons of residual range less than fifteen centimeters of air.

In experiments like this there is some choice in the geometrical conditions of bombardment and detection. If θ is the angle between an incident alpha-particle causing a transmutation and the ejected proton and if Q is the nuclear energy change in the process then we have the equation:

$$2M_NQ = M_P(M_P+M_N)V_P^2 - M_a(M_N-M_a)V_a^2 - 2M_aM_PV_PV_a\cos\theta, \quad (1)$$

where M_N = Mass of residual nucleus,
M_P = Mass of proton,
M_a = Mass of alpha-particle,
V_a = Initial velocity of alpha-particle,
V_P = Velocity of emergent proton.

This equation simply expresses the conservation of energy and momentum. (The quantity "Q" for *maximum energy* protons represents the difference between the mass of sulphur plus alpha-particle and chlorine plus proton. If the resultant chlorine nucleus is formed in an excited state, the corresponding value of Q is less: the residual energy being supposed emitted as a gamma-ray quantum.) If the protons are observed in the same direction as the incident alpha-particles θ is zero and the proton velocity is maximum for a given alpha-particle energy. This would be the most advantageous arrangement except for the presence of "natural" protons from the source of range 40 cm which mask all groups of less than this range. If observation is made at an angle of ninety degrees between alpha-ray and proton a shield can be placed between the source and the counter, eliminating the natural protons and also any projected hydrogen nuclei from hydrogen in the target. For a full survey of the groups the so-called "right angles" method of observation is therefore the best, while for determining the

[1] E. Rutherford and J. Chadwick, Proc. Phys. Soc. London **36**, 417 (1924).
[2] O. Haxel, Physik. Zeits. **36**, 804 (1935).
[3] C. E. Wynn-Williams and F. B. Ward, Proc. Roy. Soc. **A131**, 391 (1931).
[4] J. Dunning, Rev. Sci. Inst. **5**, 387 (1934); O. Haxel, Zeits. f. Physik **83**, 323 (1933); W. E. Duncanson and H. Miller, Proc. Roy. Soc. **A146**, 396 (1934).
[5] H. Geiger and H. Zahn, *Handbuch der Physik*, Vol. XXII, [2] p. 163.

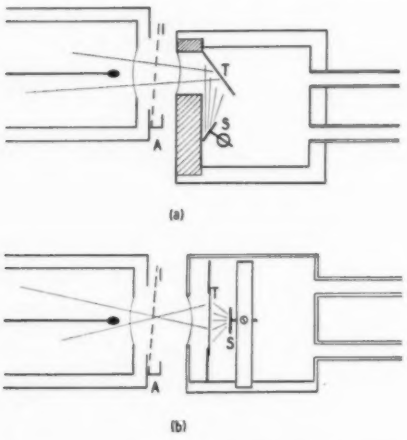

FIG. 1. Arrangements for bombardment of target and detection of protons.

maximum range of the protons the "forwards" method (protons in same direction as the alpha-rays) is more satisfactory. The forwards method allows a greater solid angle between the source and the target and consequently an increased yield of protons.

These two arrangements are illustrated in Fig. 1(a) and (b). (a) shows the "right angles" method: S is the alpha-particle source deposited on a monel metal button 9 mm diameter by exposure to the emanation from radiothorium, T is the sulphur target on cardboard backing. The activity of the source varied between 2 and 3 millicuries. Both are enclosed in a brass box which can be evacuated: the shaded wall of the box is of lead of one centimeter thickness (which served to diminish the gamma-rays reaching the counter) with a 5/8" hole covered by an aluminum foil of 4.1 cm air equivalent. The whole box was placed in a magnetic field of about 5000 gauss to bend back (and so remove) secondary electrons produced in the target. The counter opening was sealed with a mica window of 4.8 cm air equivalent. With this arrangement the minimum angle between alpha-ray and detected proton is 80° and the maximum 120° giving a solid angle of observation (the product of the solid angle between source and target and that between target and counter) of 1/1400.

The "forwards" method is shown in (b). The sulphur target was deposited on a thick gold foil by spraying a suspension of sulphur in carbon tetrachloride over the gold. The foil had an absorption greater than 8.6 cm so that the aluminum window closing the box was not bombarded by alpha-particles. In this arrangement a magnetic field is essential to bend out the beta-rays. The solid angle of observation was approximately 1/400.

In both arrangements absorption curves of the protons were plotted by interposing aluminum screens between the opening of the box and that of the counter as at A. The air equivalent of these screens was determined by weighing, 1.64 mg per square centimeter being taken as equivalent to 1 centimeter of air.

EXPERIMENTAL RESULTS

Absorption curves and nuclear energy changes

Absorption curves plotted using the right angles arrangement are shown in Fig. 2. The upper curve is for full range alpha-particles; the lower for 7.5 cm range. The sharp drop in yield shows that the 4.9 cm alpha-particles also present are not effective in causing transmutations. It will be seen that the protons form three groups of ranges 24 cm, 32 cm, and 38 cm air equivalent when full range alpha-particles are used, the values being considered good to within 1.5 cm. For this curve about one hundred particles were counted at each point. We have not included here in the diagram several runs in which the counting level was different which also showed the presence of the three groups at the ranges given. The value 8.4 cm is used for the alpha-particle range rather than the maximum value of 8.6 cm since the last two millimeters contain

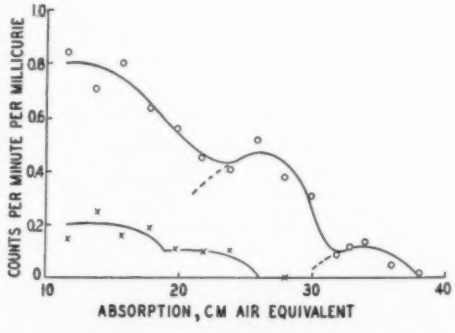

FIG. 2. Absorption curve for protons emitted at 90° to incident alpha-particles.

a very small proportion of the particles from the source. 8.4 cm is taken as a limit which is more nearly that responsible for the ends of the experimentally found proton groups. Using the range-velocity data from the Cavendish laboratory curves the nuclear energy changes "Q" corresponding to the three groups are found to be

$$-3.6\pm0.3; \quad -2.85\pm0.3; \quad -2.35\pm0.3 \text{ MEV},$$

as calculated from the upper curve, and -3.6 and -2.90 MEV from the lower, less reliable, curve. (The numbers in the third group were too small to be detected without long counting.)

In consequence of the extra momentum imparted by the recoiling nucleus the 38 cm group found above should give a group of protons in the forward direction having a range beyond that of the natural protons (40 cm). A more accurate determination of the highest "Q" value can therefore be made using the forward arrangement. The results of experiments in this way are shown in Fig. 3. Here the maximum range alpha-particles were used. A single group is seen whose range is 46 cm correct to 1.5 cm. A careful investigation beyond this range showed no signs of an additional group so this value of 46 cm presumably corresponds to a transition from the ground state of sulphur to the ground state of chlorine and can be used to compare the two masses. On this basis the calculated value of "Q" is -2.4 ± 0.2 *MEV*, in good agreement with that found previously. Expressing this energy change in terms of atomic weight units we have $Q=-0.0026$. The equation

$$_2\text{He}^4+{}_{16}\text{S}^{32}={}_{17}\text{Cl}^{35}+{}_1\text{H}^1+Q$$

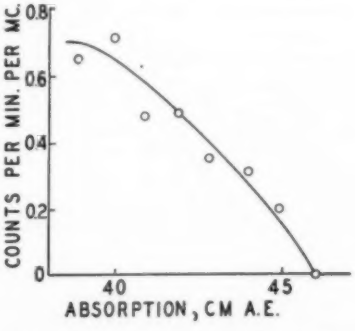

FIG. 3. Absorption curve for protons emitted in the same direction as the incident alpha-particles.

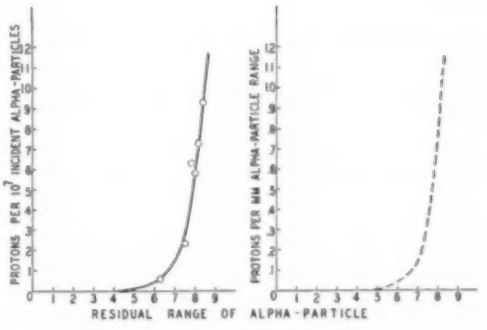

FIG. 4. Excitation curve and derived differential curve.

then becomes

$$4.0039+{}_{16}\text{S}^{32}=34.9796+1.0081-0.0026$$
$$(\pm0.0002) \qquad (\pm0.0012) \qquad (\pm0.0002)$$

and we derive the value *31.9812*($\pm$*0.0016*) for the mass of the neutral sulphur atom. The masses for helium and hydrogen are those found recently by Aston and quoted by Oliphant,[6] while the mass of chlorine is the value found by Bainbridge.[7] The energy values reported by Haxel[2] are -3.85, -2.90, -2.25 MEV. Our results, which are in good agreement with these, thus give a confirmation of his work.

Excitation curve and nuclear radius

Fig. 2 shows that there is a marked diminution in the yield as the energy of the incident alpha-particles is reduced. This is due to the fact that fewer alpha-particles are able to penetrate the barrier of the sulphur nucleus. In order to determine the form of the excitation curve experiments were made at six different alpha-particle energies—the residual range being reduced by placing thin gold or aluminum screens over the source. The procedure adopted was to plot a rough absorption curve for the emitted protons in each case and to take a mean value of the yield in the flat part of the curve between eleven and sixteen centimeters air equivalent absorption. By so doing a true excitation curve for the shortest range group is plotted, not merely a curve showing diminution of yield at one absorption which may be due to the shortening of range of a proton group to less than the

[6] M. L. Oliphant, Nature **137**, 396 (1936).
[7] K. T. Bainbridge, Phys. Rev. **43**, 378 (1933).

detected absorption. The six rough absorption curves showed that the yields of all three groups changed simultaneously, a behavior different from that found by Haxel[8] for the excitation of protons from aluminum.

The resulting excitation curve is shown in Fig. 4. As this is plotted for a thick target the excitation for a thin layer is obtained by differentiation and is shown as a dotted curve. The ordinates give the total yield in all directions for 10^7 alpha-particles incident on the target for the thick curve and yield per 10^7 alpha-particles for one millimeter target thickness for the differential curve.

The numbers available at the lower counts were not very large and therefore the curve is necessarily somewhat rough. It is interesting, nevertheless, that a reasonable estimate of the radius of the sulphur nucleus can be made even from these data, since absolute yields are determined. Thus if we assume that the sulphur nucleus has a barrier of the Gamow type and that the Gamow law for penetration holds we can say at once that the continued rise at 8 cm alpha-particle range means the barrier height exceeds the corresponding energy of 12×10^{-6} erg (7.5 MEV) or that the nuclear radius cannot be greater than 6.0×10^{-13} cm. At the same time the fact that there is an appreciable yield at 7.0 cm range means that the radius cannot be less than 4.5×10^{-13} cm for then the expected yield on the Gamow theory would be too small by a factor of one hundred. In an appendix a detailed account of a use of our excitation curve to derive a probable value for the nuclear radius is given—the value arrived at is $(5.4\pm0.3)\times10^{-13}$ cm. This is slightly higher than would be expected on the basis of Gamow's values for the radioactive nuclei but is nevertheless not unreasonable.

Nuclear spin and this reaction

According to a suggestion made by Goldhaber[9] a nuclear reaction will be probable if the nuclear spin is conserved. The present reaction is one in which a very considerable change of spin takes place since both sulphur and helium have zero spin while chlorine has a value of 5/2 and hydrogen 1/2. We estimate that our yield is similar in magnitude to that from other nuclear reactions if account is taken of the difference in penetration of the barrier. It is possible that at high energies of bombardment the conservation of nuclear spin plays a less important part than at the low energies used for the transmutation of light nuclei such as lithium and boron.

In conclusion we wish to express our thanks to Professor A. F. Kovarik for his interest and advice, to Dr. C. D. Bock for help in the setting up of a voltage stabilizer of his design and to Mr. H. L. Schultz for the construction of the amplifier.

Appendix

Derivation of the nuclear radius of $_{16}S^{32}$

We suppose the nucleus has a potential barrier of the Gamow type consisting of a cut-off Coulomb barrier falling sharply to negative potentials at a radius defined as the nuclear radius r_0. The process of disintegration is considered to be as follows:

(1) The alpha-particle must collide with a nucleus.
(2) It must penetrate into the region $r<r_0$.
(3) It must then fall to a stable level giving energy to a proton which is ejected.

If the probabilities of these processes are called P_1, P_2 and P_3 then the yield of protons observed is the product $P_1P_2P_3$. Of these three probabilities, P_1 and P_3 vary slowly with the nuclear radius while P_2, which follows the Gamow formula, is a rapidly varying function of it: thus a change of ten percent in the radius changes P_2 by a factor of five. Then if we can make an estimate of P_2 correct within a factor of five we can derive the nuclear radius correct to ten percent. We give below methods of estimating P_1 and P_3 which, together with the experimentally observed values of $P_1P_2P_3$ allow us to estimate the corresponding values of P_2, from which we can deduce the nuclear radius. The estimates of P_1 and P_2 are not accurate but since wide limits of error are permissible it is still possible to give a reasonable value for the nuclear radius.

Probability P_1

This may be estimated in two ways, the first following a theoretical approach, the second in terms of experimentally observed data. The quantum mechanical approach to the problem involves regarding a beam of alpha-particles as a plane wave which can be split into a number of partial waves of increasing angular momentum. Only that of zero

[8] O. Haxel, Zeits. f. Physik **90**, 373 (1934).

[9] M. Goldhaber, Proc. Camb. Phil. Soc. **30**, 561 (1934).

order is supposed to be effective in disintegrating (meaning only head-on—or nearly so—collisions cause disintegration). This wave has a collision cross-section equal to the square of the wave-length of the alpha-particles which is

$$\sigma=\left[\frac{h}{mv}\right]^2=\left[\frac{6\times10^{-27}}{6.6\times10^{-24}\times2.0\times10^{9}}\right]^2=2\times10^{-25}\text{ sq. cm.}$$

Or alternatively, adopting the experimental approach, we can suppose σ to be the actual cross-section of a nucleus whose radius we know lies between 4.5 and 6.0×10^{-13} and so can be estimated as 5×10^{-13} cm giving $\sigma=0.8\times10^{-25}$ sq. cm.

Now a target one square centimeter in area and of one millimeter air equivalent thickness contains 3.0×10^{18} atoms. These present an area $3.0\times10^{18}\sigma$ to the incident alpha-particles for disintegration purposes. This represents the fraction of area which is effective and so is a measure of P_1 the chance that an alpha-particle will collide with a nucleus in passing through one millimeter air equivalent of sulphur.

These two estimates therefore yield the values P_1^A, P_1^B for the probability of collision given by

$$P_1^A=2\times10^{-25}\times3\times10^{18}=6\times10^{-7},$$
$$P_1^B=0.8\times10^{-24}\times3\times10^{18}=2\times10^{-6}.$$

Probability P_2

The probability of penetration after collision is supposed to be given by the Gamow formula assuming the component of angular momentum zero is alone effective. The formula is

$$P_2=A\ \exp\frac{-2(2m)^{\frac{1}{2}}}{h}\int_{r_0}^{r}\left(\frac{2Ze^2}{r_0}-\frac{2Ze^2}{r}\right)^{\frac{1}{2}}dr,$$

$2Ze^2/r$ = energy of incident particle in the nuclear field at radius r,

$2Ze^2/r_0$ = energy at the top of the barrier.

A is a quantity depending on the energy of the bottom of the nuclear potential well which can be treated as unity for a first approximation. The evaluation of this integral gives the final numerical value

$$P_2=e^{-375.8\times10^{8}r^{\frac{1}{2}}[2u_0-\sin 2u_0]},$$

where $\cos u_0=(r_0/r)^{\frac{1}{2}}$.

Probability P_3

Having entered, how often does an alpha-particle eject a proton? This again can be approached theoretically or experimentally. Theoretically, taking P_1^A based on the wave-length of the alpha-particle the order of magnitude of P_3 is the velocity of the proton divided by the nuclear radius (assuming the proton clears the barrier). This is already well in excess of unity. Hence if we use P_1^A we can assume $P_3^A=1$.

Experimentally, Blackett and Lees have found for nitrogen disintegration that between one in two and one in ten sufficiently close collisions eject a proton. The general run of disintegration experiments indicate that there is no wide deviation from these limits. Hence using P_1^B we can take P_3^B as between 1/2 and 1/10. In either case the product P_1P_3 is of the order 10^{-6}. We wish to emphasize that in spite of an error of a factor of five which is possible in making this estimate, a value for the nuclear radius can nevertheless be derived.

Application to our experiments

We find that at 8.4 cm range we get 1.2 protons per 10^7 alpha-particles incident on a target of thickness one millimeter air equivalent. Then we have $P_1P_2P_3=1.2\times10^{-7}$. The limits of P_1P_2 can be put as 10^{-6} to 2×10^{-7} with a mean 6×10^{-7} from which we derive $P_2=0.2$ with limits 0.12 and 0.6. We now compare our experimental curves with theoretical curves for the variation of P_2 with energy seeking one which gives $P_2=0.2$ for the point at 8.4 cm range and estimating the limiting values of the radius from curves which pass through $P_2=0.12$ and 0.6. Comparative figures are given below (alpha-particle energies have been corrected for recoil motion by multiplying experimental values by 32/36)

Energy of alpha-particle	P_2	Experimental
$r_0=5.2\times10^{-13}$ cm		
12.0×10^{-6} erg	.110	.120
11.5×10^{-6} erg	.040	.045
11.0×10^{-6} erg	.015	.019
$r_0=5.4\times10^{-13}$ cm		
12.0	.200	.200
11.5	.110	.080
11.0	.030	.034
$r_0=5.7\times10^{-13}$ cm		
12.0	.60	.60
11.5	.32	.24
11.0	.09	.10

Hence we can set $5.4\pm.3\times10^{-13}$ as the nuclear radius of sulphur.

It is of some interest that the Gamow penetration formula for angular momentum zero appears to be obeyed although we do not claim that our experiments give a very rigorous test.

A Cloud Chamber Study of the Compton Effect

H. R. CRANE, E. R. GAERTTNER AND J. J. TURIN, *University of Michigan*

(Received June 10, 1936)

An experiment is described which is designed to test the photon theory of scattering in the energy region between 0.5 and 2.6 MEV. A small pencil of radiation from a thorium source is shot through a cloud chamber. A celluloid scatterer 0.8 mm thick is placed in the beam at the center of the chamber. Two thin lead sheets are placed parallel to, and on each side of, the primary beam, to absorb the scattered photons. A magnetic field is applied to determine the energies of the electrons. From the energy and direction of an electron ejected from the scatterer, the direction of the scattered photon expected from theory can be calculated, and is independent of any assumption about the energy of the primary photon. Out of 10,000 photographs taken, 300 electron-photon combinations were found. The angular and energy relations of these seem to indicate that the photon theory of scattering is valid. It is shown experimentally that the scattering of the electrons in the celluloid is of the right order of magnitude to account, at least in part, for the observed deviations of the results from theory.

INTRODUCTION

THE results recently published by R. S. Shankland[1] have incited a great deal of interest in the question of the validity of the Compton theory of photon scattering in the individual collision. Compton and Simon,[2] in 1925, performed an experiment with a cloud chamber, in which the angular relations of the secondary and tertiary electrons produced by 140 kilovolt x-rays were compared with the angles predicted by the theory. Although only a rather small amount of data was obtained the results appeared definitely to support the theory. All experiments reported subsequently were performed with Geiger counters. In 1925 Bothe and Geiger[3] performed an experiment with Geiger counters arranged in a coincidence circuit, designed to record the simultaneous appearance of the scattered photon and electron at the predicted angles. The primary photons were in this case obtained from a 70 kilovolt x-ray tube. Their results seemed to indicate that the Compton theory was valid.

Further work of this kind has been carried out at the University of Chicago since the experiments of Compton and Simon. R. D. Bennett,[4] and, later, J. A. Bearden[5] attempted to detect the simultaneous appearance of the scattered photon and the electron at the predicted angles by means of coincident Geiger counters. The results of both of their experiments were negative. The primary radiation used in these experiments was filtered x-rays. R. S. Shankland published, in January, 1936, the results of an experiment of essentially the type performed by Bennett and by Bearden. He used two sets of Geiger counters, one to record the electron and the other to record the scattered photon, placed in positions calculated from the Compton theory, and measured the rate at which coincident counts were obtained. Then, by placing the photon counter on the opposite side of the axis (at the same angle from the incident beam, but with opposite sign) he obtained a control count. He found the rate of coincidences to be the same for the two cases, which constituted evidence in direct contradiction to the predictions of the Compton theory. The fact that this experiment was done with the gamma-radiation from radon and its products, which was of much higher energy than that used in the previous experiments, invited theoretical speculation as to why the theory had so far appeared to be valid for x-rays but not for higher energy radiation.

EXPERIMENTAL METHOD

Following along the general lines of the Compton and Simon experiment, but with some modification, we have attempted to test the validity of the Compton theory for radiation between 0.5 and 2.6 MEV, especially insofar as

[1] R. S. Shankland, Phys. Rev. **49**, 8 (1936).
[2] A. H. Compton and A. W. Simon, Phys. Rev. **26**, 289 (1925).
[3] W. Bothe and H. Geiger, Zeits. f. Physik **32**, 639 (1925).
[4] R. D. Bennett, Ph.D. dissertation, University of Chicago, 1925.
[5] J. A. Bearden, Letter to A. H. Compton, quoted by Shankland (reference 1).

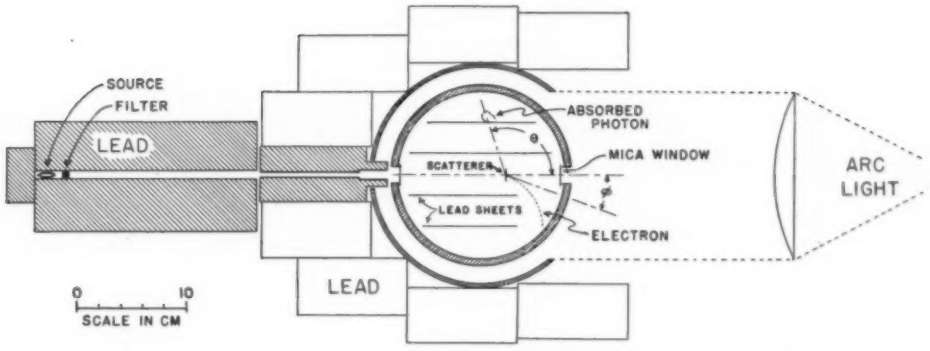

FIG. 1. Sketch of the experimental setup. Angles ϕ and θ are measured positively in the clockwise direction from the line of the gamma-ray beam; negatively in the anticlockwise direction.

the angular relationship of the electron and photon is concerned.

A thin pencil of gamma-rays was shot through a cloud chamber, as shown in Fig. 1, so as to pass through a scatterer suspended in its path. The intensity of the radiation was so adjusted that frequently a single electron appeared in the forward direction from the scatterer. Tracks of electrons of lower energy, presumably due to the absorption of scattered photons, were looked for near the four lead sheets indicated at the sides of the central gamma-ray beam. A magnetic field was applied normal to the chamber so that the energy of the electrons from the scatterer could be determined from their curvature. From the energy and the angle at which an electron was ejected, the angle of the scattered photon expected from the Compton theory could be calculated. In those photographs in which there also appeared evidence of the absorption of a scattered photon, the calculated and the observed photon angles were compared. In a similar manner, using the electron energy and the observed photon angle, the theoretical angle for the electron could be calculated and compared with the observed angle. The above calculations can be made *independently of any assumption whatever about the energy of the incident photon.* This is the important difference between the present experiment and previous experiments, in which it was always necessary to assume an energy for the primary photon.

DETAILS OF APPARATUS

The cloud chamber used was 15 cm in diameter and 2.5 cm deep, filled with air and ethyl alcohol vapor at atmospheric pressure. A mica window 12 mm in diameter and 0.2 mm thick was provided in each side of the chamber to reduce the scattering of the gamma-ray beam on entering and leaving the chamber. A magnetic field of 880 gauss was produced by a pair of water cooled Helmholz coils. The strength of the field was determined by calculation from the geometry of the coils and the current, and also by measuring the spectrum of recoil electrons from the known 2.6 MEV gamma-ray line of Th C″. A sheet of parallel light about 1 cm in depth, obtained from a 200 ampere carbon arc was projected through the chamber, and photographs were taken with a Sept 35 mm movie camera, at f 3.5 and $\frac{1}{4}$ second exposure. The entire apparatus ran automatically, expansions occurring at 30-second intervals. This rather long expansion interval was found necessary on account of the large amount of material in the chamber in the form of absorbers, etc.

The scatterer used in obtaining most of the data was a piece of celluloid, 0.8 mm thick, although in a few runs at the beginning a 0.2 mm mica scatterer was used. The lead plates parallel to the beam were $\frac{1}{4}$ mm thick, and extended from the top to the bottom of the chamber. For a source of gamma-rays a small capsule containing mesothorium and its products of about 1 millicurie strength was placed at the end of a lead collimator 30 cm long and about 5 mm inside

diameter. The walls of the collimator were 5 cm thick, and, for additional shielding, a number of lead blocks were placed around the sides of the cloud chamber, as shown in the diagram. The beam of radiation allowed to enter the chamber was filtered through about 6 mm of lead.

Results and Treatment of Data

About 10,000 photographs were taken, and the following procedure was employed in recording the data which they contained. The pictures were reprojected onto a screen, natural size. Before proceeding to each new picture, a black card was placed over the part of the field in which the recoil electrons appeared; namely, the part in front of, and to the right of, the scatterer. The angular position of any track in the chamber which was thought to indicate the absorption of a scattered photon was then recorded before the black card was removed. If a recoil electron track from the scatterer was found, its angle and energy were recorded. In this way the angle of an electron from the scatterer could not influence the choice or measurement of the "photon tracks." Some discrimination was permissible in dealing with the photon tracks, since in a few cases it was fairly certain that a track was due to the primary gamma-rays (if it was of very high energy), or that it had its origin in the path of the central beam. Such tracks were not counted. It is not probable that the position of the photon track could have influenced the measurement of the recoil electron from the scatterer, since these tracks were very distinct. All electron tracks were

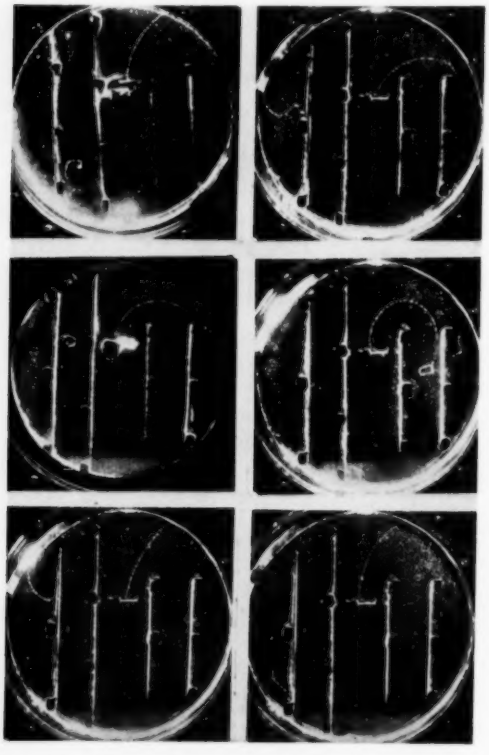

Fig. 2. Examples of cloud chamber photographs, each of which contains one recoil electron, together with evidence of the absorption of the scattered photon.

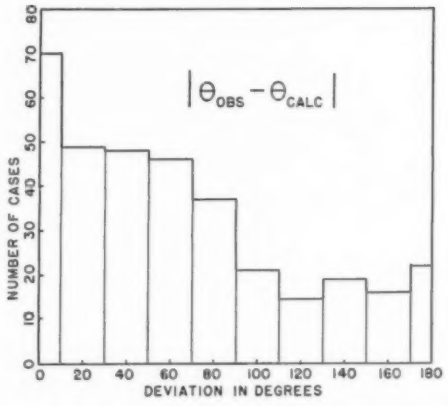

Fig. 3. Absolute values of the differences between the calculated and the observed angles of the scattered photons.

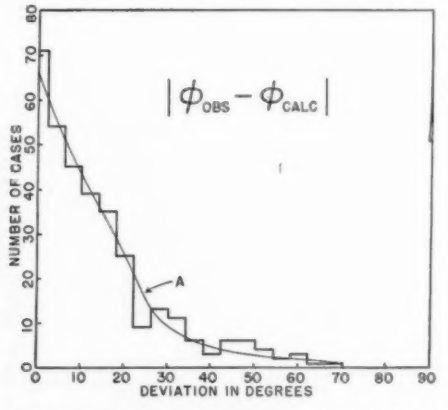

Fig. 4. Absolute values of the differences between the calculated and the observed angles of the recoil electrons.

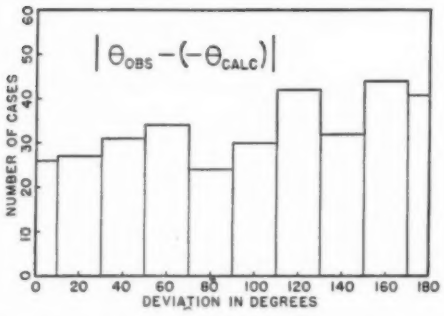

FIG. 5. Absolute values of the differences between the observed and minus the calculated angles of the scattered photons.

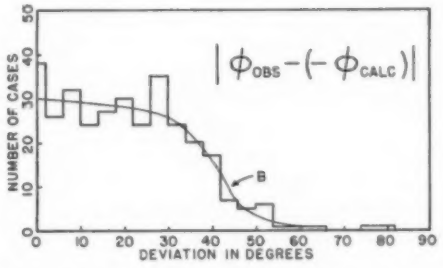

FIG. 6. Absolute values of the differences between the observed and minus the calculated angles of the recoil electrons.

measured which lay nearly enough in the plane of the light beam that an arc of about 90° was visible. After recording all the data in the manner described, only those electron-photon combinations were used which consisted of a single electron from the scatterer and a single absorbed photon. 300 such combinations were found in the 10,000 photographs. Each of the electron-photon combinations was treated as follows: (1) Using the angle and energy of the electron, the theoretical angle of the photon was calculated. (2) Using the energy of the electron and the angle of the photon, the theoretical angle of the electron was calculated. Fig. 3 shows these results plotted according to the absolute difference between the calculated and observed photon angles, and Fig. 4 shows a similar plot for the electron angles.

For the purpose of comparison, similar plots are shown (Figs. 5 and 6) of the absolute differences between the observed photon and electron angles and minus the corresponding calculated angles. These give control plots which are not influenced by asymmetry in the chamber, because spurious tracks have the same chance of appearing near the calculated angles as they have of appearing near minus the calculated angles. (See paragraph on symmetry considerations.)

DISCUSSION OF RESULTS

The results of the present experiment may be expected to answer with fair certainty the general question of whether the Compton energy and angular relations are at all valid for the individual collision, or whether the correspondence which has been established by many x-ray scattering experiments is of an entirely statistical nature. The question of how closely the angles correspond in the individual collision to those predicted by theory is a more difficult one on the basis of the data obtained here, and only the vaguest kind of answer can be attempted.

If the Compton angular and energy relationship were assumed to hold only statistically, we would expect the plots of the photon angles in Figs. 3 and 5 to be alike. Actually, they seem to show a significant difference, in a direction which indicates that the predicted Compton angles are considerably favored. The broadness of the maximum, as will be shown later, can be accounted for at least partly by the scattering which the recoil electrons suffer in getting out of the celluloid scatterer. The small errors in the angle ϕ which come about in this way make correspondingly large errors in the theoretical angle θ, especially when ϕ is small, as can be seen readily from the Compton formulas. For 1 MEV electron energy, $d\theta/d\phi$ is about 6 for $\phi=5°$, 5 for $\phi=10°$, 4 for $\phi=15°$, which produces in the θ plots considerable amplification of the broadening effect of the electron scattering.

An indication that the Compton angles are favored can be obtained in a different way, simply by considering the signs of the angles ϕ and θ. In 209 of the 300 cases ϕ and θ were of opposite sign, meaning that the lateral components of momentum of the electron and photon were opposite in direction, while in only 91 cases they were in the same direction.

The plots of the deviations of the electron angles from those calculated, shown in Figs. 4

and 6, were made in order to obtain a curve which could be interpreted more directly in terms of electron scattering. We should point out at the beginning, however, that we should expect a maximum at zero degrees for both the ϕ plots, even if the distribution of photon angles were random. Because of (1) the predominance of forward electrons (Klein-Nishina distribution) and (2) the fact that large angular ranges for θ in the backward direction correspond to small angular ranges for electrons in the forward direction, we should expect many of the differences between ϕ and ϕ calc. to be small. This is apparent in Figs. 4 and 6, but the curve in Fig. 4 is much more peaked at zero than that in Fig. 6. These, again, should have the same form if there were no correspondence of the angles in the individual collision with those predicted from the Compton theory. The ratio of the two curves, shown in Fig. 7 should, provided the breadth is due to scattering, bear some resemblance to a scattering curve for the electrons, even though it does not give it directly.

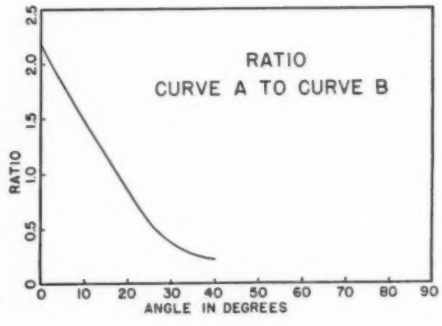

FIG. 7.

An experiment on the scattering of electrons

To determine, under the actual conditions of our experiment, whether the amount of scattering of the electrons is of the order of magnitude indicated by Fig. 7, the following experiment was performed: A sheet of celluloid of the same thickness as the scatterer used in the previous set-up was placed across the center of the cloud chamber. Recoil electrons produced by gamma-rays from the same source with the same filtration as above were allowed to pass through the celluloid, (without a magnetic field) and the angles through which they were deviated in the celluloid were measured. This gave only the projection in two dimensions of the scattering, but this is approximately the thing desired for comparison with Fig. 7, since in the other work all the angles were measured in two dimensions, and errors in the measured ϕ were due mainly to the component of scattering in the horizontal plane. The result is shown in Fig. 8. This is roughly in accord with theoretical estimates of the scattering. The fact that this curve is not as broad as that in Fig. 7 may be satisfactory, since it leaves room for some other errors in measurement, etc., which have broadening effects. From this rough indication of the extent of scattering, it seems reasonable to say that we are not compelled by the present results to look for any inherent breadth or uncertainty in the Compton angles to explain the breadth of the maxima observed. Better measurements of scattering may clarify this point.

Division of the data into energy groups

Because the suggestion has often been made that the scattering of quanta of energy large compared to mc^2 may be different from that for quanta of energy near mc^2 or below, we have analyzed the data more closely with regard to energy. The data shown in Figs. 4 and 6 were divided into groups according to the energies of the recoil electrons and plotted separately, as shown in Figs. 9 and 10. Although this was not strictly a separation according to the energy of the incident photon, it approximated it well enough for the present purpose, and placed a definite lower limit upon the photon energy. (See footnote.) The groups having electron energies from 0.3 to 0.55, 0.55 to 1.0, and 1.0 to 2.4 (photon energies above 0.5, 0.8, and 1.25 MEV, respectively), show no difference in character beyond the expected statistical fluctuations, and each group indicates that the Compton angles are favored. The numbers of cases in these groups are of course not large, but from this small amount of data, at least, there appears no reason to believe that the quanta in the low and the high energy groups are scattered differently.

The three groups in Figs. 9 and 10 automatically give some idea as to the composition of

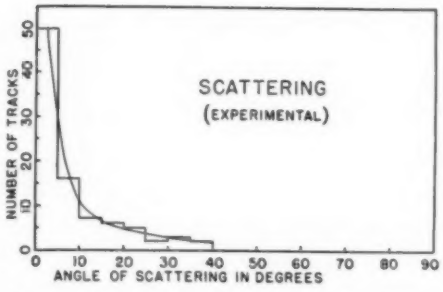

FIG. 8. Experimental curve for the scattering of electrons by 0.8 mm of celluloid.

the radiation from the mesothorium source used. This source was not old enough to have reached equilibrium with its products, and consequently there was present a larger proportion of low energy radiation than is usual with a mesothorium source. Figs. 9 and 10 show that roughly equal numbers of recoil electrons were due to quanta in the three energy regions indicated. In this the low energy component is of course accentuated, due to the larger absorption coefficient of celluloid for the lower energy radiation.

Probability of observing the scattered photon

Considering the total number of electrons and absorbed photons observed, and assuming that from $\frac{1}{2}$ to $\frac{1}{3}$ the observed electron-photon combinations are really associated, we estimate that roughly 1 photon in 50 which passed through the lead sheets was observed. This efficiency seems rather high, but several reasons can be suggested to account for it. (1) All measurable recoil electron tracks observed necessarily lie approximately in the plane of the chamber; therefore (if conservation of momentum holds) the path of the scattered photon also lies in the plane, and has a good chance of passing through one or two of the lead plates. Thus the fact that observations are restricted essentially to two dimensions does not appreciably affect the chance of observing the photon associated with an observed electron. (2) The greater majority of the photons were directed backward from the scatterer, because of the Klein-Nishina angular distribution, and were therefore of comparatively low energy (of the order of 0.25 MEV). This made them quite efficient at ejecting photoelectrons from the lead. (3) In addition to the eight lead surfaces, the top and bottom of the chamber were to some extent effective. Because of the magnetic field, electrons ejected from these surfaces had a 50 percent chance of executing a vertical helix through the visible part of the chamber.

Scattering material

Celluloid was chosen for the scattering material because of its low average atomic number and also because of its transparancy. Scattering of electrons of the energy dealt with here is mainly nuclear, and is about proportional to the square of the atomic number of the scattering material and inversely proportional to the square of the momentum of the electron. With the best lead shielding available around the chamber the background of spurious tracks is about constant, and independent of the scatterer. Too thin a scatterer will give too small a number of Compton collisions compared to the background, while too thick a scatterer gives rise to undue errors in ϕ through scattering of the recoil electrons. 0.8 mm proved to be not far from the optimum thickness.

Symmetry

The arrangement of the lead plates in the chamber was not symmetrical on the two sides of the gamma-ray beam. This had no effect on the result, however, since as many electrons were ejected having ϕ positive as having ϕ negative (by actual count). This was equivalent to interchanging the two halves of the chamber for half the data.

Simultaneity of appearance of photon and electron

The possibility of a difference in the times of appearance of the scattered electron and the photon has often been suggested to account for the failure of some of the Geiger-counter experiments to give positive results. The resolving time of a cloud chamber is about 1/25 of a second, and that of a coincidence Geiger-counter circuit of the order of 1/1000 of a second or less. If the results so far given by both the cloud chamber and the Geiger-counter technique are to be adhered to, one possible interpretation would of course be that the time difference lies somewhere between the resolving times of these two instruments. Exclusive of this argument, however, the one type of experiment seems but

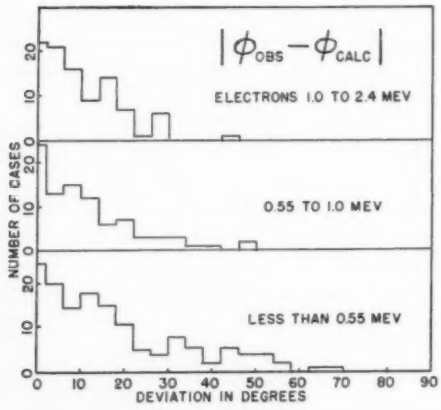

FIG. 9. The data of Fig. 4, plotted in three groups according to the energy of the recoil electrons.

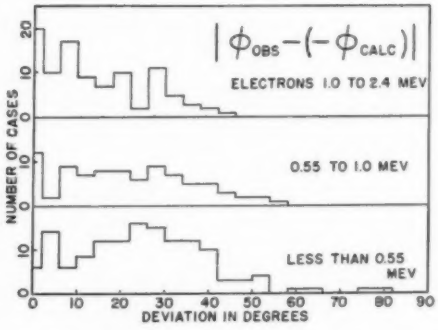

FIG. 10. The data of Fig. 6, plotted in three groups according to the energy of the recoil electrons.

little more satisfying than the other, since a time difference in the process may be imagined to lie anywhere in the large range between the above resolving time and 10^{-20} second or less. There seems at present a great likelihood that with further refinements in both methods of attack, the results of both methods will come into agreement. The desirability of further experiments along these lines can hardly be over-estimated.

This work was made possible by a grant from the Rackham Fund. The authors wish to express their appreciation for this support.

According to the Klein-Nishina formula most of the recoil electrons due to gamma-rays have nearly the maximum energy. Therefore a division of the data on the basis of electron energy seems permissible. Alternative ways of obtaining the energy of the primary gamma-ray quantum are: (1) Calculation from the energy of the recoil electron and the direction of the scattered photon. This is not satisfactory because the photon is really associated with the electron in only $\frac{1}{2}$ or $\frac{1}{4}$ of the cases. (2) Calculation from the energy and direction of the recoil electron. This is vitiated by scattering of the recoil electron. The result is rather sensitive to this.

AUGUST 15, 1936 PHYSICAL REVIEW VOLUME 50

Disintegration of Beryllium, Boron and Carbon by Deuterons

T. W. BONNER* AND W. M. BRUBAKER, *W. K. Kellogg Radiation Laboratory, California Institute of Technology*

(Received June 2, 1936)

The energy distribution of the neutrons emitted when beryllium, boron and carbon are bombarded by 0.9 MEV deuterons has been investigated. The neutrons from beryllium are attributed to the reaction

$$_4Be^9+{}_1H^2\rightarrow{}_5B^{10}+{}_0n^1+Q_1. \quad (1)$$

The energy of disintegration Q_1 is 4.25 ± 0.2 MEV. Several lower energy neutron groups attributed to excited B^{10} nuclei were observed with Q's equal to 3.7, 2.1 and 0.8 MEV. The neutrons observed when boron is bombarded by deuterons are attributed to the reactions:

$$_5B^{11}+{}_1H^2\rightarrow{}_6C^{12}+{}_0n^1+Q_2, \quad (2)$$

$$_5B^{11}+{}_1H^2\rightarrow3{}_2He^4+{}_0n^1+Q_3, \quad (3)$$

$$_5B^{10}+{}_1H^2\rightarrow{}_6C^{11}+{}_0n^1+Q_4. \quad (4)$$

The most probable of these is reaction (3); it gives rise to a group of neutrons with a continuous distribution of energies below 3 MEV. The disintegration energies observed from the other two reactions are:

$$Q_2^0=13.5\pm0.3 \text{ MEV}, \qquad Q_4^0=6.2\pm0.2 \text{ MEV},$$
$$Q_2^1=9.1\pm0.2 \text{ MEV}, \qquad Q_4^1=4.0\pm0.1 \text{ MEV}.$$

The neutrons observed when carbon is bombarded by deuterons are attributed to the reactions:

$$_6C^{12}+{}_1H^2\rightarrow{}_7N^{13}+{}_0n^1+Q_5, \quad (5)$$

$$_6C^{12}+{}_1H^2\rightarrow{}_7N^{14}+{}_0n^1+Q_6. \quad (6)$$

It is found that reaction (5) is responsible for approximately 99 percent of the neutrons from carbon and that reaction (6) is responsible for the remainder. The values of the disintegration energies are:

$$Q_5=-0.37\pm0.05 \text{ MEV} \quad \text{and} \quad Q_6=5.2\pm0.4 \text{ MEV}.$$

The calculated value of the maximum energy of the positrons from N^{13} is 1.16 MEV which is lower than the Konopinski-Uhlenbeck extrapolated value of 1.45 MEV. A complete set of values of the masses of the light elements computed from disintegration data is given.

* National Research Fellow.

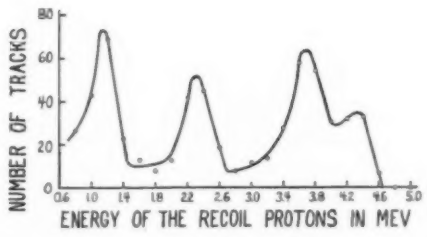

FIG. 1. The energy distribution of the recoil protons observed when beryllium was bombarded by 0.9 MEV deuterons.

IN previous papers[1] we have reported on the energy distribution of the neutrons emitted when several of the light elements are bombarded with deuterons. In the present experiments we have extended our observations to boron and carbon. Additional data concerning the neutrons from beryllium are also given. It is the object of these experiments to determine the energies liberated in the nuclear reactions in which the neutrons are produced and to investigate the relative probabilities of the different reactions.

We have continued our method of determining neutron energies by measuring the lengths of recoil proton tracks in a high pressure cloud chamber filled with methane.[1] In the case of the neutrons from boron, we have also observed recoil helium nuclei. As in our previous work, we have measured only the ranges of those recoil nuclei which were projected in nearly the forward direction. Thus recoil protons received essentially the energy of the incident neutrons, while the helium recoils received nearly 16/25 of the neutrons' energy. The cloud chamber was placed 20 cm from the target in a manner such that the neutrons made angles of 83° to 97° with the direction of the incident deuterons.

RESULTS

Beryllium

In our first report[1] on the energy of the neutrons emitted when beryllium is bombarded by deuterons we were principally interested in the maximum energy of the neutrons which are produced in the nuclear reaction:

$$ {}_4Be^9+{}_1H^2\rightarrow{}_5B^{10}+{}_0n^1+Q_1. \qquad (1) $$

However we found that there were several neutron groups with energies lower than the maximum. It is one of the objects of the present experiment to investigate more carefully these lower energy groups which are assumed to result when the B^{10} nuclei are left in excited states.

3500 stereoscopic photographs were taken when a metallic beryllium target was bombarded with 0.9 MEV deuterons. The stopping power of the methane[2] in the cloud chamber was 5.68 in this experiment and the highest energy recoil protons had track lengths of approximately 5 cm. Fig. 1 gives the energy distribution of the 580 protons whose ranges were measured. The curve indicates four neutron groups with energies of 4.52, 4.0, 2.6 and 1.4 MEV.

Since the energy of the 2.6 MEV group is very nearly the same as the energy of the neutrons from the reaction

$$ {}_1H^2+{}_1H^2\rightarrow{}_2He^3+{}_0n^1+Q_2, \qquad (2) $$

the possibility that this group is due to deuterium contamination has been considered. We find that this 2.6 MEV group is at least ten times as strong as the contamination effects observed on other targets such as Atcheson graphite, brass and $NaNO_2$. The excitation curves for the reactions (1) and (2) are quite different,[3] so a run at 0.6 MEV bombarding potential provided a conclusive means of determining whether a considerable portion of this energy group is due to contamination. At this lower voltage the intensity of the 2.6 MEV group as compared to the intensity of the higher energy groups should be five times as great if it were due entirely to contamination. The experiment showed an increase of only twenty percent, so it is apparent that only a small proportion of the neutrons in the 2.6 MEV group come from the deuteron-deuterium reaction.

The maximum neutron energy corresponds to a disintegration energy Q_1^0 of 4.25 ± 0.20 MEV which is approximately the same as we reported originally. The Q_1's associated with the lower energy groups are:

$$ Q_1^1=3.7, \qquad Q_1^2=2.1 \quad \text{and} \quad Q_1^3=0.8 \text{ MEV}. $$

[1] Bonner and Brubaker, Phys. Rev. **47**, 910 (1935); **48**, 742 (1935); **49**, 19 (1936).

[2] The composition of the gas was 85.1 percent CH_4, 13.5 percent C_2H_6, and 1.4 percent N_2.

[3] Bonner and Brubaker, Phys. Rev. **49**, 19 (1936).

These Q_1's correspond to the cases when the B^{10} nuclei are left excited to levels of 0.55, 2.15, and 3.45 MEV; one expects gamma-rays of these energies to be emitted. Crane, Delsasso, Fowler and Lauritsen[4] reported intense gamma-rays with an energy of 0.6 MEV and others with energies up to 3.3 MEV when beryllium is bombarded by deuterons. The observed gamma-rays may reasonably be attributed to excited states of B^{10}, but close correlation between the two cannot be made at present.

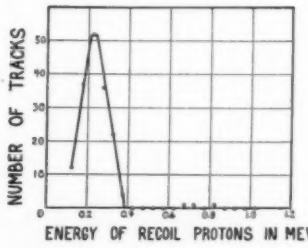

FIG. 2. The energy distribution of the recoil protons observed when carbon was bombarded with 0.88 MEV deuterons.

Carbon

Two nuclear reactions have been shown to take place when carbon is bombarded with deuterons:

$$ {}_6C^{12}+{}_1H^2\rightarrow{}_6C^{13}+{}_1H^1+Q_3, \quad (3) $$

$$ {}_6C^{12}+{}_1H^2\rightarrow{}_7N^{13}+{}_0n^1+Q_4, \quad (4) $$

$$ {}_7N^{13}\rightarrow{}_6C^{13}+e^+ +Q_5. \quad (5) $$

Reaction (3) has been carefully studied by Cockcroft and Walton,[5] Livingston and Lawrence,[6] Tuve and Hafstad[7] and by Fowler, Delsasso and Lauritsen.[8] The alternative mode of disintegration, reactions (4) and (5), in which a neutron and N^{13} are the disintegration products was first observed by Crane and Lauritsen,[9] and by Henderson, Livingston and Lawrence.[10] They made observations on the radioactive N^{13}. The neutrons were reported by Tuve and Hafstad[11] and by Newson[6] who made qualitative measurements of their energies.

It is particularly desirable to know the maximum value of Q_4 quite accurately.[12] This value, combined with Q_3 and the mass difference $({}_0n^1-{}_1H^1)$ enables one to predict the maximum energy of the positrons emitted by N^{13}. This predicted maximum positron energy should show one how to choose the end point of the experimentally determined continuous distribution curve. If, on the other hand, the maximum energy of the positrons is in the future accurately determined, then one may compute the rest mass of the neutrino from the maximum positron energy, Q_3, Q_4 and the mass difference $({}_0n^1-{}_1H^1)$. For these reasons we have attempted an accurate determination of the energies of the neutrons from reaction (4). These same questions could be solved by the data of disintegrations of the same type in one of the other light elements such as B^{10}, N^{14}, O^{16}, etc., but as Q_3, Q_4 and Q_5 are all small, the data from the disintegration of carbon are capable of the greatest precision.

Since there are two isotopes of carbon, we should also expect to observe neutrons from the reaction:

$$ {}_6C^{13}+{}_1H^2\rightarrow{}_7N^{14}+{}_0n^1+Q_6. \quad (6) $$

As C^{13} is only 1/100 as plentiful as C^{12} we should expect the yield of neutrons from reaction (6) to be much smaller than from reaction (4). We have found evidence that some of the observed neutrons are from reaction (6).

Approximately 14,500 sets of stereoscopic photographs were taken when carbon was bombarded by 0.88 MEV deuterons. For 2500 of these the chamber was operated at an expanded pressure of one atmosphere, and for the rest it was operated at 8.5 atmospheres. In the first series of runs we observed 166 tracks of recoil protons which had been projected in nearly the forward direction (0°–10°). The ranges of these protons were computed from the stopping power of the gas and the track lengths. The stopping power of the gas was determined experimentally from the mean length of the tracks of polonium

[4] Crane, Delsasso, Fowler and Lauritsen, Phys. Rev. **47**, 782 (1935).
[5] Cockcroft and Walton, Proc. Roy. Soc. **A144**, 704 (1934).
[6] H. W. Newson, Phys. Rev. **48**, 790 (1935).
[7] Tuve and Hafstad, Phys. Rev. **48**, 106 (1935).
[8] Fowler, Delsasso and Lauritsen, Phys. Rev. **49**, 561 (1936).
[9] Crane and Lauritsen, Phys. Rev. **45**, 430 (1934).
[10] Henderson, Livingston and Lawrence, Phys. Rev. **45**, 428 (1934).
[11] Tuve and Hafstad, Phys. Rev. **48**, 106 (1935).
[12] The value of Q_4 which we have found in these experiments was reported at the December (1935) meeting of the Am. Phys. Soc., Phys. Rev. **49**, 203 (1936).

alpha-particles. This value (1.06) was then corrected for the variation of stopping power with velocity;[13] the corrected value was 1.21 for protons with a range of 0.5 cm. The energies of the protons was then found from Blackett's[14] experimentally determined range-velocity curve. The energy distribution of these tracks is given in Fig. 2. The curve indicates a neutron group with a maximum energy of 0.35±0.03 MEV.

As a few tracks were observed which went entirely across the chamber, another series of runs was made when the pressure in the chamber was increased to 8.5 atmospheres. From 12,000 photographs taken when the chamber was operated at this increased pressure, we measured 223 tracks of protons with energies above 1 MEV. The few protons with energies of 2.6 MEV were probably due to neutrons from deuterium contamination, according to reaction (2). There was also an indication of a weak group with an energy of 1.8 MEV. 24 tracks of protons which had energies over 4 MEV were photographed. This group had a maximum energy of 5.6±0.4 MEV. The relative intensities of the 5.6, 1.8 and 0.35 MEV groups were 1, 3 and 300, respectively. The 5.6 and 1.8 MEV groups were probably due to reaction (6), but since their energy was almost the same as that of the neutrons from nitrogen[15] the possibility that they were due to a high contamination of nitrogen on the Atcheson graphite target cannot definitely be excluded. It is possible to explain the 3.5 to 4.0 MEV gamma-rays from carbon bombarded by deuterons by the C^{13} reaction. Approximately the right amount of energy (4.1) MEV and intensity for such gamma-rays is given by the difference between the 5.6 and 1.8 MEV neutron groups. The values of the energies of disintegration of reactions (4) and (6) were calculated to be

$Q_4 = -0.37 \pm 0.05$ MEV and $Q_6 = 5.2 \pm 0.4$ MEV.

Energy of Positrons from N^{13}

By combining Eqs. (3) and (4) we find that the maximum positron energy E_m is given by

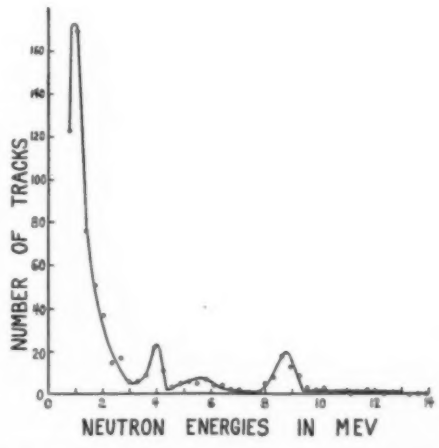

FIG. 3. The energy distribution of the neutrons from $B+H^2$ as inferred from the energy distribution of the recoil helium nuclei.

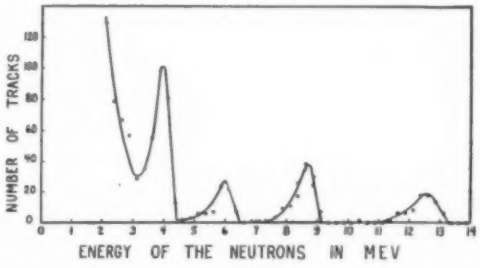

FIG. 4. The energy distribution of the neutrons from $B+H^2$ as inferred from the energies of the recoil protons.

$$E_m = Q_3 - Q_4 - 2m_e - ({}_0n^1 - {}_1H^1), \qquad (7)$$

where m_e is the rest mass of the electron (0.51 MEV). The value of Q_3 has been obtained by Fowler, Delsasso and Lauritsen[8] in this laboratory under conditions almost identical to those under which we determined Q_4. Since one is interested in the value $Q_3 - Q_4$ any errors in the energy of the bombarding particles is unimportant. The value of the mass difference $({}_0n^1 - {}_1H^1)$ is known accurately from the difference between the $H_2^{1+} - H^{2+}$ doublet as determined by the mass spectrograph. Bainbridge[16] and Aston[17] now agree that this difference is 0.00152 mass unit. One now only needs to use the binding energy of the deuteron (2.25 MEV),

[13] Rutherford, Chadwick and Ellis, *Radiations from Radioactive Substances*, p. 96.
[14] P. M. S. Blackett, Proc. Roy. Soc. **A135**, 132 (1932).
[15] As we have found from some incomplete work with nitrogen.
[16] Bainbridge and Jordan, Phys. Rev. **49**, 883A (1936).
[17] F. W. Aston, Nature **137**, 357 (1936).

which has been accurately determined by Feather, to get a $({}_0n^1-{}_1H^1)$ difference of 0.00090 mass unit.

Using the value 0.00090 for the mass difference $({}_0n^1-{}_1H^1)$ and the experimentally determined values of Q_3 and Q_4, we calculate that

$$E_m=1.16 \text{ MEV}.$$

The energy distribution of the positrons from N^{13} has been given by Fowler, Delsasso and Lauritsen[8] and by Kurie, Richardson and Paxton.[19] Our calculated value of E_m seems definitely to favor the inspection end point of the N^{13} positron spectrum (1.25 MEV) rather than the value 1.45 MEV obtained from the Konopinski-Uhlenbeck extrapolation.

Boron

The copious emission of neutrons when boron is bombarded by fast deuterons was first reported by Lauritsen and Crane.[20] Several possible reactions which will account for the neutrons are:

$${}_5B^{11}+{}_1H^2\rightarrow{}_6C^{12}+{}_0n^1+Q_8, \quad (8)$$

$${}_5B^{11}+{}_1H^2\rightarrow 3{}_2He^4+{}_0n^1+Q_9, \quad (9)$$

$${}_5B^{10}+{}_1H^2\rightarrow{}_6C^{11}+{}_0n^1+Q_{10}. \quad (10)$$

A continuous distribution of alpha-particles attributed to reaction (9) has been reported by Cockcroft and Lewis.[21] Radioactive C^{11} produced by bombarding boron with deuterons has been reported by Crane and Lauritsen,[22] Henderson, Livingston and Lawrence,[23] and by others.

We have obtained two sets of data on the energy distribution of the neutrons emitted when an amorphous boron target is bombarded by 0.9 MEV deuterons. From 5400 pairs of stereoscopic photographs taken when the chamber was filled with helium at a pressure of 6 atmospheres, 660 tracks were measured. The stopping power of the gas was determined from the mean length of the tracks of polonium alpha-particles. The neutron energy distribution deduced from these tracks is given in Fig. 3. From this curve we are not able to tell whether there are any neutrons with energies above 9 MEV or not, as the few tracks observed in this region might be attributed to recoil protons. For this reason we obtained another set of data with CH_4 in the chamber instead of He.

We have investigated the energy interval of 2 to 10 MEV with the methane-filled cloud chamber operated at an expanded pressure of 18.8 atmospheres (stopping power = 18.04). For observing the higher energy neutrons we operated the chamber at the same pressure and augmented the stopping power by placing a sheet of mica with a stopping power of 58 cm across the center of the chamber. From 5400 photographs taken with the mica and 6400 taken without the mica we have measured 1100 track lengths. The energy distribution of these recoil protons is given in Fig. 4. The ordinates of the data taken with the mica have been fitted to give the same intensity for the 9 MEV group as was obtained without the mica. The distribution curve shows four neutron groups with energies of 13.2, 9.1, 6.35 and 4.35 MEV. The rise in the distribution curves below 3 MEV indicates the presence of a continuous distribution of neutrons in this energy range. The neutron energy distribution deduced from Fig. 3 is essentially the same as that deduced from Fig. 4, except for the highest energy group; it appears to be very weak in Fig. 3, if not entirely missing. It is not clear whether this is merely a matter of statistics or is of real significance. It may perhaps be that many of the nearly head-on collisions of 13 MEV neutrons with helium nuclei are not elastic, and that a portion of the energy is liberated in the form of a gamma-ray. However, it will be necessary to do further experiments to decide between these two possibilities.

A consideration of the approximate values of the masses of the nuclei involved in Eqs. (8), (9) and (10) enables us to assign these observed neutron energies to the various equations. As reaction (8) is the only one which would give neutrons with energies greater than 7 MEV, we may be reasonably certain that the 13.2 and 9.1 MEV groups result from this reaction. The 6.35 MEV group agrees well with the energy to

[19] Kurie, Richardson and Paxton, Phys. Rev. **49**, 368 (1936).
[20] Lauritsen and Crane, Phys. Rev. **45**, 493 (1934).
[21] Cockcroft and Lewis, Proc. Roy. Soc. **A154**, 246 (1936).
[22] Crane and Lauritsen, Phys. Rev. **45**, 430 (1934).
[23] Henderson, Livingston, and Lawrence, Phys. Rev. **45**, 428 (1934).

be expected from reaction (10). We think it is likely that the 4.35 MEV group comes from reaction (10) also. The relatively large number of neutrons with energies below 3 MEV appears to have a continuous energy distribution and so is probably due to reaction (9). This disintegration into three alpha-particles and a neutron appears to be more probable than disintegration into C^{12} and a neutron according to reaction (8).

The corresponding values of the Q_8's are: $Q_8^0 = 13.5 \pm 0.3$ MEV and $Q_8^1 = 9.1 \pm 0.2$ MEV. The lower value of Q_8 results when the C^{12} nucleus is excited to a 4.4 ± 0.2 MEV level. C^{12} has been excited to this level in two other nuclear reactions. Cockcroft and Lewis[21] found two groups of alpha-particles in the reaction

$$ {}_7N^{14} + {}_1H^2 \rightarrow {}_6C^{12} + {}_2He^4 + Q_{11} \qquad (11) $$

with an energy difference of 4.2 ± 0.1 MEV. These two excitation values of C^{12} agree within the experimental errors. The first evidence for an excited C^{12} nucleus was that obtained from the study of the reaction

$$ {}_4Be^9 + {}_2He^4 \rightarrow {}_6C^{12} + {}_0n^1 + Q_{12} \qquad (12) $$

by Bothe and Becker,[24] Curie and Joliot,[25] Chadwick[26] and by others. Values ranging from 4 to 5 MEV have been obtained as the energy of the gamma-rays from this reaction and it now appears probable that the C^{12} nucleus in this reaction is excited to the same level as it is in the previous two reactions.

The corresponding values of Q_{10} gives us another means of checking the maximum energy of the continuous beta-ray spectrum in a manner similar to that which has been done in the case of N^{13}. From reactions (10) and (13)

$$ {}_5B^{10} + {}_1H^2 \rightarrow {}_5B^{11} + {}_1H^1 + Q_{13}{}^{21} \qquad (13) $$

we see that the maximum energy of the C^{11} positrons is

$$ E_m = Q_{13} - Q_{10} - 1.86 \text{ MEV} $$

(using a mass difference of ${}_0n^1 - {}_1H^1 = 0.00090$). This gives 1.05 for the value of E_m, which agrees better with the inspection end point (1.15 MEV) than with the Konopinski-Uhlenbeck value (1.3 MEV) as reported by Fowler, Delsasso and Lauritsen.[8] However, the calculated value of E_m agrees with either value within the probable error of 0.3 MEV.

Disintegration Masses of the Light Elements

It is of interest to calculate the disintegration masses of the light elements from the Q's given in this paper and the Q's reported by other investigators. Two mass differences which we shall want to use often are:

$$ 2\,{}_1H^2 - {}_2He^4 = 23.82 \text{ MEV} $$

and

$$ {}_1H^1 + {}_0n^1 - {}_1H^2 = 2.25 \text{ MEV}. $$

The first of these is the difference which we calculated previously from disintegration data[3] and the second is that found by Feather[27] from the photo-disintegration of deuterium. The first difference is very nearly the same as that recently reported by Aston[17] from new mass spectroscopic data (23.75 MEV). Using these two mass differences we can calculate the O^{16}/He^4 ratio in several different ways from the available disintegration data. For convenience we have done this in two steps. First we computed the B^{11}/He^4 ratio in three different ways and then we found the O^{16}/B^{11} ratio by several methods.

In these calculations we have used the following equations:

(a) ${}_5B^{10} + {}_1H^2 = {}_5B^{11} + {}_1H^1 + 9.11$,[21]
(b) ${}_4Be^9 + {}_1H^2 = {}_5B^{10} + {}_0n^1 + 4.25$,
(c) ${}_4Be^9 + {}_1H^2 = {}_3Li^7 + {}_2He^4 + 7.0$,[28]
(d) ${}_3Li^7 + {}_1H^1 = 2\,{}_2He^4 + 17.06$,[29]
(e) ${}_5B^{11} + {}_1H^2 = {}_4Be^9 + {}_2He^4 + 0.08$,[21]
(f) ${}_5B^{11} + {}_1H^1 = 3\,{}_2He^4 + 8.7$,[30]
(g) ${}_5B^{11} + {}_1H^2 = {}_6C^{12} + {}_0n^1 + 13.5$,
(h) ${}_7N^{14} + {}_1H^2 = {}_6C^{12} + {}_2He^4 + 13.22$,[21]
(i) ${}_8O^{16} + {}_1H^2 = {}_7N^{14} + {}_2He^4 + 2.95$,[21]
(j) ${}_6C^{13} + {}_1H^2 = {}_5B^{11} + {}_2He^4 + 5.11$,[21]
(k) ${}_6C^{12} + {}_1H^2 = {}_6C^{13} + {}_1H^1 + 2.66$,[21]
(l) ${}_5B^{10} + {}_2He^4 = {}_6C^{13} + {}_1H^1 + 3.1$,[31]

[24] Bothe and Becker, Zeits. f. Physik **76**, 421 (1932).
[25] Curie and Joliot, J. de phys. et rad. **4**, 494 (1933).
[26] J. Chadwick, Proc. Roy. Soc. **A142**, 1 (1933).
[27] N. Feather, Nature **136**, 467 (1935).
[28] Oliphant, Kempton and Rutherford, Proc. Roy. Soc. **A150**, 241 (1935).
[29] Oliphant, Kempton and Rutherford, Proc. Roy. Soc. **A149**, 406 (1935).
[30] Dee and Gilbert, Proc. Roy. Soc. **A154**, 279 (1936).
[31] Miller, Duncanson and May, Proc. Camb. Phil. Soc. **30**, 549 (1934).

and the mass differences given above.

(a)+(b)−(c)−(d) gives

$$_5B^{11}=3_2He^4-{}_1H^1+8.45\pm0.25 \text{ MEV}.$$

(c)+(d)+(e) gives

$$_5B^{11}=3_2He^4-{}_1H^1+8.32\pm0.22 \text{ MEV}.$$

Another relation is given directly by (f)

$$_5B^{11}=3_2He^4-{}_1H^1+8.7\pm0.3 \text{ MEV}.$$

The weighted mean of these values is

$$_5B^{11}=3_2He^4-{}_1H^1+8.5\pm0.2 \text{ MEV}.$$

The O^{16}/B^{11} ratio can be determined from

(g)−(h)−(i) which gives

$$_8O^{16}=_5B^{11}+2_2He^4-{}_1H^2-{}_0n^1+2.67\pm0.31 \text{ MEV}.$$

Another way to find this ratio is that used by Cockcroft and Lewis from reactions (h)+(i)+(j)+(k) which yields

$$_8O^{16}=_5B^{11}+2_2He^4-{}_1H^2-{}_0n^1+2.38\pm0.21 \text{ MEV}.$$

A third, but less direct way is that originally used by Bethe, (a)+(h)+(i)+(k)−(l) from which

$$_8O^{16}=_5B^{11}+2_2He^4-{}_1H^2-{}_0n^1+3.27\pm0.50 \text{ MEV}.$$

The weighted mean of these three values is

$$_8O^{16}=_5B^{11}+2_2He^4-{}_1H^2-{}_0n^1+2.7\pm0.3 \text{ MEV}.$$

Combining this with the value of the B^{11}/He^4 ratio leads to

$$_8O^{16}=4_2He^4-14.87\pm0.35 \text{ MEV}.$$

or $$_2He^4=4.0040+0.0001.$$

This disintegration mass of He^4 agrees with Aston's[17] new mass spectrograph value (4.0039) within the experimental errors. The mass of $_1H^1$ can be obtained only from mass spectrographic data. Aston gives the value 1.0081, and the value deduced from Bainbridge and Jordan's ($H_2^1-H^2$) difference is also 1.0081. Using the values of the masses just determined, we can now compute the masses of the other light elements. A summary of these is given below.

$O^{16}=16.0000$	$C^{11}=11.0150$	$Li^7=7.0182$
$O^{15}=15.0079$	$B^{12}=12.0179$	$Li^6=6.0170$
$N^{16}=16.0066$	$B^{11}=11.0128$	$He^4=4.0040$
$N^{15}=15.0049$	$B^{10}=10.0160$	$He^3=3.0171$
$N^{14}=14.0075$	$Be^{10}=10.0163$	$H^3=3.0170$
$N^{13}=13.0100$	$Be^9=9.0149$	$H^2=2.0147$
$C^{14}=14.0078$	$Be^8=8.0080$	$H^1=1.0081$
$C^{13}=13.0076$	$Li^8=8.0195$	$n^1=1.0090$
$C^{12}=12.0040$		

The probable errors of most of the masses is 0.0001 or 0.0002, but the probable errors of the radioactive atoms Li^8 and B^{12} may be greater. In most cases the mass values agree within 0.0002 mass units with those calculated by Oliphant,[32] from a combination of mass spectrographic and disintegration data.

In conclusion, we wish to thank Mr. Kamal Djanab for his assistance in some of the experiments. We are indebted to Professor C. C. Lauritsen for his interest in the work and to the Seeley W. Mudd fund for financial support.

[32] M. L. Oliphant, Nature **137**, 396 (1936).

The Magnetic Moment of the Li^7 Nucleus. II

J. H. BARTLETT, JR., J. J. GIBBONS, JR. AND R. E. WATSON, *Department of Physics, University of Illinois, Urbana, Illinois*

(Received June 1, 1936)

Calculation of the magnetic moment of the Li^7 nucleus, using the experimental data of Fox and Rabi and a wave function due to James and Coolidge, results in the value 3.33 nuclear magnetons.

THE magnetic moment of a nucleus is at present determined in a rather indirect way. The hfs splitting of some atomic level is found experimentally (either spectroscopically or by the molecular beam method) and the computed interaction of nucleus with the electron cloud is then used to evaluate the magnetic moment. To compute the interaction for many electrons, one must make an assumption as to the interaction operator, which is then averaged over configuration space. The averaging process requires some knowledge of the electronic wave function. One usually assumes the form of this function, and then determines its constants by the Ritz variational method.

Until quite recently, there has been no opportunity to obtain a fairly accurate check of the hyperfine structure theory, since variational wave functions were not available. The value of the magnetic moment of the lithium nucleus as calculated from the normal atom with a Fock function was shown to be in disagreement with the value calculated from ionized lithium with a Hylleraas-type function.[1,2] If the latter type of function be assumed to be the more accurate (since there is closer agreement with the experimental values of energy), and the theory of hfs supposed to be correct, then one must conclude that Fock functions are inadequate for calculation of nuclear moments.

However, the situation for lithium has been changed considerably with the computation by James and Coolidge[3] of a ground state wave function involving the interelectronic distances. It seemed, therefore, of some interest to see what the corresponding value of the magnetic moment would be.

HYPERFINE STRUCTURE FORMULA

We have extended the theory of Breit and Doermann[2] to the three-electron case. For one electron, the perturbing part of the Hamiltonian may be written as

$$H'=\frac{(e/mc)(M\cdot\mu)}{1+(E-mc^2+eA_0)2mc^2}\cdot\frac{1}{r^3}+\frac{hec/2\pi}{E+mc^2+eA_0}\left\{-\frac{(\mu\cdot\sigma)}{r^3}+\frac{3(r\cdot\sigma)(r\cdot\mu)}{r^5}\right\}$$

$$+\frac{(hec/2\pi)(e|\mathcal{E}|)}{(E+mc^2+eA_0)^2}\left\{\frac{(\mu\cdot\sigma)}{r^2}-\frac{(r\cdot\sigma)(r\cdot\mu)}{r^4}\right\}$$

$$=(B\cdot\mu)+(A\cdot\sigma).$$

It is assumed that the perturbation for three electrons is simply the sum of three such terms, each pertaining to a particular electron, i.e.

$$\sum H'=\mu\cdot\sum_{j=1}^{3}B_j+\sum_{j=1}^{3}A_j\cdot\sigma_j.$$

To find the hfs splitting for normal lithium, it is sufficient to calculate the energy displacement w for the state of highest f, and to apply the interval rule. The wave function for this state may be

[1] Results on the basis of a Fock function were obtained by Bartlett and Gibbons, Phys. Rev. **49**, 552 (1936).
[2] Breit and Doermann, Phys. Rev. **36**, 1732 (1930).
[3] H. M. James and A. S. Coolidge, Phys. Rev. **49**, 688 (1936).

written $\mu = N_1\Phi$, where Φ is the electronic function for $m_s = \frac{1}{2}$, and N is the nuclear function. Since μ_z is the only component of μ with diagonal elements, we may, for the present purpose, confine our attention to it. The perturbation is, effectively:

$$\mu_z \sum_{j=1}^{3} (B_j)_z + \sum_{j=1}^{3} (A_j)_z (\sigma_j)_z.$$

Now
$$(B_j)_z = \frac{(e/mc)}{1+[E-mc^2+e(A_0)_j]/2mc^2} \cdot \frac{1}{r_j^3} \cdot \frac{\hbar}{i} \frac{\partial}{\partial \varphi_j}.$$

The wave function of James and Coolidge is of the form:

$$\Phi = F(123)S(12\bar{3}) + F(231)S(23\bar{1}) + F(312)S(31\bar{2})$$

where the F's are space functions, the S's spin functions, and the bar denotes the electron with β-spin. This is not a function of ϕ_1, ϕ_2 or ϕ_3, but only of the mutual distances. Therefore, there will be no contribution from the B_j's. The above displacement is, then,

$$\begin{aligned} w &= \int \Phi^* (A_{1z}\sigma_{1z} + A_{2z}\sigma_{2z} + A_{3z}\sigma_{3z})\Phi d\tau \\ &= 3\int [F(123)]^2 \{A_{1z} + A_{2z} - A_{3z}\} d\tau \\ &= 3\{\int [F(123)]^2 A_{1z} d\tau + \int [F(213)]^2 A_{1z} d\tau - \int [F(321)^2] A_{1z} d\tau\}, \end{aligned}$$

since the spin functions above are mutually orthogonal. Here,

$$(A)_z = \frac{hec/2\pi}{E+mc^2+eA_0}\left(-\frac{1}{r^3} + \frac{3z^2}{r^5}\right)\mu_z + \frac{(hec/2\pi)e|\mathcal{E}|}{(E+mc^2+eA_0)^2}\left(\frac{1}{r^2} - \frac{z^2}{r^4}\right)\mu_z.$$

The first term involves $P_2(\cos\theta)$, so that there is no contribution to the integral from this. Effectively, then,

$$A_z = \frac{(hec/2\pi)e[dA_0/dr]}{(E+mc^2+eA_0)^2} \frac{\mu_z}{r^2} \cdot \frac{2}{3}, \quad \text{since} \quad \frac{z^2}{r^2} = \frac{1}{3}(P_0 + 2P_2).$$

We have to evaluate integrals such as $\int f^2 A_z dt$, where f is a known function.

$$\begin{aligned} \int f^2 A_z dt &= -4\pi \int f^2 \left(\frac{hec}{2\pi}\right) \cdot \frac{2}{3}\left(\frac{d}{dr}\frac{1}{E+mc^2+eA_0}\right) dr \cdot \mu \\ &= +\frac{8\pi}{3}\mu \int 2ff' \frac{(hec/2\pi)}{2mc^2} dr \\ &= \frac{8\pi}{3}\mu \frac{hec/2\pi}{2mc^2} f^2(0) = \frac{8\pi}{3}\mu\mu_0 f^2(0). \end{aligned}$$

The function $F(123)$ is antisymmetric in electrons 1 and 2, hence

$$w = (8\pi/3)\mu\mu_0 \cdot 3\int [2F^2(000, x_2, y_2, z_2, x_3, y_3, z_3) - F^2(x_3y_3z_3, x_2y_2z_2, 000)] d\tau_2 d\tau_3. \qquad \text{(A)}$$

This represents the energy referred to the center of gravity of the hfs multiplet. [For comparison with the simple theory (wave function separable), put $F(123) = (1/6)^{\frac{1}{2}}\{1s(1)2s(2) - 2s(1)1s(2)\}1s(3)$, etc.

Then
$$\int F(023)^2 d\tau_2 d\tau_3 = 1/6\{[1s(0)]^2 + [2s(0)]^2\}.$$

Combining, one finds that $w = \frac{1}{3}8\pi\mu\mu_0[2s(0)]^2$, which is the ordinary formula.] The doublet separation is, according to the interval rule, $\Delta s = w(2I+1)/I$. (I denotes the nuclear spin.)

Wave Function

The wave function to be used is

$$\Phi = F(123)S(12\bar{3}) + F(231)S(23\bar{1}) + F(312)S(31\bar{2}),$$

where $$F(123) = (1/\pi)^{\frac{1}{2}}\{\sum A_{kmnp} f_{kmnp}(123) + \sum B_{kmnp} g_{kmnp}(123) + \sum C_{kmnp} h_{kmnp}(123)\},$$

$$f_{kmnp}(123) = \psi_{kmnp}(123) - \psi_{kmnp}(213),$$

$$g_{kmnp}(123) = \varphi_{kmnp}(123) - \varphi_{kmnp}(213),$$

$$h_{kmnp}(123) = \chi_{kmnp}(123) - \chi_{kmnp}(213),$$

and $$\psi_{kmnp}(123) = e^{-(\gamma r_1 + \delta r_2 + \delta r_3)} r_1{}^k r_2{}^m r_3{}^n r_{12}{}^p,$$

$$\varphi_{kmnp}(123) = e^{-(\gamma r_1 + \delta r_2 + \delta r_3)} r_1{}^k r_2{}^m r_3{}^n r_{23}{}^p,$$

$$\chi_{kmnp}(123) = e^{-(\gamma r_1 + \delta r_2 + \delta r_3)} r_1{}^k r_2{}^m r_3{}^n r_{31}{}^p.$$

Here r_1 refers to the $2s$ electron, r_2 to the $1s$ electron with the same spin as the $2s$ electron, r_3 to the other $1s$ electron. James and Coolidge give the following coefficients for the approximate function $F(123)$:[3]

$$B_{1000} = 1.088500, \qquad B_{1001} = 0.583191,$$
$$B_{1010} = 0.058054, \qquad B_{1002} = -0.075465,$$
$$B_{1100} = 0.058054, \qquad B_{0^*000} = -0.970781,$$
$$B_{1020} = B_{1200} = 0.468163, \qquad B_{0^*010} = B_{0^*100} = -0.232377,$$
$$B_{1110} = -0.281807, \qquad A_{0001} = 0.196518,$$
$$C_{0001} = 0.241624.$$

The coefficients marked by the asterisk belong to terms in which the constant γ is to be replaced by γ^*. For example, -0.970781 is the coefficient of g_{0^*000} which is $[e^{-(\gamma^* r_1 + \delta r_2 + \delta r_3)} - e^{-(\gamma^* r_2 + \delta r_1 + \delta r_3)}]$. The values of the constants in the exponentials are: $\delta = 3$, $\gamma = 0.65$, $\gamma^* = 1.5$.

For brevity, write $F(123)_{r_1=0} = F(023)$, etc., and $e^{-(\gamma r_1 + \delta r_2 + \delta r_3)} = (123)$.

Then
$$F(203) = (1/\pi)^{3/2}[(-1.285018 r_2 - 0.641245\, r_2 r_3 - 0.392698\, r_2 r_3{}^2)(203) - 0.970781\{(0^*23) - (2^*03)\} + 0.232377\, r_3(2^*03) + 0.009247\, r_3(023) - 0.241624\, r_{23}(203) - 0.035859\, r_2(023)],$$

$$F(230) = f(23) - f(32),$$

where
$$f(23) = (1/\pi)^{3/2}\{(230)[1.330124\, r_2 + 0.641245\, r_2 r_3 + 0.392698\, r_2 r_3{}^2 + 0.196518\, r_{23}] - (2^*30)[0.970781 + 0.232377\, r_3]\}.$$

Integrals

Since $\int f^2(23) d\tau_2 d\tau_3 = \int f^2(32) d\tau_2 d\tau_3$, the calculation simplifies. For purposes of checking, we present the results in tabular form. Table I contains the contributions to $\int F(023)^2 d\tau_2 d\tau_3$, Table IIa the contributions to $\int f^2(23) d\tau_2 d\tau_3$, and Table IIb those to $\int f(32) f(23) d\tau_2 d\tau_3$ (except for a factor $(16/\pi)$, which multiplies everything). The entry at the head of a column gives the multiplicand, that at the left of a row the multiplier. The integral of their product is the entry in the table itself. The square

Table I. *Contributions to* $\int F(023)^2 d\tau_2 d\tau_3$.

	-1.285018 $(203)r_2$	-0.641245 $(203)r_2r_3$	-0.392698 $(203)r_2r_3^2$	-0.970781 (2^*03)	0.970781 (2^*03)	0.232377 $(2^*03)r_3$	-0.035859 $(023)r_2$	0.009247 $(023)r_3$	-0.241624 $(203)r_{23}$
-1.285018 $(203)r_2$	0.0988301								
-0.641245 $(203)r_2r_3$	0.0246589	0.0082035							
-0.392698 $(203)r_2r_3$	0.0100674	0.0041865	0.0025638						
-0.970781 (0^*23)	0.0003905	0.0000974	0.0000398	0.0000808					
0.970781 (2^*03)	-0.0032434	-0.0008093	-0.0003304	-0.0001915	0.0006438				
0.232377 $(203)r_3$	-0.0003882	-0.0001291	-0.0000659	-0.0000229	0.0000774	0.0000123			
-0.035859 $(023)r_2$	0.0000158	0.0000039	0.0000016	0.0000015	-0.0000047	-0.0000006	0.0000000		
0.009247 $(023)r_3$	-0.0000019	-0.0000006	-0.0000003	-0.0000004	0.0000009	0.0000002	0.0000000	0.0000000	
-0.241624 $(023)r_{23}$	0.0188871	0.0047559	0.0019656	0.0000881	-0.0006571	-0.0000821	0.0000033	-0.0000005	0.0036583

TABLE IIa. *Contributions to* $\int f(23)^2 dr_2 dr_3$.

	1.330124 (230)r_2	0.641245 (230)r_2r_3	0.392698 (230)$r_2r_3^2$	0.196518 (230)r_{23}	−0.970781 (2*30)	−0.232377 (2*30)r_2
1.330124 (230)r_2	0.1058900					
0.641245 (230)r_2r_3	0.0255445	0.0082035				
0.392698 (230)$r_2r_3^2$	0.0104208	0.0041865	0.0025638			
0.196518 (230)r_{23}	0.0158872	0.0038371	0.0015987	0.0024199		
−0.970781 (2*30)	−0.0033573	−0.0008093	−0.0003304	−0.0005344	0.0006464	
−0.232377 (2*30)r_3	−0.0004018	−0.0001291	−0.0000659	−0.0000668	+0.0000774	+0.0000123

TABLE IIb. *Contributions to* $\int f(23)f(32)dr_2 dr_3$.

	1.330124 (230)r_2	0.641245 (230)r_2r_3	0.392698 (230)$r_2r_3^2$	0.196518 (230)r_{23}	−0.970781 (2*30)	−0.232377 (2*30)r_2
1.330124 (320)r_2	+0.0020218					
0.641245 (320)r_2r_3	+0.0010682	+0.0005643				
0.392698 (320)$r_2r_3^2$	+0.0008961	+0.0004734	+0.0003972			
0.196518 (320)r_{23}	+0.0005082	+0.0002263	+0.0001709	+0.0001177		
−0.970781 (3*20)	−0.0009581	−0.0003079	−0.0001676	−0.0001877	+0.0004540	
−0.232377 (3*20)r_2	−0.0002513	−0.0000808	−0.0000440	−0.0000442	+0.0000724	+0.0000116

arrays are symmetrical about the main diagonal, so that only about half of the total number of entries need be given.

The integration of $F^2(123)$, etc. was straightforward for terms not involving r_{23}. For example, the first term in $\int F(023)^2 dr_2 dr_3$ is

$$(1/\pi)^3(1.285018)^2\int_0^\infty e^{-2\gamma r_2}r_2^4 dr_2\int_0^\infty e^{-2\delta r_3}r_3^2 dr_3\int_0^\pi \sin\theta_2 d\theta_2\int_0^\pi \sin\theta_3 d\theta_3\int_0^{2\pi} d\varphi_2\int_0^{2\pi} d\varphi_3$$
$$=(16/\pi).09883008.$$

For terms involving $r_{23}^2=r_2^2+r_3^2+2r_2r_3$ $(\cos\theta_2\cos\theta_3+\sin\theta_2\sin\theta_3\cos(\phi_2-\phi_3)$ the angular parts integrate to zero, leaving the integral of $(r_2^2+r_3^2)$. The terms involving r_{23} are integrated most easily with a transformed volume element,[4] in which r_{23} appears as variable of integration, between the limits $|r_2-r_3|$ and (r_2+r_3):

$$r_2^2r_3^2\sin\theta_2\sin\theta_3 d\theta_2 d\theta_3 d\phi_2 d\phi_3 dr_2 dr_3 = r_2r_3r_{23}dr_{23}\sin\theta' d\theta' d\phi' d\phi dr_2 dr_3,$$

where $\theta'=\theta_2$, $\phi'=\phi_2$, and ϕ is the angle between r_2 and r_3. The range of integration falls into two parts, one for $r_2<r_3$, and the other for $r_3<r_2$. It was found that certain terms cancel out when one integrates first from $r_3=0$ to $r_3=\infty$. For illustration, in Table IIa the entry 0.0158872 represents, except for the factor $16/\pi$, the value of,

$$(0.196518)(1.330124)\int e^{-2\gamma r_2}r_2^2 dr_2\int e^{-2\delta r_3}r_3 dr_3\int_{|r_2-r_3|}^{r_2+r_3} r_{23}^2 dr_{23}. \qquad (B)$$

The last integral in this expression is $2r_2^2r_3+(2/3)r_3^3$ if $r_3<r_2$, and $2r_2r_3^2+(2/3)r_2^3$ if $r_2<r_3$. Integrating as above, we obtain the result

$$\int_0^\infty e^{-2\gamma r_2}r_2^2\left(2r_2^2\int_0^{r_2} e^{-2\delta r_3}r_3^2 dr_3+(2/3)\int_0^{r_2} e^{-2\delta r_3}r_3^4 dr_3+2r_2\int_{r_2}^\infty e^{-2\delta r_3}r_3^3 dr_3+(2/3)r_2^3\int_{r_2}^\infty e^{-2\delta r_3}r_3 dr_3\right)dr_2.$$

The integrals appearing within the parenthesis are of the form

$$\int_0^r e^{-ar}r^n dr=(n!/a^{n+1})-\sum_{\nu=0}^{n}\frac{n!}{(n-\nu)!}\frac{r^{n-\nu}}{a^\nu} \quad\text{and}\quad \int_r^\infty e^{-ar}r^n dr=\sum_{\nu=0}^{n}\frac{n!}{(n-\nu)!}\frac{r^{n-\nu}}{a^\nu}.$$

Let us write

$$[b]_n=\frac{n!}{b^{n+1}}=\int_0^\infty e^{-br}r^n dr.$$

[4] Cf. E. A. Hylleraas, Zeits. f. Physik **48**, 475 (1928).

Then all the integrals in question which involve r_{23} can be evaluated as:

$$[a]_{m+3}[b]_{n+2}+(1/3)[a]_{m+1}[b]_{n+4}-(2/b^4)[a+b]_{m+n+2}-(8/b^5)(n+1)[a+b]_{m+n+1}$$
$$-(20/b^6)(n+1)n[a+b]_{m+n}-(40/b^7)(n+1)(n)(n-1)[a+b]_{m+n-1}$$
$$-(70/b^8)(n+1)n(n-1)(n-2)[a+b]_{m+n-2}-\cdots$$

where m and n are the powers, less one, of r_2 and r_3 appearing in the first two integrands of (B). For our integrals, this seven term formula suffices. In the example above, $a=2\gamma$, $b=2\delta$, $m=1$, $n=0$. We have then,

$$16/\pi(0.196518)\{(1.330124)[2\gamma]_4[2\delta]_3+(1/3)[2\gamma]_2[2\delta]_4-\{2/(2\delta)^4\}[2\gamma+2\delta]_3$$
$$-8(2\delta)^{-5}[2\gamma+2\delta]_2\}=(16/\pi)(0.0158872).$$

The values of the two integrals are:

$$\int F(023)^2 d\tau_2 d\tau_3=(16/\pi)0.232590, \quad \int F(230)^2 d\tau_2 d\tau_3=(16/\pi)0.450318.$$

If the second be subtracted from twice the first, the result is $(16/\pi)$ 0.014862.

The Magnetic Moment

Let us substitute in Eq. (A), and use $\Delta s=0.0267$ as determined by Fox and Rabi.[5]

$$0.0267=[8\pi(8/3)(g/1838)\mu_0^2(16/\pi)0.014862]/[(0.528\times10^{-8})^3(19.662\times10^{-17})]; \quad \mu_0=0.9174\times10^{-20}.$$

This gives $g=3.33$ nuclear magnetons for the value of the magnetic moment. This is to be compared with that of 3.29 given by Granath[6] (from measurements of hfs in Li^+ and the theory of Breit and Doermann).

Discussion

The excellent agreement between the two values of the magnetic moment, one determined from measurements on Li^+ and the other from normal Li data, would ordinarily be acceptable as strong evidence that the true value is in the immediate neighborhood. However, there are certain factors which require one to be rather cautious in drawing such a conclusion.

In the first place, our calculation involves the subtraction of two large, approximately equal, quantities. The contribution of the r_{23} terms to $\int[F(023)]^2 d\tau_2 d\tau_3$ is $(16/\pi)0.049889$; that to $\int[F(230)]^2 d\tau_2 d\tau_3$ is $(16/\pi)0.080317$. Subtracting the second from twice the first, one obtains $(16/\pi)0.019461$, which is larger than the corresponding result for all the terms i.e. $(16/\pi)$ 0.014862. This indicates the sensitiveness of the calculation to terms involving the interelectronic distances. It is quite possible that such terms could be modified in such a way that their influence on the energy would be small, but so that the nuclear moment would be changed appreciably.

Secondly, it is not known how good either the Breit-Doermann function or the James and Coolidge function is. A function may give good energy values, but yet be considerably in error near the singularities of the wave equation.

For these reasons, we prefer for the present to regard the value of the magnetic moment of the lithium nucleus as a quantity which has not been determined with great accuracy. If it should prove feasible to measure this moment in a more direct manner, then such a procedure would be much to be preferred, and it would give us more information about electronic wave functions as well.

[5] Fox and Rabi, Phys. Rev. **48**, 746 (1935).
[6] Granath, Phys. Rev. **42**, 44 (1932).

Scattering of Fast Electrons by Helium

A. L. HUGHES* AND S. S. WEST, *Wayman Crow Laboratory of Physics, Washington University, St. Louis, Missouri*

(Received June 1, 1936)

When a charged particle collides with another charged particle, the force between them varying inversely as the square of the distance, wave mechanics and classical mechanics give the same scattering formula when the particles are unlike, and different formulas when they are identical. In the particular case of scattering of electrons by electrons, wave mechanics predicts a smaller scattering than does classical mechanics, in a ratio which has a minimum of 1 to 2 at 45°. The scattering of 2000 and 4000 volt electrons by helium atoms has been investigated. For such energy values, the scattering at considerable angles (>20°) is due to the nuclei and to atomic electrons acting independently of each other. Thus it is possible to measure the ratio of the scattering by the atomic electrons to that by the nucleus and compare it with the values given by the two theories. The elastically scattered electrons are to be identified with those scattered by the nucleus while the inelastically scattered electrons are to be identified with those scattered by atomic electrons. The results are in quantitative agreement with the wave mechanical theory of collisions between electrons. A subsidiary result of the investigation is that the distribution of energies among the inelastically scattered electrons may be used to show that the velocity of the atomic electrons has a value close to that given by the Bohr theory.

THE problem of the scattering of one particle by another particle, attracting or repelling each other according to the inverse square law, has been investigated on the classical particle theory and on the wave mechanical theory. When the particles are unlike both theories lead to the same scattering formulas, but when the particles are identical the two theories lead to different scattering formulas. In this paper it is shown that, when electrons are scattered by electrons, the experimental results are decisively in favor of the wave mechanical description of the scattering process.

The formula for the scattering of electrons by bare nuclei is

$$\alpha=(Z^2e^4/4m^2v^4)\ \mathrm{cosec}^4\ (\phi/2), \qquad (1)$$

where α is the probability that an electron of mass m and velocity v will be scattered into unit solid angle, at an angle ϕ with its original direction, by a nucleus of charge Ze. (It is assumed that the electron may be moving before collision with equal probability along any path, within and parallel to the axis of a column of unit cross section, which contains the scattering nucleus.) This formula was derived by Rutherford on the classical particle theory.[1] Wave mechanics leads to precisely the same formula.[2]

For the scattering of electrons by electrons initially at rest, Darwin found that the classical particle theory gave

$$\alpha_1=(e^4/m^2v^4)\ 4\cos\phi\ (\mathrm{cosec}^4\ \phi+\sec^4\phi). \qquad (2)$$

The recoil electrons which after collision are indistinguishable experimentally from the impinging electrons are included in this formula. When, however, the problem is considered from the standpoint of wave mechanics, Mott[3] showed that it was necessary to take into account the spin of the electron. This led to the formula

$$\alpha_2=(e^4/m^2v^4)\ 4\cos\phi\ (\mathrm{cosec}^4\ \phi+\sec^4\phi - \Phi\ \mathrm{cosec}^2\ \phi\ \sec^2\phi), \qquad (3)$$

where

$$\Phi=\cos\ ((2\pi e^2/hv)\log\tan^2\phi).$$

Under our experimental conditions (angles over 20° and electron energies in excess of 2000 volts), Φ is within 2 percent of unity, and we shall therefore write $\Phi=1$. The ratio between the values of α_1 and α_2 reaches a maximum of 2 to 1 at 45°. The relationship at other angles may be inferred from Fig. 7.

Since it is easier experimentally to make relative measurements than to make absolute measurements, we arranged to measure the *ratio* of the scattering by electrons to that by nuclei, and then to compare the ratios found experimentally with those given by the two theories. We cannot secure free nuclei and free electrons for scattering measurements. The next best

* The senior author was aided in part by a grant from the Rockefeller Foundation to Washington University for research in science.

[1] E. Rutherford, Phil. Mag. **21**, 669 (1911).

[2] N. F. Mott and H. S. W. Massey, *The Theory of Atomic Collisions*, Chap. III (Oxford University Press, 1933).

[3] N. F. Mott, Proc. Roy. Soc. **A126**, 259 (1930).

thing to do is to use hydrogen or helium in which the electrons are bound so loosely to the nuclei that the binding energy can be neglected when the electrons in the beam have energies exceeding 1000 volts. In order that we may consider the gas as essentially a mixture of nuclei and electrons acting as independent scattering centers (as though they were not grouped together in atoms), the collision parameters for an appreciable deflection must be such that any one scattering event must be due *either* to a nucleus, *or* to an atomic electron, but never to both. In Fig. 1, we have drawn to scale the paths along which a 2000 volt electron must move in order to be deflected through 30° by a helium nucleus and by an electron at rest. The distance between the two centers is the most probable distance between the nucleus and an atomic electron in the helium atom. It is evident that, when a 2000 volt electron is scattered through 30° or more by a helium atom, it must have been scattered either by the nucleus, or by an atomic electron, except in those very infrequent cases in which the particles constituting the atom happen to be orientated so that the incoming electron, after being deflected by one particle, is then deflected again by a second particle before it leaves the atom.

Since there are two atomic electrons in helium to each nucleus, the ratio of the scattering by the atomic electrons in an atom to that by the nucleus will be $\alpha_1'/\alpha = 2\alpha_1/\alpha$ on the classical particle theory and $\alpha_2'/\alpha = 2\alpha_2/\alpha$ on the wave mechanical theory. α_1'/α and α_2'/α, so defined, are the quantities to be compared with the experimentally determined ratio α'/α.

We can distinguish readily between scattering by nuclei and scattering by atomic electrons by the fact that electrons lose no energy when they are scattered by nuclei but do lose energy when they are scattered by atomic electrons. In the latter case the energy of the electrons after collision is $V = V_0 \cos^2\phi$, where V_0 is the energy of the impinging electrons, and ϕ is the angle which the path of an electron makes after collision with the path of the impinging electron before collision. Consequently in the graph showing the scattered electron current as a function of the retarding potential, there should be two steps, one corresponding to those electrons

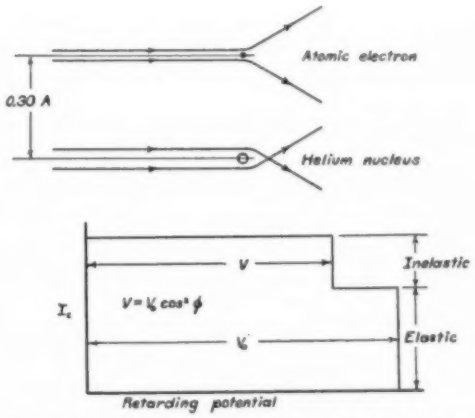

FIG. 1. *Above:* Scattering of a 2000 volt electron by an atomic electron and helium nucleus. *Below:* Theoretical scattered electron current *v.* retarding voltage curve.

which have been scattered without loss of energy and the other corresponding to those which have been scattered with loss of energy (Fig. 1). If the atomic electrons are in random motion, instead of being at rest, as we have assumed up to the present, the discontinuous step will be replaced by a sloping line indicating a range of energies instead of a single energy $V = V_0 \cos^2\phi$. The ratio of the number of electrons scattered inelastically to the number scattered elastically can be read off the experimental curves and compared with the theoretical values.

Klemperer[4] investigated the scattering of 30 to 45 kilovolt electrons by a thin collodion film. The energies of the inelastically scattered electrons were far from being grouped around the energy given by $V = V_0 \cos^2\phi$, as theory would suggest. It is probable therefore that some degree of multiple scattering was unavoidable in his experiments. It may be concluded that his results are in better accord with the wave mechanical theory than with the classical theory, the agreement being qualitative rather than quantitative. Mohr and Nicol[5] studied the angular distribution of the electrons scattered inelastically by hydrogen and helium and found ill defined humps at the angles corresponding to scattering by isolated electrons. Since their electron energies were not over 300 volts, one

[4] O. Klemperer, Ann. d. Physik **15**, 361 (1932).
[5] C. B. O. Mohr and F. H. Nicol, Proc. Roy. Soc. **A144**, 596 (1934).

cannot expect to find the scattering by the nuclei clearly separated from the scattering by the atomic electrons.

Apparatus and Experimental Procedure

The essential features of the apparatus are shown in Fig. 2. The scattering chamber consists of a brass cylinder, which was made vacuum tight by beeswax and rosin mixture. Through one end of this cylinder (perpendicular to the plane of the figure) passes the shaft of the turntable which carries the electron gun. The shaft forms part of the inside member of a tapered greased joint, the outer member being a piece of clear Bakelite. The brass cylinder of the analyzer is attached at one side of the scattering chamber. Two tubes open into the chamber, one from the pumps and one from a capillary leak connected to the gas storage reservoir. The analyzer has no opening into the main chamber except the narrow defining slits and is evacuated by means of a separate connection to the pumps.

The electron gun is mounted on a brass plate perpendicular to the turntable and extending nearly to the walls on all sides, thus rendering the scattering region field-free. On this plate is mounted a cylinder containing three slits of thin sheet platinum of dimensions 0.4×2.0 mm and 10 mm apart, and behind these is a square shell containing the filament. In the one mm thick front face of this shell is a slit of dimensions 1.0×5.0 mm with longer edges beveled 45° on the outside of the face. Between the filament and shell is applied a potential difference V_1 of 2 to 25 volts and between the shell and the rear one of the narrow defining slits a potential difference V_0 of 2000 or 4000 volts. The gun is aligned with the axis of the analyzer by removing the square shell and filament and observing through the analyzer a light placed behind the gun slits. However, the actual center of the electron beam is later found electrically by means of the analyzer, and the scattering angle is measured from that point. The angular spread of the electron beam by the latter method corresponds to about 2° rotation of the turntable. The current in the beam was kept between one and five microamperes.

The homogeneity of the electron beam with respect to energy can be seen from the solid curve in Fig. 3. However, when scattering measurements are being made under a fairly high pressure, the energy distribution of the incident electrons is that shown by the dashed curve. This spread of energies arises in the accelerating field within the gun and is unavoidable when the gun is operated in gas at an appreciable pressure. The same sort of inhomogeneity is observed in the elastically scattered electrons of Fig. 4 to 6, for these cannot be expected to be more homogeneous than the primary electrons.

The analyzer is essentially a pair of slits to define the solid angle from which electrons are received, a retarding field to measure electron energies, and a Faraday cylinder to collect the scattered electrons. The defining slits (S_1 and S_2, Fig. 2) are 0.3×2.0 mm, the slit S_3 2×9 mm, and the slit S_4 3×7 mm. The distance from S_1 to S_2 is 28 mm, from S_2 to S_3 7 mm, from S_3 to S_4 12 mm, and from S_4 to the Faraday cylinder 3 mm. The inside diameter of the Faraday cylinder is 10 mm and its depth 35 mm. S_3 is put at a potential of +45 volts with respect to S_2 to turn back any positive ions that might pass through the defining slits. Between S_3 and S_4 is applied the retarding field. The lead from the Faraday cylinder passes through an amber plug to the grid of the FP 54. The defining slits are of thin platinum sheet, other slits of thin brass.

The high voltage supply is a full-wave rectifier with filter system capable to reducing the ripple to less than 0.3 percent of the total voltage. The retarding voltage is taken off across a 50T vacuum tube with filament connected through a high resistance to the negative side of the hv

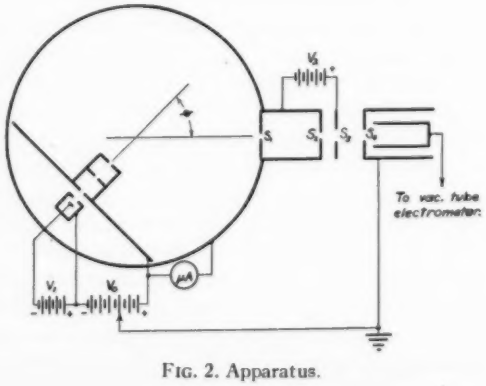

Fig. 2. Apparatus.

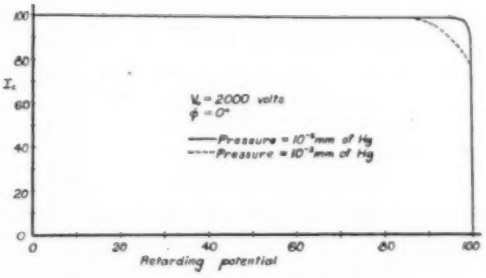

FIG. 3. Homogeneity of the electron beam.

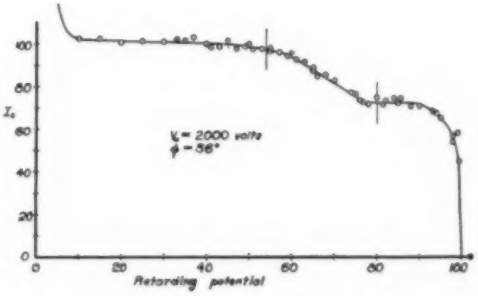

FIG. 4. Experimental curve. 2000 volts, 36°.

supply and plate to the positive side. By varying the grid bias of the 50T tube, one can obtain any retarding voltage from 2 percent to at least 99.5 percent of the accelerating voltage. Higher retarding voltages were obtained by inserting batteries in series with the HV supply. Accelerating and retarding voltages are each measured by a 0–1.0 milliammeter in series with a resistor across the line, the resistor having one megohm for each thousand volts of accelerating voltage. For the retarding voltage the resistor is that used in series with the 50T tube. The unit is capable of giving up to 6000 volts at 2 milliamperes.

Helmholtz coils are used to neutralize the earth's magnetic field. For such fast electrons as we used the adjustment of the current through the coils is not critical, since even without the coils the deflection of the beam is not large.

The gas used was purified by passing it through two charcoal traps immersed in liquid air when filling the reservoir. The helium was the commercial product, which is 95 percent pure. The reservoir is a large sylphon bellows so that the gas can be kept at atmospheric pressure as it is used. The gas flows through a capillary leak into the scattering chamber, the pressure in the chamber being kept at a constant value determined by the influx through this leak and the exhaust through a constricted line to the pumps. The pressure in the chamber can be decreased if desired by expanding the sylphon to decrease the pressure in the reservoir. A charcoal trap cooled with solid CO_2 was inserted in the intake line between leak and chamber. With the flow of gas shut off, the pressure in the chamber was less than 10^{-6} mm of mercury as measured on a McLeod gauge, whereas, with the gas fed in and the pumps on, the pressure averaged 0.025 mm of mercury. Hence for this constant flow method the impurity due to gas evolved in the scattering chamber will certainly be less than one part in a thousand. During scattering measurements the pressure of the gas can be observed constantly by means of a Pirani gauge.

The current to the Faraday cylinder of the analyzer is measured by means of an FP 54 electrometer tube with the DuBridge and Brown balanced circuit at a sensitivity of 120,000 mm/volt. No change was made in the original circuit except to insert a fine adjustment for the grid bias in order to make the open-key and closed-key zeros coincide. The tube and grounding key are enclosed in an evacuated brass case, and all leads, batteries and accessory apparatus are well shielded. The 18 volts for the operation of the circuit are supplied by large glass-cell storage batteries. The rate-of-charge method (with no grid resistor) was used, since it is more sensitive than the constant deflection method and less liable to subjective error. The maximum currents measured in the runs shown in Fig. 4 to 6 were of the order of 10^{-15} amp.

With no gas in the apparatus the observed background current for any of the scattering angles used was apparently due entirely to secondary electrons emitted where the electron beam struck metal surfaces. Except for the case of energies less than about 20 percent of the maximum energy of the beam, this background was never more than one-half percent of the current scattered from the gas and was therefore negligible.

Experimental Results

Typical retarding potential curves are shown in Fig. 4. An ordinate of 100 represents the current corresponding to an arbitrary standard reference retarding voltage, say 20 percent or 30 percent of the accelerating voltage. An abscissa of 100 represents the accelerating voltage V_0. Points on these curves were mostly taken in pairs, one at a retarding voltage V_x, say, and the next at $V_x+V_0(1-\cos^2\phi)$. From each of these pairs a value of the ratio of inelastic to elastic scattering can be calculated. (Only those pairs of which one value is to be found on the upper flat portion of the curve, and the other on the lower flat portion, are used in computing the ratio.) The deviations of these values from their mean give a measure of the error due to fluctuations in the FP 54 circuit and the beam current, which far outweighs any other error. The inelastic and elastic groups are clearly separated and enough of the flat portions is present in each case to fix their magnitudes. Note that the inelastic distribution has an energy spread which is entirely different in character from the spread in the elastic distribution due to the inhomogeneity of the original beam (see Figs. 3, and 4, 5, or 6).

Table I shows the values of the ratio α'/α of inelastic scattering to elastic scattering in helium for various scattering angles. The values in this table are plotted in Fig. 7, in which are also the theoretical curves based on the classical theory and on the Mott theory.

Discussion

It is evident from Table I or Fig. 7 that, when the impinging electrons have 2000 to 4000 volt energies, the experimental values of α'/α, the ratio of the inelastic electron scattering to the elastic electron scattering, agree well with the values calculated on the Mott theory (α_2'/α), and differ widely from the values calculated on the classical particle theory (α_1'/α). The conclusion to be drawn then is that the results are decisively in favor of the wave mechanical description of the collision of two electrons.

We now turn to a subsidiary result of the investigation. When the scattered electron current is plotted as a function of the retarding voltage, as in Figs. 4 to 6, it is found that the inelastically scattered electrons have a spread in energy which (*a*) is larger the greater the angle of scattering, and (*b*) is smaller the greater the energy of the impinging electron. From the equations for the conservation of energy and momentum of two colliding electrons, one of which has a definite velocity and the other (in our case the atomic electron) a velocity which may have any direction at the moment of impact, the range of velocities among the electrons scattered at any angle can be calculated. Jauncey[6] gave a theory of the width of the modified line in the Compton effect on the assumption that the atomic electrons, with which the photons collide, are in random motion with the speed given by the Bohr theory. The same theory gives the range in energies of scattered electrons on substituting electrons for photons. Jauncey's formula for the range in energies is

$$V_1-V_2=4\sin\phi(UV_0)^{\frac{1}{2}},$$

where V_0 is the energy of the impinging electron,

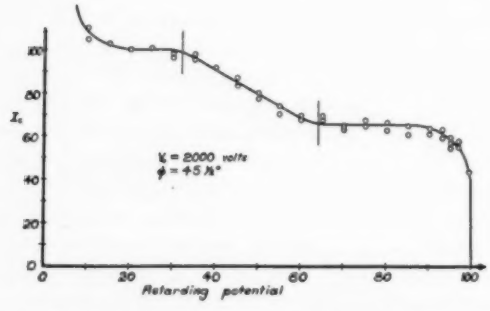

Fig. 5. Experimental curve. 2000 volts, 45.5°.

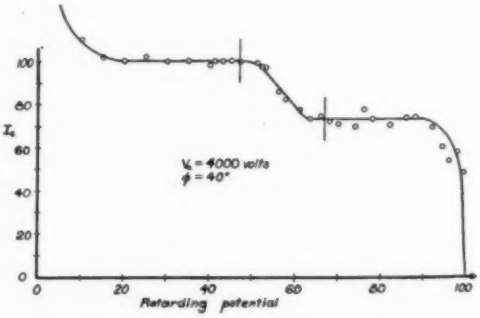

Fig. 6. Experimental curve. 4000 volts, 40°.

[6] G. E. M. Jauncey, Phil. Mag. **49**, 427 (1925).

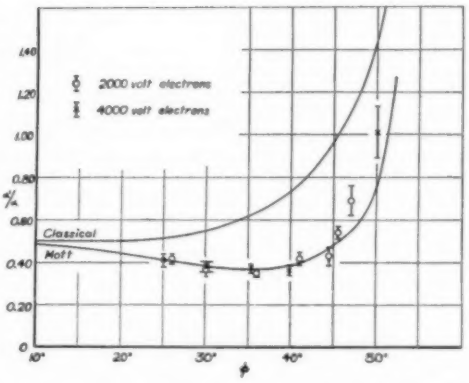

FIG. 7. Comparison of experimental ratios with theoretical ratios (continuous lines).

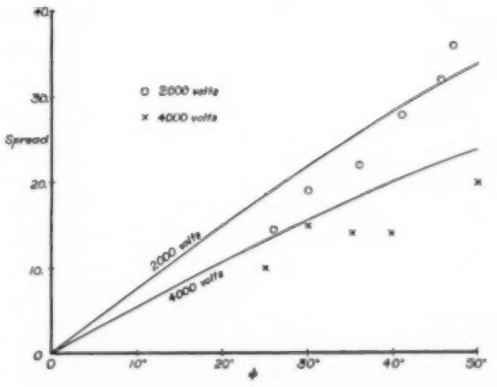

FIG. 8. Spread of energies of the inelastically scattered electrons. *Continuous lines:* theoretical ratios. *Circles* and *crosses:* experimental points for 2000 and 4000 volt electrons, and respectively.

U the energy of the atomic electrons, V_1 and V_2 the maximum and minimum energies among the electrons scattered inelastically at ϕ.[7] For U we take the ionization potential, and for V_0 the value of the energy of the impinging electrons in volts. These theoretical ranges in the energies of the inelastically scattered electrons are shown in Figs. 4 to 6 by two vertical lines. The results for all our curves are summarized in Fig. 8. It is clear that the theory describes at least the order of magnitude of the range of energies.

It is possible in principle to calculate the distribution of energy among the atomic electrons from the shape of the curve giving the distribution of energies among the scattered electrons.[7] For example, if the atomic electrons were moving in random directions with a constant velocity, then the part of the curves in Figs. 4 to 6 corresponding to the inelastically scattered electrons should be straight lines. The fact that they are practically straight lines may be taken to indicate that the velocities of the atomic electrons in helium do not deviate much from the average velocity. It must be stated, however, that, while our experimental arrangement is particularly effective for measuring the *ratio* of the inelastically scattered electrons to the elastically scattered electrons, it is not so suitable for the accurate measurement of the *distribution* of energies among the inelastically scattered electrons. Consequently, in order to get accurate experimental data from which to get information about the distribution of velocities among atomic electrons, a different type of apparatus should be used. It would be interesting to apply this method to determine accurately the velocities of atomic electrons and to find out whether or not, in atoms containing electrons of more than one kind, there is evidence of well separated velocities.

[7] G. E. M. Jauncey, following paper.

TABLE I. *Ratio of inelastic scattering to elastic scattering.*

Electron energy (volts)		Experimental α'/α	Theoretical α_1'/α	Theoretical α_2'/α
2000	26°	0.419±0.020	0.527	0.433
	30°	0.370±0.034	0.553	0.386
	36°	0.353±0.020	0.632	0.371
	41°	0.419±0.027	0.771	0.404
	44.5°	0.424±0.040	0.939	0.470
	45.5°	0.542±0.027	0.999	0.500
	47	0.690±0.047	1.120	0.558
4000	25°	0.408±0.034	0.523	0.414
	30°	0.379±0.024	0.553	0.386
	35.25°	0.375±0.022	0.608	0.372
	39.75°	0.361±0.026	0.726	0.386
	50°	1.010±0.081	1.437	0.761

Velocity Distribution of Atomic Electrons by the Method of Electron Impact

G. E. M. JAUNCEY,* *Wayman Crow Hall of Physics, Washington University, St. Louis*

(Received June 1, 1936)

When gas atoms are bombarded with electrons traveling with a speed which is large compared to the orbital speeds of the atomic electrons, a bombarding electron collides either with the nucleus or an atomic electron. In the latter case the distribution-in-energy of the electrons scattered at a given angle gives directly the distribution-in-component-velocity of the atomic electrons. The two distribution functions are of the same form.

SEVERAL years ago the author[1] extended the simple photon theory of the Compton effect to the case of the impact between an x-ray photon and a moving atomic electron and showed that the Compton modified line at a certain angle of scattering should have a width due to the motion of the atomic electrons. More recently the author[2] has shown that the distribution-in-intensity in the Compton modified band measures directly, after multiplication by a proportionality constant, the distribution-in-component velocity of the atomic electrons giving rise to the band. In these papers, the author has used the following assumptions: (a) The problem may be treated as that of the impact of a photon with an electron moving in free space but having the same velocity as the actual atomic electron; and (b) if, after applying the principles of conservation of energy and momentum in the substitute problem of (a), the kinetic energy of the recoiling atomic electron is insufficient for it to escape from the atom, the process of the substitute problem becomes inoperative and the photon must then be treated as impinging on the atom as a whole with the result that the scattered photon shows no change (or rather, a negligible change) in wave-length.

The assumption (a) is valid in the case of photon scattering because the photon having no charge is not affected by the field of the nucleus either before or after impact with the atomic electron. We now consider the impact of an outside electron with an atomic electron. An assumption similar to (a) in the case of electron scattering is only valid if the velocity of the impinging electron is so great that the diameters of the "collision areas" of the nucleus and atomic electron are both small compared with the average distance between the nucleus and atomic electron. In the preceding paper of this issue of the *Physical Review*, Hughes and West describe the scattering of fast electrons by helium. Under their experimental conditions the impinging electron is, except in very rare cases, scattered by either the nucleus or the atomic electron. We shall therefore use assumptions similar to (a) and (b) in the problem of the scattering of fast electrons by the relatively slow-moving atomic electrons.

Let v_0 be the velocity in cm/sec. of the impinging electron just before impact and v that of the scattered electron[3] just after impact. Let the direction of v be that of the x-axis and let the v_0v plane (the plane of scattering) be the xz plane. Let ϕ be the angle of scattering, u_x, u_y, u_z the velocity components of the atomic electron just before impact and u_x', u_y', u_z' the components just after impact. The direction cosines of v_0 are $\cos\phi$, 0, $-\sin\phi$. Conservation of kinetic energy gives

$$v_0^2+u_x^2+u_y^2+u_z^2=v^2+u_x'^2+u_y'^2+u_z'^2, \quad (1)$$

while conservation of momentum requires

$$v_0\cos\phi+u_x=v+u_x', \quad (2)$$

$$u_y=u_y', \quad (3)$$

$$u_z-v_0\sin\phi=u_z'. \quad (4)$$

Eliminating u_x', u_y', u_z', we obtain

$$v^2-v(v_0\cos\phi+u_x)+v_0(u_x\cos\phi-u_z\sin\phi)=0. \quad (5)$$

* The author was aided in part by a grant from the Rockefeller Foundation to Washington University for research in science.

[1] G. E. M. Jauncey, Phil. Mag. **49**, 427 (1925); Phys. Rev. **25**, 314 (1925); Phys. Rev. **25**, 723 (1925).

[2] G. E. M. Jauncey, Phys. Rev. **46**, 667 (1934).

[3] Following the usual practice, the scattered electron is distinguished from the recoil electron by the greater velocity of the former.

This is a quadratic in v/v_0 and its solution is given by formula. In Hughes and West's experiments with helium u_x/v_0 and u_z/v_0 are small with respect to unity while $\cos\phi$ and $\sin\phi$ are of the order unity. Hence, to the second power of u_x/v_0 and u_z/v_0, we have, using the plus sign of the ambiguity,

$$v/v_0=\cos\phi+\frac{u_z\tan\phi}{v_0}+\frac{(u_xu_z\sin\phi\sec^2\phi-u_z^2\sin^2\phi\sec^3\phi)}{{v_0}^2}, \quad (6)$$

while to the first power of the quantities we have for high speed impinging electrons

$$v/v_0=\cos\phi+\frac{u_z\tan\phi}{v_0}. \quad (7)$$

Now v_0 and v are the velocities just before and just after impact, respectively. They are not the actual velocities of the impinging and the scattered electron outside the atom. However, if both velocities are high, we may make the approximation that v_0 and v are the speeds outside the atom. Experimentally, velocities are measured in "volts," V_0 and V. Hence, squaring (7), we obtain to the first power of u_z/v_0

$$V/V_0=\cos^2\phi+u_z(2m/V_0e)^{\frac{1}{2}}\sin\phi. \quad (8)$$

For a given angle of scattering ϕ and a given accelerating voltage V_0 for the impinging electrons, we have from (8) a *linear* relation between V and u_z. From this it follows that, if the number of atoms per cm³ having electrons with z-component velocities u_z in the range du_z is $f(u_z)du_z$ and if a definite fraction of these electrons gives rise to $F(V)dV$ scattered electrons of energy V volts in the range dV volts,

$$f(u_z)du_z=\text{const } F(V)dV. \quad (9)$$

In virtue of the *linear* relation (8),

$$f(u_z)=\text{const } F(V_0\cos^2\phi+u_z(2mV_0/e)^{\frac{1}{2}}\sin\phi). \quad (10)$$

If $F(V)$ can be determined experimentally, $f(u_z)$ can immediately be obtained from (10), the curves of $f(u_z)$ *vs.* u_z and $F(V)$ *vs.* V having the same shape. On the other hand, if $f(u_z)$ is known from theory,

$$F(V)=\text{const } f((e/2mV_0\sin^2\phi)^{\frac{1}{2}}(V-V_0\cos^2\phi)). \quad (11)$$

In the original Bohr theory of the helium atom the two electrons were at a constant radial distance from the nucleus and therefore had velocities constant in magnitude but random in direction. In such a case[4]

$$f(u_z)=\text{const } (\neq 0), \text{ for } |u_z|\leqq C,$$
$$=0 \quad , \text{ for } |u_z|>C, \quad (12)$$

where C is the magnitude of the orbital velocity in cm/sec. Consequently, for this case, (11) and (8) give

$$F(V)=\text{const } (\neq 0), \text{ for } |(V-V_0\cos^2\phi)| \leqq C(2mV_0/e)^{\frac{1}{2}}\sin\phi$$
$$=0, \text{ for } |(V-V_0\cos^2\phi)| > C(2mV_0/e)^{\frac{1}{2}}\sin\phi. \quad (13)$$

Moreover, in this case, we may speak of a spread in the velocity (measured in volts) of the electrons scattered in the direction ϕ. From (13) it is seen that this spread is

$$V_1-V_2=4\sin\phi(UV_0)^{\frac{1}{2}}, \quad (14)$$

where V_1 and V_2 are the retarding voltages (as in Hughes and West's experiments) respectively necessary to prevent all scattered electrons from entering the Faraday cylinder and to allow all such electrons to enter the cylinder when the cylinder is placed at a scattering angle ϕ. The quantity U in (14) is the voltage equivalent of the kinetic energy of the orbital electron.

Finally, it should be noted that the conclusions of this paper are only valid under the various restrictions mentioned in the paper.

---

[4] In the more general case of a radially symmetrical atom, the probability distribution function $n(C)$ for the speed C (magnitude only) of an atomic electron is related to the probability distribution function $f(u)$ for the component velocity u in a particular direction by

$$f(u)=\frac{1}{2}\int_u^\infty\frac{n(C)dC}{C}.$$

The inverse relation is

$$n(C)=-2Cf'(C).$$

These relations are used in the kinetic theory of gases.

On the Resonance Capture of Slow Neutrons*

H. H. GOLDSMITH AND F. RASETTI, *Columbia University*

(Received June 8, 1936)

The energies of neutron groups selectively activating various elements have been measured by means of the boron absorption method. The elements Rh (3.9 minutes), Rh (44 seconds), Ag (22 seconds), In (13 seconds), In (54 minutes), Ir (19 hours) and Au (2.7 days) exhibit resonance capture for neutrons of energies between one and five volts. The elements Mn (2.5 hours), Cu (5 minutes), As (26 hours), Br (18 minutes), Ag (2.3 minutes), I (25 minutes) Re (20 hours) seem to be activated only by higher energy neutrons (30–85 volts). There are indications that Gd and Sm have resonance groups within the Cd absorption region (thermal energies).

STUDIES of the absorption of the neutrons which emerge from paraffin containing a Rn-Be source, prove that it is impossible to assign to these neutrons an absorption coefficient, in a given element, which is independent of the nature of the detector. In general, the absorption is greatest when the detector is the same element as the absorber. Such selective absorption is more pronounced when the neutrons issuing from the paraffin are first filtered through cadmium. Extensive measurements by Amaldi and Fermi,[1] of the absorption and scattering of these cadmium-filtered neutrons revealed the presence of several distinct groups. These groups are:

(1) *C group*—Strongly absorbed by Cd, $[(\mu/\rho)_{Cd}=13.5$–16 cm²/gm].

and the following groups not strongly absorbed by cadmium:

(2) *D group*—Strongly absorbed by Rh and In, $[(\mu/\rho)_{Rh}=1.6$–2.0 cm²/g; $(\mu/\rho)_{In}=3.0$–3.8 cm²/g]; activates Rh (44″) and In (54′). Cadmium absorption small $[(\mu/\rho)_{Cd}=0.05$ cm²/g].

(3) *A group*—Strongly absorbed by Ag, $[(\mu/\rho)_{Ag}=20$ cm²/g]; activates Ag (22″) and Ir (19 hr).

(4) *B group*—Moderately absorbed by Ag, $[(\mu/\rho)_{Ag}\sim 0.3$ cm²/g]; activates Ag (22″).

(5) *I group*—Strongly absorbed by I, $[(\mu/\rho)_{I}=0.7$ cm²/g]; activates I (25′).

Breit and Wigner,[2] and Bohr[3] have accounted for selective absorption on the basis of a resonance capture process. According to this explanation the *C*, *D*, *A*, *B*, *I* groups differ merely in energy. However, the energy of only one of these groups, the *C* group, can be determined directly. Various investigations show that the neutrons of this group have thermal energies. Concerning the other groups one knows only that their energies are greater than this.[3a]

It is the purpose of the experiments here described to determine the energies of a large number of neutron groups including those found by Amaldi and Fermi. The method, by which the neutron energies are measured, is based on the plausible assumption that those light nuclei (B^{10} and Li^6) which emit heavy particles on neutron capture should exhibit no sharp resonance effects. The slow neutron absorption cross section in boron (and lithium) should, therefore, be inversely proportional to the neutron velocity. It follows, that if one knows the energy as well as the absorption coefficient in boron for one group, say the *C* group, then the measurement of the absorption coefficient in boron for any other neutron group is sufficient to determine its energy. This method was first suggested by Frisch and Placzek[3b] and was employed by them in order to estimate the upper limit of the Cd absorption band. It has also been applied by Weekes, Livingston and Bethe[4] in order to obtain the energy of the neutron group which activates the 2.3′ period of Ag.

The neutron source consisted of a bulb containing radon (300–600 mc) and powdered beryllium. The source was placed at the center of a solid paraffin parallelopiped $30\times22\times7.5$ cm³.

* Preliminary reports of some of these results were presented at the meeting of the Metropolitan Section of the Am. Phys. Soc. (March 20, 1936) and at the Washington meeting. Rasetti, Fink, Goldsmith, Mitchell, Phys. Rev. **49**, 869 (1936).

[1] Amaldi and Fermi, Ricerca scient. **2**, 344 (1935); **2**, 443 (1935); **1**, 56 (1936); **1**, 223 (1936); **1**, 310 (1936).

[2] Breit and Wigner, Phys. Rev. **49**, 519 (1936).

[3] Bohr, Nature **137**, 344 (1936).

[3a] Preiswerk and v. Halban, Jr. Comptes rendus **202**, 840 (1936).

[3b] Frisch and Placzek, Nature **137**, 357 (1936).

[4] Weekes, Livingston and Bethe, Phys. Rev. **49**, 471 (1936).

A sheet of Cd (0.4 g/cm²) covered the paraffin and served to eliminate the *C* neutrons. Thin, flat detectors, 4×5 cm² (thickness given in Table I), were placed at the center of the 30×22 side and at a distance ($\leqslant 1$ cm) from the Cd sufficient to permit the interposition of the absorber. The boron absorbers were (a) Pyrex plates, each of which contained either 0.020 or 0.027 g/cm² of boron; (b) boron carbide, B_4C, containing 0.58 g/cm² of boron. The lithium absorber was LiF containing 0.22 g/cm² of lithium. The absorption of neutrons by the elements other than boron and lithium in these substances was assumed to be negligible.

In studying substances of long half-lifetime (Re, Br, Ir, As, Au, Mn) two similar detectors were symmetrically placed on opposite sides of the paraffin. On one of the sides the cadmium-filtered neutrons were absorbed by boron. This procedure ensured equal times of irradiation, expedited the measurements and obviated the necessity of correcting for the decay of the source. The small deviation from symmetry (about 5 percent, according to measurements made with a Rh detector) was taken into account in the final results. For detectors of short half-lifetime, only one side of the paraffin was used, the measurements being made with and without the absorber.

The β-activities were measured by means of an ionization chamber and Edelmann electrometer. The chamber was filled with argon at a pressure of three atmospheres. The electrons entered the chamber through a thin Al window (0.1 mm) of 6 cm diameter. Measurements with this arrangement can be made more rapidly than with Geiger-Müller counters which is a matter of importance with short period detectors. However, since the electrometer is less sensitive than the counter, the investigation was limited to those elements which exhibit strong activities.

In order to study neutrons of energies greater than thermal energies, it is first necessary to ascertain, for each detector, that appreciable activity is induced by the neutrons transmitted through Cd. From Amaldi and Fermi's work it is known that a considerable fraction (15 percent to 75 percent) of the activity exhibited by Ag (22″), Rh (44″), Br (18′), I (25′), In (54′), Mn (150′), and Ir (19 hr) is produced by neutrons which get through 0.27 g/cm² Cd. It is also known that Au (2.7 d) and Ag (2.3′) are strongly activated by such neutrons. Desiring to investigate additional neutron groups we measured roughly the relative activities induced in a number of detectors by the *C* neutrons and those of higher energy. Two similar detectors, one of which was covered with 0.4 g/cm² Cd, were placed symmetrically inside of a block of paraffin and irradiated simultaneously. The percentage activities due to the neutrons transmitted through Cd were: Dy (2.5 hr)—2.5 percent; V (3.75′)—4 percent; Mn (150′)—5 percent; Rh (3.9′)—17 percent; Br (4.2 hr)—25 percent; As (26 hr)—45 percent. Amaldi and Fermi have shown that the ratio of the number of *D* or *A* neutrons to the number of *C* neutrons in the beam issuing from a paraffin block is about three times greater than it is at a point inside the block. In view of this, our value of 5 percent for Mn is consistent with their value of 15 percent which was obtained outside the paraffin. The absorption in boron of the residual neutrons activating Dy, V, and Br (4.2 hr) was not studied because of insufficient intensity.

The results of the absorption measurements are summarized in Table I.

The meaning of the first six columns is self-evident. For the deduction of the corrected values of the mass absorption coefficients and of energies see below. Using Rh (44″) as detector, we measured absorption curves, using different thicknesses of boron absorbers, both for the neutron of thermal energies and for the *D* group. The results are plotted in Fig. 1 (uncorrected absorption curves; for the meaning of the corrected absorption curves see below).

The absorption curve, under the conditions of our experiment, will not be an exponential, mainly for two reasons: (a) the Cd filtered neutrons activating a detector may not be homogeneous in velocity, because of the breadth of the absorption band. If more than one resonance level is effective the neutrons will be even less homogeneous; (b) the absorbed beam is not parallel.

The effect of the obliquity of the neutrons in the absorber can be evaluated if one knows the angular distribution of the neutrons emerging from the paraffin. An approximate theoretical

distribution law has been derived by Fermi (private communication) for the neutrons of thermal energies. This states that the number of neutrons emitted per unit solid angle at an angle θ with the normal to the surface is proportional to $\cos\theta+3\frac{1}{2}\cos^2\theta$. Assuming this distribution and also taking into account the fact that neutrons which traverse the detector obliquely have a higher probability of being captured, we have calculated the absorption curve for homogeneous neutrons. However for relative absorption coefficients, this correction is not needed provided one uses an absorber thickness, for each detector, that will reduce the neutron intensity by the same amount; and provided that the angular distribution is the same for neutrons of different energies. Therefore, as can be seen from the table, we chose, for each detector, a thickness of boron that reduced the activity to about 50 percent.

In the case of Rh, as we had a few accurately determined points of the absorption curves, we applied the correction for obliquity in absorber and detector, and thus obtained the curves designated as "corrected" in Fig. 1. These curves do not show any appreciable departure from exponentials, although both the *C* and *D* groups are certainly inhomogeneous. However, the expected effect of the inhomogeneity on the shape of the curves is too small to be observed unless the absorption measurements are extended out to very low transmitted intensities. It thus appears that most of the deviation from an exponential in the experimental absorption curve for the *D* neutrons in boron is due to geometrical factors.

From the corrected absorption curves for the *C* and *D* neutrons we obtain the mass absorption coefficients in boron given in Table I. We note that the cross section for the *C* neutrons (500×10^{-24} cm^2) is in gratifying agreement with the values obtained by using an approximately parallel beam of neutrons and a boron or lithium detector (540×10^{-24} cm^2).

By employing the same procedure, we also obtained the corrected values of μ/ρ for all the other detectors. However, as has already been pointed out, geometrical corrections are not essential if only relative values of the absorption coefficient are required. This consideration does not apply to the absorption of the *A* neutrons in Ag detector. Here the correction employed was different because the assumption of a thin detector is not valid.

To convert absorption coefficients into the energies of the neutron groups, we must make the following assumptions: (a) the absorption cross section in boron varies as $1/v$, (b) the *C* neutrons are in thermal equilibrium, i.e. they have a Maxwellian velocity distribution, (c) the

TABLE I. *Summary of absorption measurements.*

Detector	Filter	Thickness of Detector (g/cm^2)	Period	Thickness of Absorber (g/cm^2)	Transmission %	μ/ρ (cm^2/g) corrected	E (ev)
45 Rh		0.35	44″	B 0.02	35.2	28	[0.026]
				Li 0.22	30.6	2.9	
25 Mn	0.4 g/cm^2 Cd	0.5	150′	B 0.58	43	0.73	37
29 Cu	0.4 g/cm^2 Cd	0.38	5′	B 0.58	~50	0.57	62
33 As	0.4 g/cm^2 Cd	0.5	26 hr	B 0.58	54	0.49	84
35 Br	0.4 g/cm^2 Cd	0.7 NaBr	18′	B 0.58	50	0.57	62
45 Rh	0.4 g/cm^2 Cd	0.35	44″	B 0.081	50	4.15	1.16
				Li 0.22	78	0.47	0.98
45 Rh	0.4 g/cm^2 Cd	0.35	3.9′	B 0.054	~57	4.6	~1
47 Ag	0.4 g/cm^2 Cd	0.06	22″	B 0.108	63	2.8	2.5
47 Ag	0.4 g/cm^2 Cd+0.25 g/cm^2 Ag	0.56	22″	B 0.108	60	2.1	4.5
47 Ag	0.4 g/cm^2 Cd	0.56	2.3′	B 0.58	51.5	0.54	69
49 In	0.4 g/cm^2 Cd	0.11	13″	B 0.108	~50	3	2.2
49 In	0.4 g/cm^2 Cd	0.11	54′	B 0.081 }	53 }	3.8	1.38
				B 0.108 }	43 }		
53 I	0.4 g/cm^2 Cd	0.3	25′	B 0.58	53	0.50	80
75 Re	0.4 g/cm^2 Cd	0.5	20 hr	B 0.23	64	0.83	30
77 Ir	0.4 g/cm^2 Cd	0.5	19 hr	B 0.108	46	3.5	1.6
79 Au	0.4 g/cm^2 Cd	0.25	2.7 d	B 0.108	53	2.8	2.5

neutrons detected consist of a single, relatively narrow energy band. We now discuss these three assumptions in detail.

(a) Apart from any theoretical reasons for assuming the validity of the $1/v$ law in boron and lithium, this law is supported by two experimental results: (1) the cross section in boron appears to vary as $1/v$ at least within the thermal region,[5] (2) the ratio of the absorption coefficients for the C and D neutrons is found to be the same for lithium (6.2) and for boron (6.7).

(b) It has been experimentally shown that the neutrons absorbed by Cd have, at least approximately, a Maxwellian distribution.[6] To determine what value of the energy of the thermal neutrons must be assumed as effective for the boron absorption measurements, we considered the following case: a beam of thermal neutrons is absorbed in a thickness l of a material having an absorption coefficient σ/v, and is recorded by means of a thin detector (sensitivity proportional to $1/v$). The transmitted intensity I is given by

$$I=\frac{4}{\pi^{\frac{1}{2}}}I_0\int_0^\infty x^2e^{-x^2}e^{-\sigma l/\alpha x}dx,$$

where $\alpha=(2kT/m)^{\frac{1}{2}}$. By evaluating the integral one finds that, for a transmission of 50 percent, the absorption is about the same as that of homogeneous neutrons of velocity $v=\alpha$. Therefore, we have taken the effective energy of the thermal neutrons to be kT, that is 0.026 ev, at 300°K.

(c) For the elements that show selective absorption at low energies (1–5 volts), that is, Rh (44″), Rh (3.9′), In (15″), In (54′), Ag (22″), Au (2.7 d) and Ir (19 hr), one may assume that the resonance level observed is considerably closer to zero than the average energy between nuclear levels. For these cases, we may expect the absorption measurements to give the true value of the mean energy within the resonance band. This band, however, may be quite broad.[1] Ag (22″) appears to exhibit two absorption bands of low energy (A and B), although the difference in energy observed is not very large. For the other detectors investigated, i.e. Ag (2.3′), Mn (150′), Br (18′), I (25′), As (26 hr) Cu (5′) and Re (20 hr), the absorption of boron indicates higher resonance energies (30–85 ev). Here, the energy of the lowest resonance group is probably of the order of the average distance between nuclear levels and, consequently, the observed values have a greater probability of being mean values for several absorption bands. On theoretical grounds, this must be expected to happen more frequently for heavy nuclei.

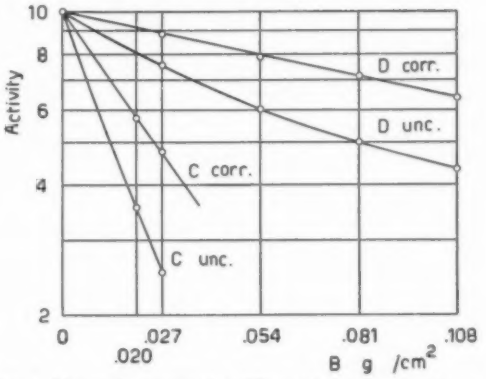

FIG. 1. Absorption curves for different thicknesses of boron. Rhodium was used as a detector.

We note that those elements which show resonance bands of low energy also exhibit larger capture cross sections in the thermal region than the elements with higher resonance levels. This conclusion, however, can be safely applied only to elements which possess a single isotope. According to the theory, the magnitude of the cross section for thermal neutrons will depend not only on the position, but also on the width of the resonance level.

When levels within or near the thermal region exist, one of the effects is to produce departures from the $1/v$ law of absorption at very low velocities. One element exhibiting such properties is Cd; Hg is probably another. We have evidence to indicate that Sm and Gd also possess a resonance level of exceedingly low energy. We measured roughly in each of these elements the ratio of the absorption coefficients for the C and D neutrons. The absorption coefficient for the D neutrons is of the order of 100 times smaller than for the C neutrons (compared with a ratio 6.7 in boron), indicating probable resonance in the thermal region.

[5] Rasetti, Mitchell, Fink and Pegram, Phys. Rev. **49**, 777 (1936).
[6] Fink, Dunning, Pegram and Mitchell, Phys. Rev. **49**, 103 (1936).

An Attempt to Calculate the Number of Energy Levels of a Heavy Nucleus

H. A. BETHE, *Cornell University*

(Received June 5, 1936)

Experiments on slow neutrons, and theoretical considerations of Bohr have shown that heavy nuclei possess an enormous number of energy levels which are very closely spaced if the nucleus is highly excited. A crude method is suggested for calculating the spacing between these levels. The method is statistical: The individual nuclear particles are supposed to move in a simple potential hole, and the energy of the complete nucleus is supposed to be the sum of the energies of the individual particles. A critical discussion of these assumptions is given in section 5. The problem then reduces itself to the calculation of the "entropy" of a Fermi gas containing a given number of particles A and having a given excitation energy Q above the zero point energy of the Fermi gas (cf. section 2 and 3). This calculation gives the total number of levels of the complete nucleus in a given energy interval irrespective of the angular momentum, which will, for most of the levels, be very large. For the theory of neutron capture, it is necessary to calculate the density of nuclear levels with a *given angular momentum* I (section 4). The spacing of nuclear levels is found to depend on the product of the mass number A and the excitation energy Q of the nucleus, and to be roughly given by

$$\Delta = 4.1 \cdot 10^6 x^4 e^{-x}/(2I+1) \text{ volts}$$
$$x = (AQ)^{\frac{1}{2}}/2.20,$$

Q being expressed in MV and I being the nuclear spin. For the capture of slow neutrons by nuclei of medium weight (A around 100), Δ is of the order 50 to 500 volts. The spacing between adjacent levels decreases rapidly with increasing atomic weight. For given atomic weight, the spacing of the nuclear levels responsible for neutron capture is wider if the capture leads to the formation of a radioactive nucleus than if a stable nucleus is formed. This explains the experimental fact that only moderately large cross sections are found for the capture of thermal neutrons leading to radioactive nuclei while the very largest cross sections are all connected with the formation of stable nuclei. The dependence of the spacing on various factors is discussed (section 6); the results seem to be in qualitative agreement with experiment.

1. STATEMENT OF PROBLEM

BOHR[1] has given strong reasons for the existence of a very great number of closely spaced energy levels for a highly excited heavy nucleus. Breit and Wigner[2] and Bohr[1] have shown that the assumption of such levels leads automatically to a completely satisfactory explanation of all phenomena connected with slow neutrons, in particular the selective absorption, the high capture cross section and the large ratio of capture to scattering. Various investigators[3] have measured the position of the neutron resonance levels for several substances. The resonances are found to lie at neutron energies ranging from about 0.1 volt (Cd) to about 50 volts (I). These measurements indicate that the spacing between adjacent energy levels of the nuclei concerned in the energy region investigated is very small, maybe of the order of 100 volts or even less.

It is the purpose of this paper to give some fairly crude calculations leading to an estimate of this spacing. We consider a nucleus containing N neutrons and Z protons. The total number of particles (mass number) will be denoted by $A=N+Z$. The nucleus will have a certain ground state of energy U_0. We are interested in the energy levels of the nucleus which lie by a certain amount Q higher than the ground state, and we ask for the density of energy levels in this region, i.e., for the number of levels between Q and $Q+dQ$ which we may call $\rho(Q)dQ$. $1/\rho(Q)$ will then be the average spacing between neighboring levels.

We shall be particularly interested in such values of Q which are just sufficient to dissociate the given nucleus A into a neutron and a residual nucleus of atomic weight $A-1$. These energy levels will be important for the capture of slow neutrons by the nucleus $A-1$. In general, the "dissociation energy" Q, i.e., the energy set free when a neutron is captured by the nucleus $A-1$, will be of the order 8 MV. This figure applies if the packing fractions of the nuclei $A-1$ and A are about equal, and represents the excess of the

[1] Bohr, Nature **137** (1936).
[2] Breit and Wigner, Phys. Rev. **49**, 519 (1936).
[3] Frisch and Placzek, Nature **137**, 357 (1936); Weekes, Livingston and Bethe, Phys. Rev. **49**, 471 (1936); Rasetti, Fink, Goldsmith and Mitchell, Phys. Rev. **49**, 869 (1936); Fillie, Nature **137**, 614 (1936); Fermi and Amaldi, Ricerca Sient. **1**, No. 7–8 (1936).

neutron mass over one mass unit. In particular cases, Q will be lower or higher than 8 MV, but it will probably lie in the interval from 5 to 10 MV for most cases (see section 6).

2. Method of Calculation

In order to estimate the "density" $\rho(Q)$ of the levels of the nucleus as a whole, we shall start from the statistical model of the nucleus; in other words, from the individual-particle picture. We are fully aware of the crudeness of this assumption, but reasons will be given below (section 5) for the belief that the density of levels will come out fairly correctly from this picture, although the wave function of a particular state of the nucleus will differ greatly from that obtained by this picture.

In this model, we shall obtain, first of all, a certain set of energy levels for the individual neutrons and protons in the nucleus. The positions of these levels will depend on the potential which we assume to act on the particles. The ground level of the *nucleus as a whole* is then obtained by filling all the lowest "individual" states with particles and leaving all the higher individual states unoccupied. An excited level of the nucleus will be obtained by taking one particle out of one of the low individual states and putting it into one of the higher individual states, or else by leaving *two* of the "low" individual states empty and having two higher individual states occupied instead, etc. In fact, for excited levels about 8 MV above the ground level of the nucleus, we shall in general have a fairly large number (of the order $\sqrt{A}$) of the individual particles "excited." Since there is a great variety of "low" individual states which may be left empty, and an equally great variety of "high" states which may be occupied by a particle, it is obvious that there will be a very large number of different ways in which a certain excitation energy of the nucleus as a whole may be realized, particularly if the energy is sufficient to have many particles excited.

The problem of finding the number of these different modes of realization is identical with the problem of finding the "probability number" (entropy) of a Fermi gas whose energy is given and has a value larger than the minimum possible energy for the gas. The solution of this problem is well-known in Fermi statistics, and it is only necessary to go one step farther in the accuracy than is usually done because usually only the logarithm of $\rho(Q)$, i.e., the entropy, is wanted while we want to calculate $\rho(Q)$ itself correctly to quantities of the relative order $1/A$ or $1/\sqrt{A}$ where A is the total number of particles.

Since we know that Fermi statistics is applicable to our problem, the probability that a given *individual-particle* state of energy ϵ is occupied, will be

$$f(\epsilon)=1/(e^{\beta(\epsilon-\zeta)}+1) \tag{1}$$

where β and ζ are two constants which have to be determined from the total number of particles N and the total energy U of the nucleus. As regards the number of particles, we have to consider neutrons and protons separately because both these numbers are given for a given nucleus. We shall, for the present, refer to neutrons alone and let U denote the total energy of the neutrons alone; U is then, of course, *not* given, but we must, later on, integrate over all possible distributions of the total nuclear energy between neutrons and protons.

The conditions determining β and ζ are then

$$N=\sum_i f(\epsilon_i), \quad U=\sum_i \epsilon_i f(\epsilon_i), \tag{2}$$

the sums extending over all possible states of an individual neutron. We now assume that the neutrons and protons are contained in a box of volume

$$\Omega=(4\pi/3)R^3, \tag{3}$$

where R is the nuclear radius. Then the number of neutron levels of energy between ϵ and $\epsilon+d\epsilon$ is given by the well-known formula

$$\varphi(\epsilon)d\epsilon=(2^{5/2}/3\pi)(MR^2/\hbar^2)^{\frac{3}{2}}\epsilon^{\frac{1}{2}}d\epsilon=(3/2)C\epsilon^{\frac{1}{2}}d\epsilon \tag{4}$$

with

$$C=(2^{7/2}/9\pi)(MR^2/\hbar^2)^{\frac{3}{2}}. \tag{4a}$$

Then (2) reduces to

$$N=(3/2)C\int f(\epsilon)\epsilon^{\frac{1}{2}}d\epsilon, \tag{5}$$

$$U=(3/2)C\int f(\epsilon)\epsilon^{\frac{3}{2}}d\epsilon. \tag{5a}$$

The number $\rho(U)dU$ of energy levels of the nucleus as a whole, between U and $U+dU$, is

An Attempt to Calculate the Number of Energy Levels of a Heavy Nucleus

H. A. BETHE, *Cornell University*

(Received June 5, 1936)

Experiments on slow neutrons, and theoretical considerations of Bohr have shown that heavy nuclei possess an enormous number of energy levels which are very closely spaced if the nucleus is highly excited. A crude method is suggested for calculating the spacing between these levels. The method is statistical: The individual nuclear particles are supposed to move in a simple potential hole, and the energy of the complete nucleus is supposed to be the sum of the energies of the individual particles. A critical discussion of these assumptions is given in section 5. The problem then reduces itself to the calculation of the "entropy" of a Fermi gas containing a given number of particles A and having a given excitation energy Q above the zero point energy of the Fermi gas (cf. section 2 and 3). This calculation gives the total number of levels of the complete nucleus in a given energy interval irrespective of the angular momentum, which will, for most of the levels, be very large. For the theory of neutron capture, it is necessary to calculate the density of nuclear levels with a *given angular momentum* I (section 4). The spacing of nuclear levels is found to depend on the product of the mass number A and the excitation energy Q of the nucleus, and to be roughly given by

$$\Delta = 4.1 \cdot 10^6 x^4 e^{-x}/(2I+1) \text{ volts}$$
$$x = (AQ)^{\frac{1}{2}}/2.20,$$

Q being expressed in MV and I being the nuclear spin. For the capture of slow neutrons by nuclei of medium weight (A around 100), Δ is of the order 50 to 500 volts. The spacing between adjacent levels decreases rapidly with increasing atomic weight. For given atomic weight, the spacing of the nuclear levels responsible for neutron capture is wider if the capture leads to the formation of a radioactive nucleus than if a stable nucleus is formed. This explains the experimental fact that only moderately large cross sections are found for the capture of thermal neutrons leading to radioactive nuclei while the very largest cross sections are all connected with the formation of stable nuclei. The dependence of the spacing on various factors is discussed (section 6); the results seem to be in qualitative agreement with experiment.

1. STATEMENT OF PROBLEM

BOHR[1] has given strong reasons for the existence of a very great number of closely spaced energy levels for a highly excited heavy nucleus. Breit and Wigner[2] and Bohr[1] have shown that the assumption of such levels leads automatically to a completely satisfactory explanation of all phenomena connected with slow neutrons, in particular the selective absorption, the high capture cross section and the large ratio of capture to scattering. Various investigators[3] have measured the position of the neutron resonance levels for several substances. The resonances are found to lie at neutron energies ranging from about 0.1 volt (Cd) to about 50 volts (I). These measurements indicate that the spacing between adjacent energy levels of the nuclei concerned in the energy region investigated is very small, maybe of the order of 100 volts or even less.

It is the purpose of this paper to give some fairly crude calculations leading to an estimate of this spacing. We consider a nucleus containing N neutrons and Z protons. The total number of particles (mass number) will be denoted by $A=N+Z$. The nucleus will have a certain ground state of energy U_0. We are interested in the energy levels of the nucleus which lie by a certain amount Q higher than the ground state, and we ask for the density of energy levels in this region, i.e., for the number of levels between Q and $Q+dQ$ which we may call $\rho(Q)dQ$. $1/\rho(Q)$ will then be the average spacing between neighboring levels.

We shall be particularly interested in such values of Q which are just sufficient to dissociate the given nucleus A into a neutron and a residual nucleus of atomic weight $A-1$. These energy levels will be important for the capture of slow neutrons by the nucleus $A-1$. In general, the "dissociation energy" Q, i.e., the energy set free when a neutron is captured by the nucleus $A-1$, will be of the order 8 MV. This figure applies if the packing fractions of the nuclei $A-1$ and A are about equal, and represents the excess of the

[1] Bohr, Nature **137** (1936).
[2] Breit and Wigner, Phys. Rev. **49**, 519 (1936).
[3] Frisch and Placzek, Nature **137**, 357 (1936); Weekes, Livingston and Bethe, Phys. Rev. **49**, 471 (1936); Rasetti, Fink, Goldsmith and Mitchell, Phys. Rev. **49**, 869 (1936); Collie, Nature **137**, 614 (1936); Fermi and Amaldi, Ricerca scient. **1**, No. 7–8 (1936).

neutron mass over one mass unit. In particular cases, Q will be lower or higher than 8 MV, but it will probably lie in the interval from 5 to 10 MV for most cases (see section 6).

2. Method of Calculation

In order to estimate the "density" $\rho(Q)$ of the levels of the nucleus as a whole, we shall start from the statistical model of the nucleus; in other words, from the individual-particle picture. We are fully aware of the crudeness of this assumption, but reasons will be given below (section 5) for the belief that the density of levels will come out fairly correctly from this picture, although the wave function of a particular state of the nucleus will differ greatly from that obtained by this picture.

In this model, we shall obtain, first of all, a certain set of energy levels for the individual neutrons and protons in the nucleus. The positions of these levels will depend on the potential which we assume to act on the particles. The ground level of the *nucleus as a whole* is then obtained by filling all the lowest "individual" states with particles and leaving all the higher individual states unoccupied. An excited level of the nucleus will be obtained by taking one particle out of one of the low individual states and putting it into one of the higher individual states, or else by leaving *two* of the "low" individual states empty and having two higher individual states occupied instead, etc. In fact, for excited levels about 8 MV above the ground level of the nucleus, we shall in general have a fairly large number (of the order $\sqrt{A}$) of the individual particles "excited." Since there is a great variety of "low" individual states which may be left empty, and an equally great variety of "high" states which may be occupied by a particle, it is obvious that there will be a very large number of different ways in which a certain excitation energy of the nucleus as a whole may be realized, particularly if the energy is sufficient to have many particles excited.

The problem of finding the number of these different modes of realization is identical with the problem of finding the "probability number" (entropy) of a Fermi gas whose energy is given and has a value larger than the minimum possible energy for the gas. The solution of this problem is well-known in Fermi statistics, and it is only necessary to go one step farther in the accuracy than is usually done because usually only the logarithm of $\rho(Q)$, i.e., the entropy, is wanted while we want to calculate $\rho(Q)$ itself correctly to quantities of the relative order $1/A$ or $1/\sqrt{A}$ where A is the total number of particles.

Since we know that Fermi statistics is applicable to our problem, the probability that a given *individual-particle* state of energy ϵ is occupied, will be

$$f(\epsilon)=1/(e^{\beta(\epsilon-\zeta)}+1) \tag{1}$$

where β and ζ are two constants which have to be determined from the total number of particles N and the total energy U of the nucleus. As regards the number of particles, we have to consider neutrons and protons separately because both these numbers are given for a given nucleus. We shall, for the present, refer to neutrons alone and let U denote the total energy of the neutrons alone; U is then, of course, *not* given, but we must, later on, integrate over all possible distributions of the total nuclear energy between neutrons and protons.

The conditions determining β and ζ are then

$$N=\sum_i f(\epsilon_i), \quad U=\sum_i \epsilon_i f(\epsilon_i), \tag{2}$$

the sums extending over all possible states of an individual neutron. We now assume that the neutrons and protons are contained in a box of volume

$$\Omega=(4\pi/3)R^3, \tag{3}$$

where R is the nuclear radius. Then the number of neutron levels of energy between ϵ and $\epsilon+d\epsilon$ is given by the well-known formula

$$\varphi(\epsilon)d\epsilon=(2^{5/2}/3\pi)(MR^2/\hbar^2)^{3/2}\epsilon^{1/2}d\epsilon=(3/2)C\epsilon^{1/2}d\epsilon \tag{4}$$

with $$C=(2^{7/2}/9\pi)(MR^2/\hbar^2)^{3/2}. \tag{4a}$$

Then (2) reduces to

$$N=(3/2)C\int f(\epsilon)\epsilon^{1/2}d\epsilon, \tag{5}$$

$$U=(3/2)C\int f(\epsilon)\epsilon^{1/2}d\epsilon. \tag{5a}$$

The number $\rho(U)dU$ of energy levels of the nucleus as a whole, between U and $U+dU$, is

found very easily from Sommerfeld's[4] derivation of the Fermi statistics. We have

$$\log \sum_{N'} \int dU' \rho(U') e^{\beta\zeta N' - \beta U'} = \sum_i \log (1+e^{\beta(\zeta-\epsilon_i)})$$

$$= (3/2) C \int \epsilon^{\frac{1}{2}} d\epsilon \log (1+e^{\beta(\zeta-\epsilon)}). \quad (6)$$

The notation is the same as in Sommerfeld's paper (Eqs. (3), (11)), except that his α has been denoted by $-\beta\zeta$. The left hand side of (6) is known to have a sharp maximum for $N'=N$ and $U'=U$. This fact makes it easy to determine $\rho(U)$ once the right hand side of (6) has been evaluated. $1/\rho(U)$ gives directly the desired spacing between the nuclear levels.

3. Evaluation of the Number of Levels

Since the excitation Q of the nucleus is small compared to the total kinetic energy U of all the nuclear particles, the "Fermi gas" is highly degenerate and the formulae known from the theory of metals may be applied. We have

$$N = C\zeta^{\frac{1}{2}}(1+(\pi^2/8)(\beta\zeta)^{-2}+\cdots), \quad (7)$$

$$U = \tfrac{2}{5} C\zeta^{5/2}(1+(5\pi^2/8)(\beta\zeta)^{-2}+\cdots). \quad (7a)$$

C may be regarded as a given constant, essentially determined by the nuclear radius. Therefor ζ is practically determined by the number of neutrons:

$$\zeta = (N/C)^{2/3}(1-(\pi^2/12)(\beta\zeta)^{-2}+\cdots). \quad (8)$$

ζ, in its turn, determines U except for a small term of the relative order $(\beta\zeta)^{-2}$. There will, therefore, be a large zero-point energy of the nucleus, plus a small additional (excitation) energy. The latter determines the constant β.

If the nucleus is in its ground state, β will be infinity. In this case, the "Fermi energy" becomes (cf. (8))

$$\zeta_0 = (N/C)^{2/3} \quad (9)$$

and the total kinetic energy of all neutrons (cf. (7a), "zero-point energy")

$$U_0 = \tfrac{2}{5} C\zeta_0^{5/2} = \tfrac{2}{5} N\zeta_0. \quad (9a)$$

From (8) and (9), we have

$$\zeta = \zeta_0(1-(\pi^2/12)(\beta\zeta_0)^{-2}+\cdots). \quad (10)$$

Inserting this into (7a), we find

$$U = \tfrac{2}{5} C\zeta_0^{5/2} + \tfrac{1}{4}\pi^2 C\beta^{-2}\zeta_0^{1/2}. \quad (10a)$$

Therefore the excitation energy is

$$Q = U - U_0 = \tfrac{1}{4}\pi^2 C\zeta_0^{1/2}\beta^{-2}, \quad (11)$$

wherefrom

$$\beta^{-2} = 4Q/\pi^2 C\zeta_0^{\frac{1}{2}} \quad (11a)$$

or, by inserting (7)

$$\beta^{-1} = (2/\pi)(\zeta_0 Q/N)^{\frac{1}{2}}. \quad (12)$$

β^{-1} is the average excitation energy of the individual particles (width of the "tail" of the Fermi distribution).

Numerically, ζ_0 turns out to be somewhat, but not very much, larger than Q. Therefore β^{-1} is of the order QN^{-1}. In other words, the excitation energy is, in our model, shared between $N^{\frac{1}{2}}$ particles.

The right-hand side of (6) can be transformed by partial integration; we obtain exactly (i.e., not only for large β)

$$(3/2) C \int \epsilon^{\frac{1}{2}} d\epsilon \log (1+e^{\beta(\zeta-\epsilon)}) = \beta C \int \epsilon^{\frac{1}{2}} d\epsilon / (e^{\beta(\zeta-\epsilon)}+1) = \tfrac{2}{3}\beta U. \quad (13)$$

Therefore

$$\Phi = \log \sum_{N'} \int dU' \rho(U') e^{\beta\zeta(N'-N)-\beta(U'-U)} = (5/3)\beta U - \beta\zeta N. \quad (14)$$

Inserting (7) (7a) we get

$$\Phi = \beta C\zeta^{5/2}\tfrac{1}{2}\pi^2(\beta\zeta)^{-2} = \tfrac{1}{2}\pi^2 C\beta^{-1}\zeta^{\frac{1}{2}} \quad (14a)$$

and with (11a) (9)

$$\Phi = \pi(NQ/\zeta_0)^{\frac{1}{2}}. \quad (15)$$

This formula contains the fundamental result of our calculations. The following calculations, down to the end of section 4, represent only refinements.

In order to obtain ρ from (14), (15) we remark that the argument of the logarithm on the left-hand side in (14) is essentially $\rho(U)$ because the integrand has a sharp maximum for $U'=U$. Therefore we put

$$\rho(Q) = \lambda(N, Q) e^{\Phi(Q)}, \quad (16)$$

where λ is a slowly varying function of Q. We shall determine λ by carrying out the summation

[4] Sommerfeld, Zeits. f. Physik **47**, 1 (1927).

in (14), regarding λ as constant over the range of N' and U' involved. We find then from (14)

$$\lambda(N, Q)\int dQ' \exp\left[\beta\zeta(N'-N) - \beta(U'-U)+\Phi(Q')-\Phi(Q)\right]=1, \quad (17)$$

having replaced the integration variable U' by Q'.

In order to evaluate (17), we consider the exponent

$$f(\beta', \zeta')=\beta\zeta(N'-N)-\beta(U'-U)+(5/3)\beta' U' - \beta'\zeta' N'-(5/3)\beta U+\beta\zeta N=((5/3)U'-N'\zeta')(\beta'-\beta) + \tfrac{2}{3}\beta(U'-U)-N'\beta(\zeta'-\zeta), \quad (18)$$

where β' and ζ' are the parameters corresponding to $N'U'$. Using the formulae (7), (7a) repeatedly, we find by an elementary calculation

$$(5/3)U'-N'\zeta'=\tfrac{1}{2}\pi^2 C\beta'^{-2}\zeta'^{\frac{1}{2}}, \quad (18a)$$

$$\tfrac{2}{3}(U'-U)-N'(\zeta'-\zeta)=-\tfrac{3}{4}C\zeta'^{\frac{1}{2}}(\zeta'-\zeta)^2 + \tfrac{1}{4}\pi^2 C\zeta'^{\frac{1}{2}}(\beta'^{-2}-\beta^{-2}), \quad (18b)$$

leaving out some terms of the relative order $(\beta\zeta)^{-2}$. Inserting into (18), we have

$$f=-C\beta\zeta^{\frac{1}{2}}[\tfrac{3}{4}(\zeta'-\zeta)^2+\tfrac{1}{4}\pi^2(\beta'-\beta)^2(\beta\beta')^{-2}]. \quad (19)$$

The exponential in (17) behaves thus as $e^{-a(\zeta'-\zeta)^2-b(\beta'-\beta)^2}$ as should be expected. The differences $\zeta'-\zeta$ and $\beta'-\beta$ may be expressed in terms of $N'-N$ and $Q'-Q$, respectively, using (9) and (12). Neglecting again some small terms, we get

$$f=-\frac{\pi}{2}\left(\frac{N}{\zeta_0 Q}\right)^{\frac{1}{2}}\left[\tfrac{1}{3}(N'-N)^2\frac{\zeta}{N}+\frac{1}{4}\frac{(Q'-Q)^2}{Q}\right]. \quad (19a)$$

This may be inserted into (17) and the integrations carried out. Then

$$\frac{1}{\lambda(N, Q)}=\int_{-\infty}^{+\infty}dQ'\int_{-\infty}^{\infty}dN' \exp\left[-\frac{\pi}{6}\left(\frac{N}{\zeta Q}\right)^{\frac{1}{2}}\frac{\zeta}{N}(N'-N)^2 - \frac{\pi}{8}\left(\frac{N}{\zeta Q}\right)^{\frac{1}{2}}\frac{(Q'-Q)^2}{Q}\right]=\frac{\pi}{48^{-\frac{1}{2}}\pi}\left(\frac{\zeta Q}{N}\right)^{\frac{1}{2}}\left(\frac{N}{\zeta}\right)^{\frac{1}{2}}Q^{\frac{1}{2}}=48^{\frac{1}{2}}Q. \quad (20)$$

Therefore we find finally (cf. (16), (15))

$$\rho(Q)dQ=48^{-\frac{1}{2}}e^{\pi(NQ/\zeta)^{\frac{1}{2}}}dQ/Q \quad (21)$$

for the number of states of the system composed of all the neutrons, having a total excitation energy between Q and $Q+dQ$. A similar expression holds for the protons. Therefore the total number of levels of the nucleus as a whole per dQ is

$$\rho(Q)=\int dQ_1 \exp\left(\pi(NQ_1/\zeta_1)^{\frac{1}{2}} + \pi(ZQ_2/\zeta_2)^{\frac{1}{2}}\right)/48Q_1Q_2, \quad (22)$$

where $Q_2=Q-Q_1$ is the excitation energy of the protons.

The integration is facilitated by the fact that, for all existing nuclei, practically $N/\zeta_1=Z/\zeta_2$. The Fermi energies $\zeta_1\zeta_2$ are given by (cf. 9)

$$\zeta_1=(N/C)^{\frac{1}{2}}, \qquad \zeta_2=(Z/C)^{\frac{1}{2}}, \quad (23)$$

so that

$$a_1=\pi(N/\zeta_1)^{\frac{1}{2}}=\pi C^{\frac{1}{2}}N^{1/6}, \quad a_2=\pi(Z/\zeta_2)^{\frac{1}{2}}=\pi C^{\frac{1}{2}}Z^{1/6}. \quad (24a)$$

The ratio a_2/a_1 is, even for uranium, only $(146/92)^{1/6}=1.08$ and for other nuclei even closer to unity. We put therefore

$$a_1=a_2=a=\pi C^{\frac{1}{2}}(\tfrac{1}{2}A)^{1/6} \quad (24)$$

and have

$$\rho(Q)=\int dQ_1 e^{a(Q_1^{\frac{1}{2}}+(Q-Q_1)^{\frac{1}{2}})}/48Q_1(Q-Q_1). \quad (25)$$

The exponential has a sharp maximum for $Q_1=\frac{1}{2}Q$. We may write

$$Q_1^{\frac{1}{2}}+(Q-Q_1)^{\frac{1}{2}}=\sqrt{2}Q^{\frac{1}{2}}(1-\tfrac{1}{8}(2Q_1-Q/Q)^2+\cdots), \quad (25a)$$

while the denominator may simply be replaced by $12Q^2$. The integration gives then

$$\rho(Q)=\tfrac{1}{12}(\pi/a)^{\frac{1}{2}}2^{\frac{1}{4}}Q^{-5/4}e^{\sqrt{2}aQ^{\frac{1}{2}}}. \quad (26)$$

From its definition (24a), the constant a may be written

$$a=\pi(A/2\zeta_0)^{\frac{1}{2}}, \quad (27a)$$

where ζ_0 is the average Fermi energy for protons and neutrons. Then (26) reduces to

$$\rho(Q)=\tfrac{1}{12}\sqrt{2}\zeta_0^{\frac{1}{4}}Q^{-5/4}A^{-\frac{1}{4}}e^{\pi(AQ/\zeta_0)^{\frac{1}{2}}}. \quad (27)$$

The value of ζ_0 follows from (9) and (4a):

$$\zeta_0=(A/2C)^{\frac{1}{2}}=(3^{4/3}\pi^{\frac{1}{3}}/8)(\hbar^2A^{\frac{1}{3}}/MR^2). \quad (28)$$

Now the nuclear volume is proportional to the atomic weight A, so that

$$R=r_0A^{1/3}, \quad (29)$$

where r_0 may be calculated from the experimental data on α-radioactivity. Assuming $R=9\cdot10^{-13}$ cm for the average radius of radioactive nuclei, corresponding to A about 222, we have

$$r_0=1.48\cdot10^{-13}\text{ cm} \quad (29a)$$

and $$\zeta_0=(3^{4/3}\pi^{\frac{1}{3}}/8)(\hbar^2/Mr_0^2)=21.5\text{ MV}. \quad (30)$$

Putting now

$$x=\pi(AQ/\zeta_0)^{\frac{1}{2}}=(AQ/2.20)^{\frac{1}{2}} \quad (31)$$

(Q in MV), we have for the spacing between neighboring levels

$$1/\rho(Q)=12\cdot(2\pi)^{-\frac{1}{2}}Qx^{\frac{1}{2}}e^{-x}. \quad (32)$$

For medium atomic weight, let us say $A=110$, and for $Q=8$ MV, we have $x=20$ and the spacing (32) becomes

$$5\cdot8\cdot10^6\cdot4.5\cdot2\cdot10^{-9}=0.4\text{ volt}. \quad (32a)$$

This is obviously too small compared to the experimental spacing between neutron resonance levels. The reasons will be explained in the following section.

4. States with Given Angular Momentum

Most of the nuclear energy levels calculated in the preceding section will have very large angular momenta. Already the angular momentum of an individual particle in a heavy nucleus is apt to run up to about 6 (see Eq. (44a), below), and if the momenta of a fairly large number of particles are added, extremely large momenta for the nucleus as a whole may result. On the other hand, only small momenta of the nucleus A are of any importance for the capture of slow neutrons by the nucleus $A-1$. The nucleus $A-1$ will, in its ground state, have a certain total angular momentum ("nuclear spin"), say I_0. The neutron must have orbital momentum $l=0$ in order to be captured by the nucleus $A-1$, and therefore total momentum $j=\frac{1}{2}$, considering its spin. The resulting state of the "compound nucleus" A must therefore have an angular momentum $I_0\pm\frac{1}{2}$. Of all the levels of the nucleus A, we should therefore consider only those with angular momenta $I_0\pm\frac{1}{2}$; and I_0 will be small compared to the "average angular momentum" of all possible states of the nucleus A. Only a small fraction of the levels considered in the preceding section will fulfill this condition.[5]

We want to calculate the probability that a nuclear level has a given angular momentum I. In order to do this, we assume that each individual particle in the nucleus has the same angular momentum j. (The value of j will be calculated later; also we shall then consider the variation of j among the particles.) The resultant of all individual particle momenta will be the moment of the nucleus, I. Following the usual procedure, we consider the *components* of the angular momenta in a given direction z. Let m_i be the z-component of the momentum of particle i, and M the z-component of the total momentum. Then

$$M=\sum_i m_i, \tag{33}$$

We want to know the probability of a given resultant M, each value of m_i from $-j$ to $+j$ being equally probable. Provided the number n of particles is large, the probability for a given M is given by the "Gauss formula"

$$p(M)=(\tfrac{2}{3}\pi nj(j+1))^{-\frac{1}{2}}e^{-3M^2/2nj(j+1)}. \tag{34}$$

To prove this, we make use of three facts:

(1) If $p_n(M)$ is the probability that n momenta have the resultant M in the z direction, we must have the "addition theorem"

$$p_{r+s}(M)=\sum_{M_1}p_r(M_1)p_s(M-M_1)$$
$$=\int_{-\infty}^{\infty}p_r(M_1)p_s(M-M_1)dM_1. \tag{34a}$$

If this is to be generally true for arbitrary values of r, s and M, then p must be of the form

$$p_n(M)=c_ne^{-\alpha M^2/n}, \tag{35a}$$

where α is a constant independent of n while c_n depends on n.

(2) The average of M^2, *viz.*

$$\overline{M^2}=\sum_M M^2p_n(M), \tag{36}$$

must be given by

$$\overline{M^2}=\sum_{ik}\overline{m_im_k}=\sum_i\overline{m_i^2}+\sum_{i\neq k}\overline{m_im_k}=n\overline{m^2}, \tag{36a}$$

since two different m's (m_i and m_k) are independent of each other, and the average value of an individual m is zero. Now

$$\overline{m^2}=\sum_{m=-j}^{j}m^2/(2j+1)=\tfrac{1}{3}j(j+1). \tag{36b}$$

On the other hand, we have from (35a)

$$\overline{M^2}=\int p_n(M)M^2dM/\int p_ndM=n/2\alpha. \tag{37}$$

Comparing (36a), (36b), (37), we find

$$\alpha=3/2j(j+1). \tag{37a}$$

(3) The total probability must be unity:

$$\int_{-\infty}^{\infty}p_n(M)dM=1. \tag{38}$$

This fixes the constant c_n in (35a).

The number of states of given total angular momentum I is, as is well known, equal to the number of states with $M=I$, minus the number of states with $M=I+1$. Since $\rho(Q)dQ$ is the total number of nuclear states in the energy interval dQ, the number of states with a given M is $\rho(Q)p(M)dQ$ and the number of energy levels with a given I therefore

$$\rho(Q)[p(I)-p(I+1)]dQ. \tag{39}$$

[5] The importance of the angular momentum for the number of nuclear states was first pointed out to me by Dr. Placzek, to whom I am indebted for this suggestion.

Since p varies slowly with its argument M, this gives

$$\rho(Q, I)=\rho(Q)(dp/dM)_{I+\frac{1}{2}}. \quad (40)$$

Here we insert (34), carry out the differentiation and then put the exponential equal to unity, since for all cases of interest $I^2 \ll nj(j+1)$. We obtain thus

$$\rho(Q, I)=\rho(Q)(2I+1)(8\pi)^{-\frac{1}{2}}(3/nj(j+1))^{3/2}. \quad (41)$$

We have now to compute $nj(j+1)\approx n(j+\frac{1}{2})^2$. We have therefore to know the average angular momentum j of the individual particles, and the number n of the particles which contribute to the resultant angular momentum of the nucleus. We know that in the ground state of a nucleus the resultant momentum is almost zero, because the momenta of the various individual particles nearly cancel each other ("closed shells"). Therefore the angular momentum of an excited state of a nucleus comes from the "tail of the Fermi distribution," i.e., from those particles whose energy is larger than the Fermi energy ζ, and from the empty states of energy smaller than ζ.

For j we have thus to take the average angular momentum of an individual particle whose energy is near ζ. We therefore calculate the number of quantum states (per unit energy) of given orbital momentum l for an individual particle of kinetic energy ζ which is enclosed in a deep spherical potential well of radius R. This problem is similar to the problem of the first appearance of an electron of orbital momentum l in the periodic system which was treated by Fermi.[6] The problem can be solved by separating the wave equation in polar coordinates, and then using the WKB (Wentzel Kramers Brillouin) method for treating the radial wave equation. This leads to the well known "quantum condition"

$$\int^R dr[(2M/\hbar^2)\epsilon-(l+\tfrac{1}{2})^2/r^2]^{\frac{1}{2}}=(n+\tfrac{1}{2})\pi, \quad (42)$$

where n is an integer and ϵ the energy of the particle. Since there is one quantum state for each integral value of n, the number of states of orbital momentum l in the energy interval $d\epsilon$ is

$$w(\epsilon)d\epsilon=\frac{d\epsilon}{\pi}\frac{d}{d\epsilon}\int^R dr\left[\frac{2M}{\hbar^2}\epsilon-\frac{(l+\frac{1}{2})^2}{r^2}\right]^{\frac{1}{2}}$$
$$=\frac{Md\epsilon}{\pi\hbar^2}\int^R\frac{rdr}{[2M\epsilon\hbar^{-2}r^2-(l+\frac{1}{2})^2]^{\frac{1}{2}}}$$
$$=\frac{d\epsilon}{2\pi\epsilon}[2M\epsilon\hbar^{-2}R^2-(l+\tfrac{1}{2})^2]^{\frac{1}{2}}. \quad (43)$$

The number of states with a given j is equal to the number of states with $l=j-\frac{1}{2}$, plus the number of states with $l=j+\frac{1}{2}$. Therefore it will be approximately proportional to

$$w'(j)=[2M\zeta R^2\hbar^{-2}-(j+\tfrac{1}{2})]^{\frac{1}{2}}, \quad (43a)$$

leaving out factors independent of j and putting the particle energy equal to ζ. The number of *particles* of angular momentum j will be proportional to $(2j+1)w'(j)$ because each level j has the statistical weight $2j+1$. Therefore the average value of $(j+\frac{1}{2})^2$ is

$$\overline{(j+\tfrac{1}{2})^2}=\int(2j+1)dj(j+\tfrac{1}{2})^2w'(j)/\int(2j+1)djw'(j)$$
$$=(2/5)\cdot 2MR^2\hbar^{-2}\zeta. \quad (44)$$

Inserting the value of ζ from (30) and R from (29), we find

$$\overline{(j+\tfrac{1}{2})^2}=(3^{4/3}\pi^{\frac{1}{3}}/10)A^{\frac{1}{3}}=0.93A^{\frac{1}{3}}. \quad (44a)$$

There remains the computation of n, which is the number of neutrons and protons having energies larger than ζ, plus the number of unoccupied states of energy smaller than ζ. Obviously, n is about four times the number of neutrons with energy larger than ζ. According to the Fermi distribution, this number is given by

$$\tfrac{1}{4}n=(3/2)C\int_\zeta^\infty\frac{\epsilon^{\frac{1}{2}}d\epsilon}{e^{\beta(\epsilon-\zeta)}+1}=3/2\frac{C\zeta^{\frac{3}{2}}}{\beta}(1-\tfrac{1}{2}+\tfrac{1}{3}-\cdots)$$
$$=3/2\frac{C\zeta^{\frac{3}{2}}}{\beta}\log 2 \quad (45)$$

or, inserting the value of β from (11a), and of C from (9), we have

$$n=\frac{12}{\pi}\log 2\left(\frac{QN}{\zeta}\right)^{\frac{1}{2}}=\frac{6\sqrt{2}\log 2}{\pi}\left(\frac{QA}{\zeta}\right)^{\frac{1}{2}}=1.87\left(\frac{QA}{\zeta}\right)^{\frac{1}{2}}. \quad (46)$$

For $A=100$, $Q=8$ MV and $\zeta=20$ MV, this would be about 12.

With this value for n, and (44a) for $j(j+1)$, we find for the number of nuclear levels with angular momentum I:

$$\rho(Q, I)=(2I+1)\rho(Q)(5/\log 2)^{\frac{1}{2}}\cdot 2^{-9/4}\cdot 3^{-2}(\zeta/Q)^{3/4}A^{-7/4}. \quad (47)$$

Inserting $\rho(Q)$ from (27), we have

$$\rho(Q, I)=2^{-15/4}\cdot 3^{-2}(5/\log 2)^{\frac{1}{2}}(2I+1)\zeta_0^{-1}\times(\zeta_0/QA)^2e^{\pi(AQ/\zeta_0)^{\frac{1}{2}}} \quad (48)$$

or, introducing the abbreviation $x=\pi(AQ/\zeta_0)^{\frac{1}{2}}$ from (31):

$$\rho(Q, I)=\frac{\pi^4\cdot 2^{\frac{1}{2}}}{432}\left(\frac{5}{\log 2}\right)^{\frac{1}{2}}(2I+1)\zeta^{-1}x^{-4}e^x. \quad (49)$$

The spacing between two levels of spin I is the reciprocal of this, *viz.*

$$\Delta=\frac{432}{2^{\frac{1}{2}}\pi^4}\left(\frac{\log 2}{5}\right)^{\frac{1}{2}}\frac{\zeta}{2I+1}x^4e^{-x} \quad (50)$$

or
$$\Delta=\Delta_0/(2I+1) \quad (50a)$$

with
$$\Delta_0=4.1\cdot 10^6x^4e^{-x}\text{ volts} \quad (50b)$$

and
$$x=(AQ/2.20)^{\frac{1}{2}},\quad (Q\text{ in MV}). \quad (50c)$$

[6] Fermi, Zeits. f. Physik **48**, 73 (1928).

In applications to the capture of slow neutrons, it should be remembered that levels with $I=I_0\pm\frac{1}{2}$ of the "final" nucleus are effective if I_0 is the "spin" of the capturing nucleus.

5. Criticism of the Method Used

We have assumed the energy levels of the nucleus as a whole to be given by the sum of the energies of the individual particles. In other words, we have taken into account the interaction between the particles only insofar as it can be expressed in terms of a potential acting on each particle (Hartree method). This method would, of course, lead to a hopelessly wrong result if we wanted to deduce the actual characteristics (wave function) of each nuclear level from it. It might, however, give fairly correct results for the number of levels in a given energy interval.

The interaction between particles will thoroughly mix the wave functions of the various nuclear levels obtained from the Hartree approximation. A group of levels which would have approximately the same energy in the Hartree approximation will, by the interaction between the particles, be drawn out into a spectrum extending over a wide energy range, probably several MV. Conversely, the wave functions of the *actual* nuclear states in a given energy interval will be linear combinations of Hartree wave functions belonging to much lower as well as much higher Hartree levels.

From these considerations, it might seem that the general behavior of the density of levels, as a function of the energy, might *in the average* be not very greatly changed by the interaction between the particles. There is, however, one fact which will somewhat invalidate this conclusion: The lowest level of the nucleus lies certainly lower than the corresponding Hartree level. It might seem that Q should be taken as the energy of a nuclear level as compared to that of the lowest *Hartree* level. Then Q would be smaller than the actual excitation energy counted from the *true* ground state of the nucleus, which we may call Q'. If we inserted Q' into our formulae we should then obtain too small a spacing between the nuclear levels.

However, we believe that this error is compensated by the fact that we are considering only nuclear levels of low angular momentum. From experience, and from some calculations made recently on light nuclei,[7] we know that the nuclear levels of low angular momentum usually lie lowest, those with high momentum highest among the levels arising from a given configuration. It may be expected that the levels of low momentum arising from "excited configurations" are depressed by the same amount, as compared to their position in the Hartree approximation, as the ground level. Thus we may expect our formulae to give us about the correct density of levels of low angular momentum if we insert for Q the actual energy of excitation above the ground state. Of course, the formulae would give us too high a density of levels of high momenta.

Another reason why we believe our formulae to be not too far wrong, is the fact that the actual levels in a given energy interval will mostly arise from Hartree levels of higher energy, simply because there is a rapid increase of the density of Hartree levels with increasing energy. Most of the levels will therefore be related to the corresponding Hartree levels in a similar way as the ground state.

6. Discussion of the Spacing of Nuclear Levels

The spacing of nuclear energy levels depends, according to formula (50), only on the product of the mass number A of the nucleus and the excitation energy Q. Light nuclei, and heavy nuclei at energies just above the ground level, should possess very few quantum states while highly excited heavy nuclei ought to have an enormous number of closely spaced levels.[1]

Table I gives the spacing between the levels with $I=0$ for various values of the product AQ. E.g., if a nucleus of atomic weight 112(Cd) captures a neutron with the evolution of about

Table I. *Spacing Δ_0 of nuclear energy levels of zero angular momentum in volts.**

QA (in MV)	100	200	400	600	800	1000	1200	1500	1800
Δ_0 (in Volts)	10^7	$2.4\cdot10^6$	$1.9\cdot10^5$	$2.1\cdot10^4$	2800	450	85	8.5	1.0

*For angular momentum I, the spacing would be $\Delta=\Delta_0/(2I+1)$.

[7] Bethe and Bacher, Rev. Mod. Phys. **8**, 82 (1936) (quoted as B), §36, Wigner and Feenberg, to appear shortly in the Phys. Rev., and unfinished calculations of Bethe and Rose.

9 MV energy, QA would be 1000 and the spacing of S levels of that nucleus only 450 volts. For higher angular momenta, the spacing between levels becomes even less, e.g., for $I=3$ it would be only 1/7 of the previous value, i.e., 60 volts. Since two values of the angular momentum ($I=I_0\pm\frac{1}{2}$, see section 4) lead to neutron capture, the distance between neutron resonance levels would be only one half of the values given. The distance between the highly excited levels of fairly heavy nuclei is thus very small indeed.

For smaller charge, the spacing between levels becomes very much larger. If we let Q be again of the order 9 MV, the spacing of levels for a nucleus such as Fe($A=55$) will be of the order of ten thousand volts, and for really light nuclei such as O($A=16$) of the order of a million volts. This explains why simple capture of neutrons is practically never found with any great intensity for really light nuclei. It would also mean that the lowest neutron resonance level for a nucleus of atomic weight around 50 will, in the average, lie at very much higher energy than for atomic weights of the order 100.

Another cause for an increased spacing of levels would be a smaller value of the excitation energy Q. In connection with the capture of slow neutrons, this would mean that the energy set free in the capture process would have to be smaller than 9 MV. This energy is given by

$$Q=M_{A-1}+M_n-M_A, \tag{51}$$

where M_{A-1}, M_n and M_A denote the (exact) masses of the capturing nucleus, the neutron and the product nucleus respectively, in energy units. In the average, nuclei of medium atomic weight have packing fractions of $-1/1000$, so that M_A-M_{A-1} will be about 0.999 mass unit. The neutron mass being almost 1.009, we find *in the average* the above-mentioned figure $Q=9$ MV (For details, see below).

However, deviations from this figure are to be expected if either of the nuclei $A-1$ or A is exceptionally stable or unstable. The greatest variations will in general come in through the product nucleus A. If this nucleus is radioactive, it is obviously less stable than if it is not. Thus it is to be expected that the energy evolution Q is smaller (in the average) if a radioactive nucleus A is produced, than otherwise. Therefore the spacing of neutron energy levels will be larger in the case of the production of a radioactive nucleus, and the first resonance level will lie at a higher neutron energy. Now it is known from the Breit-Wigner theory[2] of neutron capture that the capture probability for thermal neutrons is, cet. par., the larger the lower the energy of the first resonance level. *The probability of capture of thermal neutrons will, therefore, in the average be smaller if the capture leads to a radioactive nucleus than if it leads to a stable nucleus.*

This fact has been known for some time experimentally and has puzzled investigators to some extent. All the very large cross sections (of the order 10^{-21} cm^2 and more, e.g., Cd, Sm) for the absorption of slow neutrons are connected with the formation of stable nuclei whereas the cross section for the formation of radioactive nuclei are in general only moderately large (about 10^{-22} cm^2 or smaller). Even more marked differences should be found in the positions of the lowest resonance level for neutrons: This level should lie, in the average, at higher neutron energies for the formation of radioactive nuclei than for capture processes leading to stable nuclei.

Apart from irregularities for the individual nuclei, the value of the "dissociation energy" Q will depend on charge and mass number of the nuclei A and $A-1$. We know that generally nuclei with even charge and even mass are most stable, such with odd mass number less stable, and nuclei of odd charge and even mass number unstable to the extent of being radioactive.[8] Therefore we have to distinguish three cases:

(1) The capturing nucleus $A-1$ has *odd charge*. Its mass must then be also odd. Then the capture of a neutron will certainly lead to a radioactive nucleus of odd charge and even mass. The energy Q evolved will be comparatively small, the spacing between the neutron levels fairly large and the capture cross section for temperature neutrons only moderately large.

(2) The capturing nucleus $A-1$ has *even charge and even mass*. The nucleus produced will then have even charge and odd mass. It may be radioactive or stable. But in any case, it will have relatively higher energy in its ground state than the capturing nucleus. Therefore the energy evolved will again be comparatively small, and probably of the same order as in case (1), irrespective of whether the nucleus A is radioactive or not.

(3) The capturing nucleus $A-1$ has *even charge and odd mass*. The nucleus produced will then be of the most stable

[8] For a discussion and explanation of this fact, see B, §10.

type, i.e. even charge and even mass. The energy Q evolved will be exceptionally large, the lowest resonance level will lie at very low neutron energy and the cross section for temperature neutrons will be exceedingly large.

From these considerations it would seem that very strong capture of temperature neutrons can only be due to nuclei of even charge and odd mass number. We suggest that the neutron absorption levels at very low neutron energies which have been observed[9] for Cd, Sm and Hg are due to the abundant "odd isotopes" Cd^{111} or Cd^{113}, Sm^{147} or Sm^{179}, and Hg^{199} or Hg^{201}, respectively.

Another factor which will also increase the capture in case 3 is the factor $2I+1$ in the number of energy levels per unit energy (cf. 49). The spin I of the "resonance level" of the product nucleus A may be either $I_0-\frac{1}{2}$ or $I_0+\frac{1}{2}$ if I_0 is the angular momentum of the original nucleus $A-1$ (cf. beginning of section 4). The number of levels of the nucleus A suitable for the capture of neutrons will therefore be proportional to $2(2I_0+1)$, i.e., the larger the greater the spin of the original nucleus. Now all nuclei with even charge and even mass (class 2 above) seem to have spin $I_0=0$, while nuclei with odd mass (classes 1 and 3) have spins different from zero and therefore are more likely to capture slow neutrons.

We shall now try to compute roughly the actual values of Q to be expected and the differences in the Q values between the above-mentioned cases 1, 2 and 3. An estimate of the latter may perhaps be based on the average energy of the β-particles obtained from neutron captures of class 1. The lifetimes of the radioactive nuclei obtained from neutron capture vary from about 20 sec. to some hours or days, at least for the radioactivities known at present. According to the Sargent rule, this corresponds to energies from about 1 to 3 MV. In the average, we find therefore that nuclei of even mass number and odd nuclear charge have energies by 2 MV greater than their neighboring isobars of even charge into which they transform by emitting a β-ray. Now we may safely assume that the average packing fraction of nuclei of *odd* mass number is independent of whether their nuclear charge is even or odd, because firstly there seems to be experimentally no difference between the number of species and the abundance of these two types of nuclei, and secondly there is no theoretical reason for assuming any difference (cf. B, §10). Consequently, the energy Q evolved in the capture of neutrons by nuclei of odd weight and even charge (class 3 above) ought to be about 2 MV more than for nuclei of odd weight and odd charge (class 1). For nuclei of class 2 (even weight, even charge) we may expect about the same Q's as for class 1, because in both cases the transition goes from a more stable to a less stable type of nucleus.

A rough estimate of the *average* value of Q, i.e. the mean between the cases (2) and (3) above, may be obtained from an empirical formula for the average nuclear mass defects as a function of mass number A and charge Z, such as that derived by Weizsäcker[10] or by the author (B, §30). The energy (excess of the exact mass value over the mass number) of the most stable nucleus of atomic weight A is approximately given by (B, Eq. (186))

$$E(A)=-6.6_5A+14.2A^{2/3}+0.156A^{5/3}\cdot 135/(134+A^{2/3}), \quad (52)$$

the unit of energy being a thousandth of a mass unit. The difference in energy between the nuclei A and $A-1$ is therefore (cf. B (186b))

$$E(A)-E(A-1)=-6.6_5+9.5A^{-1/3}+0.156A^{2/3}\cdot 135(223+A^{2/3})/(134+A^{2/3})^2. \quad (52a)$$

The mass of the neutron may be calculated from the following data:

(1) The mass spectroscopic comparison of the deuteron and the proton by Bainbridge and Jordan,[11] giving

$$2H-D=0.00153\pm 0.00004 \text{ mass unit.}$$

(2) The binding energy of the deuteron as measured by Feather[12]

$$H+n-D=2.22\pm 0.06 \text{ MV}=0.00238.$$

(3) The mass of the deuteron as derived from

[9] Rasetti, Fink, Goldsmith and Mitchell, Phys. Rev. **49**, 869, 1936. Placzek and Frisch (private communication). Amaldi and Fermi, Ricerca Scientifica **1**, 11–12 (1936).

[10] Weizsäcker, Zeits. f. Physik **96**, 431 (1935).

[11] Bainbridge and Jordan, Bull. Am. Phys. Soc., 1936, Washington meeting, report 123.

[12] Feather, Nature **136**, 467 (1935). A correction of 40,000 volts has been applied to Feather's value because of the range energy relation (B, p. 123).

TABLE II. *Mass excesses of nuclei and energy evolved in neutron capture.*

A	20	50	100	150	200	240
$E(A)-E(A-1)$ (mass units)	−1.45	−1.0	0	0.75	1.4	1.9
$\bar{Q}$(MV)	9.5	9.1	8.2	7.5	6.9	6.4

disintegration data[13]

$$D=2.01445.$$

A combination of these three data gives

$$n=H+0.00085=\tfrac{1}{2}D+0.00161=1.00884. \quad (53)$$

Thus the energy $\bar{Q}$ evolved in the neutron capture will be 8.84 thousandths of a mass unit, minus the energy difference (52a). Converted into MV, this gives

$$\bar{Q}=14.4-8.8A^{-1/3}-0.145A^{2/3}\cdot 135(223+A^{2/3})/(134+A^{2/3})^2. \quad (54)$$

Table II gives the average difference between the mass excess of neighboring isotopes, $E(A)-E(A-1)$, according to the semi-empirical formula (52a), in thousandths of a mass unit, and the average energy evolved in the capture of a neutron, $\bar{Q}$, in MV. The values in the table are of course only averages, and in individual cases large deviations ought to be expected. Moreover, it seems from the observed energies of radioactive α-particles that the mass excess of heavy nuclei increases actually somewhat faster with increasing A, so that $\bar{Q}$ for $A=200$ or more may actually be about 0.5 MV smaller than indicated in the table.

Accepting the energies given in the table for the *average* energy evolved in neutron capture, we should expect values by about 1 MV *higher* for the capture by nuclei of even charge and odd mass number (class 3 above) and about 1 MV *lower* than the values of the table for the other cases (classes 1 and 2 above). Thus the odd isotopes of Cd would probably correspond to Q values slightly over 9 MV, giving for AQ a value somewhat over 1000. With a spin of $I_0=\frac{1}{2}$ (B, Table 19) for both the "odd" isotopes of Cd, we should thus expect a spacing of the nuclear levels of about 50 volts (cf. Table I, divide by $2(2I_0+1)$). For Ag, we would expect $Q=7$ MV, approximately, $AQ=800$, and, with $I_0=3/2$, a spacing of about 300 volts between neighboring levels. These figures seem reasonable, although perhaps a little high.

Turning now to the very heavy nuclei (A around 200), we should expect very many very closely spaced levels. The increase in the density of levels due to the increased number of particles A in the nucleus is, however, partly offset by the decrease in the energy evolved in the neutron capture,[14] as shown in Table II. Even so, we should expect values of QA of the order 1400 for $A=200$ (Hg, cf. Table II). This would correspond to a spacing of about 20 volts between levels with $I=0$. Now Hg^{201} has a spin of $3/2$; therefore the average spacing between the resonance levels of neutrons captured by Hg^{201} ought to be about two volts. An element of such high atomic number should have an almost continuous absorption spectrum for slow neutrons if the element belongs to class 3, i.e., has even charge and odd mass.

For elements of odd charge (or of even charge and even mass), the increase in the density of levels for high mass number should be less marked. Suppose the Q value is 1 MV less than the "average" given in Table II; which may easily happen. Then AQ is reduced to 1200 for $A=200$, i.e., not much more than for elements of medium atomic weight such as Cd. The distance between adjacent levels would, accordingly, be of the order of 10 volts. This is compatible with the observed resonance level of Au (2.5 volts.)

I wish to express my thanks to Dr. G. Placzek and Dr. L. Nordheim for interesting discussions and valuable suggestions. My thanks are also due to Dr. M. E. Rose for a critical revision of the manuscript.

[13] Cockcroft and Lewis, Proc. Roy. Soc. **A154**, 261 (1936).

[14] The importance of this factor was first pointed out to me by Dr. Nordheim.

Relativity and Nuclear Forces

HENRY MARGENAU, *Sloane Laboratory, Yale University*

(Received June 19, 1936)

To obtain an estimate of the relativity correction in nuclear problems, the Klein-Gordon theory is applied to the common forms of interaction between the neutron and the proton. Because there is an appreciable region of space in which the zero-point energy is enormous, the relativity effect is larger than would be supposed by mere inspection of binding energies. For the deuteron, it amounts to several times the binding energy if the forces have a range around 10^{-13} cm; for ranges about 3×10^{-13} cm it decreases to a few percent of the binding energy.—The calculations were based on two types of assumed interactions: the rectangular potential hole and the error function potential.

ACCORDING to the calculations of Wigner,[1] Massey and Mohr,[2] Feenberg,[3] and others the binding energy of light nuclei can be accounted for with reasonable accuracy by supposing the existence of interactions of various types between the elementary particles. It is common to these calculations that they represent the total energies as differences between large potential and slightly smaller kinetic energies, thus involving zero-point energies which are many times as great as the total energy of the nucleus. This circumstance is responsible for the fact that the binding energies are quite insensitive to the form chosen for the interaction; it allows the interaction to be specified very simply by two parameters, of which one is the width and the other the depth of the potential hole. But it also raises a question as to the basic meaning of the assumed interactions, whose precise form is rendered practically unobservable by the large amount of zero-point energy which they generate. Yet, while one might wonder about the ultimate satisfaction which the use of potential functions in connection with nuclear particles is likely to give, attention should be called to another point which is not quite so trivial and a little more definite.

It has to do with the extent to which one may safely neglect relativity corrections in the calculations mentioned. To make the argument precise let us refer to the simplest, the ordinary potential type of interaction, between a proton and a neutron, and represent it first as a potential well with vertical walls, of width a and depth D. The depth of this hole which will produce the correct binding energy of the deuteron (2.1 MEV) is easily calculated with the use of Schrödinger's equation for any given width a. It is also easy to compute, in simple classical fashion, the relative speed, v, of proton and neutron as a function of a. One then obtains the set of values listed in the first column of Table I. It is thus clear that the problem here under discussion invites inquiry.

There exists no rigorous relativistic theory for the problem of several bodies. Even if spins are entirely ignored, the two-body problem as it presents itself here, is incapable of solution. For the purpose of estimating the order of magnitude of the error in a classical calculation it may be adequate, however, to replace the two-body problem by a one-body problem using the *relativistically incorrect* procedure of introducing the reduced mass and relative coordinates. The results thus obtained are not to be trusted numerically, but they lie within a range of uncertainty peculiar to the nonrelativistic calculations. The one-body problem may then be solved by use of a relativistic modification of the Schrödinger equation. Since we do not know how to deal with the spins anyway, the suggested form is that of Klein-Gordon:

$$\nabla^2\psi+(1/\hbar^2c^2)[(E-V)^2-E_0^2]\psi=0. \qquad (1)$$

This, then, takes account of no other relativistic effects than the change of mass with velocity. If a well of width a and depth D is again chosen for V, the solution is of the same form as that of the ordinary Schrödinger equation, the energy

[1] E. Wigner, Phys. Rev. **43**, 252 (1933).
[2] H. S. W. Massey and C. B. O. Mohr, Proc. Roy. Soc **A152**, 693 (1935).
[3] E. Feenberg, Phys. Rev. **47**, 850 (1935).

TABLE I. *Binding energies of the deuteron computed under various conditions.*

$a\times10^{13}$ (cm)	$\frac{v}{c}$	D_{class} (MEV)	$D_{\text{rel.}}$ (MEV)	$D_{\text{class}}-D_{\text{rel.}}$ (MEV)
1	0.71	121.2	108.9	12.3
1.5	.49	58.7	55.8	2.9
2.0	.38	35.7	34.8	0.9
2.5	.31	24.93	24.37	0.56
3.0	.27	18.69	18.40	0.29

being determined by

$$\tan(\kappa a) = -\kappa/k.$$

But κ and k have slightly different meanings:

$$k=\left(\frac{2M}{\hbar^2}W-\frac{W^2}{\hbar^2c^2}\right)^{\frac{1}{2}},$$

$$\kappa=\left[\frac{2M}{\hbar^2}(D-W)+\frac{(D-W)^2}{\hbar^2c^2}\right]^{\frac{1}{2}},$$

where W is the binding energy.

Entries in the second and third columns of Table I show how, for a given value of a and the experimental binding energy of the deuteron, D is modified by the procedure here outlined. It is to be observed that the two values of D differ by more than 5 times the binding energy of the deuteron for $a=10^{-13}$ cm, but only by 13 percent of the binding energy for $a=3\times10^{-13}$ cm.

To compare the differences between the second and third columns of Table I with the binding energy of the deuteron (2.1 MEV) is not an altogether fair test of the theories. One should rather compute the effect of the decrease in D upon W. This was done for a variety of values of a, and it was found that the absolute error in W is about one-half the difference between the two D's.

The potential functions used in the literature (cf. in particular references 1, 2, 3) are not always of the simple type we have chosen. We wish to point out that there is no simple way of relating the results obtained for a rectangular hole to other potential functions. The average kinetic energies for the same binding energy may be widely different for two different potential troughs having approximately equal half-widths.

Feenberg[3] has done considerable work with potential functions of the type—$Ae^{-\alpha r^2}$. He has, in particular, succeeded in fitting the constants A and α to the observed binding energies for the deuteron and the alpha-particle, and suggests the values $A=165\ Mc^2$, $1/\alpha^{\frac{1}{2}}=1.34\times10^{-13}$ cm. It was thought of interest to compute the magnitude of relativity corrections for this case.

A simple method for determining the effect on the binding energy is the following. We write Eq. (1) in the form

$$(H+W+F)\varphi=0. \tag{2}$$

Here $W=Mc^2-E$, the binding energy, and $(H+W)\psi=0$ is the Schrödinger equation. The "perturbing" function F is then seen to be

$$F=-(1/2Mc^2)(W+V)^2. \tag{3}$$

If the integral over this function, weighted by ψ^2, is small, we may apply ordinary perturbation theory to compute the effect of F on W, and we may substitute the empirical value for W in (3). Thus

$$\Delta W=-(1/2Mc^2)\int(W+V)^2\psi^2 d\tau. \tag{4}$$

This expression was evaluated for Feenberg's potential function with the values of A and α cited above, ψ having been found by numerical integration of the Schrödinger equation. The result obtained was $\Delta W=-1.17Mc^2\approx0.6$ MEV. It amounts to an error of 28 percent of the binding energy. While this seems large, it must of course be remembered that a much smaller relative change in the constants of the potential function would annul it.

Relativity effects are evidently not serious as long as the range of the nuclear forces is as large as or larger than 3×10^{-13} cm. It may be that relativity corrections are of greater importance in heavy than in light nuclei.

Unfortunately, an attempt to make a correct relativistic calculation of the binding energies is blocked, chiefly by the following facts:

1. The use of *simultaneous* potentials is inconsistent with the relativistic point of view. For interactions between electrical charges this difficulty can be circumvented by the use of retarded potentials. Can this be done for nuclear constituents? *Formally* it is possible. The Hamiltonian for a group of particles then contains, besides the classical terms, an infinite sequence of terms in negative powers of c, the velocity of

light, that in c^{-1} being absent. But such procedure is, strictly speaking, not permissible. In classical electrodynamics, the retarded potentials which one encounters are solutions of Maxwell's equations; they appear as necessary generalizations of Coulomb's law. In nuclear physics, where the potential functions used hitherto are entirely arbitrary, the use of retarded functions has no meaning whatever.

2. Even if, following the classical analogy, retarded potentials are introduced, no exact calculation can be made. For there will then appear damping terms corresponding to the classical radiation reaction, permitting no stationary solution. The first of these terms is of the order c^{-3}. To avoid them, the sequence must therefore be broken off after the term in c^{-2}. But in that case, the approximation would hardly be satisfactory and the calculation of doubtful utility.

AUGUST 15, 1936 PHYSICAL REVIEW VOLUME 50

The Relation Between Electron Field Emission and Contact Electromotive Force for Liquid Mercury

DAN H. MOORE, *University of Virginia*
(Received June 13, 1936)

The relation between contact e.m.f. and the impulsive potential necessary to initiate a vacuum spark has been studied for a liquid mercury cathode. The magnitude and time of application of the impulsive potential were determined by a cathode-ray oscillograph so that possible distortion of the mercury surface produced by the electric field could be evaluated. For impure mercury no definite relation could be found. However, for carefully distilled mercury the relation between the work function and breakdown field was in qualitative but not in quantitative agreement with theory.

THE impulsive potential necessary to produce a vacuum spark has been studied by Beams[1] and Quarles.[2] Beams has investigated the field emission from a liquid mercury cathode using impulsive potentials of approximately 10^{-6} sec. duration and, by means of a rotating mirror, has shown that the luminosity appears at the anode before the cathode which suggested that the breakdown was initiated by field emission from the cathode. Quarles has measured the breakdown fields between a mercury cathode and a molybdenum anode along with the accompanying variation in the work function of the mercury. His results, although qualitative, were not in quantitative agreement with the theoretical predictions of Fowler and Nordheim.[3]

The present investigation was undertaken to extend the work of Quarles over a wider range and to find, if possible, the effect of impurities on the relation between field emission and the work function. Also the applied impulses were investigated with a high speed cathode-ray oscillograph in order that the effect of possible distortion of the mercury surface on the field measurements, as suggested by Tonks,[4] could be evaluated.

Outline of Procedure

The method consisted in measuring both the contact potential difference between a hot platinum filament and the mercury surface also the potential necessary to cause a vacuum spark between the mercury and a molybdenum sphere. The contact potential is a measure of the difference between the work functions of the two surfaces.[5, 6] The work function of platinum is assumed constant. Moreover, Cassel and Glückauf[7] have found that mercury vapor does not affect the work function of platinum. There-

[1] Beams, Phys. Rev. **44**, 803 (1933).
[2] Quarles, Phys. Rev. **48**, 260 (1935).
[3] Fowler and Nordheim, Proc. Roy. Soc. **A119**, 173 (1928).
[4] Tonks, Phys. Rev. **48**, 562 (1935).
[5] Mönch, Zeits. f. Physik **65**, 233 (1930).
[6] Eckart, Zeits. f. Physik **47**, 38 (1929).
[7] Cassel and Glückauf, Zeits. f. physik. Chemie 18 Abt. B 4–5, 347 (1932).

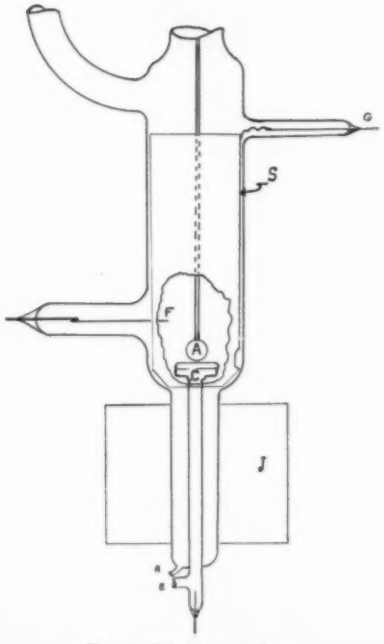

FIG. 1. Discharge tube.

fore, if the filament is kept at a fixed temperature, the change in contact potential gives the change in work function of the mercury.[8]

APPARATUS

The tube in which the measurements were made is shown in Fig. 1. It was sealed to a standard vacuum system. In order to minimize grease vapors, no stopcocks were used, all cut-offs being of the mercury type. The tube consisted of two parts—a main part about 20 cm long and 6.5 cm in diameter which was lined with a grounded nickel shield *S*, except for two openings, one for the filament leads and the other for observing the gap; a bottom part about 15 cm long and 3.8 cm in diameter, which permitted the removal of the mercury system without disturbing the rest of the tube, also gave space for packing dry ice in the jacket *J* to reduce mercury vapor pressure. An upper part, not shown, contained an aluminum support for the iron rod which held the sphere in place. Above this there was space for the rod and sphere to be lifted by an electromagnet out of the way while making measurements on contact potentials. The platinum filament *F*, 0.2 mm in diameter and 2.5 cm long was inserted from the side and welded to 100 mil nickel wire supports. The cathode consisted of the mercury contained in an iron cup *C*. The cup was 3.5 cm in diameter and the bottom fitted tightly into a 12 mm glass tube which conveyed the mercury from the condenser of a still. The mercury after overflowing the cup, thus changing the cathode surface, returned to the still through the tube *R*. The iron served to prevent the overflowing mercury from setting up charges which would interfere with the electrometer readings. The molybdenum spherical anode *A* was 2 cm in diameter and, when in position for a breakdown, was from 0.7 to 1.5 mm above the mercury surface, this distance being carefully measured each time with a telescope with micrometer eyepiece. The tube was mounted on a

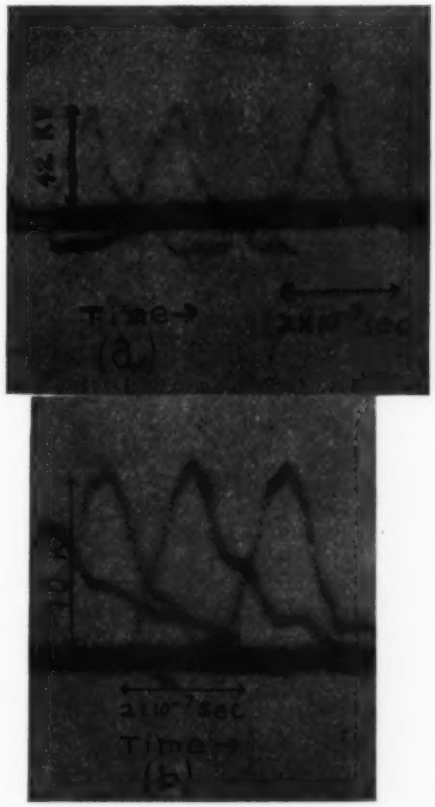

FIG. 2. Oscillograms of the impulse when the spark occurred (a) at the auxiliary gap, (b) at the vacuum gap.

[8] Compton and Langmuir, Rev. Mod. Phys. **2**, 145 (1930).

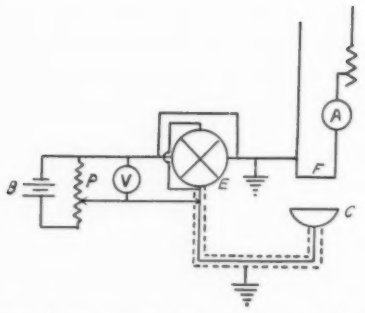

FIG. 3. Electrometer circuit for measuring contact potentials.

heavy table which floated on automobile inner tubes.

The impulses from the Marx circuit, set for 100 kv, were applied to the anode through the upper part of the tube. In parallel with the vacuum gap was a small condenser and an auxiliary gap of brass spheres illuminated with ultraviolet light. This gap, at first narrow, was gradually widened until a discharge took place in the vacuum tube, the final spacing giving a measure of the applied potential from which the field at the mercury surface was calculated. Fig. 2a gives oscillograms of the impulse when the breakdown occurred in the auxiliary gap. In this case the gap was set for 42 kv. Fig. 2b shows oscillograms of the breakdown in the mercury-molybdenum gap. The breakdown occurs at 70 kv, which is higher than the voltages used when the accompanying contact potential was measured. The potential rises in 1.1×10^{-7} sec.

The electrometer circuit used in making the contact potential measurements is shown in Fig. 3. The filament F and two quadrants of the electrometer, E, were grounded while the other two quadrants, the mercury cup C, and leads, connected as shown, were well shielded. All connections were soldered. After flashing the filament it was heated with a fixed current sufficient for thermionic emission. The quantity of charge that flowed from filament to mercury depended upon the potential difference between the two surfaces and upon the time. Therefore, for a given time interval, the deflection of the electrometer could be reduced to volts. A zero deflection would correspond to zero difference between contact and applied electromotive forces.

TABLE I. *Data on commercial mercury.*

Contact potential Pt−Hg (volts)	Field (volts per cm)	Contact potential Pt−Hg (volts)	Field (volts per cm)
−0.82	486,000	−0.88	520,000
−0.83	491,000	−1.20	530,000
−0.89	490,000	−0.79	725,000
−0.95	495,000	−1.40	730,000

TABLE II. *Data on purified mercury.*

Contact potential Pt−Hg (volts)	Field (volts per cm)	Contact potential Pt−Hg (volts)	Field (volts per cm)
−0.65	320,000	−0.76	650,000
−1.00	590,000	−0.79	435,000
−0.80	460,000	−0.92	445,000
−0.46	590,000	−0.82	475,000

RESULTS AND CONCLUSIONS

The results were summarized in Tables I and II and in the graph of Fig. 4. The data for Table I were taken on ordinary commercial mercury. With the exception of three values there is little variation in either contact potential or field strength necessary to produce discharge. The three varied values were obtained after the system had been either opened to air and again evacuated or after the mercury surface had been definitely changed by shaking the mercury out of the cup. An explanation of the constant results is

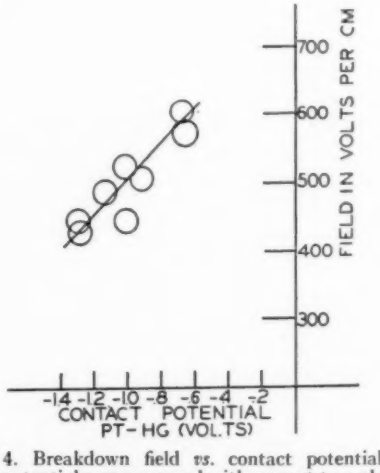

FIG. 4. Breakdown field *vs.* contact potential. The contact potential was measured with respect to a platinum filament.

that the surface was completely covered with a layer of impurities which did not flow off with the usual overflowing caused by distilling. The erratic results obtained when the surface was definitely changed indicated that the surface layer had been changed to a layer of patches, since the contact potential measurements depended on the average value of the work function while the breakdown depended on the local condition immediately under the anode. These patches could easily be seen.

The data for Table II were taken on mercury which had been purified according to the process outlined by Roller.[9] Before the mercury was transferred to the system, the still and discharge tube were baked out at 350°–400°C, the vacuum system being torched out in the meantime. Liquid air was used on the traps.

Under the conditions the values were much more erratic than in the previous case, there being at no time any correlation between contact potential measurements and breakdown fields. This would seem to indicate that there were only impurities enough to form patches and not enough to cover the surface completely at any time.

The curve of Fig. 4 was obtained after the mercury had been further purified by distilling it four times in air at a pressure slightly less than one atmosphere. This caused thick films of oxide to be formed over the surface which were removed each time by pouring the mercury through a filter paper funnel. The process evidently removed most of the impurities so that there were not enough left to form patches. The tube was also again baked out at about 400°C for eight hours before the clean mercury was introduced into it. The mercury was further purified by vacuum distillation after it was placed in the system.

The curve is similar to that obtained by Quarles. It has almost the same slope, but extends to higher breakdown fields. The contact potentials are only relative so that his values cannot be compared with these. Neither can the values of Fig. 4 be compared with those given in the Tables, for different platinum filaments at different temperatures were used.

[9] Roller, J. Opt. Soc. Am. **18**, 357 (1929).

The reason for the breakdown fields being so much lower than those predicted by theory is not apparent. With the short impulses shown by the oscillograms, it is difficult to believe that they are due to error in measurement as a result of surface distortion of the mercury. According to the theory of Tonks, even if there were waves on the mercury surface of amplitude 8.3×10^{-5} cm before the application of the field, it would require a time of 1.5×10^{-5} sec. to cause rupture with the highest fields here used (7×10^{5} volts/cm). The oscillograms show that the fields were applied for less than one-hundredth of this time. It is impossible to say whether disturbances of this magnitude were already present, but such disturbances would have to be due either to thermal agitation or to external mechanical causes. Mandelstam[10] has developed a theory for the roughness of liquid surfaces due to thermal agitation and, by means of light scattering, Gans[11] has tested the theory for liquid mercury surfaces finding that, at ordinary temperatures, the average roughness height is only of the order of 10^{-9} cm. No ripples could be observed on the surface and, during the experiment, mechanical vibrations were prevented by the air cushion mounting. It is therefore difficult to assume that the field measurements could be in error by a factor of approximately one hundred, which would be a necessary assumption in order to obtain agreement with theory.

It was found that the breakdown potentials were consistently higher if the wave fronts of the impulse were made steeper. On the average, the values were 4 or 5 percent higher, which cannot be attributed to distortional ripples since the same increase for solids has been found by Snoddy (unpublished). Moreover, this is accounted for by the finiteness of the time required to initiate a vacuum discharge.

In conclusion I wish to express my sincere appreciation to Dr. J. W. Beams for suggesting the experiment and for his continued interest and guidance. I also wish to express my appreciation to Dr. L. B. Snoddy for his assistance in taking the oscillograms and for the privilege of discussing this paper with him.

[10] Mandelstam, Ann. d. Physik **41**, 609 (1913).
[11] Gans, Ann. d. Physik **74**, 231 (1924).

On Space Quantization in Time Varying Magnetic Fields

LLOYD MOTZ, *Columbia University* AND M. E. ROSE,* *Institute for Advanced Study*

(Received June 11, 1936)

The transitions between states of different space quantization which take place when an atom is passed through a weak inhomogeneous magnetic field are calculated by approximate methods taking into account the coupling between the nucleus and the orbital electrons. Two types of field are considered, namely, the field introduced by Majorana and the one introduced by Güttinger. For the Majorana field a discussion of the cases I arbitrary $J=\frac{1}{2}$, J arbitrary $I=\frac{1}{2}$, and I and J arbitrary with explicit application to the nitrogen atom is given. For the Güttinger field the general equations are set up for a field of any strength and are then applied to the case $I=J=\frac{1}{2}$.

INTRODUCTION

THE effect of a rapidly varying magnetic field on an atom of total angular momentum $\mathbf{F}\hbar$ in a definite state of space quantization given by the magnetic quantum number m_F has been discussed separately by Majorana[1] and Güttinger[2] for two different types of fields. These authors have given definite expressions for the transition probabilities for the transitions from a state characterized by m_F to a state characterized by m_F' which do not take into account the coupling between the various components of F. The formula of Majorana was tested experimentally by Frisch and Segrè.[3] When these experiments are interpreted in the light of an extension by Rabi[4] of the above considerations to the case of an atom with nuclear spin, excellent agreement with the formula of Majorana is found. Further developments of these ideas were a new method for measuring the nuclear spin and a method for determining the sign of the nuclear magnetic moment. This last method has recently been applied to the case of the hydrogen atom.[5]

It was explicitly assumed in these experiments that there was vanishing transition probability between the hyperfine structure (hfs) levels characterized by different values of the total angular momentum $\mathbf{F}$. It is the purpose of this paper to investigate this point and to extend the work of Güttinger and Majorana to include the possibility of such transitions between different hfs states characterized by different values of the total angular momentum vector $\mathbf{F}$. The Güttinger-Majorana transitions involve as a parameter the ratio of the Larmor frequency to the frequency of rotation of the magnetic field. The process considered by us will involve in addition the hfs separation between the different F levels. It is to be hoped that by measurement of such transition probabilities one will be able to measure the hfs separation of these levels in cases which would otherwise be inaccessible to the experimenter, as may be the case in nitrogen.

THE CASES $I=\frac{1}{2}$, J ARBITRARY AND $J=\frac{1}{2}$, I ARBITRARY

The wave equation for the general case of an atom with nuclear spin $\mathbf{I}\hbar$ and electronic angular momentum $\mathbf{J}\hbar$ in a magnetic field $\mathbf{H}$ with the assumption of a cosine interaction between $\mathbf{I}$ and $\mathbf{J}$ is

$$i\hbar\dot{\Psi}=(\mathcal{H}_0+\mathcal{H}_1)\Psi$$
$$=\{\mathcal{H}_0+\mu(g_j\mathbf{J}+g_i\mathbf{I})\cdot\mathbf{H}+\alpha(\mathbf{I}\cdot\mathbf{J})\}\Psi, \quad (1)$$

where $\mathcal{H}_0$ is the energy operator for the field-free atom neglecting hfs effects, g_i and g_j are the Landé g factors for the nucleus and the electronic configuration, respectively, $\mu=e\hbar/2mc$ (the Bohr magneton), and α measures the strength of the electron-nucleus coupling and is proportional to the hfs energy separation.

$$\alpha=\Delta W/I(2J+1) \quad I<J$$
$$=\Delta W/J(2I+1) \quad I>J \quad (2)$$

where $\Delta W=W_{F=I+J}-W_{F=|I-J|}$, that is, the difference between the hfs energy levels belonging to the extreme values of F. The dot in (1) signifies differentiation with respect to the time.

* Now at Cornell University.

[1] E. Majorana, Nuovo Cim. **9**, 43 (1932).
[2] P. Güttinger, Zeits. f. Physik **73**, 169 (1931).
[3] R. Frisch and E. Segrè, Zeits. f. Physik **80**, 610 (1933).
[4] I. I. Rabi, Phys. Rev. **49**, 324 (1936).
[5] J. M. B. Kellogg, I. I. Rabi and J. R. Zacharias, Phys. Rev. **49**, 641A (1936).

A state of definite space quantization will be described by the normalized and orthogonal wave functions $\psi(m_i, m_j)$ which are eigenstates for the operator $\mathfrak{H}_0$. Here the strong field representation is employed so that m_i and m_j are the projections of I and J respectively along the Z axis. We shall treat the term $\mathfrak{H}_1$ as a perturbation. The general Ψ will then be represented as a superposition of the states $\psi(m_i, m_j)$.

$$\Psi=\sum_{m_i m_j} b_{m_i m_j}\psi(m_i, m_j)e^{-iE_0 t/\hbar}, \tag{3}$$

where E_0 is the eigenvalue of the operator $\mathfrak{H}_0$ and does not depend on m_i and m_j. The equations of motion for the probability amplitudes $b_{m_i m_j}$ become

$$i\hbar\dot{b}_{m_i m_j}=\sum_{m_i' m_j'}(m_i m_j|\mathfrak{H}_1|m_i' m_j')b_{m_i' m_j'} \tag{4}$$

or explicitly

$$\begin{aligned}
i\hbar\dot{b}_{m_i m_j}&=[\mu(g_i m_i+g_j m_j)H_z+\alpha m_i m_j]b_{m_i m_j}\\
&+\mu g_j(H_x-iH_y)[(J-m_j)(J+m_j+1)]^{\frac{1}{2}}b_{m_i m_j+1}/2\\
&+\mu g_j(H_x+iH_y)[(J+m_j)(J-m_j+1)]^{\frac{1}{2}}b_{m_i m_j-1}/2\\
&+\mu g_i(H_x-iH_y)[(I-m_i)(I+m_i+1)]^{\frac{1}{2}}b_{m_i+1,\,m_j}/2\\
&+\mu g_i(H_x+iH_y)[(I+m_i)(I-m_i+1)]^{\frac{1}{2}}b_{m_i-1,\,m_j}/2\\
&+\alpha[(I-m_i)(I+m_i+1)(J+m_j)(J-m_j+1)]^{\frac{1}{2}}\\
&\times b_{m_i+1,\,m_j-1}/2+\alpha[(I+m_i)(I-m_i+1)\\
&\times(J-m_j)(J+m_j+1)]^{\frac{1}{2}}b_{m_i-1,\,m_j+1}/2.
\end{aligned} \tag{5}$$

The solutions of these equations will depend on how the magnetic field H is chosen. We shall treat first the field introduced by Majorana in which it is supposed that the atom passes in the neighborhood of a point where the field vanishes, a situation which can be easily realized experimentally. In a reference system moving with the atom this field is given by

$$H_x=\text{constant}=A, \quad H_y=0, \quad H_z=-ct. \tag{6}$$

It will be convenient to introduce the dimensionless quantities

$$\begin{aligned}
t&=(\hbar/\mu c)^{\frac{1}{2}}\tau, \quad \eta=(\alpha/2\hbar)(\hbar/\mu c)^{\frac{1}{2}},\\
\rho_{i,\,j}&=(g_{i,\,j}\mu A/2\hbar)(\hbar/\mu c)^{\frac{1}{2}}
\end{aligned} \tag{7}$$

and to set

$$b_{m_i m_j}=\varphi_{m_i m_j}\exp i[g_i m_i+g_j m_j)\tau^2/2-2\,\eta m_i m_j\tau], \tag{8}$$

so that $|b_{m_i m_j}|=|\varphi_{m_i m_j}|$. The parameters η and $\rho_{i,\,j}$ are characteristic of the theory and are essentially those mentioned above. The quantity k introduced by Majorana is just $4\rho_j^2/g_j$ and can be interpreted as the ratio of the Larmor frequency at the minimum field ($\tau=0$) to the frequency of rotation of the field at that point. Also η^{-2} is seen to be proportional to the change in Larmor angle during one period of the hfs precession.[6]

We shall consider first the special case of both I and $J=\frac{1}{2}$ (for example H and Tl). Then for the field given in (6) the equations (5) in the notation (7) and (8) become

$$\begin{aligned}
id\varphi_1/d\tau&=\rho_j\varphi_2 e^{-i(g_j\tau^2/2-\eta\tau)}+\rho_i\varphi_3 e^{-i(g_i\tau^2/2-\eta\tau)},\\
id\varphi_2/d\tau&=\rho_j\varphi_1 e^{i(g_i\tau^2/2-\eta\tau)}+\eta\varphi_2 e^{-i\tau^2(g_j-g_i)/2}\\
&\quad+\rho_i\varphi_4 e^{-i(g_i\tau^2/2+\eta\tau)},\\
id\varphi_3/d\tau&=\rho_i\varphi_1 e^{i(g_i\tau^2/2-\eta\tau)}+\eta\varphi_2 e^{-i\tau^2(g_j-g_i)/2}\\
&\quad+\rho_j\varphi_4 e^{-i(g_j\tau^2/2+\eta\tau)},\\
id\varphi_4/d\tau&=\rho_i\varphi_3 e^{i(g_i\tau^2/2+\eta\tau)}+\rho_j\varphi_3 e^{i(g_j\tau^2/2+\eta\tau)},
\end{aligned} \tag{9}$$

where the indices 1, 2, 3 and 4 represent the index pairs $(m_i, m_j)=(\frac{1}{2}, \frac{1}{2})$, $(\frac{1}{2}, -\frac{1}{2})$, $(-\frac{1}{2}, \frac{1}{2})$ and $(-\frac{1}{2}, -\frac{1}{2})$, respectively.

An exact solution of these equations can not be carried out even though one makes the obviously valid simplification $g_i=0$. However, it is possible to obtain approximate solutions by considering either of the two quantities ρ_j or η as a small perturbation parameter. The former case is the more interesting physically. Therefore we set

$$\varphi_k=\sum_{\nu=0}^{\infty}\rho_j{}^{\nu}\varphi_k{}^{(\nu)}, \quad k=1, 2, 3, 4 \tag{10}$$

and take $\rho_j\ll 1$.

The condition $\rho_j\ll 1$ implies that the field rotates very rapidly in the neighborhood of $\tau=0$. One therefore expects the transitions to occur in this region since the field here is strongly nonadiabatic.

We shall seek solutions of (9) which are governed by the following boundary conditions:

At $\tau=-\infty$, $|\varphi_l|=1$ for some one l, all others $=0$. In terms of the expansion (10) these become

$$|\varphi_k{}^{(0)}|^2=\delta_{kl}, \tag{11}$$

$$\varphi_k{}^{(0)}\varphi_k{}^{(1)*}+\varphi_k{}^{(0)*}\varphi_k{}^{(1)}=0, \tag{11'}$$

$$\varphi_k{}^{(0)}\varphi_k{}^{(2)*}+\varphi_k{}^{(0)*}\varphi_k{}^{(2)}+|\varphi_k{}^{(1)}|^2=0. \tag{11''}$$

[6] That is, the time during which the two vectors **I** and **J** precess about their resultant **F**.

The zero-order solutions satisfy the differential equations[7]

$$d\varphi_1^{(0)}/d\tau=0, \qquad d\varphi_4^{(0)}/d\tau=0,$$
$$id\varphi_2^{(0)}/d\tau=\eta\varphi_3^{(0)}e^{ig_j\tau^2/2}, \tag{12}$$
$$id\varphi_3^{(0)}/d\tau=\eta\varphi_2^{(0)}e^{-ig_j\tau^2/2}.$$

These equations are just those found by Majorana for the case $J=\frac{1}{2}$, $I=0$ with his k replaced by $2\eta^2$.[8]

From (12) it follows that if initially the atom is prepared in either of the states corresponding to φ_3 or φ_4, then in zero-order no transitions with respect to a fixed direction in space will occur since we must have for all τ

$$\sum_1^4|\varphi_k|^2=\text{constant}=1. \tag{13}$$

In fact in zero-order of approximation the selection rule $\Delta m\equiv\Delta(m_i+m_j)=0$ is obeyed for the case of general I and J. The operator I_z+J_z commutes with the Hamiltonian in (1) when $H_z=H_y=0$ but I_z and J_z separately do not. It must be pointed out that during the course of the process the direction of the field has been reversed. Hence a transition from a state of space quantization (m_i, m_j) to a state (m_i', m_j') corresponds to a transition to a state with space quantization $(-m_i', -m_j')$ with respect to the field. Therefore in this approximation an atom originally in the state $(\pm\frac{1}{2}, \pm\frac{1}{2})$ goes over completely into the state $(\mp\frac{1}{2}, \mp\frac{1}{2})$ with respect to the field.

If we take φ_3 as the initial state, the zero-order solutions are

$$\varphi_1^{(0)}=\varphi_4^{(0)}=0,$$
$$\varphi_3^{(0)}=C_1F(-i\eta^2/2g_i\,;\,\tfrac{1}{2}\,;\,-ig_i\tau^2/2)$$
$$+(-ig_j/2)^{\frac{1}{2}}C_2\tau F(-i\eta^2/2g_j+\tfrac{1}{2}\,;\,3/2\,;\,-ig_j\tau^2/2),$$
$$\varphi_2^{(0)}=C_1'F(i\eta^2/2g_j;\,\tfrac{1}{2}\,;\,ig_j\tau^2/2)$$
$$+(ig_j/2)^{\frac{1}{2}}C_2'\tau F(i\eta^2/2g_j+\tfrac{1}{2}\,;\,3/2\,;\,ig_j\tau^2/2), \tag{14}$$

where $F(a\,;b\,;x)$ is defined by

$$F(a\,;b\,;x)=\frac{\Gamma(b)}{\Gamma(a)}\sum_{n=0}^{\infty}\Gamma(a+n)x^n/\Gamma(b+n)n!.$$

[7] We have set $g_i=0$ throughout. It is possible to take it into account exactly but it is easily seen that it has little effect on the final result.

[8] Reference 5, Eq. (5).

The integration constants C_1, C_2, C_1' and C_2' are not independent. One finds from (12) that

$$C_2'=-(2i/g_j)^{\frac{1}{2}}\eta C_1, \quad C_2=(-2i/g_j)^{\frac{1}{2}}\eta C_1'.$$

C_1 and C_2 are determined from (11). The probability in zero-order for the transition $(-\frac{1}{2}, \frac{1}{2})$ to $(\frac{1}{2}, -\frac{1}{2})$ can now be determined from the asymptotic values of $\varphi_2^{(0)}$ and $\varphi_3^{(0)}$ at $\tau=\infty$. Before we give this result, we shall consider the contribution to the transition probabilities from first-order terms. Since the transitions $\varphi_3\to\varphi_1$ and $\varphi_3\to\varphi_4$ are forbidden in zero-order, we shall obtain the first-order corrections to these transitions. This is not necessary for the transitions which are not excluded in zero-order. We find from (9) and (11″) that

$$\varphi_1^{(1)}=-i\int_{-\infty}^{\tau}\varphi_2^{(0)}e^{-i(g_j\tau^2/2-\eta\tau)}d\tau,$$
$$\varphi_4^{(1)}=-i\int_{-\infty}^{\tau}\varphi_3^{(0)}e^{i(g_j\tau^2/2+\eta\tau)}d\tau. \tag{15}$$

In evaluating $\varphi_1^{(1)}(\infty)$ and $\varphi_4^{(1)}(\infty)$ we make use of the integral representations of the confluent hypergeometric functions[9] which enter from (14). The final results for the transition probabilities with respect to the field are[10]

$$|\varphi_4|^2=(2/g_j)\pi\rho_j^2(1-e^{-2\pi\eta^2/g_j}),$$
$$|\varphi_3|^2=1-e^{-2\pi\eta^2/g_j}+0(\rho_j^2),$$
$$|\varphi_2|^2=e^{-2\pi\eta^2/g_j}+0(\rho_j^2), \tag{16}$$
$$|\varphi_1|^2=(2\pi/g_j)\rho_j^2e^{-2\pi\eta^2/g_j}.$$

The quantity η is a measure of how rapidly the field rotates when $\rho_j=0$ in the region where the transitions occur. For $\eta\ll1$ and $\rho_j=0$ the field rotates very rapidly so that the vectors **I** and **J** will not be able to follow the field and there will be complete transitions with respect to it, $|\varphi_2|^2\to1$, $|\varphi_3|^2\to0$. The effect of $\rho_j\neq0$ is to make the rate of rotation of the field finite. For $\eta\ll1$ in this case, J will behave differently from I since it is coupled more strongly to the field than I is. One will expect to find m_i changing

[9] Whittaker and Watson, *Modern Analysis*, fourth edition, p. 352. The confluent hypergeometric function $M_{k,\,m}(x)$ defined by Whittaker and Watson is related to the function given in (14) by

$$M_{km}(x)=x^{m+1/2}e^{-x/2}F((1/2)+m-k\,;\,2m+1\,;\,x).$$

[10] As expected from physical considerations the results are independent for the sign of A even in the general case.

more readily with respect to the field than m_j. This is borne out by the results in (16).

The transition probabilities for the case where the initial state corresponds to φ_2 can be obtained from (16) by interchanging φ_2 and φ_3 and φ_1 and φ_4 because of the symmetry of Eq. (9).

For the case $J=\frac{1}{2}$ and I arbitrary (alkali atoms, Ag, etc.) the zero-order results may be found exactly as in the case of $I=J=\frac{1}{2}$ treated above. If the initial state is $(m_i, -\frac{1}{2})$, one finds that with respect to the field (with $g_i=0$)

$$|\varphi_{-m_i+1,\,-\frac{1}{2}}|^2=1 - \exp\left[-2\pi\eta^2(I-m_i+1)(I+m_i)/g_j\right], \quad (17)$$

$$|\varphi_{-m_i,\,\frac{1}{2}}|^2=\exp\left[-2\pi\eta^2(I-m_i+1)(I+m_i)/g_j\right].$$

All other probability amplitudes are, in accordance with the selection rule in zero-order, identically zero; i.e., with respect to the field, $m\rightarrow -m$. If one does not set $g_i=0$, one obtains a result of the form (17) with g_j-g_i replacing g_j. This also applies to all cases given below. When one proceeds to the first order calculation, the probability amplitudes $\varphi_{-m_i,\,-\frac{1}{2}}$, $\varphi_{-m_i+2,\,-\frac{1}{2}}$ and $\varphi_{-m_i\pm 1,\,\frac{1}{2}}$ will have values different from zero and the selection rule becomes $m\rightarrow -m$, $-m\pm 1$. To terms up to ρ_j^n the selection rule is $m\rightarrow -m$, $-m\pm 1$, $\cdots$ $-m\pm n$.

The case $I=\frac{1}{2}$ and J arbitrary (F^{19}, P^{30}, Cd^{111}, etc.) is the same analytically as the case $J=\frac{1}{2}$, I arbitrary. Again confining ourselves to the zero-order we find, if the initial state is $(-\frac{1}{2}, m_j)$, that transitions can occur only to the state $(\frac{1}{2}, m_j-1)$ with respect to a fixed direction. With respect to the field we have

$$|\varphi_{-\frac{1}{2},\,-m_j+1}|^2=1 - \exp\left[-2\pi\eta^2(J-m_j+1)(J+m_j)/g_i\right], \quad (17')$$

$$|\varphi_{\frac{1}{2},\,-m_j}|^2=1-|\varphi_{-\frac{1}{2},\,-m_j+1}|^2.$$

In the paper cited in reference 4, Rabi has shown how one may obtain the sign of the nuclear magnetic moment in the case that the separation of neighboring hfs energy levels is very large compared to the Zeeman splitting. He assumes that there are no transitions between states of different total angular momentum F under the given experimental conditions. This assumption seems very plausible. Since the hfs energy levels are very far apart, the electron-nucleus coupling is very strong and one does not expect this coupling to be broken down in a weak field, which is the character of the field in the immediate neighborhood of the point where the transitions actually take place. In the special case which we have considered, namely, $\rho_j=0$, the assumption can be rigorously justified. In our discussion we considered that initially ($\tau=-\infty$) the atom was prepared in a certain state of space quantization specified by particular values of m_i and m_j. It is possible to describe this state in terms of wave functions labeled with the weak field quantum numbers f, m, and the wave function of such a state (definite m_i, m_j) will be given as certain linear combinations of the latter type wave functions.[11] In the present formulation of the problem we cannot prepare ($\tau=-\infty$) the atom in a state of definite f and m and seek the probability amplitudes for various f, m states at the end of the experiment ($\tau=\infty$) since it has no meaning to speak of pure f, m states when the field is so large. A valid procedure is to transform from the (m_i, m_j) scheme to the (f, m) scheme in the region where the transitions take place, that is, where the field is weak and where states of definite f and m are possible. Considering the case $I=\frac{1}{2}$, J arbitrary or $J=\frac{1}{2}$, I arbitrary we find, according to the above procedure, that in the limit $\eta\rightarrow\infty$ the modulus of the probability amplitude for a state of given f does not change as one passes through the origin $\tau=0$, so that for this case $\Delta f=0$.

In the general case I, J arbitrary the validity of the assumption may be inferred though not rigorously demonstrated from the following considerations. In Eq. (1) we could just as well have included the term $\alpha(\mathbf{I}\cdot\mathbf{J})$ in the unperturbed part of the Hamiltonian, $\mathcal{H}_0$, considering only the external field as a perturbation. Instead of using the strong field notation we could now write down a set of equations corresponding to (5) for the weak field probability amplitudes, b_{fm}. In doing this however, we have to remember that $\mathcal{H}_0$ now depends on f and m and that our differential equations will contain exponential terms, *viz.*

$$i\hbar\dot{b}_{fm}=\sum_{f'm'}(fm|\mathcal{H}_1|f'm')b_{f'm'}e^{i(E_{fm}-E_{f'm'})t/\hbar}. \quad (18)$$

[11] Condon and Shortley, *The Theory of Atomic Spectra* (Cambridge, 1935) pp. 73–78. For the purpose of our argument the knowledge of the exact numerical values of these coefficients is not essential.

For the hfs energy levels very far apart, $E_{fm}-E_{f'm'}$ is very large for $f\neq f'$ compared to the Zeeman levels. Thus the coefficients $b_{f'm'}$ with $f\neq f'$ will be multiplied by a very rapidly oscillating term, as compared to coefficients $b_{fm'}$ and we may consider such terms as being relatively small.

The Nitrogen Atom. The Case of Arbitrary I and J

As a particular example in which both I and J are different from $\frac{1}{2}$ we shall treat the case $I=1$, $J=3/2$ in detail. The nitrogen atom (N^{14}) in the normal state ${}^4S_{3/2}$ comes under this case. If we attempt to carry out an approximation calculation as was done in the previous section, we find in zero-order ($\rho_j=0$) that the $(2I+1)(2J+1)=12$ states split into six groups, the states in each group having the same value of m. There are two states ($m_i=1$, $m_j=3/2$) and ($m_i=-1$, $m_j=-3/2$) whose probability amplitudes are constant; two groups of two states each ($m_i=0$, $m_j=-3/2$), ($m_i=-1$, $m_j=-\frac{1}{2}$) and ($m_i=1$, $m_j=\frac{1}{2}$), ($m_i=0$, $m_j=3/2$) whose probability amplitudes satisfy differential equations of the Majorana type,

$$id\varphi_{0,\ -3/2}/d\tau=6^{\frac{1}{2}}\eta\varphi_{-1,\ -1/2}\exp i[g_j\tau^2/2-\eta\tau],$$

$$id\varphi_{-1,\ -1/2}/d\tau=6^{\frac{1}{2}}\eta\varphi_{0,\ -3/2}\exp -i[g_j\tau^2/2-\eta\tau], \tag{19}$$

$$id\varphi_{1,\ 1/2}/d\tau=6^{\frac{1}{2}}\eta\varphi_{0,\ 3/2}\exp i[g_j\tau^2/2+\eta\tau],$$

$$id\varphi_{0,\ 3/2}/d\tau=6^{\frac{1}{2}}\eta\varphi_{1,\ 1/2}\exp -i[g_j\tau^2/2+\eta\tau], \tag{19'}$$

the superscripts 0 on the φ's being omitted since we shall consider only zero-order solutions; and finally two groups of three states each $(m_im_j)=(1,-3/2)$, $(0,-\frac{1}{2})$, $(-1,\frac{1}{2})$ and $(m_im_j)=(1,-\frac{1}{2})$, $(0,\frac{1}{2})$, $(-1,3/2)$. The first three of these satisfy the equations

$$\begin{aligned}id\varphi_1/d\tau&=6^{\frac{1}{2}}\eta\varphi_2\exp -i[g_j\tau^2/2-3\eta\tau],\\ id\varphi_2/d\tau&=6^{\frac{1}{2}}\eta\varphi_1\exp i[g_j\tau^2/2-3\eta\tau]\\ &\quad+8^{\frac{1}{2}}\eta\varphi_3\exp i[g_j\tau^2/2+\eta\tau],\\ id\varphi_3/d\tau&=8^{\frac{1}{2}}\eta\varphi_2\exp -i[g_j\tau^2/2+\eta\tau],\end{aligned} \tag{20}$$

where the indices 1, 2 and 3 represent the index pairs $(1,-3/2)$, $(0,-\frac{1}{2})$ and $(-1,\frac{1}{2})$, respectively. The probability amplitudes for the second set of three states in the order $(-1,3/2)$, $(0,\frac{1}{2})$ and $(1,-\frac{1}{2})$ satisfy equations which can be obtained from (20) by changing the sign of g_j. The transitions with respect to a fixed direction must take place within a group, i.e., $\Delta m=0$ so that there will be an integral of the form (13) for each group of states separately. That is

$$\sum_{m_im_j}|\varphi_{m_im_j}|^2\delta_{m_i+m_j,\ m}=1 \text{ for every } m.$$

If we choose our atom initially with a definite value of m, then the probability amplitudes corresponding to all other values of m will be identically zero.

In the case that the initial state is one for which $m=\pm\frac{1}{2}$ we have a system of three equations to solve. These equations cannot be solved without further approximation. An interesting case is the one in which the hfs separation is small. That is, we take $|\eta|\ll 1$ but $\rho_j\ll|\eta|$ so that we may consistently consider terms of second order in η.

We introduce into (20) the expansions

$$\varphi_k=\sum_0^\infty\eta^\nu\varphi_k^{(\nu)}.$$

The determination of each $\varphi_k^{(\nu)}$ now reduces to quadratures. For the case $|\varphi_k(-\infty)|=\delta_{k1}$, the approximations which one needs are

$$\begin{aligned}&\varphi_1^{(0)}=e^{i\lambda},\quad \lambda=\text{constant},\quad \varphi_2^{(0)}=\varphi_3^{(0)}=0,\\ &\varphi_1^{(1)}=0,\quad \varphi_2^{(1)}=-6^{\frac{1}{2}}ie^{i\lambda}\int_{-\infty}^{\tau}e^{ig_jx^2/2}dx,\quad \varphi_3^{(1)}=0,\\ &\varphi_1^{(2)}=-6^{\frac{1}{2}}e^{i\lambda}\int_{-\infty}^{\tau}e^{-ig_jx^2/2}\int_{-\infty}^{x}e^{ig_jy^2/2}dydx.\end{aligned} \tag{21}$$

The transition probabilities are

$$\begin{aligned}|\varphi_{-1,\ 3/2}|^2&=1-12\pi\eta^2/g_j,\\ |\varphi_{0,\ 1/2}|^2&=12\pi\eta^2/g_j,\\ |\varphi_{1,\ -1/2}|^2&=0(\eta^4).\end{aligned} \tag{22}$$

This gives to the order of approximation considered the further selection rule $m_i\rightarrow -m_i\pm 1$, $m_j\rightarrow -m_j\mp 1$. If the initial state corresponds to φ_2, i.e., $(0,-\frac{1}{2})$, the transition probabilities are given by

$$\begin{aligned}|\varphi_{-1,\ 3/2}|^2&=12\pi\eta^2/g_j,\\ |\varphi_{0,\ 1/2}|^2&=1-28\pi\eta^2/g_j,\\ |\varphi_{1,\ -1/2}|^2&=16\pi\eta^2/g_j.\end{aligned} \tag{23}$$

When the initial state corresponds to φ_3, the probabilities are given by (22) with $\varphi_{1,\ -\frac{1}{2}}$ and $\varphi_{-1,\ 3/2}$ interchanged and the numerical factor 12 replaced by 16. If the initial state is one for which $m=\pm 3/2$ (Eqs. (19) or (19′)), the hfs separation can be taken into account exactly. Then for the case of both m values the probability that a transition $(m_i, m_j)\rightarrow(-m_i\pm 1, -m_j\mp 1)$ take place is

$$1-\exp\left[-12\pi\eta^2/g_i\right]\cong 12\pi\eta^2/g_j \text{ for } |\eta|\ll 1. \quad (24)$$

And the probability for the transition $(m_i m_j)\rightarrow(-m_i-m_j)$ is

$$\exp\left[-12\pi\eta^2/g_i\right]\cong 1-12\pi\eta^2/g_j \text{ for } |\eta|\ll 1. \quad (24')$$

Proceeding in exactly the same manner as for the nitrogen atom, we find for the case of arbitrary I and J for the transitions $(m_i m_j)\rightarrow(-m_i\pm 1, -m_j\mp 1)$ to terms of order η^2

$$|\varphi_{-m_i-1,\ -m_j+1}|^2 = 2\pi\eta^2(I+m_i+1)(I-m_i)(J-m_j+1)(J+m_j)/g_j, \quad (25)$$

$$|\varphi_{-m_i+1,\ -m_j-1}|^2 = 2\pi\eta^2(I-m_i+1)(I+m_i)(J+m_j+1)(J-m_j)/g_j$$

and

$$|\varphi_{-m_i,\ -m_j}|^2 = 1-|\varphi_{-m_i-1,\ -m_j+1}|^2-|\varphi_{-m_i+1,\ -m_j-1}|^2. \quad (25')$$

If one proceeds to higher orders of approximation, one finds that transitions of the type $m_i\rightarrow -m_i\pm n$, $m_j\rightarrow -m_j\mp n$ enter in the nth order approximation and that the corresponding transition probabilities are of order η^{2n}. One may regard such transitions as being equivalent to n successive transitions of the type $(m_i, m_j)\rightarrow(-m_i\pm 1, -m_j\mp 1)$ each of these taking place with a probability given by (25), that is, of order η^2. One may consistently consider approximations of the nth order in η only if $\rho^2\ll\eta^n$.

All the above results are seen to depend on η^2 when the nuclear g factor is neglected so that the transition probabilities are independent of the sign of the nuclear magnetic moment. This is not the case when g_i is not neglected. The effect of including the nuclear g factor is to change our results by an amount of order of 0.1 percent so that from a practical standpoint one may consider the transition probabilities to be independent of the sign of the moment in all cases.

The Rotating Magnetic Field

In this section we shall treat the case of a magnetic field of constant magnitude H rotating with constant angular velocity ω. It is convenient in this treatment to follow the procedure of Güttinger[2] who has given a general discussion of the wave equation when it contains parameters a_i which themselves depend explicitly on the time. Let us consider a system with a Hamiltonian which contains a set of parameters a_i. The wave equation for the stationary states of such a system is

$$\mathcal{H}(p, q, a_i)\psi_n=E_n(a_i)\psi_n. \quad (26)$$

If the parameters a_i are not functions of the time, one obtains the orthogonal set of solutions (in what follows we consider a single parameter a)

$$\cdots\psi_n(q, a)\cdots.$$

If, however, the parameters are definite functions of the time, the wave equation becomes

$$\mathcal{H}(p, q, a(t))\Psi=i\hbar\dot{\Psi}. \quad (27)$$

The general state Ψ can now be expanded in terms of the solutions of (26)

$$\Psi=\sum_n b_n(t)\psi_n(q, a(t)), \quad (28)$$

where the $b_n(t)$ are the probability coefficients we seek and obey the differential equations

$$\dot{b}_m-iE_m b_m/\hbar+\sum_n{}'\dot{a}\left(\frac{\partial\mathcal{H}}{\partial a}\right)_{mn}\frac{b_n}{(E_n-E_m)}=0. \quad (29)$$

The accent means that the term $n=m$ is to be excluded from the sum.

Let (x, y, z) define a stationary coordinate system relative to which we have a magnetic field $\mathbf{H}$ ($|\mathbf{H}|=$const.) rotating with constant angular velocity

$$H_x=H\cos\omega t,$$
$$H_y=H\sin\omega t.$$

Let (ξ, η, ζ) define a system of coordinates rotating with the field in such a manner that $\mathbf{H}$ always points in the direction ξ and ζ always coincides with z. We shall consider the transitions which an atom makes when placed in a field of this sort. In order that the results may be applicable to fields of any strength we shall label our

states in terms of the energy levels of the atom in a constant magnetic field. This can be done by the method employed by Heisenberg and Jordan[12] for the determination of the atomic energy levels in the anomolous Zeeman effect. We must transform the perturbing part, $\mathcal{H}_1$, of the Hamiltonian in Eq. (1) to diagonal form. This gives rise to the system of equations

$$W(rl/W)-\sum(rl|\mathcal{H}_1|r'l')(r'l'/W)=0 \quad (30)$$

where the indices r, r' and l, l' take on all possible values of m_i and m_j respectively for a given choice of I, J and $m=m_i+m_j$. The energy levels are the roots of the equations obtained by equating to zero the determinant $|W\delta_{rl,\,r'l'}-(rl|\mathcal{H}_1|r'l')|$. Let the roots of these equations be $W_1, W_2, \cdots$. Using these roots to label our states we now rewrite Eq. (29) as

$$\dot{b}_{W_m}-i/\hbar(E_0+W_m)b_m+\sum_n{}'\dot{a}(\partial\mathcal{H}/\partial a)_{mn}\frac{b_n}{(W_n-W_m)}=0. \quad (29')$$

To proceed further we require the expression (M_η is taken diagonal)

$$\dot{H}_x(\partial\mathcal{H}/\partial H_x)+\dot{H}_y(\partial\mathcal{H}/\partial H_y)=\omega HM_\eta, \quad (31)$$

where $M_\eta=\mu(g_jJ_\eta+g_iI_\eta)$.

Substituting (31) into (29′) we get

$$\dot{b}_{W_m}-\frac{i}{\hbar}(E_0+W_m)b_m+\omega H\sum_n{}'(W_m|M_\eta|W_n)\frac{b_{W_n}}{(W_n-W_m)}=0. \quad (32)$$

The matrix elements $(W_m|M_\eta|W_n)$ can be found with the aid of the transformation functions (m_im_j/W) obtained from the solution of (30). We have

$$(W_m|M_\eta|W_n)=\sum_{\substack{m_i'm_j'\\ m_i''m_j''}}(W_m/m_i'm_j')\times(m_i'm_j'|M_\eta|m_i''m_j'')(m_i''m_j''/W_n). \quad (33)$$

And since the matrix elements $(m_i'm_j'|M_\eta|m_i''m_j'')$ are well known, the elements $(W_m|M_\eta|W_n)$ can now be easily found.

[12] W. Heisenberg and P. Jordan, Zeits. f. Physik **37**, 26 (1926).

We shall consider as a particular example the case $I=J=\frac{1}{2}$. For this case the transformation function and the energy levels can be found from the formulae (18), (26) and (28) of reference 13 by placing $m=0$ and $k=\frac{1}{2}$ in these formulae and remembering that we are now dealing with the nuclear spin so that the nuclear g factor will enter. If we carry out all the necessary calculations, we find for the equations of motion of the probability amplitudes for this simple case (placing $g_i=0$)

$$\dot{b}_{W_1}-\frac{i}{\hbar}(E_0+W_1)b_{W_1}+\omega\kappa\left\{\left(\frac{\kappa}{2\gamma^{\frac{1}{2}}}+\frac{1}{2}\right)^{\frac{1}{2}}\frac{b_{W_3}}{W_3-W_1}+\frac{\alpha}{2}[\tfrac{1}{2}(\kappa\gamma^{\frac{1}{2}}+\gamma)]^{-\frac{1}{2}}\frac{b_{W_4}}{W_4-W_1}\right\}=0,$$

$$\dot{b}_{W_2}-\frac{i}{\hbar}(E_0+W_2)b_{W_2}+\omega\kappa\left\{\left(\frac{1}{2}-\frac{\kappa}{2\gamma^{\frac{1}{2}}}\right)^{\frac{1}{2}}\frac{b_{W_3}}{W_3-W_2}+\frac{\alpha}{2}[\tfrac{1}{2}(\gamma-\kappa\gamma^{\frac{1}{2}})]^{-\frac{1}{2}}\frac{b_{W_4}}{W_4-W_2}\right\}=0,$$

$$\dot{b}_{W_3}-\frac{i}{\hbar}(E_0+W_3)b_{W_3}+\omega\kappa\left\{\left(\frac{1}{2}+\frac{\kappa}{2\gamma^{\frac{1}{2}}}\right)^{\frac{1}{2}}\frac{b_{W_1}}{W_1-W_3}+\left(\frac{1}{2}-\frac{\kappa}{2\gamma^{\frac{1}{2}}}\right)^{\frac{1}{2}}\frac{b_{W_2}}{W_2-W_3}\right\}=0,$$

$$\dot{b}_{W_4}-\frac{i}{\hbar}(E_0+W_4)b_{W_4}+\frac{\omega\kappa\alpha}{2}\left\{[\tfrac{1}{2}(\kappa\gamma^{\frac{1}{2}}+\gamma)]^{-\frac{1}{2}}\frac{b_{W_1}}{W_1-W_4}+[\tfrac{1}{2}(\gamma-\kappa\gamma^{\frac{1}{2}})]^{-\frac{1}{2}}\frac{b_{W_2}}{W_2-W_4}\right\}=0, \quad (34)$$

where E_0 is the energy of the atom corresponding to $\mathcal{H}_0$ of Eq. (1); where

$$\kappa=\mu g_jH, \quad \gamma=\kappa^2+\alpha^2;$$

and where α is defined by Eq. (2). The energy differences which appear in the denominators of (34) are

$$\begin{aligned}W_3-W_1&=\tfrac{1}{2}(\alpha+\kappa-\gamma^{\frac{1}{2}}),\\ W_4-W_1&=\tfrac{1}{2}(\alpha-\kappa-\gamma^{\frac{1}{2}}),\\ W_3-W_2&=\tfrac{1}{2}(\alpha+\kappa+\gamma^{\frac{1}{2}}),\\ W_4-W_2&=\tfrac{1}{2}(\alpha-\kappa+\gamma^{\frac{1}{2}}).\end{aligned} \quad (35)$$

The desired probability amplitudes will be given by the solutions of Eqs. (34). The general

solutions of these equations are

$$b_{W_n}=\sum_{m=1}^{4} A_{nm}C_m e^{(i/\hbar)(E_0+\hbar\lambda_m)t}, \qquad (n=1, 2, 3, 4), \quad (36)$$

where the λ_m are the roots of the equation

$$\left|i\left(\lambda-\frac{W_m}{\hbar}\right)\delta_{mn}-\frac{\omega H(W_m|M_y|W_n)}{W_n-W_m}\right|=0 \quad (37)$$
$$n\neq m$$

and the A_{nm} are to be determined by substituting (36) back into (34). These expressions are too lengthy to be set down explicitly. The C_m are the four arbitrary constants of integration which must be determined by the normalization and the initial conditions. Let us suppose that initially ($t=0$) the atom is in a state characterized by the energy W_k so that initially $|b_{W_k}|^2=1$ and all the others are zero. Then at any other time, t, later we shall have

$$b_{W_n}=\frac{1}{\Delta}\sum_{m=1}^{4} A_{nm}A^{km}e^{(i/\hbar)(E_0+\hbar\lambda_m)t}, \qquad (38)$$

where Δ is the determinant of the matrix $((A_{nm}))$ and A^{km} is the cofactor of the element A_{km}. The quantities $|b_{W_n}|^2$ give the probabilities of transition from the initial state.

The authors wish to express their appreciation to Professor I. I. Rabi for suggesting this problem and for invaluable advice and to Professors G. Breit and W. Pauli for interesting and helpful discussions. One of us (L. M.) would also like to thank Mr. Julian Schwinger of the Columbia University physics seminar for interesting and helpful discussions on various phases of this problem.

AUGUST 15, 1936 PHYSICAL REVIEW VOLUME 50

Sound Absorption and Velocity in Mixtures

D. G. BOURGIN, *University of Illinois, Urbana, Illinois*

(Received October 18, 1935)

The effects of (a) collision excitation probabilities dependent on the internal energy specification of the impinging molecules; (b) transitions in both colliding members; (c) triple and higher order collisions; (d) viscosity and conduction, are considered with reference to sound propagation. A comparative study is made of the generalized Kneser-Ruttgers method and the writer's method of investigation. It is shown that the two are developments of the same physical theory and may be looked upon as a thermodynamic and a kinetic theory transcript respectively. In particular, ω_i (a parameter, dependent on the frequency, which determines the degree to which equilibrium conditions are attained) plays a central role, implicitly, in the former method as well as in the latter. The kinetic theory transport equation interpretation of the use of C_∞ instead of $3k/2$ is noted. It is shown that for impurity contamination, the Kneser special assumptions and formulae fall out as consequences of the general mixture theory if certain approximations are valid. The triple collision hypothesis for H, O, O_2 mixtures is discussed and alternative explanations are suggested. The main contributions of this paper from the experimenter's viewpoint are the formulae for absorption and velocity in mixtures, derived by the two methods referred to above, in convenient form for application.

THE first objective of this paper is the exhibition of a conveniently applied expression for sound absorption in mixtures of gases. The extensive experimental[1] work inaugurated on impurities in gases and gas mixtures emphasizes the timeliness of the calculations presented here. In the first paper on supersonics[2]

[1] Three techniques have been followed in the experimental work. The first utilizes the piezoelectric oscillator in the way devised by G. W. Pierce, Proc. Am. Acad. Arts and Sci. **60**, 271 (1925). The second employs the acoustic interferometer invented and developed by J. C. Hubbard, Phys. Rev. **38**, 1011 (1931); **41**, 523 (1932). The third is concerned with absorption measurements by means of reverberation times. It is not restricted to any particular frequency region and owes its exploitation to V. O. Knudsen, J. A. S. A. **3**, 126 (1931).

[2] D. G. Bourgin, Nature **122**, 133 (1928); Phil. Mag. **7**, 821 (1929); Phys. Rev. **34**, 521 (1929); J. A. S. A. **5**, 108 (1932); Phys. Rev. **42**, 721 (1932); designated as I, II, III, IV, V respectively. In the interest of historical completeness, the work of Jeans' *Kinetic Theory of Gases* and K. F. Herzfeld and F. O. Rice, Phys. Rev. **31**, 691 (1928), may be mentioned. Both these investigations are on the pre-quantum theory model and the last named is, in fact, really a continuous fluid theory entirely macroscopic in perspective. Cf. I for discussion of the relation of this highly original theory to the writer's.

published by the writer, there is given a theory of sound absorption in mixtures, and later communications[3] simplify some of the findings. This research is, in a sense, a culmination of the previous work as regards simplifications and nomenclature on the one hand and certain natural generalizations on the other. For the case of impurities in a single gas, the empirical postulate of Kneser[4] expressed in the notation of this paper $k_{12} \sim aB + bB^2$ and the contingent formulae are shown to be logical consequences of a sub-case under the general theory.

The quantum theory of sound propagation making use of the concept of lags in adjustment of internal energy states was originally proposed and developed in its present form by the writer.[2] While the physical basis of the theory has undergone little improvement, there has, however, been real advance in the presentation of the formulae in a manner more amenable to the needs of the experimenter and in the application of the theory to specific gases.[5] As an alternative to the writer's method for developing the physical consequences of the theory, modification of a method used by Einstein[6] for investigating dissociating gases may be employed. This choice is to some extent a matter of individual preference as pointed out by Richards.[7] The impression that there is greater complexity in the writer's method is, in his opinion, unfounded as the sequel will show, and due possibly to a lack of realization that the original developments of I are completely general for n states, and accordingly slightly more formidable in appearance than a treatment for two states with which comparison is ordinarily made. The second objective of this paper is to discuss the two methods comparatively, and it is shown that the methods are almost completely equivalent.[8] This purpose is carried out in part by developing both the writer's and the Kneser-Ruttgers modification of Einstein's method (hereafter abbreviated to K.R. method)[9] for the mixture formula, and also by the discussion in the appendix. This appendix contains material whose introduction would impede the direct derivation of the main formulae of the paper.

In order to make this paper self-contained, the physical theory will be briefly reviewed. Consider a gas A maintained at temperature T_0. Under the influence of collisions some kinetic energy is taken up by the internal states of the atoms or molecules of A, but this is exactly balanced on the average by the internal energy given back. If the temperature be raised by the small amount δT, the increment in the number of molecules in the excited state i, after the passage of sufficient time, is, of course, $(\partial A_i/\partial T)\,|_{T=T_0}\delta T$ where A_i represents the number of i state molecules in unit volume, and is given mathematically by the Maxwell-Boltzmann formula. Since kinetic theory considerations are central in this paper it is more desirable to use K, the kinetic energy per molecule determined from the mean square of the velocity, rather than T, so that the increment may also be written $(\partial A_i/\partial K)\,|_{K=K_0}\delta K$. However if too short a time interval is taken, this new equilibrium value for state i is not attained. We may take account,

[3] Reference 2, II, V.

[4] H. O. Kneser, V. O. Knudsen, Ann. d. Physik **21**, 682 (1935) and other papers of their own to which the authors refer.

[5] The penetrating papers of Richards, and Richards and Reid (scattered through the 1933 and 1934 issues of the Journal of Chemical Physics) contain an excellently balanced analysis of the application of theory to experiment and should not be overlooked by students endeavoring to orient themselves in this field. Though written from the viewpoint of the Einstein method, the authors have evidently a thorough understanding of the writer's method as well. Special mention ought be made of H. O. Kneser's work in interpreting his own and others' experimental work, for it has gone far in making this field significant, cf. reference 4. The papers already mentioned and those in reference 6 contain more adequate bibliographies. In the forefront of important contributors whom the reader may consult for other phases of supersonic work, one lists W. P. Pielemeyer, Phys. Rev. **36**, 1006 (1930); **41**, 833 (1932); A. Eucken and R. Becker, Zeits. f. physik. Chemie **B20**, 467 (1933); P. S. H. Henry, Proc. Camb. Phil. Soc. **28**, 249–255 (1931–32).

[6] The first presentation by H. O. Kneser contained inconsistencies which fortunately "balanced" out. The correct application was made by Ruttgers. A. Einstein, Sitz.-Ber. Berlin Acad. 380, 1920. H. O. Knese, Ann. d. Physik **5**, 761 (1931); Ruttgers, Ann. d. Physik **5**, 350 (1933).

[7] There is a difference in result in the sense that $\mathbf{C}_\infty$ replaces $3k/2$, but this is not an essential distinction. Cf. appendix, section (B).

[8] The criticism of the Kneser theory in paragraph 1 of IV, reference 2, implied that a microscopic state separation had to be imposed for completeness. When this is done, one obtains the theory described here as the K.R. method which is shown to be essentially equivalent to the writer's formulation. The extension of the original Kneser-Ruttgers work to more than two states was made by Richards, who, in fact, remarked the similarity to the three state calculation made by the writer in IV.

[9] The material on the K.R. method may be omitted by the reader without sacrificing the completeness of the derivations of the new results of this paper. Cf. reference 27.

mathematically, of such a condition by multiplying by a parameter ω_i whose value is determined by this time interval. Evidently $|\omega_i| \leqslant 1$.

If sound waves are propagated in the gas, the mean kinetic energy in any small region is an approximately harmonic function of the time. Hence the time interval referred to above, which is available for adjustment of the internal states to the external translational energy fluctuation, is evidently determined by the period or more conveniently the frequency of the kinetic energy oscillations. Furthermore, since the energy quanta in the excited states have a finite mean life they are not, on the average, immediately restored to the gas as translational energy; that is to say a phase lag must subsist in the relationship between external and internal energy changes. It is then clear that the parameters ω_i must be functions of ν involving phase lags. Now quite without any mathematics it seems clear that when the period of the sound wave is nearly the same as that of the mean life of the energy quantum of some state, an influence on the sound propagation may be expected. The degree of this influence is dependent on the amounts of internal energy exchanged at this particular 'mean life' rate. Roughly then the effect should be proportional to $(\partial A_i/\partial K)\epsilon_i$ where ϵ_i is the energy associated with the ith excited state. This will perhaps be clearer if we recall that the Laplace value for the velocity of sound depends on the ratio of the specific heats which in turn involves a sum over i of terms of just the form $(\partial A_i/\partial K)\epsilon_i$. In this connection it may be remarked that the Laplace formula may be maintained formally if, because of the dependence of the internal state populations on ω_i, one introduces 'effective' specific heats dependent on ν.

Evidently the fidelity of reproduction in the internal states of the kinetic energy variation and accordingly the values of the ω_i and the 'mean lives' depend on the ease with which external and internal energies are exchanged in collision. One therefore introduces transition probability factors. A natural notation is k_{ij}^{σ}. The subscripts indicate that a molecule originally in state i goes to state j because of the collision. The superscript σ marks the fact that the colliding molecule under whose influence the transition was accomplished was in state σ. Later double transitions will be considered—the early part of this paper considers only single transitions so that the second molecule remains in state σ though its translational energy may, of course, be affected. The units for k_{ij}^{σ} are so chosen that the number of collision-inspired transitions from state i to state j in unit time and volume is given by $A_i A_\sigma k_{ij}^{\sigma}$.

Among the important questions of modern physics and chemistry are those associated with collision processes. A satisfactory quantum theoretic treatment of individual atomic and molecular collisions does not exist as yet because of the complexity both of the physical situation and the analysis. However statistical information may be obtained from the interpretations of sound data afforded by the lag theory of sound just sketched. This required information is embodied in the values of the collision transition probabilities k_{ij}^{σ}. Explicit connections between these transition probabilities and the experimentally determinable magnitudes such as the absorption, velocity, specific heat, etc., of the gases involved, are important ends of this paper and others in this field. From this point of view it would seem essential to consider collisions between molecules of different types in order to gain an idea of the factors influencing the effectiveness of collision, that is to say, a theory of sound propagation in *mixtures* is demanded.

The main ideas of the theory of sound for a single gas may be carried over in their entirety to the case of a mixture of gas A and gas B. As a measure of economy A and B will also stand for the number of molecules of each gas in unit volume. Two sets of parameters must now be used, namely ω_{A_i} and ω_{B_r}. For collisions in which A type molecules change their state, the small letters[10] k_{ij}^{σ} and g_{ij}^{σ} will be used. The first has already been defined. The second refers to collisions between an A type molecule in state i and a B molecule in state σ, thus $A_i B_\sigma g_{ij}^{\sigma}$ gives the number of molecules of gas A, originally in

[10] The notation used in previous papers is slightly different, i.e., $\mathfrak{f}_{ij} \equiv k_{ij}^{i}$ and the average value $f_{ij} \equiv \Sigma_\sigma (A_\sigma k_{ij}^{\sigma}/A - A_i)$, $\sigma \neq i$. The new notation lends itself to clearer exposition. Cf. appendix, section (A), for indication of equivalence of results. For $i, j = 1, 2$ there is really no difference in notations.

state i, which change to state j in unit time and volume because of AB collisions. The capitals K_{rs}^{σ} and G_{rs}^{σ} are used for transitions of the molecules of gas B. The first refers to the case that the colliding molecules are B_r and B_s respectively, and the second that they are B_r and A_s. In general i and j will be used as scripts for any of the n states of gas A molecules and r and s will be used similarly for gas B. However σ is used indiscriminately for reasons of convenience since it will usually be associated with a summation sign. This dual usage will cause no confusion because the symbols to which σ is attached already differentiate between the two gases.

The various transition factors[11] are not independent for the principle of detailed balancing requires that

$$A_i k_{ij}^{\sigma} = A_j k_{ji}^{\sigma}, \quad A_i g_{ij}^{\sigma} = A_j g_{ji}^{\sigma},$$
$$B_r K_{rs}^{\sigma} = B_s K_{sr}^{\sigma}, \quad B_r G_{rs}^{\sigma} = B_s G_{sr}^{\sigma}. \tag{1}$$

The rate of change in i state populations contributed by double collisions is denoted by $D(A_i)$, the definition of $D(B_i)$ is similar

$$D(A_i) = -\Sigma_{\sigma,j} A_i A_\sigma k_{ij}^{\sigma} - A_j A_\sigma k_{ji}^{\sigma} + A_i B_\sigma g_{ij}^{\sigma} - A_j B_\sigma g_{ji}^{\sigma}. \tag{1a}$$

Evidently (cf. Eq. 1), $D(A_i)=0$ for equilibrium conditions. The effects of triple collisions as well as collisions in which both partners undergo transitions may be incorporated into these developments. The explicit modifications are given in the appendix (Eqs. 15 ff.).

The assumption of a lag in adjustment of the internal energy states may be expressed formally by writing for the change[12] in state i (or r) concentration of gas A (or B)

$$\delta A_i = (A_i/A)\delta A + \omega_{A_i} A'_i \delta K; \quad \delta B_r = (B_r/B)\delta B + \omega_{B_r} B'_r \delta K \tag{2a}$$

where A'_i, B'_r stand for $\partial A_i/\partial K$ and $\partial B_r/\partial K$. For the developments of this paper the simplifying assumptions $\omega_{A_i} \equiv \omega_A$; $\omega_{B_r} \equiv \omega_B$ are made. The rate of change in occupants of state i due to passage of a sound wave[13] is denoted by ΔA_i (or ΔB_i).

$$\Delta A_i \equiv \delta D(A_i) = -\Sigma_{\sigma,j}\delta A_\sigma (A_i k_{ij}^{\sigma} - A_j k_{ji}^{\sigma}) + \delta A_i A_\sigma k_{ij}^{\sigma} - \delta A_j A_\sigma k_{ji}^{\sigma} + \delta B_\sigma (A_i g_{ij}^{\sigma} - A_j g_{ji}^{\sigma})$$
$$+ \delta A_i B_\sigma g_{ij}^{\sigma} - \delta A_j B_\sigma g_{ji}^{\sigma} + \delta g[\ ] + \delta k[\ ]. \tag{3a}$$

$\delta k[\ ]$, $\delta g[\ ]$ are generic notations for the totality of terms in the variations δk_{ij}^{σ}, δk_{ji}^{σ} and δg_{ij}^{σ}, δg_{ji}^{σ}.

Since the relative number of molecules in the various states depends on temperature alone at equilibrium, merely increasing A or B by amounts δA or δB will not disturb the exact balance of internal and external energy collision exchanges; i.e., $\Delta A_i/\delta A$, $\Delta A_i/\delta B$ at constant K is 0. This is easily verified analytically for the substituion of $(\delta A/A)A_i$, for δA_i gives for the coefficient of δA in Eq. (3a), $D(A_i)/A$ or 0 at equilibrium; similarly for terms in δB. Thus only the second terms of Eq. (2a) play a role in ΔA_i or ΔB_r.

Next we notice that the coefficients of δA_σ and δB_σ are 0 by the principle of detailed balancing, Eq. (1). The transition probabilities are dependent solely on K. The terms $\delta k[\ ]$, $\delta g[\ ]$ might be difficult to calculate directly. Fortunately, however, they may be eliminated since $L_{r\to 0}\Delta A_i = L_{\omega_A \to 1}\Delta A_i = 0$. We have, in fact,

$$0 = L_{r\to 0}\Delta A_i = \Sigma_{j,\sigma}\delta k[\ ] + \delta g[\ ] + \delta K[A'_i(A_\sigma k_{ij}^{\sigma} + B'_\sigma g_{ij}^{\sigma}) - A'_j(A_\sigma k_{ij}^{\sigma} + B_\sigma g_{ji}^{\sigma})]. \tag{3.1a}$$

We introduce the averaged probabilities[14]

[11] If desired, the Einstein radiation transition probabilities may be added. Cf. I, reference 2.

[12] The δK is supposed so small that the distribution function is not appreciably modified.

[13] The equivalent notation in IV, reference 2, is $(\Delta)_T$ for D and $\Delta = \Delta(\Delta)_T$ for the present Δ and has caused readers some confusion. Authors employing the K.R. developments write d/dt and Δ for our D and δ respectively.

[14] The work would be more perspicuous, no doubt, if instead of the n state model with the one ω value a two state model ($i, j = 1$ or 2) were used just as in the K.R. method in the succeeding paragraphs. The more general situation is taken in order to emphasize the fact that it is the ω and not the number of states that determines the behavior of the gas. The text treatment involves $\Sigma_j(R_{ij} - (N'_j/N'_i)R_{ji})$ independent of i, i.e., $\Sigma_j R_{ij}(\epsilon_i - \epsilon_j/\epsilon - \epsilon_j)$, where ϵ is the average energy. If $B \equiv 0$ the pure gas equations with $\omega_i \equiv \omega$ are obtained. The general case $\omega_i \neq \omega$ is taken up in I, and IV of reference 2. Cf. also appendix.

$$R_{ij}=\Sigma_\sigma A_\sigma k_{ij}^{\sigma}/A\,;\quad P_{ij}=\Sigma_\sigma B_\sigma g_{ij}^{\sigma}/B\,;\quad A_iR_{ij}=A_jR_{ji},\quad \text{etc.}\,;$$
$$S_{rs}=\Sigma_\sigma B_\sigma K_{rs}^{\sigma}/B\,;\quad Q_{rs}=\Sigma_\sigma A_\sigma G_{rs}^{\sigma}/A. \tag{3.2a}$$

Accordingly,[15]
$$\Delta A_i/\delta K=-(\omega_A-1)\Sigma_j A(A'_iR_{ij}-A'_jR_{ji})+B(A'_iP_{ij}-A'_jP_{ji}),$$
$$\Delta B_r/\delta K=-(\omega_B-1)\Sigma_j B(B'_rS_{rs}-B'_sS_{sr})+A(B'_rQ_{rs}-B'_sQ_{sr}). \tag{4a}$$

These are key equations[16] in our development of the theory.

By making use of the equations of the kinetic theory of gases it is possible to obtain another expression for $\Delta A_i/\delta K$, $(\Delta B_r/\delta K)$. Thus one may solve for ω_A and ω_B, and substitute these values in Eq. (4a) to give $\Delta A_i/\delta K$; $\Delta B_r/\delta K$ directly in terms of the R's and P's, etc. The kinetic theory equations required may be looked upon as being modifications of the transport equation.

The first is

$$\frac{\partial}{\partial t}\begin{Bmatrix}A\\B\end{Bmatrix}=-\frac{\partial}{\partial x}\begin{matrix}A\\B\end{matrix}v. \tag{4.1a}$$

v is the mass motion velocity.

Next, according to the equipartition principle, A and B molecules have equal translational energies. Since their mass motions are also equal, there is no collision term and we may write, with $N=A+B$,

$$\frac{\partial}{\partial t}(m_AA+m_BB)v=-\frac{\partial}{\partial x}\left(\frac{2}{3}NK\right), \tag{4.2a}$$

$$\frac{\partial}{\partial t}NK=-\frac{\partial}{\partial x}\left(\frac{5}{3}NKv\right)+\Delta K, \tag{4.3a}$$

$$\frac{\partial}{\partial t}\begin{Bmatrix}A_i\\B_r\end{Bmatrix}=-\frac{\partial}{\partial x}\begin{Bmatrix}A_i\\B_r\end{Bmatrix}v+\Delta\begin{matrix}A_i\\B_r\end{matrix}. \tag{4.4a}$$

ΔK is the translational energy change due to collision. These equations have already been given in (I) and (II) (cf., however, the correction given in footnote 2 of (III)). For the rest we set

$$\delta N=|\delta N|e^{j(\nu t-x/\lambda)}\,;\quad \delta K=|\delta K|e^{j(\nu t-x/\lambda)},\quad \text{etc.} \tag{4.5}$$

and neglect products involving two variationals. *Note ν is 2π times the frequency while λ is $1/2\pi$ times the wave-length.*

Eqs. (4.1a) and (4.4a) are therefore

$$j\nu\delta A=jA\delta v/\lambda, \tag{4.11a}$$
$$j\nu\delta A_i=jA_i\delta v/\lambda+\Delta A_i, \tag{4.41a}$$

whence
$$\Delta A_i=j\nu[\delta A_i-A_i\delta A/A]\quad=j\nu\omega_AA'_i\delta K. \tag{4.411a}$$

On equating this value for ΔA_i to that given in Eq. (4a), there results

$$\delta Kj\nu\omega_AA'_i=-(\omega_A-1)\delta K\Sigma_jAA'_i[R_{ij}=(A'_j/A'_i)R_{ji}]+BA'_i[P_{ij}-(A'_j/A'_i)P_{ji}].$$

Accordingly
$$\omega_A=\frac{1}{1+j\nu/\Sigma_jA(R_{ij}-(A'_j/A'_i)R_{ji})+B(P_{ij}-(A'_j/A'_i)P_{ji})} \tag{5a}$$

[15] For the single gas $F(\omega)$ in Kneser's notation is our ω, cf. Eq. (18) of reference 6. In Ruttger's paper his Eq. 23 is effectively $\omega_1N'_1\delta K=-\Delta N_1$. Cf. Eq. (5a). Ruttgers goes through several steps to obtain his Eq. (24) which is our Eq. (2a). Of course these equations already occur in I, reference 2.

[16] Since all developments of the theory by the writer use Eq. (4a) as a basic equation, it may be accepted by the reader not interested in detail as a sort of postulate along with the kinetic theory equations (Eq. 4.1a, 4.4a).

and therefore,

$$\Delta A_i = \frac{j\nu A^\cdot{}_i \delta K}{1 + j\nu/A\Sigma_j[(R_{ij} - (A^\cdot{}_j/A^\cdot{}_i)R_{ji}) + B(P_{ij} - (A^\cdot{}_j/A^\cdot{}_i)P_{ji})]}.$$

Similarly

$$\Delta B_r = \frac{j\nu B^\cdot{}_r \delta K}{1 + j\nu/B\Sigma_s[s_{rs} - (B^\cdot{}_s/B^\cdot{}_r)s_{sr} + A(Q_{rs} - (B^\cdot{}_s/B^\cdot{}_r)Q_{sr})]}. \tag{5.1a}$$

Sinçe ΔK is the negative of the internal energy change due to collisions, it may be written down immediately as $\Delta K = -\Sigma_i \Delta A_i \epsilon_i{}^A + \Sigma_r \Delta B_r \epsilon_r{}^B$, with $\epsilon_i{}^A$ the ith energy state value for gas A.

The succeeding six paragraphs indicate the K.R. approach to essentially the formulae already derived. To facilitate comparison with the K.R. method, let us introduce the auxiliary notation $a_i = UA_i$ and $a = UA$, i.e., a_i and a are the number of molecules in the volume U, while A_i and A are the concentrations or number in unit volume. We remark now that in the developments of the theory one may either maintain the volume fixed while permitting the molecule count a to change, or associate different volumes with a fixed molecule count a. The equivalence is immediate from $a = UA$,

i.e., $$(\delta a/a)_U = -(\delta U/U)_a. \tag{6}$$

The first viewpoint with $U \equiv 1$ and fixed (so that $a_i \equiv A_i$, $a \equiv A$) is used in the writer's developments; the second is followed in the K.R. argument. Consider ΔA_i. It has been demonstrated that δA and δB drop out of Eq. (3a) which means that all the results obtained must be consistent with A and B being held constant.[17] Since U is considered fixed on the writer's viewpoint, this is the same as saying that a and b may be taken fixed. For later comparison with Eq. (3b) it is desirable to write ΔA_i with U introduced explicitly. From what has just been said it is evident that

$$\Delta A_i \equiv \Delta(a_i/U)|_{U,\, a,\, b} \equiv (1/U)\Delta a_i|_{a,\, b}. \tag{6.1}$$

If the K.R. viewpoint of variable U be adopted the notation ΔA_i might be expected to mean $a_i \Delta(1/U) + \Delta a_i/U$. We proceed to show in conformity with the result Eq. (6.1) that, using the K.R. method, again only the second term enters.

For the K.R. method[18] Eq. (1a) is written down as before

$$\begin{aligned} &D(A_1) = (1/U)D(a_1) = A_1{}^2 k_{12}{}^1 + A_1 A_2 k_{12}{}^2 - A_2{}^2 k_{21}{}^2 - A_2 A_1 k_{21}{}^1 + A_1(B_1 g_{12}{}^1 + B_2 g_{12}{}^2) - A_2(\cdots), \\ &D(A_2) = (1/U)D(a_1) = \cdots, \quad D(B_1) = \cdots, \end{aligned} \tag{1b}$$

where i, j of Eq. (1a) are restricted to the values 1, 2.

The variations may of course be carried out precisely as in the writer's method, but to maintain parallelism with the usual forms of development, one writes

$$\left(\frac{A_2}{A_1}\right) = \frac{k_{21}{}^\sigma}{k_{12}{}^\sigma} = \frac{g_{21}{}^\sigma}{g_{12}{}^\sigma} = e^{-(\epsilon_2{}^A - \epsilon_1{}^A)/kT} = \mu_A; \quad A_1 = \frac{A}{1+\mu_A};$$

$$\left(\frac{B_2}{B_1}\right) = \frac{K_{21}{}^\sigma}{K_{12}{}^\sigma} = \frac{G_{21}{}^\sigma}{G_{12}{}^\sigma} = e^{-(\epsilon_2{}^B - \epsilon_1{}^B)/kT} = \mu_B; \quad B_1 = \frac{B}{1+\mu_B}.$$

Then

$$(\Delta A_i) = -[\{\Sigma^2{}_{\sigma=1} A_\sigma k_{21}{}^\sigma + \Sigma^2{}_{\rho=1} B_\rho g_{21}{}^\rho\}[\delta(\mu_A A_1) - \delta A_2] + (\mu_A A_1 - A_2)\delta\Sigma_\sigma A_\sigma k_{21}{}^\sigma + \Sigma^2{}_{\rho=1} B_\rho g_{21}{}^\rho], \tag{3b}$$

referring to Eq. (1a) or (1b). The last block of terms vanishes because of Eq. (1). It would be more in keeping with the spirit of a K.R. method development to express A_i in terms of a_i/U and then factor out the U term, and vary only a_i. This would give for the right side above

$$-\{\Sigma^2{}_{\sigma=1} a_\sigma k_{21}{}^\sigma + \Sigma^2{}_{\rho=1} b_\rho g_{21}{}^\rho\}[\delta(\mu_A a_1) - \delta a_2]U + 0. \tag{3.1b}$$

[17] The fact that ΔA was proved independent of δA is immediate confirmation.

[18] In the K.R. work only the first collision change is taken into account in the single gas case. However the generalization is simple to make, and is, besides, of small effect probably because of the relative fewness of $A_2 A_2$ collisions; cf. Richards, references 5, 8.

The equivalence with Eq. (3b) follows from

$$\delta(\mu_A A_1)-\delta A_2-(1/U)\{\delta(\mu_A a_1)-\delta a_2\}=-(\delta U/U)\{\mu_A a_1-a_2\}=0.$$

The vanishing of the term on the right is the precise analogue of the disappearance of the δA term on the writer's method from Eq. (3a), as is obvious on writing $(\delta A/UA)=(\delta B/UB)$ for $-(\delta U/U^2)$. It appears from this last remark that though the δ symbol implies variation of A or U, the true value of ΔA_i (Eq. 3b) is also obtained if δ be considered as a partial variation at constant volume, cf. Eq. (6.1). Thus we are again justified in writing $\Delta(A_i)\equiv(1/U)\Delta a_i|_{a,\ b\ \text{fixed}}$. Also,

$$\delta\mu_A=\delta A_2/A_1=(A'_2/A_1-(A'_1/A_1)\mu_A)\delta K,\quad A'_2=-A'_1;$$

$$\therefore\quad \delta(\mu_A A_1)-\delta A_2=A_1\delta\mu_A+(A/A_1)\delta A_1=-A'_1(A/A_1)\delta K+(A/A_1)\delta A_1. \tag{2b}$$

We assume now that D and δ are commutative, i.e., $\Delta A_i\equiv\delta D(A_i)\equiv(D\delta A_i)_{U=1}$. Evidently $D(f)$ is a time rate so that if all variations are harmonic in time, i.e., $\delta f=|\delta f|e^{i\nu t}$, then

$$D(\delta A_i)_{U=1}\equiv\Delta A_i=j\nu(\delta A_i)_{U=1}. \tag{5b}$$

This equation is the analogue of Eqs. (4.11) and (5a). Solving Eqs. (3b) and (5b) simultaneously one obtains the value of $(1/A'_1)(\delta A_i/\delta K)_{U=1}$ (which is called ω_A in the writer's work) and $\Delta A_i/\delta K$. Evidently the results are exactly Eqs. (5a) and (5.1a) again. The writers who employ the K.R. development would however write the results in terms of the a's instead of the A since later the U variations are considered basic

$$\Delta a_1=-\Delta a_2=j\nu a'_1\delta K/[1+j\nu/(a/U)(R_{12}+R_{21})+(b/U)(P_{12}+P_{21})]. \tag{5.1b}$$

The other equations introduced in the K.R. method are

$$\rho_A V=Am_A,\quad \rho_B U=Bm_B, \tag{4.1b}$$

$$pU=nkT,\quad \text{the equation of state}^{19} \tag{4b}$$

and the equation for adiabatic change[20]

$$(aC_{A_\infty}+bC_{B_\infty})\delta T+(\epsilon_2{}^A-\epsilon_1{}^A)\Delta a_1+(\epsilon_2{}^B-\epsilon_1{}^B)\Delta b_1+p\delta U=0, \tag{4.3b}$$

$$V^2=\delta p/\delta\rho,\quad \text{where } V \text{ is the velocity of sound.} \tag{4.2b}$$

C_{A_∞} is the effective specific heat per mol. at constant volume of gas A when the sound frequency is "very high." The meaning of this last condition as well as the distinction between $3k/2$ and C_{A_∞} or C_{B_∞} is taken up in appendix E.

These equations, too, when expressed in variational forms are exactly equivalent to the set (4a–4.4a) used by the writer. In particular the central equation (4.3b) is the thermodynamic statement of Eq. (4.3a). As verification Eq. (4.3a) goes to

$$(N\delta K+K\delta N)j\nu=(j/\lambda)(5NKv/3)+\Delta K. \tag{6.2}$$

Making use of Eq. (4.11a), this is

$$(N\delta K-\tfrac{2}{3}K\delta N)j\nu=\Delta K. \tag{6.3}$$

Recalling $\delta N/N=-\delta U/U$, this is

$$N\delta K+\tfrac{2}{3}KN(\delta U/U)=\Delta K=-(\Delta A_1(\epsilon_2{}^A-\epsilon_1{}^A)+\Delta B_1(\epsilon_2{}^B-\epsilon_1{}^B)). \tag{64}$$

The equation of state is $pU=nkT$, with $n=NU$, and it may either be taken from the set (4b) or from kinetic theory. Hence

$$(3kn\delta T/2)+p\delta U-(\Delta K)U=0\quad\text{if}\quad K=3kT/2. \tag{6.5}$$

This is Eq. (4.3b) with $aC_{A_\infty}+bC_{B_\infty}=3kn/2$. Cf. appendix D for removal of this restriction.

[19] The results may be generalized by using other relations between p, T, U or N, K, m for the equation of state—the effect is on the coefficient p/ρ (or K/m). Cf. Richards for use of the van der Waals equation.

[20] C_{A_∞}, C_{B_∞} is the "effective" frequency free term for the range up to the last absorption band.

From Eqs. (4.1a) and (4.3a), in conjunction with Eq. (4.5), one has immediately for $\delta N/\delta K$,

$$\delta N/\delta K=(\Delta K-j\nu N)/(j\nu K-j(5/3)(KV/\lambda)), \tag{7a}$$

where $V=\lambda\nu$ is the velocity of sound. An expression for $\delta N/\delta K$ is also obtained from Eqs. (4.1a) and (4.2a), whence on elimination and substitution of the equipartition value $K=3kT/2$ there results

$$V^2=\frac{kT}{\mathbf{m}}\left[\frac{-Nk(5/2)j\nu+(3/2)k(\Delta K/\Delta T)}{-Nk(3/2)j\nu\ +3k/2(\Delta K/\Delta T)}\right] \tag{8a}$$

with $\mathbf{m}$, the mean mass,[21] i.e. $=(Am_A+Bm_B)/N$. Furthermore, one remarks that

$$A\dot{}_1\epsilon_1{}^A+A\dot{}_2\epsilon_2{}^A=A\dot{}_1(\epsilon_1{}^A-\epsilon_2{}^A)=\frac{d}{dT}(A_1\epsilon\dot{}_1{}^A+A_2\epsilon_2{}^A)\frac{dT}{dK}=AC_A/(3k/2);$$

where C_A is the ordinary internal specific heat per molecule of gas A similarly for C_B. They may be considered measured at 0 frequency. The end result[22] is

$$V^2=\frac{kT}{\mathbf{m}}\left[1+k\Big/\left(\frac{3}{2}k+\frac{1}{N}\left\{\frac{AC_A}{1+j\nu/A\Gamma_{11}+B\Gamma_{12}}+\frac{BC_B}{1+j\nu/A\Gamma_{21}+B\Gamma_{22}}\right\}\right)\right], \tag{8.1a}$$

$$\Gamma_{11}=R_{12}+R_{21};\quad \Gamma_{22}=S_{12}+S_{21};\quad \Gamma_{12}=P_{12}+P_{21};\quad \Gamma_{21}=Q_{12}+Q_{21}.$$

Now $kT/m\equiv p/\rho$ and this will be the factor used hereafter, cf. reference 19.

In accordance with the general principle of replacement of δN by δU in going from the writer's to the K.R. calculation, we first combine Eqs. (4b) to (4.2b) to get $\delta U/\delta T$, whence substituting the value of $\delta U/\delta T$ from Eqs. (4.3b) and (5.1b) we have

$$V^2=\frac{p}{\rho}\left[1+k\Big/\left(\frac{AC_{A\infty}+BC_{B\infty}}{N}+\frac{1}{N}\left\{\frac{AC_A}{1+j\nu/A\Gamma_{11}+B\Gamma_{12}}+\frac{BC_B}{1+j\nu/A\Gamma}\right\}\right)\right]. \tag{8.1b}$$

Except for the occurrence of $(AC_{A\infty}+BC_{B\infty})/N$, henceforth written $\mathbf{C}_\infty$, in the place of $3k/2$ the final equation (Eq. (8.1a) and Eq. (8.1b)) deduced by either method is the same (and has been given before by the writer for specialized k_{ij}).

The calculation of main interest for the purpose of this paper is the absorption. The sound wave may be represented as $e^{-x/\lambda\sin\phi}e^{j(\nu t-x/\lambda\cos\phi)}$. Since ϕ is small for nearly all practical cases

$$\cos\phi/\cos 2\phi\sim 1$$
$$\mu=2\sin\phi\sim\tan 2\phi.$$

This approximation[23] gives the absorption formula a considerable advantage in simplicity over the strictly rigorous results, i.e.,

$$\mu=\text{absorption coefficient per wave-length}\div 2\pi=\nu D(\mathfrak{C}_p-\mathfrak{C}_v)/(\mathfrak{C}_p\mathfrak{C}_v+\nu^2D^2)=2\nu kD/\mathfrak{C}_p\mathfrak{C}_v+\nu^2D^2. \tag{9}$$

The notation of V is adhered to here, namely

$V^2=V_0{}^2e^{2i\phi}$, $V_0{}^2$ is the real part of V^2, cf. Eqs. (8.1).

$$\mathfrak{C}_V=\ _\infty+\frac{1}{N}\left[\frac{AC_A}{1+\nu^2/\Sigma_A{}^2}+\frac{BC_B}{1+\nu^2/\Sigma_B{}^2}\right]=\text{"effective" specific heat per mol. at constant volume,}$$

$\mathfrak{C}_p=\mathfrak{C}_V+k=$"effective" specific heat per mol. at constant pressure,

$\Sigma_A=A\Gamma_{11}+B\Gamma_{12}$; $\Sigma_B=B\Gamma_{22}+A\Gamma_{21}$ (Cf. Eq. (8.1a) and Eq. (10.3)),

$$D=\frac{1}{N}\left\{\frac{AC_A}{\Sigma_A(1+\nu^2/\Sigma_A{}^2)}+\frac{BC_B}{\Sigma_B(1+\nu^2/\Sigma_B{}^2)}\right\},$$

$\mathbf{C}=\mathbf{C}_i+\mathbf{C}_\infty$; $\mathbf{C}_i=(AC_A+BC_B)/N$.

[21] $\mathbf{m}$ replaces the slightly awkward notation (cf. reference 2 of III). N/S used in V and earlier.
[22] Called Eq. (2.1) in V, reference 2.
[23] The factor 2 takes care of the fact that intensities and not amplitudes are being compared.

Fortunately, the rather forbidding expression in Eq. (9) may be simplified by removing factors of $(1+\nu^2/\Sigma_A^2)(1+\nu^2/\Sigma_B^2)$ from numerator and denominator. Thus

$$\mu=\left\{\frac{\dfrac{\nu k}{N}\left\{\dfrac{AC_A}{\Sigma_A}\left(1+\dfrac{\nu^2}{\Sigma_B^2}\right)+\dfrac{BC_B}{\Sigma_B}\left(1+\dfrac{\nu^2}{\Sigma_A^2}\right)\right\}}{\mathbf{C}_\infty(\mathbf{C}_\infty+k)\left[1+\dfrac{\nu^2}{\Sigma_A^2}\right]\left[1+\dfrac{\nu^2}{\Sigma_B^2}\right]+(2\mathbf{C}_\infty+k)\mathbf{C}_i+\dfrac{\nu^2}{N}\left\{\dfrac{AC_A}{\Sigma_B^2}+\dfrac{BC_B}{\Sigma_A^2}\right\}(2\mathbf{C}_\infty+k)+\mathbf{C}_i^2+\dfrac{\nu^2}{N}\left\{\dfrac{AC_A}{\Sigma_B}+\dfrac{BC_B}{\Sigma_A}\right\}}\right\}$$

$$=\frac{\left\{\dfrac{\nu k}{N}\left[\dfrac{AC_A}{\Sigma_A}\left(1+\dfrac{\nu^2}{\Sigma_B^2}\right)+\dfrac{BC_B}{\Sigma_B}\left(1+\dfrac{\nu^2}{\Sigma_A^2}\right)\right]\right\}}{(\mathbf{C}+k)\mathbf{C}+\nu^2\left\{\dfrac{1}{\Sigma_A^2}\left(\mathbf{C}_\infty+\dfrac{BC_B}{N}+k\right)\left(\mathbf{C}_\infty+\dfrac{B}{N}C_B\right)\right.}\tag{9.1}$$

$$\left.+\frac{1}{\Sigma_B^2}\left(\mathbf{C}_\infty+\frac{AC_A}{N}+k\right)\left(\mathbf{C}_\infty+\frac{AC_A}{N}\right)+\frac{2ABC_AC_B}{N^2\Sigma_A\Sigma_B}\right\}+\nu^2(\mathbf{C}_\infty+k)\mathbf{C}_\infty.$$

Very often the following approximations are permissible:

$$BC_B/N\mathbf{C}_\infty,\quad AC_A/N\mathbf{C}_\infty\ll 1.\tag{9.2}$$

This allows us to write the denominator as nearly

$$(\mathbf{C}_\infty+k)\mathbf{C}_\infty[(\Sigma_A^2+\nu^2)(\Sigma_B^2+\nu^2)/(\Sigma_A\Sigma_B)^2].$$

The approximate expression for μ is now

$$\mu=\frac{\nu k}{N}\left[\frac{AC_A\Sigma_A}{(\mathbf{C}_\infty+k)\mathbf{C}_\infty(\Sigma_A^2+\nu^2)}+\frac{BC_B\Sigma_B}{(\mathbf{C}_\infty+k)\mathbf{C}_\infty(\Sigma_B^2+\nu^2)}\right].\tag{9.3}$$

This is sufficiently near to being a sum of effects due to each gas separately to make the result easy to comprehend physically.[24]

So far all the work done on supersonics has assumed pair collisions to be the only significant ones. It is, however, easy to extend the result to triple and higher order collisions and indeed the formulae maintain their appearance, except that the $\begin{Bmatrix} k_{ij} & \cdots & G_{rs} \\ R_{ij} & & Q_{rs} \end{Bmatrix}$ assigned to n body collisions have an $n-1$ degree factor in the gas concentrations; i.e., A^pB^q, $p+q=n-1$ rather than the normal first degree term in A or B. The general triple collision is, of course,

$$A_iB_jB_K\rightarrow A_\sigma B_\tau B_\gamma.\tag{10}$$

This sort of collision is omitted just now because its inclusion complicates the expressions for ω_A and ω_B. Cf. Appendix, section C.

Consider the case

$$A_1B_\tau B_\sigma\rightarrow A_2B_\tau B_\sigma\tag{10.1}$$

with the transition probability $k_{12}{}^{\tau s}$ in the forward direction and $k_{21}{}^{\tau s}$ in the reverse. Evidently the contribution to ΔA_1 is

$$(\Sigma_{\tau,\sigma}B_\tau B_\sigma k_{12}{}^{\tau s})\delta A_1-(\Sigma_{\tau,\sigma}B_\tau B_\sigma k_{21}{}^{\tau s})\delta A_2.\tag{10.2}$$

On comparing with Eqs. (3a) and (3.2a) it is plain that it is only necessary to add the terms

[24] The appearance of Eq. (9.3) suggests that the parameter $Z=\nu/N$ will rid the result of pressure dependence *provided* Σ_A and Σ_B depend only linearly on A and B. Cf. Richards for a single gas.

$\Sigma_{r,\ s}B_rB_sk_{12}{}^{rs}/B^2$ and $\Sigma_{r,\ s}B_rB_sk_{21}{}^{rs}/B^2$ to P_{12} and P_{21} in Eq. (3.2a) in order to include this triple collision[25] effect. Since for the two state gas model $A'_1=-A'_2$ there results[26]

$$B\Gamma_{12}=B(P_{12}+P_{21})+\Sigma_{r,\ s}B_rB_sk_{21}{}^{rs}$$
$$=B\left(\frac{1+\mu_A}{1+U_B}\right)\left[(g_{21}{}^1+\mu_Bg_{21}{}^2)+\frac{B}{1+U_B}(k_{21}{}^{11}+\mu_Bk_{21}{}^{12}+\mu_B{}^2k_{21}{}^{22})\right]. \tag{10.3}$$

Of course similar terms may be added for A. In this way Σ_A and Σ_B may be considered made up of terms in A, B, A^2, $B^2\cdots A^n$, B^n depending on the order of collisions assumed important.[27]

By making the arbitrary assumption that $k_{12}{}^1$ was proportional to B (and, in the case of H_2O in O_2, to B^2 also) Kneser has been able to get agreement with experiment for impurity contamination.[28] To understand why such a proposal works and what the deeper relation is with collision probabilities we shall derive the impurity contamination case as a special instance of the mixture formulae. We may start either with the definition of ω_A and ω_B, Eq. (5a); or with Eq. (9.3). The Kneser 'normal' situation arises when $B((1+\mu_A)/(1+\mu_B))(g_{21}{}^1+\mu_Bg_{21})$ dominates all other terms in Σ_A and Σ_B. For generality the derivation is given with the weaker assumption $AC_A\Sigma_A\gg\Sigma_BBC_B$, then

$$\omega_B\sim 1,\quad \omega_A\sim 1/(1+j\nu/\Sigma_A).$$

The result for the absorption is, therefore,

$$\mu=\frac{(\nu k/N)(AC_A\Sigma_A)}{(\mathbf{C}_\infty+k)(\mathbf{C}_\infty)[\nu^2+(1+C_AA/N(\mathbf{C}_\infty+k))(1+AC_A/N\mathbf{C}_\infty)\Sigma_A{}^2]}. \tag{9.4}$$

If, *furthermore*, $AC_A\ll C_{\infty A}N$ (cf. Eq. (9.2)) there results

$$\mu=\frac{(\nu k/N)(AC_A\Sigma_A)}{\mathbf{C}_\infty(\mathbf{C}_\infty+k)(\nu^2+\Sigma_A{}^2)}. \tag{9.5}$$

Kneser's 'normal' case is given by suppressing the A and B^2 terms in Σ_A (cf. Eq. (10.3)). The formula proposed for H_2O in O_2 merely suppresses the A term,[29] leaving $B\Gamma_{12}$ alone. It is, however, to be noticed that $\mathbf{C}_\infty$ in Eq. (9.5) is the mean specific heat. Written out in detail

$$N^2\mathbf{C}_\infty(\mathbf{C}_\infty+k)=B^2(C_{A\infty}-C_{B\infty})^2+NB(C_{B\infty}-C_{A\infty})(k+2C_{A\infty})+N^2C_{A\infty}(C_{A\infty}+k). \tag{9.6}$$

For the case of $B\sim H_2O$ and $A\sim O_2$ for instance, using the values $C_{A\infty}=5k/2$, $C_{B\infty}=1k/2$ the variation of $\mathbf{C}_\infty(C_\infty+k)$ is only about 0.005 in the range from 0 to 1 percent H_2O.[30] A similar remark holds generally for experiments at low frequencies. At higher frequencies the maximum shifts in the direction of increasing B and the variation of the Eq. (9.6) term can no longer be neglected unless $C_{A\infty}$ and $C_{B\infty}$ are equal.

[25] The derivation on the K.R. method is equally easy.

[26] Unless there is special reason to assume the associated k factor large, the terms with μ_A, μ_B, $\mu_B{}^2$ may probably be dropped.

[27] The experimenter interested only in an applicable result of this investigation is referred to Eqs. (9.1), (9.3), (9.4), (9.5), (11.1), (12), and (12.1). For convenience of reference, using $K_{21}{}^{2/K}$ as the "reaction rate" for $B_2A_jA_K\rightarrow B_iA_jA_K$,

$$\Sigma_A=A(k_{21}{}^1+\mu_Ak_{21}{}^2)+B\left(\frac{1+\mu_A}{1+\mu_B}(g_{21}{}^1+\mu_Bg_{21}{}^2)\right)+B^2\frac{(1+\mu_A)}{(1+\mu_B)^2}\{k_{21}{}^{211}+\mu_Bk_{21}{}^{212}+\mu_B{}^2k_{21}{}^{222}\}$$

+

$$\Sigma_B=B(K_{21}{}^1+\mu_BK_{21}{}^2)+A\left(\frac{1+\mu_B}{1+\mu_A}\right)\{G_{21}{}^1+\mu_AG_{21}{}^2\}+A^2\frac{(1+\mu_B)}{(1+\mu_A)^2}\{K_{21}{}^{211}+\mu_AK_{21}{}^{212}+\mu_A{}^2K_{21}{}^{222}\}.$$

[28] Of course this is only a special type of behavior of impurities. (For other possibilities cf. remarks on the classification of mixtures.) However, this special case seems the one of greatest practical interest at this time.

[29] Kneser, Knudsen, reference 4, p. 691.

[30] The anomalous appearance of Knudsen's $\mu\sim\log B$ curves for H_2O at low frequencies is not explained by this and may credibly be due to the B^2 term. The double transition collisions ought perhaps be looked into. Cf. Eq. (15.5).

The explanation for the triple collision effect as advanced by Kneser and Knudsen is that a reaction of the form $2H_2O+O_2 \rightleftarrows 2H_2O_2$ takes place and hence these are very efficient triple collisions. However, apart from objections based on chemical considerations, a rough computation shows that this efficiency must be unreasonably high even under favorable interpretations. If W represents the fraction of the total number of the triple collisions of Kneser-Knudsen type actually effective for absorption and a prime (here and below) indicates an excited molecule and Z_{33}, Z_3, Z_2 stand for the number of collisions of type $H_2O+H_2O+O_2'$, $O_2'+O_2+O_2$, $O_2'+O_2$ respectively then Kneser and Knudsen[29] have shown that $W \sim B\Gamma_{12}/Z_{33}$. Their experiments give $B\Gamma_{12} \sim 5 \cdot 10^8 (B/N)^2$. In order to throw in relief the relation of other physical collision processes that may be postulated to account for the experimental data we shall write $Z_{33} \sim (B/N)^2 Z_3 = (B/N)^2 (Z_3/Z_2) Z_2$. With the values $Z_2 \sim 4 \cdot 10^9$ and $Z_3/Z_2 \sim 10^{-3}$ at normal pressure and a temperature of 20°C there results $W \sim 10^2$. Granting that this impossible result may be ascribed to the grossness of the collision number estimates, there remains the indication that practically every $H_2O+H_2O+O_2'$ collision would have to involve an O_2' internal energy change effective in absorption. This is extremely unlikely and casts doubt on the suggestion that these are the important collisions.

The Kneser-Knudsen results may be explained in another way, however,—namely one involving an increase in the effective number (rather than the efficiency) of the collisions. Specifically we may assume loosely-bound complexes of the sort AB, $(O_2 \cdot H_2O)$ or alternatively BB $(H_2O \cdot H_2O)$ in the mixture. The known strong field of O_2 and other arguments of a qualitative nature lends some support to the first of these conjectures. For the AB union there are two types of binary collisions of importance: (a) $A'B+AB$, and (b) $A'B+B$. If r is the fraction of B molecules occurring as components of the complex AB, the collision frequency for case (b) is $\sim 2r(1-r)(B/N)^2 Z_2$ and for (a) is less accurately $\sim r^2 (B/N)^2 Z_2$. The assumptions, (justifiable in such a rough preliminary survey), made here, are that $r \ll 1$, that the ratio of vibrating O_2 molecules is unaffected by association and, for (b), that if all excited O_2 molecules were associated the collision frequency for $H_2O \cdot O_2' + O_2$ would be closely that for $O_2' + O_2$. For (a) it is assumed that the collision number is the same, considering now *all* O_2 molecules associated, as for pure O_2. Comparison with the expression for Z_{33} occurring on the Kneser-Knudsen hypothesis (treated supra) indicates that for $r > 5 \cdot 10^{-4}$ for (b) and $r > 10^{-3}$ for the (a) collisions, the postulated association would increase the collision frequency and thus give a more plausible (smaller) W value. Of course, if both (a) and (b) collisions are of comparable efficiency, the collision frequency increase is still greater.

The ingenious suggestion of the H_2O polymerization is due to Professor H. M. Mott-Smith, and may be treated in similar fashion, though it is apparently not so plausible as the first type of association. The writer owes much to the staff of the Department of Physical Chemistry of this university for clarifying discussion of the H_2O polymerization possibility and the chemical aspects of the Kneser-Knudsen peroxide reaction hypothesis. A test of $O_2 \cdot H_2O$ (or even $H_2O \cdot H_2O$) association seems in order—either by sound methods, pressure isotherms, or light absorption spectra of O_2 under various concentrations of H_2O as impurity (or *vice versa*). Since the (a) type collisions depend on the squared concentration of O_2, this supposition might be checked by using a high N_2 atmosphere with O_2 and H_2O present in variable amounts in a sound mixture experiment.

Eq. (9.3) (in special cases the more exact Eq. (9.1) may be necessary) suggests a classification of mixtures[31] dependent on the relative size of the terms in Σ_A and Σ_B. The detailed investigation is entirely like that just given (cf. Eq. (9.5)) for the impurity contamination type.

The velocity[32] in the mixture is

$$V^2 = (kT/\mathfrak{m})(1 + R\mathfrak{C}_V/\mathfrak{C}_V^2 + \nu^2 D^2). \tag{11}$$

[31] There is obviously a difference in type between the $\mu \sim \log \nu$ and the $\mu \sim \log B$ curves. The first set are expected to give rise to two maxima of the same general shape.

[32] Strictly speaking, the true (velocity)^2 is $V_0^2 \cos^2 \phi$, Eq. (11), whereas what we are calculating is $V^2 \cos 2\phi$, but the difference is negligible.

A common factor of $[(1+\nu^2/\Sigma_A{}^2)(1+\nu^2/\Sigma_B{}^2)]^{-1}$ in numerator and denominator cancels and there results[33]

$$V^2=-\frac{p}{\varrho}\left\{1+\frac{k(\mathbf{C}+\nu^2\{C_{\mathrm{I}}/\Sigma_B{}^2+C_{\mathrm{II}}/\Sigma_A{}^2\}+\nu^4\mathbf{C}_\infty/(\Sigma_A\Sigma_B)^2)}{\mathbf{C}^2+\nu^2\{(C_{\mathrm{II}}/\Sigma_A)^2+(C_{\mathrm{I}}/\Sigma_B)^2+2(C_AC_B/\Sigma_A\Sigma_B)\}+\nu^4(C_\infty/\Sigma_A\Sigma_B)^2}\right\}, \tag{11.1}$$

where

$$C_{\mathrm{I}}=\mathbf{C}_\infty+(AC_A/N),\quad C_{\mathrm{II}}=\mathbf{C}_\infty+(BC_B/N). \tag{11.1}$$

The point of inflection of least abscissa[34] for the $V^2\sim\log\nu$ curve with B fixed is approximately

$$\nu_i=[\mathbf{C}/\{(C_{\mathrm{I}}/\Sigma_B)+(C_{\mathrm{II}}/C_A)\}\{1-\mathbf{C}\mathbf{C}_\infty/\Sigma_A\Sigma_B(C_{\mathrm{I}}/\Sigma_B+C_{\mathrm{II}}/\Sigma_A)^2+\cdots\}]. \tag{12}$$

For the impurity contamination case the results are written using Σ_A for compactness though, as before, the A term is supposed to be of minor importance.

$$V^2=-\frac{p}{\varrho}\left\{1+\frac{k[(\mathbf{C}_\infty+AC_A/N)+\nu^2\mathbf{C}_\infty/\Sigma_A{}^2]}{(\mathbf{C}_\infty+AC_A/N)^2+(\nu^2/\Sigma_A{}^2)\mathbf{C}_\infty{}^2}\right\},\quad \nu_0\sim(\mathbf{C}/\mathbf{C}_\infty)\Sigma_A. \tag{12.1}$$

Appendix

(A) Previous papers of the writer used the notation $\mathbf{f}_{ij}=k_{ij}{}^i$ and $f_{ij}=\Sigma_\sigma{}'N_\sigma k_{ij}{}^\sigma/(N-N_i)$, $\sigma\neq i$. This separation was more one of form rather than fact for the derivation given neglected terms in $\partial f_{ij}/\partial N_\sigma$ and is valid only when $\mathbf{f}_{ij}=f_{ij}$.[35] Since the results are all stated in terms of the symbols[36] R_{ij}, we have only to use the correct generalized form of R_{ij} as given in the text to have accurate interpretations in all cases,[37] i.e.,

$$R_{ij}=\Sigma_\sigma N_\sigma k_{ij}{}^\sigma/N=(N_i\mathbf{f}_{ij}+(N-N_i)f_{ij})/N \tag{13}$$

rather than the value

$$R_{ij}{}'=(2N_i(\mathbf{f}_{ij}-f_{ij})+Nf_{ij})/N \tag{13.1}$$

used in earlier papers.

Although this result for R_{ij} has already been established in a simple manner in the text (cf. Eq. (3.2a)), in the interest of continuity with the notation in previous papers, we shall now show that the addition of $\partial f_{ij}/\partial N$ terms does indeed bring the earlier expression (Eq. (13.1)) into conformity with Eq. (13).

Reference to I and IV shows that f_{ij} occurs in $D(N_i)$ with the coefficient $N_i(N-N_i)$. The new terms in the coefficient of δN_i, because of inclusion of $\partial f/\partial N_\sigma$ terms, are

$$(\partial f_{ij}/\partial N_i)(N-N_i)N_i-(\partial f_{ji}/\partial N_i)(N-N_j)N_j. \tag{13.2}$$

Evidently

$$\frac{\partial f_{ij}}{\partial N_i}=\frac{1}{N-N_i}f_{ij},$$
$$\frac{\partial f_{ji}}{\partial N_j}=\frac{1}{N-N_j}f_{ji}{}^i=\frac{N_i}{N_j}\frac{1}{(N-N_j)}f_{ij}{}^i=\frac{N_i}{N_j}\frac{1}{(N-N_j)}\mathbf{f}_{ij}. \tag{13.3}$$

---

[33] The general equation of velocity in mixtures was given in the author's early papers, reference 2, I, II, V—the one given here is simpler because of algebraic reductions and also a superior nomenclature, besides including triple collision effects in the Γ's.

[34] Cf. appendix for remarks about the inflection point calculations.

[35] A similar assumption is made in Richards' paper, J. Chem. Phys. **1**, 863 (1933). Kneser's and Ruttgers' work uses a single type of collision as being significant so that the differentiation does not arise there. M. Rose, J. Chem. Phys. **2**, 260 (1934), mentions this point.

[36] It is assumed that the notation and ideas are fairly familiar to the reader either from say 1, IV of reference 2, or from reading the first section of this paper.

[37] Unfortunately, careless proofreading overlooked the omission of two whole phrases in the derivation of ΔN_i in IV and may possibly account for some difficulty in reading Richards has alluded to. However, I, reference 2, contains virtually the same derivation. In Eqs. (1.07), (1.08) all terms are of course inside the differentiating operators. Another error of obvious type is the omission of summation signs at the top of page 724. The correct statement is, of course, that $\Sigma_i(\Delta K_i)=N\Sigma_iN'{}_iA_i\epsilon_i\delta K$. A number of correspondents have inquired about the proof that $\Sigma_i(A_i-\Sigma_is_j)\Delta K_i=S\Sigma_iN'{}_i\epsilon_i\delta K$. The direct verification is tedious. The truth of the relationship is patent on realizing that for vanishing frequencies there is perfect adjustment. With $L_{\nu\to0}(\omega_i-1/j\nu)=(A_i-\Sigma_is_j)/S$ there follows

$$L_{\nu\to0}\Sigma_i(\Delta K_i)\frac{\omega_i-1}{j\nu}=\Sigma_i(A_i-\Sigma_js_j)\Delta K_i$$
$$=-\Delta K=C_i\delta K=\Sigma_iN'{}_i\epsilon_i\delta K.\qquad\text{Q.E.D.}$$

As errata in V may be mentioned the omission of squares from the $N_1\Gamma_{11}+N_2\Gamma_{12}$ and $N_1\Gamma_{21}+N_2\Gamma_{22}$ terms in the definition of $\mathfrak{S}_\nu$. Also the definition of D omits the factors $(1+\nu^2/\Sigma^2{}_A)^{-1}$; $(1+\nu^2/\Sigma^2{}_B)^{-1}$ in the coefficients of AC_A/Σ_A and BC_B/Σ_B. These two inadvertencies do not affect Eq. (7.2) of that paper.

Therefore

$$NR_{ij}'-N_i\mathbf{f}_{ij}+N_if_{ij}=N_i\mathbf{f}_{ij}+(N-N_i)f_{ij}=NR_{ij}. \tag{13.4}$$

(B) The text treatment has established that except possibly for C_∞ in place of $3k/2$ the K.R. and the writer's methods lead to similar results. The text work has, however, restricted itself to a single ω characterizing each gas, but the equivalence of the methods is obviously not dependent on this simplification. As an exercise in point we may derive the result for a single gas

$$\Delta A_i=-(\omega_i-1)A\Sigma_j\{(A^\cdot{}_iR_{ij})-(A^\cdot{}_jR_{ji})(\omega_j-1)\} \tag{14}$$

used in I and IV, by the K.R. method. The calculation will, incidentally, enable the reader to see at once how multiple collision transitions fit in. If, then,

$$\mu_2=A_2/A_1\cdots;\qquad \mu_i=A_i/A_1;\qquad A_i=\mu_iA/1+\mu_2+\mu_3+\cdots\mu_n \tag{14.1}$$

we may write

$$\begin{aligned}D(a_1)/U&=-[(A_1\mu_2-A_2)\Sigma_\sigma A_\alpha f_{21}{}^\sigma+(A_1\mu_3-A_3)\Sigma A_\alpha f_{31}{}^\sigma+\cdots(A_1\mu_i-A_i)\Sigma f_{i1}{}^\sigma A_\sigma+\cdots\\&=0\text{ at equilibrium,}\end{aligned} \tag{14.2}$$

$$\begin{aligned}D(a_i)/U&=\cdots\\\Delta a_1/U&=-A\{(\delta(A_1\mu_2)-\delta A_2)R_{21}+(\delta(A_1\mu_3)-\delta A_3)R_{31}+\cdots(\delta(A_1\mu_i)-\delta A_i)R_{i1}+\cdots\end{aligned} \tag{14.3}$$

It is easy to see that

$$\delta\mu_i=(A^\cdot{}_i/A_1-(A^\cdot{}_1/A_1)\mu_i)\delta K. \tag{14.5}$$

On substituting these values in Eq. (14.2) and adopting the notation $\delta A_i/\delta K=\omega_i=\delta a_i/U\delta K$ one arrives at Eq. (14) for $i=1$. In exactly the same way, the general case ($i=2, 3, \cdots n$) may be determined so that in all cases Eq. (14) is reproduced. On specializing the range i, j as 1, 2, 3, there results the case treated in IV, etc., thus verifying that the results of that paper may be arrived at by the K.R. method.

(C) The collisions treated so far have been restricted to change in only one of the colliding molecules.[38] More general collisions may be introduced into the theory at the expense of complicating the resulting formulae. Consider for instance the collision taking A_iA_j into A_kA_h respectively. The transition probabilities are written $f^{ij}{}_{ik,\ jh}$ and $f^{kh}{}_{ki,\ hj}$. The contribution of these collisions[39] to ΔA_i is

$$-A_kf^{kh}{}_{ki,\ hj}\left[\delta\left(\frac{A_iA_j}{A_k}\frac{\mu_k\mu_h}{\mu_i\mu_j}\right)-\delta A_h\right]. \tag{15}$$

This may be shown easily enough to reduce to

$$-A_kA_hf^{kh}{}_{ki,\ hj}\left\{\frac{A^\cdot{}_i}{A_i}(\omega_i-1)+\frac{A^\cdot{}_j}{A_j}(\omega_j-1)-\frac{A^\cdot{}_k}{A_k}(\omega_k-1)-\frac{A^\cdot{}_h}{A_h}(\omega_h-1)\right\}. \tag{15.1}$$

Accordingly the term $A_kf^{kh}{}_{ki,\ hj}$ adds to the other terms of R_{ki}; $A_hf^{kh}{}_{ki,\ hj}$ adds to those of R_{hj} and the other two terms are easily seen to be parts of R_{ik} and R_{jk} for they are, respectively, A_k/A_i and A_h/A_j times the first named. Cf. Eq. (3.2a).

By analogy with the case of the mixture whose treatment immediately follows, one would expect as a modification in the three state pure gas model that, instead of getting a second degree denominator in $j\nu$ for ω_i ($i=1, 2, 3$), we should get a cubic. The writer has not tested this however.

We consider now the case of simultaneous transitions in the partners of a double collision. The *new* terms in $D(A_i)$ are

$$-(A_iB_jf^{ij}{}_{ik,\ jh}-A_kB_kf^{kh}{}_{ki,\ hj}). \tag{15.2}$$

On passing to ΔA_i these become

$$-(\delta A_iB_jf^{ij}{}_{ik,\ jh}+\delta B_jA^\cdot{}_if^{ij}{}_{ik,\ jh}-(\delta A_kB_h+A_k\delta B_h)f^{kh}{}_{ki,\ hj}; \tag{15.3}$$

then with the argument leading to Eq. (4a) we have here for the *new* terms

$$\begin{aligned}\Delta A_i&=-(\omega_A-1)\Sigma_{h,\ j,\ h}(A^\cdot{}_iB_jf^{ij}{}_{ik,\ jh}-A^\cdot{}_kB_kf^{kh}{}_{ki,\ hj})-(\omega_B-1)\Sigma_{k,\ j,\ h}(A_iB^\cdot{}_jf^{ij}{}_{ik,\ jh}-A_kB^\cdot{}_kf^{kh}{}_{ki,\ hj}),\\\Delta B_j&=\cdots.\end{aligned} \tag{15.4}$$

Evidently the solution for ω_A, ω_B is the ratio of a linear to a quadratic polynomial in $j\nu$. Thus the expressions for the absorption and velocity will *not* be of the simple type given in the text. The complex velocity of sound may be written down at once as may also the expression for $\mathfrak{C}_v$, $\mathfrak{C}_n$, D after which the deduction of the expression for μ and $|V|$ is a matter of straightforward reduction. The algebra involved in manipulating the resulting expressions appears to be so

[38] The redistribution of internal energies in an excited molecule has not yet been explicitly recognized in the equations.
[39] To balance the use of the K.R. method here, the double transitions in mixtures, treated next, is discussed by the writer's method.

heavy that a complete discussion will not be attempted in this paper. Perhaps the most important double transition to be expected is that written as $(A_1B_2)\rightarrow(A_2B_1)$. The formulae will be expressed for this case

$$\omega_A=\frac{j\nu S_1+l}{(j\nu)^2+j\nu m+l},\qquad \omega_B=\frac{j\nu S_2+l}{j\nu m+(l-\nu^2)},$$

$$V^2=\frac{p}{\rho}\left[\frac{\mathfrak{C}_v+k-j\nu D}{\mathfrak{C}_v-j\nu D}\right]=\left(\frac{p}{\rho}\left[1+\frac{j\nu k}{j\nu\mathbf{C}_\infty+(1/N)\{\omega_A AC_A+\omega_B BC_B\}}\right]\right), \tag{15.5}$$

$$\mathfrak{C}_v=\mathbf{C}_\infty+\frac{1}{N}\left\{AC_A\Big/\left(1+\nu^2\left\{\frac{\nu^2+m(m-S_1)-l}{\nu^2(mS_1-l)+l^2}\right\}\right)+BC_B\Big/\left(1+\nu^2\left\{\frac{\nu^2+m(m-S_2)-l}{\nu^2(mS_2-l)+l^2}\right\}\right)\right\},$$

$$D=\frac{1}{N}\left[\frac{AC_A(ml-S_1l+\nu^2S_1)}{l^2+\nu^2(m^2-2l)+\nu^4}+\frac{BC_B(ml-S_1l+\nu^2S_2)}{(l-\nu^2)^2+\nu^4}\right],$$

$$S_1=\Sigma_A+(A'_1B_1(1+\mu_A)f^{21}{}_{21,\ 12}-A_1B'_1(1+\mu_B)f^{12}{}_{12,\ 21})/A'_1,$$

$$S_2=\Sigma_B-(A'_1B_1(1+\mu_A)f^{21}{}_{21,\ 12}-A_1B'_1(1+\mu_B)f^{12}{}_{12,\ 21})/B'_1,$$

$$l=(\Sigma_A\Sigma_B)+(\Sigma_A)A_1(1+\mu_B)f^{12}{}_{12,\ 21}+(\Sigma_B)B_1(1+\mu_A)f^{21}{}_{21,\ 12},$$

$$m=\Sigma_A+\Sigma_B+A_1(1+\mu_B)f^{12}{}_{12,\ 21}+B_1(1+\mu_A)f^{21}{}_{21,\ 12}.$$

(D) To complete the comparison of the K.R. and the writer's methods, it will now be shown how, by slight modification, the fundamental equations may be made to yield C_∞ in place of $3k/2$. It may be verified in fact that it is sufficient to replace the coefficients 2/3 and 5/3 in Eqs. (4.2a) and (4.3a) by k/C_∞ and $1+k/C_\infty$ respectively. These changes are given their interpretation by the assumption of an external energy no longer identical with the translational energy. We have now

$$\begin{aligned}K&=C_\infty T\\&=[C_\infty/3k/2](\tfrac{1}{2}m(\overline{u^2+v^2}+w^2)),\end{aligned} \tag{16}$$

where u, v, w are the component velocities of the molecules.[40]

(E) By way of further elucidation of the interpretations given in IV, one remarks that, physically speaking, increasing the sound frequency has as net result complete ankylosis of all states eventually. However, if some states have a long mean life, the frequency at which ankylosis for them is practically total may very well leave the other states only slightly affected. (The relation $dK/dT=3k/2$ preserves the true physical model.) For computational purposes over this first range, one may consider the rest of the states absolutely, instead of merely relatively, unaffected. This amounts to having, instead of a single term of this independent nature (namely $3k/2$), the sum $3k/2+d/dT\Sigma_i A_i\epsilon_i=C_\infty$ where the summation includes only the short life states, thus giving a mathematically convenient, though physically fictional, representation.

(F) In view of the remarks just concluded in this appendix, as well as the comparative study made in the text, we may say that the K.R. and the writer's methods differ almost solely in the fact that the last uses the language of kinetic theory while the first uses that of thermodynamics and chemical reactions. We have shown that not only is there equivalence in the end result, namely the expression for the velocity of sound, but also in the separate steps and basic assumptions. It would seem to the writer that the kinetic theory formulation is more "natural" since the mechanism and processes involved are kinetic in nature. Furthermore the use of concentrations (i.e. A_i) rather than total populations (a_i) has on the one hand the advantage of clarity and on the other almost automatically excludes errors arising from manipulations[6] with U. From the practical viewpoint perhaps the most important difference is connected with the writer's *explicit* introduction of the ω_i. These not only give logical sequence to the steps of the argument, but are essential to the definition of the classes of states which act as *units* (i.e., ω_i is the same for these states)—that is to say, precision is given to statements such as "states . . . come in or drop out together."[41]

(G) Of course, finite amplitude, viscosity, conductivity,[42] etc., may affect the absorption and sound velocity to some degree. As a formal scheme the last two agencies may be incorporated approximately (as in II) by adding the term $s\partial^2v/\partial x^2$ to Eq. (4.2a) and $\vartheta\partial^2K/\partial x^2$ to Eq. (4.3a). ω_A and ω_B are unaffected. (Cf. Eq. (5a).) The method of the text yields directly

$$\begin{aligned}V^4\mathbf{m}(\omega_AAC_A+\omega_BBC_B+NC_\infty)+V^2\{&-j\nu(s(\omega_AAC_A+\omega_BBC_B+NC_\infty))+\mathbf{m}NC_\infty\vartheta\\&-\tfrac{2}{3}K[\omega_AAC_A+\omega_BBC_B+NC_\infty+k]\}+\tfrac{2}{3}j\nu KN\vartheta-s\vartheta NC_\infty\nu^2=0,\end{aligned} \tag{17}$$

from which the information of interest may be obtained, but the paper is already too long for consideration of the μ and $|V|$ expressions here.

(H) The remainder of this appendix is devoted to some comments on IV. If the physical ideas of IV be adhered to, the three states referred to there are the ground state $\epsilon_3=0$, the excited state ϵ_1 of appreciable occurrence and of long mean

---

[40] The coefficient kT/m (of V^2) becomes $C_\infty T/m$ which is again p/ρ.

[41] Richards, reference 5.

[42] Cf. II, reference 2, and also Rocard, J. d. Physik **1** (1930).

life, and ϵ_2, the short life state (or, if the proper specific heat contribution of the internal energy states is to be maintained, a single equivalent state for all those of short life). It will be supposed then that ϵ_2 is closely $C_v-\epsilon_1$. With the $3k/2$ theory, the three state calculation is necessary. If the shorter lived of the two states is lumped with the translational energy, only a two state calculation is needed for fair approximation.[43]

We shall show now that whether or not this change be made in the final equations, i.e., C_∞ for $3k/2$, the term $\Sigma N_i A_i \epsilon_i / \Sigma s_j$, which[44] is the component of interest in the main results of IV, always reduces, except for small correction terms, to $C_i - C_1$, i.e., the long lived $i=1$ state "drops out" of the internal specific heat. Under hypothesis A of that paper R_{21} and R_{31} are very small. Therefore

$$\Sigma_i{}' \frac{N_i A_i \epsilon_i}{\Sigma s_j} = \frac{\Sigma_i N_i \Sigma_K (R_{iK} - (N_K/N_i) R_{Ki}) \epsilon_i}{\frac{1}{2}\Sigma_j \Sigma_K R_{jK}} \sim \frac{s_1 N_1 \epsilon_1}{s_2+s_3} + \frac{N_3 A_2 \epsilon_2}{s_2+s_3}\,; \tag{18}$$

also

$$\frac{A_2}{s_2+s_3} \sim \left(s_2 - \frac{N_3}{N_1} R_{23} \right) \Big/ R_{23}+R_{32} = \frac{R_{23}\epsilon_2}{(\epsilon_2-\mathfrak{e})R_{23}+R_{22}}, \tag{18.1}$$

where $\mathfrak{e}$ is the mean value of ϵ, i.e., $(\epsilon_1\mu_1+\epsilon_2\mu_2)/(1+\mu_1+\mu_2)$; $\mu_i = N_i/N_3$. Hence the further reduction

$$= \frac{\epsilon_2(1+\mu_1+\mu_2)}{(\epsilon_1\mu_1+\epsilon_2(1+\mu_1))(1+\mu_2)} \sim 1.$$

Thus to terms in μ_1 and $s_1/(s_2+s_3)$

$$\frac{\Sigma N_i A_i \epsilon_i}{\Sigma s_j} \sim N_3 \epsilon_2 = (d/dK)(N_1\epsilon_1+N_2\epsilon_2) - N_1\epsilon_1 = \frac{C_i - N_1\epsilon_1}{3k/2} = \frac{C_i - C_1}{3k/2}.$$

It is manifest then that Eq. (2.092) of IV is a refinement of the grosser theory expressed by Eq. (2.021) and does, indeed, reduce to it when small correction terms are neglected.

If now the $3k/2$ be changed to C_∞ the results of IV may be considered as a second order approximation with *three types*[45] of *excited states*. We have then[46]

$$C_\infty = 3k/2 + (d/dT)N_3\epsilon_3, \qquad C_i = (d/dT)(N_1\epsilon_1 + N_2\epsilon_2).$$

It is easy to see that the reduction of $\Sigma N_i A_i \epsilon_i / \Sigma s_j$ is precisely the same as before (cf. Eq. (11.2)) to $C_i - C_1$.

The value of ν_0 in Eq. (2.10) of IV, as is obvious from the context, lacks a term. The value should be[47]

$$\nu_0 \sim \frac{N s_1 (3k/2 + C_i)}{\{3k/2 + (\Sigma N_i A_i \epsilon_i / \Sigma s_j)\}\left(1 - \dfrac{s_1}{s_2+s_3}\left(\dfrac{3k/2+C_i}{3k/2+(\Sigma N_i A_i \epsilon_i/\Sigma s_j)}\right)\right)}.$$

From the results stated in Eq. (18.2) above this we get

$$\nu_0 \sim \frac{N s_1 C_v}{(C_v - C_1)\left(1 - \dfrac{s_1}{s_2+s_3}\dfrac{C_v}{C_v - C_1}\right)}.$$

---

[43] Of course the results of the $3k/2$, three state theory are not the same as those of the two state C_∞ theory, for in the latter case the lumped internal energy states are assumed absolutely free of frequency dependence whereas in the former the weak frequency modifications are included, but the concordance is much better than that between say a two and a three state $3k/2$ (or C_∞) formula. Cf. IV, reference 2, for discussion of mean life interpretations.

[44] $A_i = \Sigma_j (R_{ij} - (N_j/N_i)R_{ji})$; $s_i = \Sigma_K R_{iK}$.

[45] There is no necessity to assume that ϵ_3 has the lowest energy.

[46] This covers the case of one very short lived state and two others, both long lived but of different orders.

[47] The value of ν_0 given above has been obtained after extensive approximation. If Eq. (2.091) of IV, reference 2, be written

$$V^2 = \frac{p}{\rho}\left\{1 + \frac{a_2+a_1\nu^2+\nu^4}{b_2+b_1\nu^2+\nu^4}\right\}$$

the inflection point for the $V^2 \sim \log \nu$ curve is determined as the root of a fourth degree equation in ν^2. Neglecting all but the last two terms there is obtained

$$\nu_0^2 \sim \frac{\beta_2}{\beta_1(1 - [4(\beta_2-\alpha_2)/\beta_1(\alpha_1-\beta_1(\alpha_2/\beta_2))])}.$$

This is further approximated as $(\beta_2/\beta_1)^{\frac{1}{2}}$. Throughout the parameter of smallness is s_1/s_2+s_3. In cases where this ratio is not excessively small, enough detail has been indicated to enable the reader to supply the next higher terms. The neglect of higher degree terms in the eighth degree equation for ν_0 is supported by the observation that for $\nu_0 = (\beta_2/\beta_1)^{\frac{1}{2}}$ the ratio of the neglected terms to those retained involves powers of s_1/s_2+s_3.

The Kelvin Temperature of the Ice Point

J. R. ROEBUCK, *Physics Laboratory, University of Wisconsin*

(Received June 11, 1936)

The data on the Joule-Thomson effect of the author and his colleagues are used to calculate the value of the ice point on the Kelvin thermodynamic scale from the data on the coefficients of volume and pressure expansion found in the literature. The gases involved are air, helium, argon and nitrogen. The results are, air 273.158, helium 273.168, nitrogen 273.125 and the most probable value 273.16±0.02. These are compared with accepted values. The use of a helium mixture to give the ice point precisely as the reciprocal of the coefficient of volume expansion is suggested.

THE scale as well as the readings of the ice point ($T_{ice} \equiv T_i$) on the constant volume gas thermometer differ from those on the constant pressure thermometer and both are in general different for each real gas which is employed. A knowledge of the thermodynamic properties of the real gas makes possible the conversion of the various gas scale readings into the corresponding readings on the Kelvin thermodynamic scale. The Kelvin temperature of the ice point may thus be deduced precisely from a combination of the thermometer readings at the ice and steam points with data on the specific heat, and data on either pv, the Joule-Thomson effect, or the Gay Lussac-Joule effect. This article is concerned primarily with the calculation and discussion of the Kelvin temperature of the ice point derived from the constant pressure thermometer readings and our Joule-Thomson data. For the corresponding calculations from the constant volume thermometer readings, it is necessary to introduce pv data in the computation of λ, the variation of intrinsic energy with volume at constant temperature. The availability of Joule-Thomson data for air, helium, nitrogen and argon permits a more accurate and comprehensive treatment than has yet been possible.

AIR

An earlier article[1] gave data on the Joule-Thomson coefficient, μ, for air, which was employed in the equation

$$T_i = -\frac{1}{\alpha} + \frac{T_i(T_i+100)}{100\alpha}\rho_0 \int_{273}^{373} -\mu C_p d\frac{1}{T} = -\frac{1}{\alpha} + D \quad (1)$$

to give $T_i = 273.15°$K. In this D has a value of about 1° for air. Hence, for a precision of 0.01° in T_i, D and therefore μ, must be known to about 1 percent. The μ data are probably somewhat better than this.

Inconsistencies in the reports on the values of α and β as measured by Chappuis made it advisable to consult his original article[2] which is not available in our library. He reports the following data from his two series of measurements on air.

	p_0	100α	100β
(a)	1001.948	0.367267	0.367449
(b)	999.626	0.367298	0.367424

He averages these two series for his final values. In order to observe the resulting variation, T_i has been calculated independently from each value of α by means of Eq. (1), with the following results:

p_0(mm)	100α	α^{-1}	D	T_i
1001.948	0.367267	272.281	0.916	273.197
999.626	0.367298	272.258	0.916	273.174
				Average 273.186

In the second article[3] on air, the data for μ, were combined with the available data on C_p and on pv, to calculate $\lambda \equiv (du/dv)_T$ over a considerable range of pressure and temperature. These data for λ were used to calculate T_i from the available values of β. It is necessary to interpolate the λ data to obtain their value at appropriate pressures. This was done by an approximation using a linear formula. Unfortunately the approximation is not nearly close enough as has been pointed out.[4]

The calculation has consequently been repeated. The data of Table 26 of the second air

[1] Roebuck, Proc. Am. Acad. **60**, 537 (1925).

[2] Chappuis, Trav. et Mem. du Bureau int. des poids et mesures **13**, 1907.

[3] Roebuck, Proc. Am. Acad. **64**, 287 (1930).

[4] Keyes, Proc. Am. Acad. **66**, 349 (1931).

TABLE I. *Values of* $\lambda/p^2\times10^3$ *at various pressures (atmospheres) and temperatures (°C).*

p/t	−100	−75	−50	−25	0°	25	50	75	100	150	200
1	6.182	5.681	4.194	3.351	2.779	2.381	1.919	1.597	1.340	1.066	0.795
20	7.680	6.185	4.596	3.511	2.800	2.445	1.810	1.626	1.362	0.970	0.765
60		7.252	5.113	3.546	2.774	2.204	1.915	1.605	1.356	0.979	0.737
100		8.453	4.502	3.700	2.605	2.109	1.771	1.580	1.342	0.946	0.718
140		5.858	3.472	2.181							

article[3] have been used to calculate λ/p^2 of Table I.

The value of λ/p^2 at any one temperature is not quite independent of pressure but seems to first increase slightly and then decrease with rising pressure. The change of λ/p^2 between 1 and 20 atmos. over the range 0–100°C, averages 0.12 percent per atm. The range of pressure involved in the calculations of λ is less than one atmosphere. This makes the error in λ introduced by the variation of λ/p^2, small enough to be entirely neglected. The value of λ/p^2 at 100°C and 1 atm. (1.078) was obviously out of line with the values around it, and by plotting and comparison, was shifted to 1.340.

As in the previous article[3] these values of λ were used in the equation

$$T_i=\frac{1}{\beta}+\frac{(T_i+100)T_i}{100p_0\beta}\int_{273}^{373}-\lambda d\frac{1}{T}=\frac{1}{\beta}+E \quad (2)$$

to calculate the value of T_i. The data show that E is about 1° while $1/\beta$ is about 272.2. Three different smoothing procedures for the λ data gave for the integral the values of 4.617, 4.544, and 4.593×10^{-6} where the extremes are about 1 percent from the mean. A 1 percent variation in this integral results in 0.01° variation in T_i. Eq. (2) applied to Chappuis data[2] gives

p_0(mm)	100β	β^{-1}	E	T_i
1001.948	0.367449	272.150	0.965	273.115
999.626	0.367424	272.165	0.968	273.133
			Average	273.124

The uncertainty in E is probably larger than in D in the corresponding calculations for α.

The arithmetical average of the four Chappuis values of T_i is 273.159.

Eumorfopoulos' data[5] were used in the first paper on air[2] to compute T_i. In this paper he gives no positive statement as to his final value for α. Henning[6] uses the average of the four values given by Eumorfopoulos. It seems preferable to take the unweighted average of the separate determinations themselves. This gives $\alpha=3.6706\times10^{-3}$, $\alpha^{-1}=272.435$ and $T_i=273.131$.

This value could be given more weight if the doubt expressed by Callendar as to the coefficient of expansion of mercury could be removed by correction. But Eumorfopoulos gives no original readings and no statement of the coefficient used in the calculations. This value of T_i falls well inside the range of the other more satisfactory data but must be given small importance in fixing the final value of T_i.

HELIUM, α DATA

As with air, T_i was calculated by the use of Eq. (1), from the helium[7] data for μ. D is here of the order of 0.2°. Moreover the precision of the μ data for helium is decidedly superior to the same for air. C_p for helium[7] is independent of both pressure and temperature in this range. The errors in D are therefore well below the desired 0.01°.

Between −50 and 150°C, μ for helium is almost a linear function of T, so that

$$\mu=\mu_0+a(T-T_0), \quad (3)$$

in which $\mu_0=-5.96\times10^{-2}$ °C/atm., $a=-1.9\times10^{-5}$/atm. Eq. (3) was used to integrate Eq. (1), setting $C_p=\text{const.}=7.42\times10^{-5}$ cal/g ×°C at 1 atm. with μ and C_p independent of p. As a check, μ was assumed constant at its average value and D was thereby increased by about 1 percent.

Hence $$D=-3.127/v_0\alpha.$$

By using $\alpha=3.660\times10^{-3}$, $v_0=5607$ cc/g at 1 atm. and 0°C, and using the gas law we have the results

$$D=-0.152p_0=-0.2005p_0',$$

where p_0 is the initial pressure in atmospheres and p_0' the same in meters of mercury.

Henning and Heuse[8] have measured α for He with great care. Table II Nos. 1–5 lists their results. The values of D calculated as above are

[5] Eumorfopoulos, Proc. Roy. Soc. **A81**, 339 (1908).

[6] Henning, *Temperaturmessungen*, (1915).
[7] Roebuck and Osterberg, Phys. Rev. **43**, 60 (1933).
[8] Henning and Heuse, Zeits. f. Physik **5**, 308 (1921).

TABLE II. *Helium* α [*see Eq.* (*1*)].

No.	p_0	$\alpha\times10^5$	Weight	α^{-1}	$-D$	T_i	Average	Author
1	0.50	36589	3	273.306	0.100	273.206		
2	0.52	36603	3	273.201	0.104	273.197		
3	0.76	36591	4	273.291	0.152	273.139		Henning
4	1.10	36582	6	273.358	0.221	273.137	(273.164)	and
5	1.12	36581	6	273.265	0.225	273.140	273.156	Heuse[8]
6	0.991	36585	3	273.336	0.199	273.137		Heuse[9]
7	0.390	36597	4	273.246	0.078	273.168		
8	0.533	36591	5	273.269	0.107	273.162		Heuse
9	0.727	36587	7	273.321	0.146	273.175	(273.172)	and
10	0.994	36579	9	273.381	0.199	273.182	273.174	Otto[10]

Note: p_0 is given in meters of mercury as in their articles.
Weighted Average 273.164.

used to compute T_i. In the "average" column is the average weighted according to their numbers, and for comparison with it is the unweighted average (in parentheses).

Heuse[9] somewhat later carried out careful measurements in which the effect, if any, of absorption on the walls was experimentally eliminated. His single result is given in Table II, No. 6. Apparently absorption of the helium on the walls is not a material factor.

The last group of values Table II, Nos. 7–10, by Heuse and Otto[10] were obtained by an experimental procedure materially different from that used by Henning and Heuse.[8] In Table II the range of variation in the data Nos. 1–5 is $2\frac{1}{2}$ times that in Nos. 7–10, and the average T_i is a little larger in this latter group. This greater spread however is due to Nos. 1 and 2 at low pressures. Nos. 3–5 are more consistent than Nos. 7–10. It would seem that this group Nos. 1–5 hardly deserves the implied criticism of the later paper.[10] No weighting numbers are given for Nos. 7–10 but they are supplied in Table II, as the measurements at the higher pressures have a distinct advantage. It introduces however little difference in the average.

The maximum D is 0.23°K so that for a precision of 0.01° in T_i, 5 percent error in μ may be tolerated. The experimental error in μ is estimated as below 1 percent. The weighted average of T_i in Table II is 273.164.

HELIUM DATA, β

Eq. (2) given above was used to calculate T_i. The helium[11] data for λ is much more consistent than that for air, due to more consistent μ and pv data. The data in the article on helium[11] proved λ to be closely proportional to p^2, and this relation was used to calculate the values of λ at the pressures involved in the integration. The λ values at 1 atm. when plotted as a function of T give a straight line in the range 0° to 100°C so that

$$\lambda-\lambda_0=K(T-T_0), \tag{4}$$

where $K=-2.359\times10^{-7}$. These relations of λ to T and p are used to integrate Eq. (2), from which

$$E=-2.207\times10^{-2}p_0$$

where p_0 is in meters of mercury and the effect on E of the small variation of β may be neglected.

The data are presented in Table III, with the resultant E and T_i. The maximum value of E is 0.025°K, so that for a precision of 0.01°K, error up to 40 percent in E may be tolerated. The error in λ estimated earlier[11] is 15 percent.

Henning and Heuse[8] measured β and their readings are given as Nos. 1–5 in Table III. The spread in the corresponding values of T_i, namely 0.057, is slightly less than in the T_i from their α values, namely 0.069. The average value of T_i is however larger than in any other group of measurements discussed here. It suggests some slight systematic error. The size of the values is however not a sufficient reason for discarding the data.

Heuse[9] measured β as well as α, in his work eliminating experimentally the effect of absorption on the walls. The α data of Table II No. 6 give $T_i=273.137$ which is near the low end of the observed values. The β data of Table III No. 6 give $T_i=273.202$ near the largest of the observed values. The average, 273.170 falls near the general average.

Heuse and Otto[10] measured β and their data are given in Nos. 7–10 of Table III. The spread of 0.071 in T_i is the same as in their work on α, namely 0.069, and slightly larger than 0.057 in the corresponding series on β by Henning and Heuse.

It is worthy of note that the spreads in the α and β groups of data are nearly alike, so that the usual opinion that β is more accurately measurable than α is not supported.

Keesom, van der Horst and Taconis[12] have

[9] Heuse, Zeits. f. Physik **37**, 159 (1926).
[10] Heuse and Otto, Ann. d. Physik (5) **394**, 1027 (1929).
[11] Roebuck and Osterberg, Phys. Rev. **45**, 332 (1934).
[12] Keesom, Van der Horst and Taconis, Physica **1**, 331 (1934).

TABLE III. *Helium data* [*see Eq. (2)*].

No.	p_0	$\beta\times10^7$	Weight	β^{-1}	$-E$	T_i	Average	Author
1	0.50	36595	4	273.261	0.011	273.250		Henning and Heuse[6]
2	0.52	36599	4	273.231	0.011	273.220		
3	0.76	36598	6	273.239	0.017	273.222		
4	1.10	36601	9	273.217	0.024	273.193	(273.217)	Heuse[9]
5	1.12	36600	9	273.224	0.025	273.199	273.211	Heuse and Otto[10]
6	0.991	36600	4	273.224	0.022	273.202		
7	0.390	36611	4	273.142	0.009	273.133		
8	0.533	36602	5	273.209	0.012	273.197		Keesom, van der Horst, & Taconis[12]
9	0.727	36611	7	273.142	0.016	273.126	(273.157)	
10	0.994	36604	9	273.194	0.022	273.172	273.158	
11	0.508	36608.6	9	273.1598	0.0112	273.1486		
12	0.750	36607.9	9	273.1650	0.0166	273.1484		Keesom & van Santen[13]
13	0.967	36607.3	9	273.1695	0.0213	273.1482	273.148	
14	1.000	36609	4	273.157	0.0221	273.135		

Weighted average 273.174. p_0 is in meters of mercury.

measured the pressure coefficient of helium, β (called α by them), with amazing consistency. Their data are Nos. 11–13 in Table III. They use pv data to compute T_i from their gas thermometer readings. Their T_i values (average 273.144) are slightly smaller and not as consistent as the values calculated here by μ data. If consistency were the sole criterion, this extraordinary group of measurements would lessen the uncertainty by a factor of 150, below the next most consistent group.

Keesom and van Santen[13] also measure β No. 14 of Table III for Helium with great care, and although they say it is to be considered as a preliminary measurement, it deserves to be considered here. Their correction again exceeds ours as they make $T_i=273.127$.

The weighted average for Table III is 273.174, which is slightly larger than 273.164, the weighted average from Table II. The average omitting Nos. 1–5 Table III is 273.156 so that this difference is due entirely to Henning and Heuse's work.

Giving equal weights we find the α and β data lead to 273.169° as the general average for helium.

ARGON DATA, α

It is to be regretted that argon has not been employed in thermometer work, at least for α, as good μ data are now available.[14] As soon as C_p is measured carefully, λ data will be available for computing the correction for β. Argon has properties of inertness, cheapness, simple purification, moderately low T_c, freedom from diffusion difficulties. These indicate argon as a valuable addition to the list of thermometric gases.

The value of α may be obtained from the measurements of Holborn and Schultze[15] on the isotherms of argon. $\alpha=3.676\times10^{-3}$ from these data, which by the use of the μ data as above give $T_i=273.10$. This is as close to the more carefully measured values as should be expected.

NITROGEN DATA, α

We have recently completed the Joule-Thomson measurements on nitrogen.[16] When we use Eq. (1), in which $v_0=800.01$ cc/g as obtained from I. C. T., C_p and μ as obtained from the above article on nitrogen, the integral comes out 4.608×10^{-5}. This is slightly smaller than 4.706 for air and larger than that 4.013 for argon. So that

$$T_i=1/\alpha+0.6605p_0,$$

where p_0 is in atm. The variation of α for nitrogen is just small enough to be neglected in D.

The nitrogen data on α are collected in Table IV. The values of T_i are more erratic than the same observers with the same apparatus obtained with helium. The average value of T_i (273.124) is distinctly smaller. If any of the nitrogen is absorbed on the walls of the container, one might expect less to be absorbed at the higher temperature, thus making the observed coefficient too large and therefore T_i too small. The observed difference from helium ($0.045=273.169-273.124$) is well within the spread of the nitrogen values (0.113) but still somewhat larger than these latter would lead one to expect. This may indicate some absorption.

TABLE IV. *Nitrogen α data* [*See Eq. (1)*].

No.	$p$atm.	$\alpha\times10^7$	α^{-1}	D	T_i	Authors	
1	0.2895	36630	273.000	0.191	273.191	Henning and Heuse[6]	273.134
2	0.6711	36679	272.635	0.443	273.078		
3	1.461	36742	272.168	0.965	273.133		
4	0.5135	36664	272.747	0.339	273.086	Heuse and Otto[10]	273.119
5	0.7015	36668	272.717	0.463	273.180		
6	0.9568	36699	272.486	0.632	273.118		
7	1.3086	36734	272.227	0.864	273.091		
8	1.3184	367315	272.246	0.871	273.117	Chappuis[17]	
			Average		273.124		

[13] Keesom and Van Santen, Proc. Amst. Acad. **34**, 3 (1933).
[14] Roebuck and Osterberg, Phys. Rev. **46**, 785 (1934).
[15] Holborn and Schultze, Ann. d. Physik **352**, 1109 (1915).
[16] Roebuck and Osterberg, Phys. Rev. **48**, 450 (1935).
[17] Buckingham, Bull. Bur. of Stand. **3**, 237 (1907).

TABLE V. *Summary.*

Gas	Coeff.	Factor	No.	T_i	Observer	Averages
Air	β	λ	1	273.122	Chappuis	
			1	273.140	Chappuis	
	α	μ	1	273.174	Chappuis	
			1	273.197	Chappuis	273.158
He	β	λ	5	273.211	Henning and Heuse	
			1	273.202	Heuse	
			4	273.158	Heuse and Otto	
			1	273.119	Keesom and Horst	
			3	273.148	Keesom and Horst and Taconis	
			1	273.135	Keesom and van Santen	
	α	μ	5	273.156	Henning and Heuse	
			1	273.137	Heuse	
			4	273.174	Heuse and Otto	273.168
N	α	μ	3	273.134	Henning and Heuse	
			4	273.125	Heuse and Otto	273.125
			1	273.117	Chappuis	
		Average = 273.158				

Weighted av. divergence from 273.158 = 0.023

Max. divergence from 273.158 = $\begin{cases} +0.053 \\ -0.041 \end{cases}$

Probable error = 0.017

$\therefore T_i = 273.16 \pm 0.02$.

TABLE VI. *Historical summary.*

Date	T_i	Author
1903	273.13	Berthellot[18]
1907	273.08	Berthellot[17]
1907	273.17	Buckingham[17]
1915	273.09	Henning[6]
1918	273.10	Griffiths[19]
1919	273.36	Hoxton[16]
1920	273.14	Keyes[20]
1921	273.20	Henning and Heuse[8]
1925	273.15	Roebuck[1]
1926	273.2	Henning and Jaeger[21]
1926	273.1	I. C. Tables
1929	273.14	Schames[22]
1929	273.18	Birge[23]
1930	273.16	Heuse and Otto[24]
1936	273.16	Roebuck

FINAL VALUE OF T_i

The data are collected in Table V. The number of separate determinations is listed under No. At the bottom are given the average 273.158 where each determination is given the same weight, the average divergence 0.023° of the separate determinations from 273.158, the maximum divergences +0.053° and −0.041° and the probable error 0.017. Except for the measurements by Keesom, van der Horst and Taconis, the irregularities have the appearance of a haphazard variation, within these narrow limits. Under such circumstances an arithmetic average—which also makes the mean square divergence a minimum—is sufficient.

Taking account of these variations one may set

$$T_0 = 273.16 \pm 0.02$$

as the best value.

This choice is slightly higher than the value of Keesom, van der Horst and Taconis (273.148). It may be noted that consistency does not exclude systematic errors: that the effect of absorption on the walls is to lower the measured value of T_i: that the measured values using air and nitrogen fall slightly below those using helium: that the helium average (273.168) exceeds that chosen (273.16): and that the effect of mercury vapor, as discussed below, if present, will also lower the measured value of T_i. That is a value slightly larger than that of Keesom, van der Horst and Taconis seems the more probable. Moreover if one combines their value (273.148) with the best of the other work, probably Heuse and Otto's work with helium (273.166), the result (273.157) agrees with the conclusion above.

Table VI presents a set (not exhaustive) of values in chronological order from the literature. The influence of Berthellot's excellent work kept the accepted value low, in spite of the, as now appears, better estimate of Buckingham. In general the values calculated with the aid of Joule-Thomson data have run higher than those using more indirect means. The spread of the estimates seems of late to be narrowing and one can expect with considerable confidence that the final value will lie between 273.14 and 273.18.

The provision of satisfactory Joule-Thomson data has simplified the α and β measurement situation by allowing the use of higher p_0, and the examination of the effect of variation of p_0 separately from the effect of the reduction to the Kelvin scale. The effect of wall absorption still needs investigation particularly for the gases of the nitrogen group.

CARNOT'S PRINCIPLE

Since the variation of the values of T_i with different gases in the thermometer, falls within the range of what may reasonably be called

[18] Berthellot, Trav. et Mem. du Bureau Int. des poids et Mesures **13**, 1903.
[19] Griffiths, *Methods of Measuring Temperature*, 1918.
[20] Keyes, J. Am. Chem. Soc. **42**, 54 (1920).
[21] Henning, *Handbuch der Physik* (Geiger and Scheel.) Vol. IX p. 537.
[22] Schames, Zeits. f. Physik **57**, 804 (1929).
[23] Birge, Phys. Rev. Supplement **1**, 59 (1929).
[24] Heuse and Otto, Ann. d. Physik **396**, 778 (1930).

experimental error, one may conclude that T_i is not dependent experimentally on the gas used. The thermodynamic scale as defined by Kelvin, depends for its uniqueness on the deduction usually made by the logical use of the first and second laws of thermodynamics, that the efficiency of the reversible engine is the same whatever actual working material be used in the engine. That is, the thermal and mechanical properties of all working materials are always so proportioned as to lead to this result.

A most interesting aspect of the experimental independence of T_i on the gas used, is the confirmation it affords of the experimental correctness of this efficiency deduction. It should be noted that the measurements of α and β used above must be classed with the finest experimental work ever done. That what is effectively an extrapolation into unknown temperatures should yield agreement of this order is of great significance.

Mercury Vapor

As ordinarily used, the surface of mercury in the pressure reading device is separated from the thermometer bulb by a capillary tube. With the mercury at room temperature and the bulb in ice, there is the possibility of mercury vapor diffusing into the bulb or being carried over by the gas during adjustments, and condensing there. In the extreme case, where enough diffused over to saturate the bulb at 100°, its presence would decrease the measured T_i by 0.27°C. This is many times greater than the expected error of the measurement. This maximum effect might seldom occur, but a small portion of it is quite serious. The practice of holding the mercury column continuously, at the freezing point should eliminate this possibility. The bulb should never be at the ice point without the mercury column being there also, particularly during adjustment of the mercury level.

Gas Mixtures

In the experiments on He-air mixtures[7] the straightline isenthalpic curves of small negative slope for helium, shift with increasing proportion of air, to strongly curved lines of larger positive slope. The same situation holds for both helium-nitrogen and helium-argon mixtures. The slope of these curves at 1 atm. pressure passes through the zero value while the curvature is still small. At one composition, the point of zero slope moves toward lower pressure with rising temperature. It is consequently possible to choose a composition such that

$$\int_{273}^{373} -\mu C_p d\frac{1}{T} = 0$$

and hence in Eq. (1), $D=0$. For this composition

$$T_i = 1/\alpha_{100}{}^0$$

without any modification. The value of D for helium is small enough that only very moderate precision in this choice of mixture is required. For those special conditions the mixture acts as a perfect gas. To make the choice it is necessary to know C_p and μ as functions of composition and temperature. Our as yet unpublished data promise to be adequate for μ but such C_p data are still lacking.

The situation above applies to α from the constant pressure gas thermometer. For the reduction of the constant volume gas thermometer readings to the Kelvin scale by means of Eq. (2) above, it is necessary to know λ over the required pressure and temperature range. The experimental evidence seems to show that λ goes to zero only at zero pressure. That is, the reduction of E to zero by a manipulation of composition does not appear possible as judged from the mixture data which is at present available.

It is planned to proceed with Joule-Thomson measurements on carbon dioxide and on hydrogen. T_i computed with these new data as well as with β for nitrogen will be given in a future article.

We wish to thank the Wisconsin Alumni Research Foundation whose assistance made available part of the time spent on this work.

My colleague Dr. H. Osterberg has helped me in many ways.

Magnetic Anisotropy of Nickel-Cobalt Single Crystals

J. W. SHIH, *National Research Institute of Physics, Academia Sinica, Shanghai*

(Received June 16, 1936)

The magnetic anisotropy of nickel-cobalt single crystals in the face-centered cubic range has been investigated with a pendulum magnetometer. The direction for easiest magnetization changes from <111> to <100> as the cobalt content increases from 3 to 10 percent and changes back to <111> when cobalt is more than 20 percent. Powell and Fowler's theory in regard to the relations between the direction of easiest magnetization and the crystalline structure, is again inadequate to explain these results, as in the case of iron-cobalt alloys. The anisotropy constants were calculated both from these monocrystalline specimens of Ni-Co alloys and from the polycrystalline specimens tested by H. Masumoto. The discrepancy between the two sets of values is too large to be accounted for by experimental errors in the present work.

IN a previous investigation[1] on the magnetic properties of iron-cobalt crystals, it was found that the direction for the easiest magnetization in the body-centered cubic range of this system changes from the tetragonal axis at the iron end to the trigonal axis as the cobalt content increases. The transition occurs at about 42 percent cobalt. The results disagree with the theory of Powell and Fowler[2] concerning the deviation of the direction of magnetization from that of magnetizing field. In this paper, similar work on the nickel-cobalt system will be reported.

According to Powell and Fowler, in the case of a face-centered cubic lattice, the crystalline field, assumed to represent the interaction of the spin moment of electrons responsible for ferromagnetism and the orbital moment of the atom to which they belong, has a maximum lying in the tetragonal direction. With this assumption the trigonal axis becomes the direction for easiest magnetization. This has been found true for nickel.[3] It is of interest to see whether or not this idea holds for the nickel-cobalt system, which, from 0 to 70 percent[4] cobalt, has the same space-lattice as nickel.

Nickel was obtained from the International Nickel Company, New York. It contained 99 percent Ni, 0.3 percent Co and small quantities of iron, silicon and carbon. The cobalt used here was of the same kind as in the writer's previous work, namely, 99.3 percent pure. For the preparation of alloys and their monocrystals the slow solidification method was again adopted. The alloys were prepared, as before, in an induction furnace with moving coil. The alloy crystals of low cobalt content are more easily recrystallized in large sizes than those of high cobalt compositions. Ingots were first etched in nitric acid, of higher concentration for higher cobalt, and then in a concentrated solution of ferric chloride. Sometimes the mixture of these two solutions was more effective than either separately. The brightest etch planes were found to be of form {111}.

On account of the fact that these alloys were too soft to make exact oblate spheroids on a rapidly rotating shaft,[5] we modified the previous method for the preparation of specimens by sticking on the end of an iron rod of required diameter a thin plate which had been ground on an oil stone to a definite orientation and thickness, and filing it gently to shape without power drive. The resulting spheroid, which is not quite so perfect in shape as a lathe-filed specimen, was then slightly etched to remove the strained surface. After annealing in a hydrogen atmosphere at 900°C for three hours, the orientation was determined by the Laue method. From the shape of the Laue spots we know that the specimens obtained in this way are much more free from strain than those obtained by machining. Some constants of the specimens are given in Table I. Orientation is defined as before, a perfect $(01\bar{1})$ specimen having $\alpha=45°$, $\beta=0°$.

[1] J. W. Shih, Phys. Rev. **46**, 139 (1934).
[2] F. C. Powell, Proc. Roy. Soc. **A130**, 167 (1930).
[3] S. Kaya, Sci. Rep. Tohoku Imp. Univ. [1] **17**, 639 (1928); W. Sucksmith, H. H. Potter and L. Broadway, Proc. Roy. Soc. **A117**, 471 (1928).
[4] H. Kühlewein, Physik. Zeits. **31**, 626 (1930); A. Osawa, Sci. Rep. Tohoku Imp. Univ. [1] **19**, 109 (1930).
[5] L. W. McKeehan, Rev. Sci. Inst. **5**, 265 (1934). We are informed that the original method has been modified so that softer crystals can now be handled by it, as will shortly be described by L. W. McKeehan, R. G. Piety and J. D. Kleis in this journal.

TABLE I. *Constants of crystal specimens.*

Percent Co by Synthesis	Density at room temp. g cm^{-3}	Volume cm^3	Thickness cm	Diameter cm	Demagnetizing factor N	$\alpha°$	$\beta°$
3	8.940	0.002972	0.0250	0.443	0.520	45	2
10	8.888	0.002778	0.0248	0.451	0.503	40	0
20	8.881	0.00166	0.0230	0.360*	0.580	45	0
40	8.785	0.00204	0.0210	0.376	0.515	45	10
50	8.790	0.00147	0.0203	0.339†	0.548	45	7
65	8.825	0.001873	0.0227	0.388	0.534	45	5

*For [111] and [011] only; along [100], dia. =0.358 cm and N =0.585.
† For [111] and [011] only; along [100], dia. =0.343 cm and N =0.543.

For magnetic measurement a pendulum magnetometer was used, of the same general design as before except for a few parts. The solenoid for producing uniform field was constructed with a length of about 25 cm instead of 20 cm. It produces a quite uniform field region sufficiently large so that the effect of its inhomogeneity on the displacement of specimen is inappreciable. The two coils for the nonuniform field were separated by $R\sqrt{3}$, where R is the mean radius of either, rather than by R as in the magnetometer first used. In order to eliminate external mechanical disturbances the moving part of the magnetometer on which the specimen rests was hung from a heavy and damped system suspended from a fixed support. With a field gradient of 2 oersteds, cm^{-1} and a magnification by the microprojector of about 740 times, a deflection of 20 cm or more may easily be obtained for almost all the specimens. The largest difference in deflection due to anisotropy is then about 6 cm. The probable error in the measurement is less than one percent, somewhat lower than in the previous work, the volume of the specimens being determined more accurately. The results are shown in Figs. 1 and 2. The saturation values of I here obtained are reasonably close to those previously reported by others.[6]

It is very interesting to note that the direction of easiest magnetization changes from <111> to <100> as the cobalt content increases from 3 to 10 percent, but when cobalt increases to more than 20 percent it changes back to <111>. The 20 percent alloy shows almost no difference in magnetization among the three principal axes. If its elementary crystals are easily magnetized in all directions, a polycrystalline material will be expected to have high permeability in low field. This is in agreement with Masumoto's findings.[6] By comparing the irreversible parts of the magnetization curves it is apparent that both the 40 and 50 percent Co alloys are magnetically harder than the others. This is probably due to the mechanical strain introduced in the process of preparation, since only these two specimens were made partly by machine and partly by hand. The strain is also evident from the shape of the Laue spots which are a little elongated in radial directions. In spite of this the I_p–H_e curves along the preferred direction show a rather sharp bend near saturation. This is the way a perfect crystal should behave according to the generally accepted view of the process of magnetization. For other directions we did not notice, beside the main bends, any small corners either on the uncorrected or on the corrected I–H curves as some investigators have reported both in pure ferromagnetic substances[7] and in alloys.[8]

The area enclosed between the magnetization curves for any two directions represents the energy difference of magnetization between these two directions. Due to the fact that the equatorial plane of the specimen is not in general

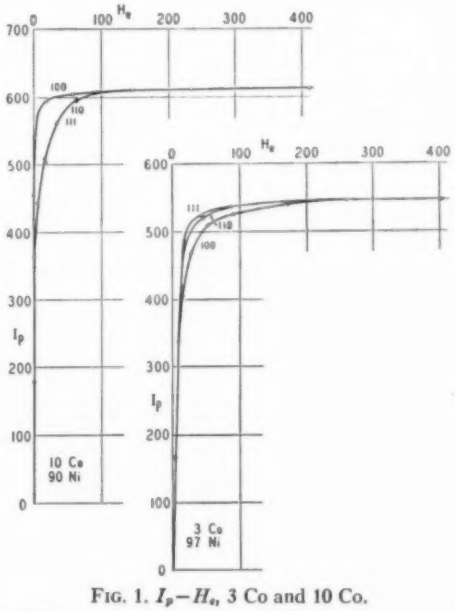

FIG. 1. I_p–H_e, 3 Co and 10 Co.

[6] H. Masumoto. Sci. Rep. Tohoku Imp. Univ. [1] **16**, 321 (1927).

[7] G. J. Sizoo, Zeits. f. Physik **56**, 649; **57**, 106 (1992).
[8] F. Lichtenberger, Ann. d. Physik [5] **15**, 45 (1932).

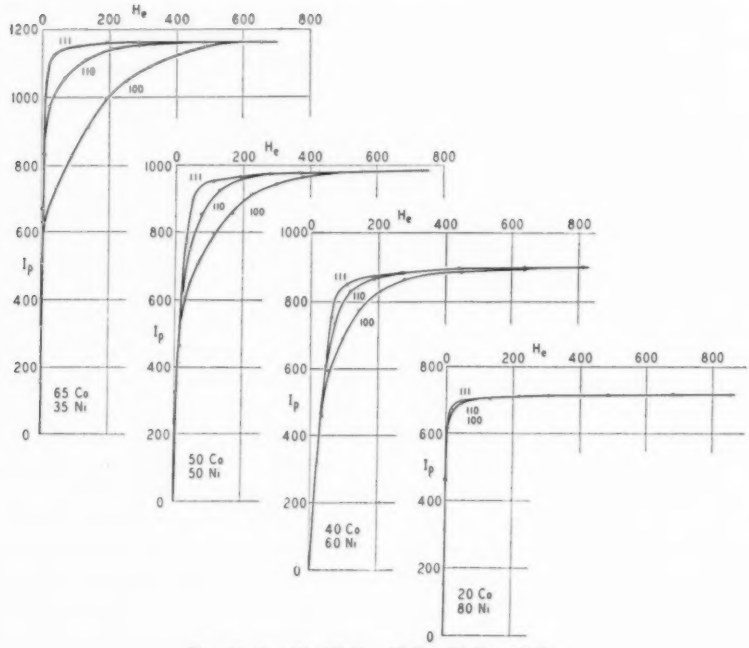

FIG. 2. $I_p - H_e$, 20 Co, 40 Co, 50 Co, 65 Co.

exactly parallel to the $(01\bar{1})$ plane the measured energy differences will generally be less than they should be. This nonparallelism can be corrected as we shall see later. The experimental and the corrected values of $W_{111}-W_{100}$ are given in Table II, while in Fig. 3 only the corrected values are plotted against the composition. It may be emphasized that the anisotropy constant for 65 percent Co has much the highest absolute value so far reported for face-centered cubic crystals. The value of $W_{111}-W_{100}$ for pure nickel in the first column was obtained by McKeehan[9]

TABLE II. *Differences of energy of magnetization, orientation factors and anisotropy constant. Eq. (1)*

Percent Co	$W_{111}-W_{100}$ uncorrected 10^4 erg. cm^{-3}	Orientation factors $f_{111}-f_{100}$	Anisotropy constant K 10^6 erg. cm^{-3}	$W_{111}-W_{100}$ corrected 10^4 erg. cm^{-3}	K Polycrystals* 10^6 erg.cm^{-3}
Pure Ni	−1.67	—	−2.5	—	−5.5
3	−0.298	0.3325	−0.448	−0.298	—
10	+0.38	0.331	+0.574	+0.384	+4.4
20	$-0.087<z<0$	0.333	$-0.13<z<0$	$-0.089<z<0$	—
40	−2.08	0.299	−3.47	−2.32	−15.1
50	−3.54	0.314	−5.63	−3.75	−27.5
65	−7.80	0.320	−12.2	−8.14	—

* Data of H. Masumoto.[6]

[9] L. W. McKeehan, Tech. Publication No. 554 of the Am. Inst. Min. and Met. Eng., August 1934; Trans. A. I. M. E. **111**, 11 (1934).

from Kaya's[8] measurements. From the figures we see that the transition of the easiest direction for magnetization from <111> to <100> probably occurs at about 5 percent and that from <100> to <111> at about 19.5 percent cobalt.

Now let us consider whether Powell and Fowler's theory is valid in the light of these results. In general the direction dependent energy[10] of a cubic crystal may be expressed as

$$W = 2K(\alpha_1^2\alpha_2^2+\alpha_2^2\alpha_3^2+\alpha_3^2\alpha_1^2) = 2Kf, \quad (1)$$

where the α's are the direction cosines of a magnetization vector with respect to the tetragonal axes, and K is the so-called anisotropy constant. In his notation, Powell's result may be reduced to the above form by letting

$$K = 1/4NI\gamma, \quad (2)$$

where

$$\gamma = 5/2(G^4/N^4)\{1/2-5(p^4+q^4+r^4)/2\},$$
$$N = 3kT_c/(y+2)\mu_B, \quad p=\alpha_1, q=\alpha_2, r=\alpha_3. \quad (3)$$

The sign of K, and hence that of γ, depends upon the direction of easiest magnetization.

[10] N. S. Akulov, Zeits. f. Physik **67**, 794 (1931).

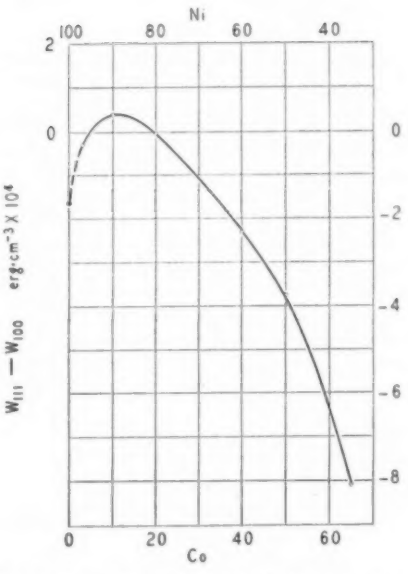

FIG. 3. $W_{111} - W_{100}$, nickel-cobalt single crystals.

If this direction is <111>, K is negative; if <100>, K is positive. This means whenever the direction for easiest magnetization changes, the sign of γ will reverse. In order to fit the experimental findings of the nickel-cobalt alloys the direction of the crystalline field, G, or rather the directions of its crystallographically equivalent maxima, must change twice, once at 5 percent Co and again at 19.5 percent Co. Suppose that the interaction between the electrons and the atoms (and hence the direction of maximum G) depends more or less upon the electron configuration inside the atoms of an elementary domain. It is hard to see why the electron pattern, which has been changed by the addition of a few cobalt atoms, should be restored to the original configuration when more cobalt is added.

Furthermore, for the alloys of the transition composition, the constant K must pass through zero. We do not know much about the nature of K. If it is represented by Eq. (2), then, when K becomes zero, either N or γ is equal to zero. Since N, which corresponds to Weiss's molecular field, seems necessarily to exist in all ferromagnetics and we cannot take special values for α_1, α_2, α_3, such as 1, 0, 0, or $1/\sqrt{2}$, $1/\sqrt{2}$, 0, to make the factor f in Eq. (1) equal to zero, G has to be zero. In other words the interaction of the orbital and the spin moments ceases in the transition alloys. The reason for this is again hardly conceivable. In brief, Powell and Fowler's theory is inadequate to explain the fact that the easiest direction for magnetization of a ferromagnetic changes in one and the same lattice structure.

As we have mentioned above, the energy difference of magnetization may be corrected for the imperfect cutting of specimens. This can be done by finding the orientation factors, f, of the component of magnetization, I_p, parallel to the direction under consideration. Having f_{111}–f_{100} and W_{111}–W_{100}, K may be computed. From the value of K, the true energy difference of magnetization for perfect cutting was calculated. These are given in the fifth column of Table II. The anisotropy constant may also be obtained from the I–H curve for polycrystalline substances by the following formula[11]

$$K = 5A/2, \tag{4}$$

where

$$A = \int_0^{I_\infty} H dI. \tag{5}$$

From Masumoto's[6] data, K for pure nickel and for the 10, 40 and 50 percent Co alloys was thus evaluated. Evidently the discrepancies between these values and those from single crystal data are much too large to be ascribed to the experimental errors in the present work. It is to be noted that small differences in the demagnetizing factors of the rods used by Masumoto would account for large differences in A. Furthermore, no correction for the width of the hysteresis loop, which may be considerable for polycrystalline specimens with high cobalt content, has been made in reducing his data. The sign of this correction is such that it would reduce the absolute (negative) values of K for 40 and 50 percent Co. It should also be remembered that Messkin and Somin[11] assumed random orientation of microcrystals in deriving their formula for K, and this condition may not exist in actual rods.

In conclusion the author wishes to express his appreciation to Mr. S. T. Pan for valuable aid throughout the work.

[11] W. S. Messkin and B. F. Somin, Zeits. f. Physik **98**, 610 (1936).

LETTERS TO THE EDITOR

Prompt publication of brief reports of important discoveries in physics may be secured by addressing them to this department. Closing dates for this department are, for the first issue of the month, the eighteenth of the preceding month, for the second issue, the third of the month. The Board of Editors does not hold itself responsible for the opinions expressed by the correspondents.

Communications should not in general exceed 600 words in length.

Nuclear Spin and Magnetic Moment of Li^6

The spin of the Li^6 nucleus and the h.f.s. separation, $\Delta\nu$, of the $^2S_{\frac{1}{2}}$ state have been measured by the atomic beam method of zero moments. The apparatus was that used in the work of K^{41}.[1] As in the case of potassium a study was made of the beam intensity as a function of the current in the tubes producing the inhomogeneous magnetic field. The resulting curve was analyzed for the determination of the spin and $\Delta\nu$.

One zero moment peak due to Li^6 was found in the region indicated by the measurements of Fox and Rabi.[2] No other peaks were found, which suggests a spin of 2/2 or 3/2. However, on the basis of this evidence alone a spin of 4/2 or greater could not be excluded, since the Li^7 background for currents lower than that corresponding to the Li^6 peak could mask any additional zero moment peak.

By extending the method of analysis used to determine the spin of K^{41} [1] and Rb^{87} [3] it was found possible by means of the Li^7 peak data to calculate the Li^7 background in the neighborhood of the Li^6 peak and thus obtain a difference curve due to the Li^6 zero moment atoms alone. The intensity and shape of this resultant Li^6 peak is in excellent agreement with the expected intensity and shape for a spin of 2/2, as is shown in Table I. The ratio of the currents at which the Li^6 and Li^7 peaks occur was found to be

$$I_P(Li^6)/I_P(Li^7) = 0.193 \pm 0.8 \text{ percent}.$$

This yields

$$\Delta\nu(Li^6)/\Delta\nu(Li^7) = 0.290 \pm 0.8 \text{ percent}.$$

Taking the value 0.0267 cm^{-1} for the $\Delta\nu$ of Li^7 as given by Fox and Rabi[2] we obtain

$$\Delta\nu(Li^6) = 0.0077 \pm 0.0001 \text{ } cm^{-1}.$$

The ratio of moments for the two isotopes of lithium is given by

$$\mu_6/\mu_7 = [\Delta\nu(Li^6)/\Delta\nu(Li^7)] \times [\{2I/(2I+1)\}_6/\{2I/(2I+1)\}_7] = 0.258 \pm 0.8 \text{ percent}.$$

Using the value 3.28 for the moment of Li^7 as calculated by Breit and Doerman[4] we obtain 0.85 nuclear magnetons for the magnetic moment of Li^6.

It is of considerable interest to note that this value is the same as that reported for the deuteron.[5]

We are indebted to Professor I. I. Rabi and others of this laboratory for their interest and assistance.

TABLE I.

	Expected			Observed
	2/2	3/2	4/2 or greater	
Peak intensity in percent	2.86	2.15	1.72 or less	2.7 ±.2
Half width of Li^6 peak / Half width of Li^7 peak	1.63	1	.77 or less	1.6 ±.2

J. H. MANLEY
S. MILLMAN

Columbia University,
July 18, 1936.

[1] Manley, Phys. Rev. **49**, 921 (1936).
[2] Fox and Rabi, Phys. Rev. **48**, 746 (1935).
[3] Millman and Fox, Phys. Rev. **50**, 220 (1936).
[4] Breit and Doerman, Phys. Rev. **36**, 1262 (1930).
[5] Kellogg, Rabi and Zacharias, Am. Phys. Soc., Rochester meeting, 1936.

The Electric Moment of the $^1\Sigma_+$ to O^+ Transition in the Continuum of Cl_2

In the course of a theoretical discussion of the continuous spectrum of chlorine, Gibson, Rice and Bayliss[1] evaluated the matrix component of the electric moment giving the value as $4.77\times10^{-10}\times0.016\times10^{-8}$ e.s.u. cm. Mulliken[2] has since pointed out that there is an error in this calculation, as it does not agree with the value $4.77\times10^{-10}\times0.067\times10^{-8}$ e.s.u. cm, obtained from the formula

$$D^2_{n''n'} = (3hC/8\pi^3)\int(k_\nu d\nu/\nu).$$

(In this formula we follow the notation of Gibson, Rice and Bayliss; in particular note that our $k_\nu N$ is equal to Mulliken's k_ν.) We have found that the discrepancy was due to an arithmetical error in our calculation, and we now obtain $4.77\times10^{-10}\times0.073\times10^{-8}$ e.s.u., which would seem to be in sufficiently good agreement with Mulliken's value. This correction has no effect on the rest of our calculations.

It may be of interest to remark that Mulliken's formula for $D^2_{n''n'}$ may be shown by comparison with the formulas of Gibson, Rice and Bayliss to be equivalent, at sufficiently low temperatures where v'' is always zero, to $\Sigma^2_{E'FE''J''J'} = 1$, where the summation is taken over all states of the continuum. This relation can be proven, in a manner similar to that used in the proof of spectroscopic stability,[3] by taking into account the fact that the vibrational eigenfunctions corresponding to the continuum form a complete orthogonal set.

G. E. GIBSON
O. K. RICE

Chemical Laboratory,
University of California,
July 17, 1936.

[1] Gibson, Rice and Bayliss, Phys. Rev. **44**, 198 (1933).
[2] Mulliken, Phys. Rev. **46**, 562 (1934).
[3] See Van Vleck, *Electric and Magnetic Susceptibilities*, p. 137.

On the Theory of Neutron Absorption in Aqueous Solutions

Measurements of the absorption of slow neutrons are usually made by the use of solid absorbers and detectors, in definite positions relative to the source and the bodies of water or paraffin. Interpretation of the results involves the geometrical problems of diffusion of the neutrons, the various angles at which they strike the absorbing layers, and the effects of scattering. The difficulty of getting reliable answers to these questions forms a distinct disadvantage of the procedure.

The purpose of this note is to point out the possibility of using another method, involving no geometrical difficulties. The substances used are placed in solution, in a vessel large enough ($\gtrsim$20 cm radius) for practically all the neutrons to be absorbed within it. The theory is extremely simple, since we use only the velocity distribution of the neutrons, and are not concerned with their distribution in space.

Fermi[1] has derived a general velocity distribution formula, valid for all energies markedly greater than the vibrational energies of H_2O: i.e., for energies at which the protons scatter as if free. If the absorption of the solute obeys the Breit-Wigner formula,[2]

$$\sigma_{\text{cap}}=\sigma_{\text{res}}\cdot(v_0/v)\Gamma^2/\{(E-E_0)^2+\Gamma^2\}, \tag{1}$$

one finds from Fermi's formula that the velocity distribution is given, in and above the resonance region, by

$$n(v)dv=dv\cdot(2\lambda Q/v^2)[\{(E-E_0)^2+\Gamma^2\}/\{(E-E_0)^2+\Gamma^2(1+\lambda/\lambda_{\text{res}})\}]\times\exp\{-(2\beta/\pi)\tan^{-1}\gamma/(v-v_0)\}\cdot\{1+0(\beta^2)\} \tag{2}$$

with

$$\beta=(\pi/2)(\Gamma/E_0)(\lambda/\lambda_{\text{res}})\{1+\lambda/\lambda_{\text{res}}\}^{-\frac{1}{2}},\qquad \gamma=(v_0/2)(\Gamma/E_0)\{1+\lambda/\lambda_{\text{res}}\}^{\frac{1}{2}}, \tag{3}$$

Q = number of neutrons/sec. leaving source,
λ = mean free path for scattering by protons,
$\lambda_{\text{res}}=1/N_d\sigma_{\text{res}}$ = mean free path for capture at velocity v_0,
N_d = concentration of detector solute (atoms/cm^3).

The number of atoms per second activated by resonance neutrons is

$$A_{\text{res}}=\int_{\substack{\text{resonance}\\ \text{region}}}v N_d\sigma_{\text{cap}}n(v)dv=2Q\beta\{1-\beta+0(\beta^2)\}. \tag{4}$$

This will be the measured activation if the solution contains a considerable concentration of cadmium, which absorbs the thermal neutrons very strongly. The number of neutrons reaching thermal velocities per second is $Q-A_{\text{res}}$; and in the absence of cadmium they will be absorbed partly by the protons[3] and partly by the detector, giving an activation

$$A_{\text{therm}}=(Q-A_{\text{res}})/(1+\tau_d/\tau) \tag{5}$$

with τ = mean lifetime for capture of thermal neutrons by protons.

$\tau_d=1/N_d\sigma_{\text{therm}}v_{\text{therm}}$ = mean lifetime for their capture by detector. The total activation without cadmium is then

$$A=A_{\text{res}}+A_{\text{therm}}=\{A_{\text{res}}+QN_d\tau\sigma_{\text{therm}}v_{\text{therm}}\}/\{1+N_d\tau\sigma_{\text{therm}}v_{\text{therm}}\}. \tag{6}$$

This equation contains the known quantities A_{res} and A (in arbitrary units), and N_d, and the unknowns Q and $\tau\sigma_{\text{therm}}v_{\text{therm}}$. Thus from measurements of A_{res} and A for two values of N_d, we can determine $\tau\sigma_{\text{therm}}v_{\text{therm}}$ and Q (in same units as the A's). Then from (4) we get the values of β for the two N_d's. Since β does not depend linearly on $\lambda/\lambda_{\text{res}}=N_d\lambda\sigma_{\text{res}}$, we can determine $\lambda\sigma_{\text{res}}$ and Γ/E_0.

E_0 may be determined by measuring A_{res} with different amounts of boron added to the solution of detector plus cadmium. For boron the absorption cross section is

$$\sigma_B=\text{constant}\cdot v^{-1}, \tag{7}$$

so that the absorption is characterized by a mean lifetime $\tau_B\sim$(concentration of boron)$^{-1}$. For not too large N_d ($\lambda_{\text{res}}\gg v_0\tau_B$), we have[1]

$$n(v)dv=2\lambda Qv(v+\lambda/\tau_B)^{-3}dv, \tag{8}$$

whence

$$A_{\text{res}}\sim(v_0+\lambda/\tau_B)^{-3}. \tag{9}$$

From measurements of A_{res} for two different values of τ_B, v_0 can be found as the single positive root of a cubic equation.

In the case of substances for which one cannot make $N_d\tau\sigma_{\text{therm}}v_{\text{therm}}$ appreciable compared to unity, one cannot get satisfactory results by using (6) as described. We can still determine E_0. Then from (6) and (1),

$$A_{\text{therm}}=A-A_{\text{res}}=QN_d\tau\sigma_{\text{therm}}v_{\text{therm}}=Q(v_0\tau/\lambda)\cdot(\lambda/\lambda_{\text{res}})(\Gamma/E_0)^2. \tag{10}$$

Here $(v_0\tau/\lambda)$ is known, since τ/λ can be found from the results on substances for which (6) can be used as described. Also β is now in general extremely small. Dividing (10) by (4) and using (3) we have

$$A_{\text{therm}}/A_{\text{res}}\cong\pi^{-1}(v_0\tau/\lambda)(\Gamma/E_0)\{1+\lambda/\lambda_{\text{res}}\}^{\frac{1}{2}}=\delta. \tag{11}$$

This quantity δ serves just as well as would β for getting $\lambda\sigma_{\text{res}}$ and Γ/E_0.

Thus by relative activation measurements one gets all three of the constants in (1), in terms of two standard quantities, λ and the constant in (7). Although there are of course certain technical difficulties, the method is probably not without technical advantages; and it certainly has marked advantages on the side of interpretation.

The writer wishes to thank Professor H. A. Bethe for helpful conversations.

W. H. Furry

Ann Arbor, Michigan,
July 27, 1936.

[1] E. Fermi, *Zeeman Festschrift* (The Hague, Nijhoff, 1935), p. 128.
[2] G. Breit and E. Wigner, Phys. Rev. **49**, 519 (1936).
[3] E. Fermi, Phys. Rev. **48**, 570 (1936).

The Velocity of Radio Waves

While making observations upon the different layers of the ionosphere, it occurred to us that if a receiving station B on the ground could be made to transmit a return wave to the sending station A at the exact instant of reception, the velocity of the radio wave could be measured at station A. The transmitting station A sends out 60 short pulses per second according to the method of Breit and Tuve. Each

pulse is less than five microseconds in duration. These pulses are received at Station *B* and appear as a broad line upon an oscilloscope which is kept in synchronism with the pulses by the commercial 60 cycle line connecting the two stations. Station *B* is also sending out 60 pulses per second. These produce a second broad line upon the oscilloscope at *B*. When these two lines are brought into coincidence by means of a phase changer the wave from *B* to *A* is acting precisely like a wave reflected from the ionosphere. The observer at *A* perceives two lines upon his oscilloscope, one due to his own pulse and the other due to a pulse which has traveled virtually from *A* to *B* and back again to *A*. The spot on his oscilloscope is being pulled across the screen at the rate of 1500 inches per second. He can therefore measure the time distance between the two lines with great accuracy. Twice the distance between the two stations divided by the time gives the required velocity.

Using this method we have found that the velocity of the ground wave between Fairmont and Morgantown is somewhat less than two-thirds the velocity of light. The station *B* was first set up by Davis and Elkins College, Elkins, W. Va., 80 kilometers away. At this distance with the power permitted, the ground wave was too weak for accurate measurement. The reflecting station was therefore moved to Fairmont State Teachers College, Fairmont, W. Va. The base line between the sending and receiving stations is now 20.3 km or 40.6 km for the total distance of transmission.

The velocity of propagation of any type of signal (light, heat, radio, x-ray, sound, etc.) may be measured by this method.

R. C. Colwell
A. W. Friend
N. I. Hall
L. R. Hill

Department of Physics,
West Virginia University,
July 27, 1936.

The Isotopes of Cobalt and Their Radioactivity

Dunning and his collaborators[1] have measured the absorption of slow neutrons in cobalt and found a large cross section: 35×10^{-24} cm^2, while Fermi and his co-workers[2] have shown that this slow neutron absorption is accompanied by the emission of gamma-radiation. This indicates that the process involved in the slow neutron absorption is radiative capture of the neutron to form an isotope heavier by one mass unit than the nucleus responsible for the capture. Since the only known isotope of cobalt has been Co^{59}, discovered by Aston, this radiative neutron capture should give rise to a water-sensitive radioactivity; but the only activities which have been observed in Co bombarded by neutrons are a 2.5-hour period which has been chemically shown[3] to be due to Mn^{56}, and a 20-minute period which is water-sensitive[4] and hence probably due to an isotope of cobalt, but is far too weak to be the only consequence of the quite large slow neutron absorption mentioned above. The process responsible for that absorption, then, has not so far been identified.

In the present work, cobalt was examined in a mass spectrograph described by Sampson and Bleakney,[5] the source of ions being a molecular beam of cobalt chloride ionized by slow electrons. Co^{57} was found as the $CoCl^+$ ion, peaks being observed at mass numbers 92 ($Co^{57}Cl^{35}$), 94 ($Co^{57}Cl^{37}$ and $Co^{59}Cl^{35}$), and 96 ($Co^{59}Cl^{37}$). Difficulty was experienced in obtaining cobalt ions from metallic Co, and the mass 57 was obscured by impurities. The abundance of Co^{57} is quite small: the ratio Co^{57}/Co^{59} being about $1/600\pm20$ percent. Assuming the packing fraction to be -9, from Aston's curve, the atomic weight comes out to be 58.93, in agreement with the accepted chemical value of 58.94.

The existence of two stable isotopes of Co presented the possibility that another water-sensitive radioactivity might be produced by neutron bombardment, and it seemed likely that it might be a long-period activity. Accordingly, a cylinder of metallic Co was bombarded for nearly a month with neutrons from a Ra-Be source of about 68 mc, source and detector being immersed in a large vessel of water. After it had been removed from the neutron source, the Co exhibited quite a strong activity, as measured with a thin-walled tube counter, almost all of which persisted after the decay of the known short-lived radioactivities. No appreciable decay has occurred in more than two weeks' observation of this activity, indicating that the half-life is of the order of a year or more. The measurements are not very accurate since the number of counts is only about four times the background. The growth of the long-period radioactivity has been observed in another Co cylinder exposed to the neutron source and removed and examined at intervals. The large intensity of this activity after bombardment for a time, short compared with the half-life, indicates that the equilibrium intensity is very big, so that this activity should be adduced to explain the large slow neutron cross section of Co.

Since Ni has stable isotopes of masses 58 and 60, we attribute Rotblat's[4] short-period activity to Co^{58}, formed by the capture of a neutron in Co^{57}; while the long-period activity just mentioned is likely to be due to Co^{60}. This assignment is made on a basis of comparison of the abundances of the Co isotopes with the relative intensities of the two radioactivities, but could be checked if the bombardment of copper with fast neutrons led to the reaction

$$_{29}Cu^{63}+{}_0n^1\rightarrow{}_{27}Co^{60}+{}_2He^4,$$

a possibility which should be examined.

We are indebted to Dr. Clyde K. Emery and the Cedars of Lebanon Hospital, of Los Angeles, California, for a gift of radon, and the American Philosophical Society for financial aid in constructing the mass spectrograph.

Milo B. Sampson
Louis N. Ridenour
Walker Bleakney

Palmer Physical Laboratory,
Princeton University,
July 29, 1936.

[1] Dunning, Pegram, Fink and Mitchell, Phys. Rev. **48**, 265 (1935).
[2] Fermi, Amaldi, d'Agostino, Rasetti and Segrè, Proc. Roy. Soc. **149**, 522 (1935).
[3] Fermi, Amaldi, d'Agostino, Rasetti and Segrè, Proc. Roy. Soc. **146**, 483 (1934).
[4] Narliker and Sastry, Nature **136**, 515 (1935).
[5] Sampson and Bleakney, Phys. Rev. In press.

Tests of the Validity of X-Ray Crystal Methods of Determining e

The procedure in determining the electronic charge, e, from measurements of x-ray diffraction angles and the density of crystals has been repeatedly criticized on the ground that while the density measurements are averages of a large volume, say 10 cc of crystal, the x-rays are diffracted from a surface layer as determined by "extinction" only about 4×10^{-4} cm thick, a very small fraction of the total volume in an *entirely specialized location*. Partial answers to this criticism in the form of experiments by Allison and Armstrong comparing different orders of reflection and by Y. C. Tu comparing determinations of e with different crystals have rendered its validity much less probable. Criticisms have continued nevertheless.

Work at this Institute in which calcite powder of grain size 2×10^{-4} cm and *less* was used closes this question completely, we believe, leaving no ground whatever for the criticism and placing the x-ray-crystal determinations of e on a very solid experimental foundation. With a Seeman-Bohlin spectrograph used so that the diffraction deviates the nickel $K\alpha_1$ and $K\alpha_2$ rays through nearly 180°, precision determinations of the grating constant of the calcite powder grains for three different sets of Miller indices were made, sufficient to establish with high accuracy the entire geometry of the microscopic calcite lattice structure in centimeter units. (The acceptance of x-ray grating wave-length values is of course involved here.) The density of the *identical powder sample* used for the diffraction was also established with a high degree of precision by pycnometric methods and this proved to be in excellent agreement with the density of macroscopic calcite. A computation of the extinction coefficients for all three Miller indices used yielded penetration depths for half-intensity in the shallowest cases twice as great as the largest crystal grains in the powder sample.

Assuming that Cu $K\alpha_1$ has the wave-length 1.5406×10^{-8} cm (Bearden's value determined with ruled gratings) our work yields the following absolute values for finely powdered calcite

$$\text{the density } \rho = 2.71022 \pm 0.00035 \text{ gram/cc},$$
$$\text{the characteristic angle } \beta = 101^\circ\ 54'\ 18'' \pm 48'',$$
$$\Phi(\beta) = 1.09602 \pm 0.00048,$$
$$\text{the grating constant of the cleavage planes } d = 3.0345\times10^{-8} \pm 0.0015 \text{ cm},$$
$$\text{the electronic charge } e = 4.799 \pm 0.007 \times 10^{-10} \text{ e.s.u.}$$

The *powder* method was selected as the most conclusive test after rejection as inconclusive of a long series of studies of *macroscopic* calcite in which precise comparisons were made of the diffraction angles for Bragg reflection from the surface and Laue reflection by interior planes with the beam transmitted through the crystal by using both the two crystal spectrometer and a precision photographic spectrometer. No difference to our precision of a part in six thousand was found between Bragg and Laue angles but further studies with the photographic spectrometer shook our faith in the method as a conclusive answer to all implications of the criticism mentioned in our first paragraph because (1) even with excellent cleaved calcite having a narrow rocking angle even Laue reflection seems to come predominantly from exit and entry surfaces and (2) certain new and unexplained phenomena observed in Laue reflection[1] emphasized the desirability of a statistical method which would render both density and diffraction angle determinations free from the peculiarities of individual crystals and of individual regions in one crystal.

An extended report of this work is in preparation.

The funds for these investigations which have continued over a period of three years were derived from the Frances Hayes Watters Memorial Research Fund given to the California Institute of Technology by Dr. Leon L. Watters of New York. We are grateful for this opportunity to express our deep appreciation of his gift.

California Institute of Technology,
June 3, 1936.

JESSE W. M. DUMOND
V. L. BOLLMAN

[1] See letter to the editor, Phys. Rev. **50**, 47 (1936), describing these phenomena in Laue reflection.

The Heavy Particle Component of the Cosmic Radiation

A survey of 8500 photographs taken of a Wilson cloud chamber of 7 liters volume and which was sensitive for 1.5 seconds indicates that about 1 percent of the ionization produced by cosmic rays at sea level is due directly to heavy particles. Some of the tracks are nearly as dense as alpha-particle or slow proton tracks and can be seen in the chamber for an equivalent path length of over 40 cm in air. 21 tracks were estimated to be between 50 and 200 times as dense as a fast electron track and 23 tracks between 10 and 50 times as dense. These heavy tracks were of such a density of ionization that their range, assuming them to be protons, would not be sufficient to penetrate the wall of the chamber. Protons with a range of 21 meters (5.6×10^7 ev) and thus capable of tripping the Geiger-counter controls would have an ionization of only 6 times that of an electron.[1] 7 tracks were observed in which the ionizing particle that apparently tripped the Geiger counter had a density of ionization of from 5 to 20 times that of an electron. There were 7 more photographs in which the ionizing particle produced a track of from 2 to 5 times the density of the usual electron track. 21 tracks with densities 3 to 10 times that of an electron track were found that had not tripped the counter but had passed through the chamber in the 0.2 second before the expansion. Tracks older than this and of this density could not be reliably distinguished from old electron tracks. 3 photographs were obtained that showed two or more heavy tracks coming from a point in the wall of the chamber. The common origin of these tracks indicates that they possibly have been the result of a disintegration. It is not unlikely that a large fraction of the heavy particles may be the secondary products of some type of disintegration. One cannot tell whether the heavy particles are protons or alpha-particles, but the apparent width of the tracks as a function of their age indicates that they are probably protons.

Department of Physics,
University of California,
July 16, 1936.

R. B. BRODE
H. G. MACPHERSON
M. A. STARR

[1] H. Bethe, *Handbuch der Physik*, 2nd edition, Vol. 24/1, p. 522 (1933).

Proceedings of the American Physical Society

MINUTES OF THE SEATTLE MEETING, JUNE 17–19, 1936

THE 206th regular meeting of the American Physical Society was held in the lecture rooms of the Physics Department of the University of Washington, Seattle, Washington, June 17 to 19, 1936. The meeting consisted of six three-hour sessions, two of which ran concurrently. The morning session of Wednesday, June 17, was devoted to a symposium on x-rays with the following invited papers.

1. **Tests of the Validity of the X-Ray Crystal Method of Determining *e*.** J. W. M. DUMOND, *California Institute of Technology.*
2. **Recent Work in the Widths of X-Ray Spectrum Lines.** F. K. RICHTMYER, *Cornell University.*
3. **Quality of Röntgen-Rays, Its Measurement and Importance.** R. R. NEWELL, *Stanford University School of Medicine.*
4. **Some Theoretical Questions Related to the Excitation of X-Ray Levels.** F. BLOCH, *Stanford University.*

The afternoon session of the same day took the form of a joint meeting with the Astronomical Society of the Pacific. Two invited papers were presented, as follows:

1. **Recent Cosmic-Ray Studies.** CARL ANDERSON, *California Institute of Technology.*
2. **Galactic Rotation.** J. A. PEARCE, *Dominion Astrophysical Observatory.*

A portion of Thursday morning, June 18, was spent in joint session with the American Mathematical Society, at which time Professor H. P. Robertson presented, by invitation, a paper upon *Geometry and Physical Space-Time.*

The larger part of the Thursday morning session and two concurrent Thursday afternoon sessions were employed for the presentation of thirty regular and ten supplementary contributed papers, abstracts of which appear below. At a business meeting held during the Thursday morning session the society voted to hold the 210th regular meeting of the American Physical Society on the Pacific Coast at the California Institute of Technology at Pasadena, California on or about December 18 and 19, 1936.

On Friday morning the invited papers listed below were presented.

1. **Ferromagnetism in Telephony: An Illustration of Industrial Research.** O. E. BUCKLEY, *Bell Telephone Laboratories.*
2. **The Present Status of β-Decay Theory.** GEORGE GAMOW, *George Washington University.*

The society met at luncheon Friday noon at the Hotel Edmond Meany, after which members of the Physics Department of the University of Washington exhibited their high voltage researches at the Swedish Hospital.

Attendance at the various sessions ranged from 70 to 160 persons.

PAUL KIRKPATRICK,
Local Secretary for the Pacific Coast.

ABSTRACTS

1. The Elimination of the Effect of Stray Sound upon the Measurement of Acoustic Absorption by the Parallel Beam Method. PAUL M. HIGGS AND F. A. OSBORN, *University of Washington.*—Frequency modulated sound collimated by a parabolic mirror is regularly reflected from a plane surface of the material under investigation and received upon a microphone placed at the principal focus of a second parabolic mirror. This arrangement has highly directional characteristics and is relatively insensitive to extraneous noises or to any sound which does not enter the receiving mirror in a direction parallel to its axis. Measurements are practically independent of the acoustic characteristics of the room in which the apparatus is placed. The operation of the apparatus and the interpretation of results are complicated by the reflection of sound back and forth between the two mirrors. The resultant standing wave system may cause large fluctuations of the sound field intensity at the foci of both mirrors and at the plane of the absorbing material. Under these conditions the intensity of the incident sound beam is influenced by the absorption of the material under test. The formation of standing waves may be prevented by introducing a region of constant high absorption in the vicinity of the foci of the mirrors.

2. High Pressure Afterglow in Nitrogen. JOSEPH KAPLAN, *University of California at Los Angeles.*—The auroral afterglow in nitrogen has been studied at pressures higher than those used in the earlier experiments. As the pressure is increased, the Goldstein-Kaplan bands in the discharge which originate on $v'=1$ increase in intensity relatively to those which originate on $v'=0$. The energy in the $v'=1$ level is 12.22 volts, and the energy of two $A^3\Sigma$ molecules in the $v=0$ level is 12.28 volts. The enhancement

of the $v'=1$ level appears therefore to be due to the increased number of collisions between metastable nitrogen molecules with increased pressure. This phenomenon points to a mechanism from which nitrogen afterglows may derive their long lives. The $v'=1$ Goldstein-Kaplan level contains only a slightly larger energy than that necessary for the production of two ^2D nitrogen atoms. This suggests the existence of predissociation on the $v'=1$ level, and thus provides a mechanism for the regeneration of metastable atoms in the afterglow and hence a means of prolonging the afterglow. The intensity of the afterglow increases with the pressure as does the relative intensity of the first-positive bands which originate on the $B^3\pi$ levels $v'=16$, 17 and 18.

3. The Shape of the β-Ray Spectrum of P^{32}. ERNEST M. LYMAN, *Radiation Laboratory, University of California.*—The magnetic β-ray spectrum of a strong sample of P^{32} has been investigated by means of a magnetic spectrograph and Geiger counter in order to determine the shape of the momentum distribution curve, particularly in the region of the upper limit. Preliminary investigation has shown that the shape of the curve is in agreement with the Konopinski-Uhlenbeck modification of the Fermi theory and with cloud chamber results[1] over the middle portion of the spectrum. However, at about 6000 $H\rho$ the experimental curve begins to deviate from the theoretical one adjusted to fit the major portion of the spectrum, falling rapidly to the $H\rho$ axis and ending at about 7300 $H\rho$, while the theoretical curve terminates at 8500 $H\rho$. The discrepancy seems too great to be explained on the basis of instrumental and experimental errors.

[1] F. N. D. Kurie, J. R. Richardson and H. C. Paxton, Phys. Rev. **49**, 368 (1936).

4. Conservation of Photons in General Relativity. H. P. ROBERTSON, *Princeton University.*—Kermack, McCrea and Whittaker* have shown that a photon description of the radiation field in general relativity is consistent with Planck's law $E=h\nu$, on the assumptions (1) the path of each (isolated) photon is a null-geodesic, along which (2) the energy-momentum 4-vector is carried by parallel transport. We here show that these two assumptions are necessary consequences of the field equations, whenever and to whatever extent the internal structure of the field allows it to be replaced by a corpuscular aggregate.

* Proc. Roy. Soc. Edinburgh **53**, 31 (1932).

5. Deuteron Induced Radioactivities of Antimony and Tin. J. J. LIVINGOOD, *Radiation Laboratory, University of California.—Antimony.* An exposure of 1 hour to 1 microampere of 5-million electron-volt deuterons caused the following radioactivities in an antimony target.

HALF-LIFE		YIELD (H^2 PER DISINTEGRATION)
52±4 days	(Negative electrons)	1.4×10^{7}
68±3 hours	(" ")	0.7×10^{7}
25±3 hours	(" ")	1.2×10^{8}

The yields have been corrected for finite time of exposure. A further activity of 2 or 3 minutes is probably due to adsorbed O^{18} and N^{14}. No chemical analysis has been made. The 68-hour activity probably corresponds to the 2.5 day half-life observed by Fermi after neutron bombardment. *Tin.* A tin target exposed to 3.5 microamperes for 3 hours was chemically separated (by Mr. Seaborg of the Chemistry Department) into indium, tin and antimony fractions. The observed radioactivities were

HALF-LIFE		YIELD (H^2 PER DISINTEGRATION)
In 27±2 hours	(Negative electrons)	4.0×10^{7}
Sn 27±2 hours	(" ")	1.5×10^{7}
Sb 52±8 days	(" ")	3.0×10^{8}
Sb 13±1 hour	(Positrons ?)	5.6×10^{8}

Two shorter periods were also observed. The similarity of the tin 52-day period with that when Sb is bombarded, and the apparent identity of their absorption curves in Al, suggest that Sb^{122} or Sb^{124} is the active isotope, formed in one case by

$_{51}Sb^{121,\,123}+{}_1H^2\rightarrow{}_{51}Sb^{122,\,124}+{}_1H^1$ and in the other by

$_{50}Sn^{120,\,122}+{}_1H^2\rightarrow{}_{51}Sb^{122,\,124}+W$ where W is a gamma-ray.

6. Temperature Dependence of Geiger-Müller Counter Characteristics. D. B. COWIE, *Bartol Research Foundation of the Franklin Institute. (Introduced by E. O. Lawrence.)*—Observations were made over a wide temperature range of the counting rates and starting potentials of a group of Geiger-Müller counters. The resultant increase in the number of discharges recorded as the temperature increased has been attributed to thermionic emission from the walls of the counter. With this assumption as to the variation in rate of discharge with temperature, one would expect that the order of magnitude of the rates would vary inversely as the work functions of the metals involved. Experiment with nickel oxide and copper oxide counters shows this to be true. No change in rate was observed as the temperature was decreased from room temperature to below 0°C, which is in agreement with the fact that thermionic emission would be negligible over this range. A further study revealed that starting potentials were also affected by temperature with the result that at 100°C an argon-filled copper oxide counter would start to count a hundred volts lower than at room temperature. The experiment was repeated with other counters with the same result.

7. Transition Phenomena in the Condensation of Silver Vapor on Clean and Gas-Covered Tungsten. MILO B. SAMPSON and PAUL A. ANDERSON, *State College of Washington.*—In a tube which had been subjected to severe outgassing, sealed from the pumps, and gettered with vaporized barium, duplicate tungsten filaments, dissimilar only with respect to the condition of their surfaces, were bombarded with gas-free silver vapor supplied by a molybdenum foil oven which could itself be thoroughly outgassed by flashing. One of the tungsten filaments was cleaned by flashing at 2800°K while the other was allowed to retain the oxygen coating which persists after flashing at 1400°K. Permanent condensation of silver on the gas-covered filament occurred only after its temperature had been lowered to 900°K and typical transition effects appeared. At the same vapor stream intensity permanent condensation on the clean tungsten occurred at 1220°K, approximately the temperature of the vaporizing oven, and none of the characteristic critical phenomena could be detected. It is

probable that transition ("critical temperature") effects in the condensation of metal on metal as observed by Estermann, Cockcroft, and others are conditioned by the presence of surface films of gas and vapor and disappear when such films are removed.

8. Photographic Infrared Absorption Spectrum of Heavy Acetylene (C_2HD) and Internuclear Distances in the Acetylene Molecule. G. HERZBERG, *University of Saskatchewan*, F. PATAT, *University of Göttingen*, AND H. VERLEGER, *Technische Hochschule Darmstadt.*—In continuation of previous work[1] we have further investigated the absorption spectrum of C_2HD in the photographic infrared with the aim of definitely deciding between our values for the internuclear distances in the acetylene molecule and those of Bradley and McKellar.[2] Using an absorbing length of 16.5 m of 50 percent heavy acetylene we have found a number of new C_2HD bands. The comparison of the combination differences $\Delta_2F''(J)$ of different bands proves conclusively the correctness of our previous numbering of the lines and thereby of our values for the internuclear distances. The results are summarized in the accompanying table in which also values for HCN have been included which have been recalculated from the data of Bartunek and Barker,[3] as well as the value for the C−H distance in CH_4 of Ginsburg and Barker.[4] The coincidence of the C−H distance in C_2H_2 and HCN as calculated independently with the aid of the C_2HD and DCN spectra is within 0.001A. The values of the distances for the corresponding free radicals, included in the table for comparison, are appreciably larger.

	In C_2H_2	In HCN	In CH_4	In Radical
r_0(C−H)	1.057A	1.057A	1.093A	1.127A
r_0(C−C)	1.204	——	——	1.311
r_0(C−N)	——	1.154	——	1.171

[1] G. Herzberg, F. Patat and J. W. T. Spinks, Zeits. f. Physik **92**, 87 (1934).
[2] A. McKellar and C. A. Bradley, Phys. Rev. **46**, 236, 341, 664 (1934).
[3] P. F. Bartunek and E. F. Barker, Phys. Rev. **48**, 516 (1935).
[4] N. Ginsburg and E. F. Barker, J. Chem. Phys. **3**, 668 (1935).

9. A Magazine Plate Camera for Photography in Vacuum. K. E. FITZSIMMONS, *State College of Washington.*—A magazine plate camera which provides for 8 to 16 separate exposures on $3\frac{1}{4}\times4$ inch plates without breaking the vacuum has been built for use with a high magnification electron microscope. Visual focusing of the image formed by the electron beam on a fluorescent screen is possible before each exposure. The camera is compact and the mechanical operation is smooth and positive. The camera is presumably generally adapted to photography in vacuum apparatus.

10. Absolute Values of the Electron Drift Velocity in the Rare Gases. R. A. NIELSEN, *Stanford University.* (*Introduced by N. E. Bradbury.*)—Absolute values of electron drift velocities in electric fields have been determined for nitrogen and the rare gases. The method employed is that of the high frequency electrical shutter recently used to measure electron mobilities in hydrogen.[1] The experimental values obtained are compared with those predicted by the Compton mobility equation using both kinetic theory and Ramsauer atomic cross sections. In addition, further comparison between experiment and theory is furnished by studying the effect of variable cross sections on the mobility as predicted by the equation of Morse, Allis and Lamar.[2] It is shown that the observed effects can be accounted for only by the occurrence of inelastic collisions of electrons with atoms or molecules, and that the random energies of the electrons are of a magnitude which is in agreement with this hypothesis.

[1] N. E. Bradbury and R. A. Nielsen, Phys. Rev. **49**, 388 (1936).
[2] Morse, Allis and Lamar, Phys. Rev. **48**, 412 (1935).

11. Attempts at Disintegration Using Lithium Ions. BERNARD B. KINSEY, *Radiation Laboratory, University of California.* (*Introduced by E. O. Lawrence.*)—A source of lithium ions is described and a method of accelerating them to energies of the order of a million volts is considered. A beam of 10 microamperes of lithium ions at about a million volts energy was directed onto targets of lithium and beryllium. In order to reduce the number of α-particles of 8-cm range, resulting from hydrogen contaminations on the targets, the latter were deposited on a sheet of molybdenum, by evaporation in vacuum, the sheet being previously outgassed by heating. With either target, no neutrons were observed, and no disintegration particles with range greater than 2 cm were observed. It is concluded that if such ionizing particles are emitted, there is less than one disintegration in 10^{13} incident lithium ions.

12. The $^1\Sigma^*-{}^1\Sigma$ Band System of Copper Deuteride. MYRON A. JEPPESEN, *The Pennsylvania State College.**—The copper deuteride bands have been photographed and an analysis has been made of the $^1\Sigma^*-{}^1\Sigma$ system. The resolving power is sufficient to permit an independent analysis of the $Cu^{63}D$ and $Cu^{65}D$ isotopic bands. The most important vibrational and rotational constants are given in Table I. The most reliable value of ρ for $Cu^{65}D$ to $Cu^{63}D$ from the present work is 0.999503. The calculated value from mass spectrograph data is 0.99952. A comparison with Heimer and Heimer's[1] CuH analysis gives a value of ρ for $Cu^{63}D$ to $Cu^{63}H$ equal to 0.7131. The calculated value is 0.7129. The electronic isotope displacement of CuD relative to CuH is 19 cm^{-1}.

TABLE I.

	$Cu^{63}D$		$Cu^{65}D$	
	$^1\Sigma$	$^1\Sigma^*$	$^1\Sigma$	$^1\Sigma^*$
ωe	1384.38 cm^{-1}	1213.16 cm^{-1}	1383.65 cm^{-1}	1212.60 cm^{-1}
$x_e\omega_e$	19.14	20.65	19.12	20.45
$y_e\omega_e$	0.037	−0.41	0.027	−0.45
T_e	0	23412	0	23412
B_e	4.03754	3.5199	4.03353	3.5182
α_e	0.09140	0.0898	0.09103	0.0919

* To be read by title only.
[1] A. Heimer and T. Heimer, Zeits. f. Physik **84**, 222 (1933).

13. Continuous Measurement of Changes in the Electronic Work Function during the Fusion of Tin. PAUL A. ANDERSON, *State College of Washington.*—A slight modification of the method for measuring contact differences of potential previously reported[1] has made possible con-

tinuous observation of progressive alterations in the work function of a metal surface down to time intervals of a few seconds. Applied to study the change in work function attending the transformation of gamma-tin to liquid tin the method yields electron current-time curves which are similar to temperature-time fusion curves. The break in the current-time characteristic does not coincide with the disappearance of the solid phase but follows it after a measurable time interval. The slope of the curve beyond the break-point is finite, decreasing from a high positive value to zero as the temperature of the liquid tin is raised. If, as is unlikely, these effects are due to liberation of adsorbed gas the curves provide a means of following the desorption continuously. They may indicate a persistence of the regularly orientated lattice structure of solid tin beyond the melting point. The contact difference of potential between gamma-tin and liquid tin is found to be 0.17 volt. The liquid tin has the lower work function in agreement with the photoelectric measurements of Goetz which, uncorrected to the true thresholds at 0°K, yield the value 0.16 ev for the difference between the work functions.

[1] P. A. Anderson, Phys. Rev. **47**, 958 (1935); **49**, 320 (1936).

14. A Controlled Mercury-Pool Device for High Voltage and Current Rectification and Switching. TYNG M. LIBBY, *The Pacific Telephone & Telegraph Company*, JOSEPH E. HENDERSON AND DONALD H. LOUGHRIDGE, *University of Washington*.—A vertical water-jacketed Pyrex cylinder having an anode at the upper end, a mercury pool cathode at the lower end, and a nozzle located between them and connected to a mercury boiler constitutes a new type of rectifier and switch. The boiler and nozzle system maintains a relatively high vapor pressure in the region of the cathode while the water-jacket temperature maintains a low vapor pressure and corresponding high sparking potential in the region of the anode. When the water-jacket is electrically connected to the cathode its shielding action prevents the establishment of significant potential gradients through the high pressure region by the anode potential and the sparking potential is high. When a moderate a.c. voltage is impressed between the water-jacket and cathode, the high pressure vapor is ionized periodically and the rectifier passes current during the positive half-cycle of anode voltage, the value of the average current being limited by the voltage, circuit resistance and duration of the conducting period. By varying the phase relation between the voltages impressed upon the water-jacket and the anode, the instantaneous value of the anode voltage at which the arc is initiated for each cycle can be varied at will over approximately the entire positive half-cycle. This device has successfully rectified 3000 to 40,000 volts with a maximum inverse peak of 80,000 volts, and currents up to the capacity of the available voltage supply.

15. Accommodation Coefficient and Molar Heat of Various Hydrocarbon Molecules. OTTO BEECK, *Shell Development Company, Emeryville*.—The accommodation coefficient α as defined by the equation $T_1-T_2=\alpha(T_1-T)$, T being the temperature of the surface and T_1 and T_2 being the mean temperatures of the gas molecules before and after the collision, respectively, has been measured for paraffin hydrocarbons up to 8 carbon atoms, a number of olefins, and some other unsaturated hydrocarbons on an ordinarily clean nickel surface at 140°C. The measurements were made by means of a molecular beam method at pressures of some 10^{-5} mm Hg. Argon and hydrogen were used as standards. The probable error of the relative measurements is less than one percent. A simple relationship between α, the molar heat at zero pressure C_{v_0}, and the molecular weight M was found, represented for paraffins by the equation: $\alpha(C_{v_0}+R/2)=c_1M$. Combined with the equation $C_{v_0}=c_2M+c_3$, which represents C_{v_0} in terms of the molecular weight, we arrive at

$$\alpha=c_1M/(c_2M+c_3+R/2)$$

where c_1, c_2 and c_3 are experimental constants and R the universal gas constant. Theoretical consequences and practical applications of these relationships will be discussed.

16. Further Simultaneous Measurements of Density and Surface Tension. L. E. DODD, *University of California at Los Angeles*.—Since the work previously reported,[1] further measurements have been made by the method there described, and with increased precision. In particular, measurements have been made on a series of some ten alcohols. Experience with this method shows that it is generally possible to take three successive measurements on a given liquid with an expected extreme range in the density values of not more than 0.25 percent, and a mean deviation (i.e., mean of the individual deviations from the average value) of 0.10 percent, or less.

[1] Phys. Rev. **48**, 487 (1935).

17. *K* X-Ray Absorption Spectrum of Bromine. S. T. STEPHENSON, *State College of Washington*.—The *K* x-ray absorption spectrum of Br in solid AgBr and in each of the vapors CH_3Br, C_2H_5Br and Br_2 is obtained with a double crystal ionization spectrometer. AgBr and Br_2 show secondary fine structure close to the main edge, the structure for AgBr being similar, as might be expected, to that of KBr and other bromides of cubic crystal structure. No significant shift, due to chemical combination, in the positions of the edges of the compounds is found except in the case of Br_2 whose edge appears shifted about $1.1\pm.5$ volts to the long wave-length side of the others. The widths of the edges as obtained by the usual triangle method are as low as 3 to 5 volts in some runs; these widths, of course, being very sensitive to small changes in the vertical adjustment of the calcite crystals. These values are smaller than those given for bromine in the literature reviewed, but might be expected from a consideration of data on emission line widths.

18. Positron Theoretic Deviations from the Klein-Nishina Formula. EDWIN A. UEHLING,* *University of California*.—On the basis of their theory of the positron,

Dirac and Heisenberg have predicted that deviations of order α in the Klein-Nishina formula for the scattering of light (of $\nu \sim mc^2/h$) by electrons would exist. Pauli has remarked that insofar as polarization effects considered by these authors are concerned, no such deviations should occur, since the polarization charge and current does not radiate. These polarization effects have been treated by considering the fields produced by the electron as classically describable. This treatment leaves out of account interchange effects between the electron and the "negative energy sea" electrons. In these interchange terms no unambiguous separation of proper energy and positron theoretic singularities is possible, and one must use Serber's method to eliminate them. Even on doing this, and renormalizing vacuum polarization effects to zero for the classical limit, terms remain which give finite deviations from the Klein-Nishina formula for $\nu \sim mc^2/h$. These have not been calculated.

* National Research Fellow.

19. Energy Liberation in Stellar Interiors. R. M. LANGER, *California Institute of Technology.*—Enough is known about the mechanisms of nuclear processes to permit a calculation of the reactions which would take place in a mass of matter originally preponderantly ordinary hydrogen heating gradually under gravitational contraction. The equations which occur can be solved approximately and for limited intervals of time. They lead to a theory of the stellar energy supply which has very desirable features. In the temperature range between 10^8 and 10^9 the formation of neutrons considered as an energetic state of hydrogen becomes considerable. The concentrations of positive and negative electrons also play a very important role. The interaction of these constituents to form deuterons and more complex nuclei then proceeds at a rate which depends essentially only on the partial pressure of protons and the temperature. Under assumptions for these which probably approximate the actual conditions the rate of energy liberation falls in the observed range. Moreover except at extremes of pressure the system is thermally stable at some temperature between 10^8 and 10^9. The presence of positrons in equilibrium at these temperatures has interesting consequences in connection with other problems of stellar interiors.

20. A Two-Stage Oil Diffusion Pump of Metal for Use on Large Volumes. JOSEPH E. HENDERSON, *University of Washington.*—A large two-stage all metal oil diffusion pump suitable for use on large volumes has been built and tested. The pump consists of the usual umbrella type of high vacuum stage backed by a stage possessing clearances of 1 mm or less. The nozzle for this stage provides an updraft which cannot clog with oil. Sufficient speed for this stage has been provided by making this nozzle surround the water jacket for the high vacuum stage. The pump, with clearances adjusted to 1 mm, worked successfully against a coarse vacuum of 0.3 mm of Hg. Upon replacing a single stage pump with a two-stage pump having the same size and length of throat the vacuum with no leak was reduced by one-sixth and the vacuum with leak to one-third. The coarse vacuum in each case was about 4 microns (including vapors). Large volumes may be successfully evacuated using less expensive coarse pumps or with the system closed for extended periods if the leak is not too large. The pump eliminates, to a large extent, the difficulties encountered in the initial evacuation of large volumes. A model of the pump is at present operating on the 800 kv x-ray tube having a volume of 200 liters.

21. The Effect of Wind upon the Electric Potential Gradient at the Earth's Surface. JOSEPH G. BROWN, *Stanford University.*—In a recent paper by the author[1] a theory of the local variation of the gradient based upon the daily cycle of turbulence, convection and subsidence was proposed. The present paper deals with the effect of wind upon the diurnal-variation and accounts for the results by modifications in this cycle. The 25-year records of Ebro Observatory are used to obtain results. Mean curves for days of continuous N-W wind and S-E wind are compared with days with calm nights. It is shown that direction of wind is important in determining the mean value of the gradient, but the form of the diurnal-variation is largely determined by speed. In general strong winds greatly reduce the amplitude and emphasize the single maximum. Days with calm nights, however, increase the amplitude and emphasize the double maximum. These results are in harmony with the proposed theory. The number of hours of sunshine is an important factor in determining seasonal differences. It is believed that observed diurnal-variations at all stations can be accounted for almost completely by considering phase relations between unitary and local variations and prevailing seasonal and wind conditions.

[1] J. G. Brown, Ter. Mag. **40**, 413–424 (1935).

22. A Long Period Positron Activity. L. JACKSON LASLETT, *Radiation Laboratory, University of California. (Introduced by E. O. Lawrence.)*—Frisch[1] has reported a long period positron activity produced in fluorine by alpha-particle bombardment; this he has attributed to Na^{22}. A long period positron activity of the character described by Frisch has been observed in Mg after bombardment with 5 MEV deuterons. This may be attributed to the reaction $Mg^{24}+D^2 \rightarrow Na^{22}+He^4$. The half-life may be tentatively given as 9 months and the upper limit for the positron energy as 0.4 MEV. It is hoped to have some cloud chamber information on the energy spectrum available in time for the meeting. The production of a positron emitter of such long half-life is of theoretical interest, as will be discussed by Mr. Lamb in another paper.

[1] Nature **136**, 220 (1935).

23. The Unobservable Decay of Na^{22}. W. E. LAMB, JR., *University of California. (Introduced by J. R. Oppenheimer.)*—According to Laslett, Na^{22} may be formed by bombarding Mg with deuterons.

$$Mg^{24}+D \rightarrow Na^{22}+\alpha. \qquad (1)$$

Na^{22} emits positrons with an upper limit ~500 kv and a half-life ~200 days. According to the Fermi theory of β-decay, it can also decay by the alternative process of K electron capture and neutrino emission. We have extended the calculations of Yukawa and Sakata to the case of Uhlenbeck-Konopinski coupling, and find for the ratio of the number of nuclei excited to the number of positrons emitted:

	Fermi	Uhlenbeck-Konopinski
$\Delta i=0$	1.2	4.7
$\Delta i=1$	2.1	30.4

The half-life puts Na^{22} near the second Sargent curve and thus indicates a spin change $\Delta i=1$. It would seem possible to check this feature of the theory by comparing the positron activity of the sample with the number of α-particles emitted, according to (1), in its activation.

24. The Effect of a Magnetic Field upon the Photoelectric Properties of Iron. Donald H. Loughridge and N. Kermit Olsen, *University of Washington.*—Measurements near 2200A with a magnetic field of about 5000 gauss, arranged to be perpendicular to the light beam, in a saturated electric field of over 200 volts, have shown practically no change in the emission of an iron cylinder when the magnetic field was applied. While the emission was always slightly less, with the field on, by about 1 to 2 percent, this was of the same order of magnitude as the experimental error. The iron cylinder was coated with electrolytically deposited iron and induction furnace heating in connection with long baking of the glass tube gave good reproducible photoelectric conditions where purity of surface is so essential. The necessary sensitivity of the FP-54 electrometer circuit was of the order of 180,000 mm per volt. The long wave-length limit, determined by the spectral response curve, with a single monochromator, was about 2500A; a little lower than that measured by Cardwell.

25. On the Elementary Interpretation of Showers and Bursts. J. R. Oppenheimer, *California Institute of Technology.*—The theoretical formulae for ionization and radiation losses of electrons and pair production by photons, have as a consequence that an electron or photon of very high energy will form sprays of electrons, positrons and γ-rays as it passes through matter. For an incident energy of 3×10^9 ev, the maximum of the probable number of electrons and positrons occurs at 2.2 cm Pb, and 45 cm Al; the maximum values attained are 12 and 2.3, respectively. For an incident energy of 10^{12} ev, the maximum occurs at 6 cm Pb, and gives about 2000 electrons and positrons and a comparable number of photons. The energy distributions observed in the cloud chamber, and the transition and absorption curves both for showers and for bursts, are in good agreement with these calculations. Apart from the experimental evidence against the validity of the theoretical formulae, the strongest argument against this interpretation of showers is that the number of showers and bursts observed under great thicknesses of absorber is far too high to be accounted for by fluctuations.

26. Production of Pairs and Compton Electrons by Gamma-Radiation from the Bombardment of Lithium by Protons. L. A. Delsasso, W. A. Fowler and C. C. Lauritsen, *California Institute of Technology.*—Stereoscopic cloud chamber photographs have been taken of pairs and Compton electrons ejected from thin sheets of carbon and lead by the gamma-radiation from lithium bombarded by protons. The distribution in total energy of the pairs indicates that most of the radiation is concentrated in a band or line at approximately 17 MEV.

27. A Wilson Cloud Chamber for the Study of Showers. R. B. Brode, H. G. MacPherson and M. A. Starr, *University of California.*—A completely automatic Wilson cloud chamber 30 cm in diameter and 10 cm deep has been constructed for the study of cosmic-ray showers. The chamber is compressed by air which forces up a duraluminum diaphragm fastened to the chamber base by a ring of sheet rubber making a gas tight connection. The Geiger-counter control releases the air pressure back of the chamber diaphragm in about 0.001 sec., and estimated from the width of the tracks, the time before complete expansion is between 0.01 and 0.02 sec. Illumination is provided by eight 150-watt, 110-volt tungsten lamps which are connected to 230 to 260 volts for from 0.05 to 0.10 sec. depending upon the particular gas used. Well exposed pictures are obtained with this illumination at $f:3.5$. An expansion ratio of 12.5 percent is required for a mixture of three parts ethyl alcohol to one part water when the chamber is filled with two atmospheres of nitrogen. A system of gauze and velvet in front of the diaphragm provides a good background for photography and reduces turbulence to such an extent that the apparent curvature of tracks, with zero magnetic field, is less than that of a track of 20 meters radius. Details of the rapid release mechanism and of the automatic resetting system will be given.

28. Characteristics and Energy Balance in Gaseous Discharge Lamps Containing Carbon Dioxide. T. J. Killian and R. S. Prescott, *Barkon Tube Lighting Corporation, Seattle.*—The design, construction and operation of lamps containing carbon dioxide are discussed. By the use of probe electrodes and a cathode-ray oscilloscope wave forms and space potentials are obtained. With a given set of electrodes the independent variables are tube length, tube diameter, gas pressure and current. The total power, voltage gradient, efficiency and stability are studied as functions of these. Results are obtained for both direct and alternating-current operation. From these results an approximate energy balance is calculated. A comparison of these characteristics is made with those of discharge tubes containing noble gases.

29. Proton-Proton Forces and the Mass Defect Curve. Robert Serber,* *California Institute of Technology.*—The experiments on the scattering of protons by protons show the existence of proton-proton forces which are not small compared to the proton-neutron forces. There probably also exist similar neutron-neutron forces. These forces must of course be included in calculations of the binding

energies of the nuclei. If the proton-proton and neutron-neutron forces are supposed to be of the Wigner (ordinary) type, the binding energy per particle should increase rapidly with increasing number of particles in the nucleus. If the forces are supposed to be of the Majorana (exchange) type, the binding energy per particle should decrease rapidly with the number of particles. The approximate constancy of the observed binding energy per particle thus indicates that the proton-proton and neutron-neutron forces are of neither the pure Wigner nor the pure Majorana type, but consist of a linear combination of the two. The proper combination is approximately two-thirds Majorana interaction and one-third Wigner interaction. A simple form of coupling between the heavy particles and the electron-neutrino field can be made to give essentially this result.

* National Research Fellow.

30. New Determinations of Gyromagnetic Ratios for Ferromagnetic Substances. S. J. BARNETT, *University of California at Los Angeles and California Institute of Technology.*—Since the last publication* new and extensive measurements have been made on a number of substances, including electrolytic iron, cold rolled steel, nickel, permalloy, Hopkinson's nickel-iron alloy, pure cobalt, cobalt alloyed with a few percent of copper, cobalt alloyed with nickel (Bloch's alloy) and Preuss' iron-cobalt alloy. All the work has been done by methods differing only slightly from those used by the author in the last work on rotation-by-magnetization. The values of the gyromagnetic ratio obtained range from about $1.02\times m/e$ (nickel-iron) to about $1.10\times m/e$ (pure cobalt), with mean errors in a number of cases of much less than 1 percent. Earlier values have been confirmed. No *certain* difference has been found between results obtained with the magnetizing coil fixed to the earth and magnetizing coil fixed to the vibrating body.

* Proc. Am. Acad. Sci. **69**, 119 (1934).

31. Infrared Absorption Spectra and Molecular Structure of HNCO (Cyanic Acid), HCOOH (Formic Acid) and CH_3OH (Methyl Alcohol). G. HERZBERG, *University of Saskatchewan,* AND H. VERLEGER, *Technische Hochschule Darmstadt.*—Using an absorbing column of 4 m for HNCO and 16.5 m for HCOOH and CH_3OH the following absorption bands in the photographic infrared have been found:

	λ	ν
HNCO	10310A	9700 cm^{-1}
HCOOH	9800A	10200 cm^{-1}
CH_3OH	9490A	10540 cm^{-1}

The fine structures of all these bands are well resolved on our plates. From the complicated structure of the HNCO band it follows that unlike N_2H^1 which is isosteric to HNCO, in the latter molecule the three atoms NCO do not even approximately lie on a straight line. The HCOOH band is surprisingly simple indicating that the molecule is very nearly a symmetrical top. The CH_3OH band is also comparatively simple (P, Q and R branch). It is to be interpreted as a $\|$ band, the moment of inertia calculated from the distance of the lines agreeing well with what one would expect for the moment of inertia about an axis perpendicular to C—O.

[1] G. Herzberg, F. Patat and H. Verleger, Zeits. f. Elektrochemie **41**, 522 (1935).

32. Two Gyromagnetic Models (with Demonstrations). S. J. BARNETT, *University of California at Los Angeles and California Institute of Technology.*—(1) A rigid frame can be rotated by an electric motor in either direction and at different speeds, about a vertical axis. The frame carries two similar and symmetrical electric motors, whose axes can move in altitude only, and whose motion is resisted by springs which keep the axes horizontal when the motors are not in rotation or when the frame is not in rotation. In the latter case they rotate in opposite directions when power is applied. Similar flywheels are on the two ends of each shaft, one painted red, the other white. To one looking along the axes, when horizontal, wheels with different colors rotate in opposite directions. The rotors represent Ampère's whirls, with magnetic moments and angular momenta. By the (automatic or manual) operation of a few switches the instrument can be made to simulate (on the classical theory) the complete process of magnetization-by-rotation. (2) This behaves similarly, and also permits demonstration of the converse effect. It consists of a student sitting on the well-known roller-bearing stool, and holding two bicycle wheels properly oriented and spun.

33. Two Afterglow Phenomena in Nitrogen. JOSEPH KAPLAN, *University of California at Los Angeles.*—This is a preliminary report on two afterglow phenomena. It has been found that the relative intensities of the two second-positive bands λ4356 and λ4344 were different in the afterglow than in the electrical discharge which is described below. λ4356 originates on the $v'=4$ vibrational level of the $C^3\pi$ state of N_2. λ4344 originates on $v'=0$. In the afterglow the ratio I_{4356}/I_{4344} is much larger than in the discharge. This difference may prove to be the means of determining whether the auroral and night-sky radiations are produced by electrical discharges or by afterglows. When a weak discharge is passed through the old Rayleigh-Lewis active nitrogen, the afterglow is quenched and the spectrum is characterized by the fourth-positive bands of nitrogen, which do not appear in the weak discharge spectrum of nonglowing nitrogen. When a weak discharge is passed through the "auroral" afterglow, there appears a yellowish flash which is much brighter than the original afterglow. The spectrum of this flash contains the first-negative bands of N_2^+ and some of the first-positive bands which originate on high vibrational levels of the $B^3\pi$ electronic state of nitrogen. These preliminary results show clearly that the most probable origin of the auroral spectrum lies in an excitation of "auroral" active nitrogen.

34. Improved Manometer and Pressure Control. T. J. KILLIAN, *Barkon Tube Lighting Corporation, Seattle.*—The uniform space conduction path manometer and pressure control reported previously has been improved.[1] Its construction and use in controlling the pressure in gaseous discharge lamps containing carbon dioxide is

described. The characteristics and pressure range with various other gases are reported. Its lack of moving parts and instantaneous positive action suggest many laboratory uses.

[1] T. J. Killian, Phys. Rev. **49**, 647A (1936).

35. The Density of Nuclear Levels. J. R. OPPENHEIMER AND R. SERBER,* *University of California.*—The high probability of radiative absorption of neutrons, and the selective absorption of slow neutrons, may be understood, as Bohr, Breit and Wigner have shown, by taking into account states of the nucleus plus neutron system in which the neutron shares its energy with other particles. In order to see whether the incidence of these levels is high enough to account for their observed effects, one may make a rough estimate of the number N of such states in a given energy range ΔE by supposing that the nuclear particles are confined to a sphere of radius ρ, that the mean potential energy of a nuclear particle is not much affected by the excitation of another, and that collisions between nuclear particles remove accidental degeneracies. On this basis, and taking account of exclusion principle and spin for neutrons and protons, one finds

$$N\Delta E=(\Delta E/E')(\gamma/5)^{\frac{1}{2}}\exp(5\pi/3\gamma);\quad \gamma=[8ME'\rho^2/\hbar^2]^{3/5}.$$

Here M is the proton mass, and E^1 is the sum of the kinetic energy of the neutron and the mass defect of the normal state of nucleus and neutron with respect to the unexcited nucleus and free neutron. The most probable number of particles to share the energy is $2\pi\gamma/3$. With reasonable values of ρ this leads to level densities consistent with both slow and fast neutron collision phenomena.

* National Research Fellow.

36. Deuteron Induced Radioactivities in Ruthenium and Copper. J. J. LIVINGOOD, *Radiation Laboratory, University of California.—Ruthenium.* Using 5 million electron-volt deuterons, with a 2-hour exposure to 2.5 microamperes, the following radioactivities were produced in a ruthenium target:

HALF-LIFE		YIELD (H^2 PER DISINTEGRATION)
44±3 days	(Negative electrons)	2.5×10^7
40±4 hours	(" ")	0.8×10^7
4±1 hour	(" ")	1.5×10^7

The yields have been calculated for saturation, by correcting for the finite length of exposure. No chemical separations have been made. *Copper.* Filings of some of the commercial copper from part of the cyclotron that has received stray bombardment over several months' use, have been examined for long period activity. After the chemical separation of the 14.5-day radio-phosphorous contamination activity, a residual effect with half-life of 146±10 days has been observed. This consists of negative electrons with a half-value absorption thickness of 0.005 cm Al and a range of 0.025 cm Al (energy equal to 0.31 MEV by Feather's relation), and in addition a gamma-ray of intensity one-seventh that of the electrons. Assuming a bombarding current of 0.1 microampere, and 4 days' total exposure the saturation yield is of order 10^7 deuterons per active atom. Isotopes possibly responsible are radio Ni^{63} or Fe^{59}, formed by

$$_{29}Cu^{65}+{}_1H^2\rightarrow{}_{28}Ni^{63}+{}_2He^4$$

or

$$_{29}Cu^{65}+{}_1H^2\rightarrow{}_{26}Fe^{59}+{}_2He^4+{}_2He^4.$$

Chemical analysis thus far has given no unambiguous answer. It is possible that the activity is due to some impurity in the commercial copper.

37. Stopping Power of Foils for High Speed Deuterons. L. JACKSON LASLETT, *Radiation Laboratory, University of California. (Introduced by E. O. Lawrence.)*—As reported at a previous meeting of the Physical Society,[1] the Berkeley magnetic resonance accelerator has been modified so that a beam of deuterons with energy above five million electron volts can be brought out of the accelerating chamber to spend its entire range in air. The decrease caused in the range of this beam by the interposition of various foils was measured by using as detector a movable shallow ionization chamber connected to a galvanometer. These approximate values for the "air-equivalent" of the foils were converted into values for the atomic stopping power for these elements (Al, Cu, Pt) by measuring the foil thicknesses either with natural alpha-particles or by weighing. It was found that for deuterons of the speed used (about 2×10^9 cm/sec.) the stopping powers did not differ markedly from those given by Mano.[2] In the case of Pt, the stopping power for deuterons was 20 percent higher than Mano's value, but the cumulative experimental errors may perhaps have been this high.

[1] D. Cooksey and E. O. Lawrence, Bull. Washington Meeting (Abs. 33).
[2] Mano, J. de physique **5**, 628 (1934).

38. The Polarity Changes of Elements When in Various Combinations of Couples to Form a Cell. LOUIS A. G. BLANCHET, *New Orleans, Louisiana.*—The polarity changes of elements when in various combinations of couples and put in a solution in order to form a cell have been investigated. The polarity results are given in tabular form. From these data a polarity determinant is found which involves a more definite consideration of atomic and molecular constants than those from which results have heretofore been reckoned. The determinant is computed for each element, and arranged in the descending order of values. This order is found to be identical with the arrangement of elements in which each element, with a preceding or succeeding element in couple combination manifests when put into an electrolyte, a negative and a positive polarity, respectively. However, this order of the elements is different from the order laid down in the electromotive force series. Because the polarity determinant of one element is greater than the polarity determinant of the other with which it is coupled, in one instance, than in another, and its momentum less; and because it will not be overcome by the one with the lesser polarity determinant, yet greater momentum, it will show this by manifesting positive polarity; yet when in couple combination in which its polarity determinant is less yet momentum greater than the polarity determinant of the other element, it will show this difference by manifesting negative

polarity. The formula enables one to predict the polarity that will be manifested by any two elements coupled in an electrolyte to form a cell.

39. The Analysis of Interferometer Patterns of Hα. WILLIAM V. HOUSTON, *California Institute of Technology.*—One of the principal difficulties in the study of the fine structure of the Balmer lines is the interpretation of the observed intensity pattern in terms of the elementary spectral components. Since the interferometer pattern is periodic, the intensity as a function of the order of interference can be expressed as a Fourier series, of which the coefficients provide a natural description of the pattern. These coefficients can then be expressed as functions of the positions, intensities, and breadth parameters of the component lines. Although these equations are not such as to be easily inverted and solved, it is possible to set up a criterion for the suitability of an assumed set of parameters. This criterion is based on minimizing the integral of the square of the difference between the observed and assumed curves. Although this procedure is laborious, it is objective and definite, and provides a method for the analysis of any interferometer pattern. A preliminary trial of the method has been made on two curves for Dα, taken under different conditions of excitation. The relative intensities are different in the two cases, and the separation of the principal components is about two percent less than the theoretical separation.

40. The Nature of the Effect of the Sign of Charge on Ions in the C. T. R. Wilson Cloud Condensation Experiments. ARTHUR F. KIP AND LEONARD B. LOEB, *University of California.*—Careful studies in an improved form of cloud chamber of the type in which Wilson originally studied the charge preference using water with different gases and using organic liquids in air have shown that the character of the companion impurity molecules making up the gaseous ion does *not* exert any marked influence on the sign preference in condensation by changing the vapor pressure of the drop. The values of the expansion ratios producing cloudy condensation in various vapors are shown below. Definite sign preference for one or the other ion in some cases must be noted. The results in chloroform and ethyl iodide are at variance with observations by Przibram. Since the ionic constituent molecules exert no influence sign preference using the J. J. Thomson theory of condensation requires the following additional assumptions: (1) That there is a definite surface orientation of the molecules in the droplet. (2) That molecules condense more readily when oriented in particular directions relative to the surface molecules, i.e., that the van der Waals forces have preferential directions. (3) That the molecules have dipole moments so directed and of such magnitude that favorable or unfavorable orientation of the molecules in the intense electrical fields near the surface of charged droplets can result.

No Sign Preference

Formula	Vapor	$E\pm$
C_6H_6	Benzene	1.73
$C_6H_5NO_2$	Nitrobenzene	1.45
$ChCl_3$	Chloroform	1.83

Negative Ion Preference

		E_-	E_+
H_2O	Water	1.25	1.31
C_2H_5I	Ethyl Iodide	1.82	2.11

Positive Ion Preference

		E_-	E_+
C_2H_5OH	Ethyl Alcohol	>1.29	1.26
CH_3OH	Methyl Alcohol	1.37	1.33
$C_2H_4O_2$	Acetic Acid	1.54	1.45
C_4H_9Br	Butyl Bromide	>1.52	1.48

E = Expansion Ratio.

AUTHOR INDEX TO ABSTRACTS OF THE SEATTLE MEETING

Anderson, Paul A.—No. 13
——see Sampson

Barnett, S. J.—Nos. 30, 32
Beeck, Otto—No. 15
Blanchet, Louis A. G.—No. 38
Brode, R. B., H. G. MacPherson and M. A. Starr—No. 27
Brown, Joseph G.—No. 21

Cowie, D. B.—No. 6

Delsasso, L. A., W. A. Fowler and C. C. Lauritsen—No. 26
Dodd, L. E.—No. 16

Fitzsimmons, K. E.—No. 9
Fowler, W. A.—see Delsasso

Henderson, Joseph E.—No. 20
—— see Libby
Herzberg, G., F. Patat and H. Verleger—No. 8
—— **and H. Verleger**—No. 31
Higgs, Paul M. and F. A. Osborn—No. 1
Houston, William V.—No. 39

Jeppesen, Myron A.—No. 12

Kaplan, Joseph—Nos. 2, 33
Killian, T. J.—No. 34
—— **and R. S. Prescott**—No. 28
Kinsey, Bernard B.—No. 11
Kip, Arthur F. and Leonard B. Loeb—No. 40

Lamb, W. E., Jr.—No. 23
Langer, R. M.—No. 19
Laslett, L. Jackson—Nos. 22, 37
Lauritsen, C. C.—see Delsasso
Libby, Tyng M., Joseph E. Henderson and Donald H. Loughridge—No. 14
Livingood, J. J.—Nos. 5, 36
Loeb, Leonard B.—see Kip
Loughridge, Donald H.—see Libby
—— **and N. Kermit Olsen**—No. 24
Lyman, Ernest M.—No. 3

MacPherson, H. G.—see Brode

Nielsen, R. A.—No. 10

Olsen, N. Kermit—see Loughridge
Oppenheimer, J. R.—No. 25
—— **and R. Serber**—No. 35
Osborn, F. A.—see Higgs

Patat, F.—see Herzberg
Prescott, R. S.—see Killian

Robertson, H. P.—No. 4

Sampson, Milo B. and Paul A. Anderson—No. 7
Serber, Robert—No. 29
—— see Oppenheimer
Starr, M. A.—see Brode
Stephenson, S. T.—No. 17

Uehling, Edwin A.—No. 18

Verleger, H.—see Herzberg

Proceedings of the American Physical Society

MINUTES OF THE ROCHESTER MEETING, JUNE 22–23, 1936

THE 207th regular meeting of the American Physical Society was held at Rochester, New York on Monday and Tuesday, June 22 and 23, 1936 on the new River Campus of the University of Rochester. There were three parallel sessions for the reading of ten-minute contributed papers on Monday morning. The presiding officers were F. K. Richtmyer, President of the Society, H. M. Randall, Vice President, F. L. Fairbanks, and Bradford Noyes. The attendance at the meeting was about four hundred.

A symposium on *Some Problems in Applied Physics* was held on Tuesday morning at nine-thirty o'clock in Strong Auditorium with F. K. Richtmyer presiding. The invited papers were as follows:

1. **Applied Physics in Photography,** C. E. K. MEES, *Eastman Kodak Company.*
2. **Some Properties of Adsorbed Films on Composite Surfaces,** IRVING LANGMUIR, *General Electric Company.*
3. **Physics in Optical Instrument Manufacture,** W. B. RAYTON, *Bausch and Lomb Optical Company.*
4. **Some Applications of the Electron Theory of Solids,** FREDERICK SEITZ, *University of Rochester.*

The attendance at this symposium was about three hundred and fifty.

Tours were arranged for the Bausch and Lomb Optical Company, Eastman Kodak Company, and the Taylor Instrument Company. The Taylor Instrument Company also served a complimentary luncheon to one hundred and twenty members of the Society.

On Monday evening at six-fifteen o'clock there was a joint dinner with the Rochester Section of the Optical Society of America in Todd Union. President Richtmyer presided and the after-dinner speakers were Carl Bausch and Lee A. DuBridge. There were one hundred and twenty guests at the dinner. Immediately following the dinner members of the Society attended a performance of *Madame Butterfly* in the University Stadium.

Meeting of the Council. At its meeting held on Monday, June 22, 1936 the deaths of one fellow (George A. Hoadley) and of two members (E. O. Dieterich and Edward J. Lorenz) were reported. Sixteen candidates were elected to membership. *Elected to Membership:* Wilmer C. Anderson, Alfredo Banõs, Jr., Charles L. Critchfield, Byron E. Eldred, C. Drummond Ellis, Allen Fowler, Alex Frosch, Royal M. Frye, J. Ogden Hancock, Hazimu Kawamura, Robert Langmuir, Elizabeth Royon, Arthur Shambon, Sin-itiro Tomonaga, John W. Tynan, and Elizabeth H. Wyckoff.

The regular scientific program of the Society consisted of thirty-nine contributed papers of which numbers 11, 23, 28, 32, and 35 were read by title. The abstracts of these papers are given in the following pages. An *Author Index* will be found at the end.

W. L. SEVERINGHAUS, *Secretary*

Abstracts

1. Extrapolated Ranges from Number-Distance Curves. Allen King and W. M. Rayton, *University of Rochester.* (*Introduced by T. R. Wilkins.*)—To obtain the ranges of alpha-particles from Wilson chamber data, frequently the integrated plot of the number-distance distribution is used. The straight line portion of this graph is extrapolated to the distance axis to obtain the intercept from which one may calculate the mean range by the equation: $R=I-\pi^{\frac{1}{2}}\alpha/2$ in which α is the parameter for the distribution curve. Since, in the distribution curve, one plots the number of tracks with lengths between l_0 and $l_0+\Delta l_0$ against l_0, the question arises: what is the best representation of the area beyond l_0? G. C. Laurence,[1] Kurie,[2] and others plot the number of tracks with lengths greater than l_0 against l_0. On the other hand, Meitner and Freitag,[3] Philipp and Donat,[4] etc. include the number of tracks at l_0 in this sum. Actually, neither method best approximates the area from l_0 to infinity. A better value to plot is $N_0'=(N_r/(N-N_0))\cdot N$ in which N_r is the number of tracks with lengths greater than l_0; N_0 is the number with lengths between l_0 and $l_0+\Delta l$; and N is the total number of tracks observed. This relation has been applied to polonium data obtained by one of us.

[1] G. Laurence, Phil. Mag. (7) **5**, 1027 (1928).
[2] F. Kurie, Phys. Rev. **41**, 701 (1932).
[3] Meitner and Freitag, Zeits. f. Physik **37**, 481 (1926).
[4] Philipp and Donat, Zeits. f. Physik **52**, 759 (1929).

2. The Alpha-Ray Ranges of Uranium Isotopes. W. M. Rayton and T. R. Wilkins, *University of Rochester.*—A Wilson chamber has been applied to an investigation of the ranges of the alpha-ray emitting isotopes of uranium. The use of an extremely thin evaporated film of uranium, and a helium-air mixture in the chamber, enabled us completely to resolve the alpha-ray groups corresponding to uraniums I and II. Some evidence for the existence of the suggested alpha-emitting actino-uranium was found. Certain difficulties with the so-called extrapolated number-distance range make it advisable to determine the mean ranges. This has been done in terms of the mean range of polonium alpha-rays,—a substance known to emit a homogeneous group. The values we obtain for the ratio of the mean ranges of U I and U II to that of polonium are 0.6902 $\pm$0.00054 and 0.8356$\pm$0.00063 respectively. These correspond to mean air ranges, at 15°C and 760 mm pressure, of 2.625 cm and 3.179 cm if we use the value 3.805 cm for polonium, as determined by Lewis and Wynn-Williams.[1]

[1] Proc. Roy. Soc. **A136**, 349 (1932).

3. Proportional Counter for Studying Neutron Intensities and Neutron Stimulated Nuclear Disintegrations. Robley D. Evans and M. H. Kanner, *Massachusetts Institute of Technology.*—A simple counter for neutrons has been developed by equipping a cylindrical lithium-cathode (2 cm by 12 cm) tube-counter (filled with He at 16 cm Hg) with a large diameter (No. 18 B. & S. Ni) polished wire anode. At voltages of 0 to 70 volts below the gamma-ray threshold of *ca.* 1700 volts the device acts as a proportional amplifier responding to the alpha-ray and probably to the H^3 disintegration products emitted from the wall when neutrons are captured by the lithium cathode. At these voltages it is insensitive to intense gamma-rays from the neutron source. Because of the gain by gas amplification within the counter, a less sensitive amplifier is required than when the usual lithium ionization chamber and linear-amplifier combination is employed. Efficiency and low noise level are retained or enhanced by this simplification of the technique. The present pulse amplifier and recorder is compact, portable, fully a.c. operated and very rugged. Plane-parallel and other electrode forms are being studied to seek greater flexibility and wider applicability. The counter's negligible sensitivity to beta-rays and intense gamma-radiation suggests its use with electrode materials such as C, Mg, Al, P, S, Cr, Zn, and many others for direct observation of alpha-rays or protons produced in nuclear disintegrations by neutrons.

4. Counter Statistics for Chain Disintegrations. L. I. Schiff, *Massachusetts Institute of Technology.*—The theory advanced in an earlier paper on the statistical analysis of counter data (in press) is extended to include chain or series disintegrating sources. It is shown that this theory gives the expected number of counts correctly when the Bateman expressions for the relative populations of the different substances in the chain during transient equilibrium are used as the expectation functions of a particle through the counter, provided that the mean lives of all members of the chain are either large or small compared to the resolving time of the counter and circuit. In the intermediate case, where the mean life of one or more of the decaying products is of the order of magnitude of the resolving time, the theory becomes much more complicated. It is developed explicitly for one such intermediate life product in a series, and is capable of further extension. The necessity for and the method of accounting for the relative efficiencies of the various products of disintegration in producing counts are shown.

5. Cosmic-Ray Disintegrations in Light Elements. Gordon L. Locher, *Bartol Research Foundation of the Franklin Institute.*—A preliminary report is given of a series of counter-controlled cloud chamber investigations of cosmic-ray bursts in light elements. Elements of low atomic number are used, since their nuclear constitutions and the energies required to produce nuclear transformations in them are better known than are those of heavy ones. The results so far obtained confirm previous work on bursts in light elements,[1] in showing that nuclear secondaries are emitted. These nuclear particles usually emanate from the walls of the cloud chamber, but sometimes originate in the gas (argon); comparison of the frequencies of their occurrence in random expansions and expansions controlled by counters in various configurations excludes the possibility that these tracks are merely of radioactive origin. The probability of obtaining a nuclear track on a counter-controlled photograph increases as the configuration of counters is altered to respond to bursts of increasing size. The cloud machine is arranged to expand swiftly, and

makes a small stroke, in order to reduce distortion of tracks. A minimum amount of massive material was used in constructing the apparatus, to reduce the number of secondary centers of disintegration in surrounding materials; this is particularly important, since the secondary centers are produced partially, if not wholly, by non-ionizing emissions.

* G. L. Locher, Phys. Rev. **45**, 296A (1934).

6. The Production of Bursts of Cosmic-Ray Ionization from Various Materials. C. G. MONTGOMERY AND D. D. MONTGOMERY, *Bartol Research Foundation of the Franklin Institute.*—Three spherical steel ionization chambers, placed at the corners of a triangle, were connected to the grid of a single vacuum tube electrometer. The chambers had a diameter of three inches, a wall thickness of a millimeter, and were filled with argon to a pressure of 300 pounds per square inch. Bursts of ionization, in the three chambers, from material placed above them, were recorded photographically. The rates of production of bursts greater than 1.6×10^5 ion pairs from small thicknesses of magnesium, iron and lead were measured. The rates of occurrence per atom were found to be approximately proportional to the square of the atomic number of the producer. The effective collision radius for lead was found to be about 2×10^{-13} cm for bursts of the sizes measured when the number of burst-producing rays was taken equal to the number of cosmic rays recorded by Geiger counters.

7. Gamma-Rays of Lithium and Fluorine Under Alpha-Particle Bombardment. KARL C. SPEH, *Yale University.*—The quantum energy of the Γ-rays induced in lithium and fluorine under bombardment by polonium α-particles has been determined, and its variation with the energy of the incident beam has been studied. In the case of lithium no change in energy was observed as the range of the incident α-particles was reduced from 3.9 cm to 2.5 cm. This is taken to support the interpretation of the radiation as due to excitation of the lithium nucleus without capture of the α-particle. At an incident range of 3.9 cm the induced fluorine radiation is shown to consist of two components. When the incident range is reduced to 3.1 cm the harder component disappears. Possible explanations are discussed, and the existence of a hitherto undetected proton group of low energy is suggested.

8. Collisions of Alpha-Particles with Sulphur Nuclei. R. L. ANTHONY, *Yale University.*—More than 700,000 thorium C and C′ alpha-particle tracks have been photographed in a Wilson chamber filled with a mixture of 70 percent hydrogen sulphide and 30 percent hydrogen. The collisions with sulphur nuclei were studied by replacing the film in the camera and projecting. A range velocity curve for recoil sulphur atoms has been constructed by plotting the measured ranges against the calculated velocities for 60 selected forks. This curve is compared with those of other workers in this field. It is shown that the formula of Blackett and Lees, $R=kmz^{-1}f(v)$, where R, m, z, and v are the range, mass, atomic number, and velocity of the recoil atom, does not apply, and that this formula should be modified to take into consideration the electronic structure of the atoms for the case of recoil atoms of low energies. No disintegrations of sulphur nuclei were observed. (Maximum reduced air range of alpha-particles in the chamber was 7.8 cm.) The methods of measurement and calculation have been thoroughly checked by applying them to collisions of alpha-particles with protons.

9. Reversible Change of Thermal Energy Accompanying Adiabatic Change of Magnetization in Nickel. T. C. HARDY, *Columbia University.*—The experimental method devised by A. Townsend[1] has been so improved as to permit a study of the magneto-caloric effect in materials for which the total hysteretic energy increase is small in comparison with the reversible thermal energy changes which occur during a half cycle of magnetization. The present specimen of nickel is the same as that used by Miss Townsend, except that it has been annealed at 1100°C for 2 hours in hydrogen at atmospheric pressure and cooled to room temperature in 10 hours. The hysteresis loss per half cycle is approximately 1200 ergs/cm³. As the magnetization is decreased from near saturation to, approximately, the knee of the magnetization curve, the thermal energy decreases almost linearly with magnetizing field by the amount, 9000 ergs/cm³. Below the knee of the curve, the magnetization decreases rapidly to zero and the thermal energy decreases by an additional 16,000 ergs/cm³. On remagnetization the same process is reversed, except for the addition of the hysteresis heat, which appears in the region of most rapid variation of magnetization with field. Throughout the entire process the decrease of thermal energy is several times greater than the external work done by the specimen on the magnetizing currents.

[1] Phys. Rev. **47**, 306 (1935).

10. Coercive Force in Single Crystals of Silicon Ferrite. K. J. SIXTUS, *Research Laboratory, General Electric Company.*—The coercive force H_c of ten single crystal disks of silicon ferrite with different orientation has been measured. The field was applied in various directions in the plane of the disks and H_c determined in these directions using a null method. H_c varied considerably in each disk; in a crystal which had very nearly a (110) plane parallel to the surface it changed between 0.10 and 0.35 oersteds. The direction of maximum and minimum H_c is not determined by those tetragonal ([100] or [010]) axes lying in or nearly in the plane of the disk but by the direction of the [001] axis which is most nearly perpendicular to that plane. In all samples H_c had a minimum in a direction at right angles to the [001] axis, a maximum in the direction of the projection of the [001] axis upon the plane of the disk. The absolute value of the minimum depends on the direction of the [100] or [010] axis, the value of the maximum on the direction of the [001] axis in a disk. The results are discussed on the basis of Bloch's theory of coercive force.

11. The Magnetic Moment of the Proton. J. M. B. KELLOGG, I. I. RABI, *Columbia University*, AND J. R. ZACHARIAS, *Hunter College of the City of New York*.—We have applied to the measurement of the magnetic moment of the proton the methods which we used for the deuteron as reported at the last Washington meeting. We find the h.f.s. separation for the normal state of the H atom to be 0.0482 cm^{-1} from which we calculate the nuclear moment to be 2.85 ± 0.15 nuclear magnetons as compared with 0.85 ± 0.03 for the deuteron. The ratio of the two moments, 3.35, should be more accurate than the individual moment measurements. Assuming simple additivity in the deuteron the neutron moment is 2 nuclear magnetons.

12. Orientation in Thin Layers of Stearic Acid by Electron Diffraction. K. H. STORKS, *Bell Telephone Laboratories, Inc.* (*Introduced by L. H. Germer.*)—Electron diffraction patterns have been obtained from films of stearic acid, by the reflection method and also by the transmission method. For transmission, films are prepared by evaporation from alcohol solution directly upon a previously prepared foil of "rezoglas." This backing foil is 100A thick and does not contribute appreciably to the diffraction pattern. (Cellulose nitrate films of 300A thickness have also been used.) A single crystal of stearic acid on rezoglas gives a rectangular array of diffraction spots corresponding to the monoclinic alpha-modification. A crystal is always oriented with its (001) plane in the plane of the foil. Transmission patterns have also been obtained from stearic acid deposited upon gold films which had previously been sputtered upon rezoglas. The spot pattern of stearic acid is obtained superposed upon Debye-Scherrer rings of gold. For reflection experiments, stearic acid layers have been formed upon polished nickel by evaporation, and upon other materials. At glancing incidence an electron beam strikes many crystals. Diffraction patterns consist of diffuse spots forming broad bands inclined 33° to the surface plane. This must be the inclination of long hydrocarbon chains to the surface normal. Separations of these bands correspond to 2.5A spacing between carbon atoms.

13. An Effective Method for Using Low-Melting Metals for X-Ray Tube Targets. T. R. FOLSOM, *New York Memorial Hospital*.—Experiments were conducted to develop a more economical target for a 600,000-volt c.p. x-ray machine. A target which was found to be very practical consists of a very thin, stretched disk of copper, upon which lead is plated to 1/100 of an inch. Two years of experience has shown that it will stand up under 10 ma electron bombardment at 600,000 volts under constant use. This method seems applicable for experimental cases, where a low-melting point metal is desired as a target.

14. An Illumination Meter for Photographic Laboratory Work. AGNES TOWNSEND, *Barnard College*.—A simple type of photometer is described and its application in the teaching and practice of photography is discussed. The instrument employs as a standard a 2.2-volt lamp operated from dry cells and a neutral photographic wedge for making the comparison. Measurements can be made with sufficient accuracy for many purposes with illuminations as low as 0.01 meter candles. The photometer can be used to determine the illumination on the ground glass of a camera or on the easel of an enlarger where a measurement of the maximum and minimum illuminations is sufficient to specify the range required of the photographic emulsion and the exposure needed. The meter can be used also to obtain exposure *versus* density curves for photographic films and papers.

15. The Polarimetric Determination of Optical Properties. RICHARD MAURY EMBERSON, *University of Missouri*. (*Introduced by H. M. Reese.*)—A study has been made of the polarimetric method of determining the optical properties of a surface. The experimental work was done with a polarimeter, which was designed and constructed in the university shops. The equations used in the computation of results were based on the theoretical work of Dr. Thornton C. Fry. It was found that certain instrumental errors profoundly affected the results. When the observed data were freed of these errors, a decrease was noted in the variation of the computed optical constants of a surface with the angle of incidence at which the data were obtained. Studies were made of thin metallic films deposited on glass. The results indicated that, while the computed film thicknesses were of the correct order of magnitude, they were not independent of the angle of incidence of observation. Also, the computed thicknesses were always complex, with the imaginary part negative and about the same size as the real part.

16. Angular Momentum in Certain Optical Problems. F. T. HOLMES, *University of Virginia*.—Fresnel showed that ordinary plane polarized light is split into two beams of equal intensity, which are circularly polarized in opposite senses, by passage through his compound prism. The experiment has been performed using plane polarized Zeeman *s* components. The result is that, in accordance with what one would expect classically, each of the *s* component beams is split into two beams by the Fresnel compound prism. Thus, before the spectroscopic analysis, the high and low frequency *s* components were indistinguishable within the limits of observation. This inability to distinguish between positively and negatively polarized linear photons may be common to all optical systems. By assuming one-to-one correspondence between ellipticity, observable angular momentum, and the angle between direction of propagation and the angular momentum vector, it follows from our experimental knowledge that: (1) The observable angular momentum of a beam of photons (of each photon?) in a homogeneous isotropic field-free medium is vectorially constant in time; (2) In general, an optical measurement, by ordinary methods, of ellipticity or of angular momentum produces a vectorial change in the angular momentum of the beam of photons (of each photon?) on which the observation was made.

17. Reflecting Power of Evaporated Metal Films in the Near and Far Ultraviolet. G. B. SABINE, *Cornell Uni-*

versity.—The reflecting power of evaporated metal films from the visible to 450A has been determined for the following elements: Aluminum, antimony, beryllium, bismuth, cadmium, chromium, copper, gold, iron, lead, magnesium, manganese, molybdenum, nickel, palladium, platinum, silver, tellurium, tin, titanium, zinc, and zirconium. Photographic methods were used. From the visible to 2400A, a quartz mercury arc with calibrated wire screens and a prism spectrograph were employed. From 2400A to 450A it was necessary to use a vacuum spectrograph with grating, a discharge tube and oiled photographic film, observing the precautions for their employment outlined by Harrison and Leighton.[1] The accuracy of the work in the near ultraviolet is of the order of three percent and in the far ultraviolet not better than five percent. Curves of reflecting power against wave-length for these metals will be shown.

[1] J. Opt. Soc. Am. **20**, 313 (1930).

18. Mean Lives of Potassium Doublets λ4047–4 and λ3447–6. DAVID SINCLAIR AND HAROLD W. WEBB, *Columbia University.*—The mean lives of the potassium doublets λ4047–4 and λ3447–6 were measured by the alternating voltage method previously described.* The radiation was excited in a sealed-off Pyrex tube by low voltage electrons from a hot cathode. A sodium hydride vacuum photoelectric cell was used as the detecting system. Optical filters were used to isolate the two doublets which were treated as a single line. The mean life of λ4047–4 was found to be 3.79×10^{-7} sec., the mean life of λ3447–6 to be 8.50×10^{-7} sec., with an estimated precision of one percent. The results were obtained on the assumption that the radiation decays exponentially after excitation. The correctness of this and other assumptions was demonstrated by means of a low frequency excitation voltage of distorted wave form which simulated the conditions at high frequency. The mean lives were found to be the same for vapor pressures ranging from 4×10^{-5} mm to 10^{-2} mm. This can be accounted for by the assumption that only 10 percent of the absorbed λ4047–4 and λ3447–6 is re-emitted at these wave-lengths. Absorption measurements were found to be consistent with this assumption.

* H. W. Webb, Phys. Rev. **24**, 113 (1924); F. G. Slack, Phys. Rev. **28**, 1 (1926); P. H. Garrett, Phys. Rev. **40**, 779 (1932).

19. Hyperfine Structure and Wave-Length of the Infrared Hg I 6^1P-7^1S Line. M. H. M. HUNT AND J. S. CAMPBELL, *Institute of Applied Optics, University of Rochester.*—The hyperfine structure of the mercury arc line λ10,140 produced in an air-cooled Cooper-Hewitt tube has been photographed with a Fabry-Perot interferometer at mirror separations ranging from 10 to 60 mm. The nine expected components give six completely resolved groups in a pattern of total width, $238\ \text{cm}^{-1}\times10^{-3}$. The total magnetic separations of isotopes 199 and 201 in 6^1P_1 are 185 and 171, respectively, in only fair agreement with the values 181 and 165 obtained by Schüler and Keyston from 6^1P-8^1S.[1] The principal components due to isotopes 200, 202 are resolved showing a relative shift of 17, while the less directly obtained 199–201 shift is somewhat smaller than this. Since the average shift in 7^1S obtained by Schüler from λ6234 is about 30, it follows that 6^1P has a shift of approximately 12 between consecutive even isotope levels. An interferometric wave-length determination gives 10,139.881A for the strongest component of isotope 201, and 10,139.811 as the wave-length of the center of gravity.

[1] Zeits. f. Physik **72**, 423 (1931).

20. On the Spectrum of Ce IV. R. J. LANG, *University of Alberta, Edmonton, Canada.*—Further progress has been made in the analysis of this spectrum. Some twenty energy levels have been found, including two members of the *F* series which are of interest because of their bearing on the structure of the rare earths.

21. The Pure Rotation Spectrum of Water Vapor. H. M. RANDALL, N. GINSBURG, D. M. DENNISON, AND R. L. WEBBER, *University of Michigan.*—These measurements begun in 1934 include 130 lines within the spectral region between 18 and 75 μ. The highest resolution yet applied by gratings in this part of the spectrum has been employed with the result that the lines are very narrow and well separated. In fact quite complete resolution is possible for lines as near together as 0.6 cm^{-1}, while lines considerably closer are readily shown to be double or triple. This has been accomplished by the use of gratings having 1200 and 900 lines per inch and slit widths of a millimeter or less. For lines of the longest wave-lengths the gratings had 360 lines per inch and the slit widths varied from 1 mm to 1.4 mm. The results give promise of yielding very satisfactorily to analysis. Already somewhat more than one-third of these lines together with the longest of the measurements obtained by Wright and Randall have been classified. Energy levels have been obtained up to and including $J=6$ and some for $J=7$. For these higher levels, it has been found that the stretching of the molecule due to centrifugal force gives rise to a very large change from the calculated levels, of the order of magnitude of 100 cm^{-1}.

22. Pressure Effect in the HCN Bands in the Near Infrared. S. D. CORNELL AND WILLIAM W. WATSON, *Yale University.*—According to Herzberg and Spinks[1] the lines of the HCN absorption band at 1.04μ are considerably more broadened by increase in HCN gas pressure than are the lines of the HCl overtone bands with increase in HCl pressure. They also reported the broadening to decrease with increasing molecular rotation. Quantitative measurements of line-widths in the 1.04μ band at different HCN pressures, however, indicate no dependence on *J*. The half-widths increase linearly with pressure, the change being 0.56 cm^{-1} per atmosphere. This value is actually slightly less than that observed by H. Becker for the first harmonic band of HCl. These results indicate that dispersion forces are the predominant broadening influence, in agreement with the predictions of theory similar to that of H. Margenau[2] for broadening by foreign gases. The observed pressure broadening gives no evidence for molecular association.

[1] Herzberg and Spinks, Proc. Roy. Soc. **A147**, 434 (1934).
[2] H. Margenau, Phys. Rev. **49**, 596 (1936).

23. The Electrical Charge of Mammalian Red Blood Cells Under Normal Conditions and in the Anemias. LAURENCE S. MOYER AND HAROLD A. ABRAMSON, *Biological Laboratory, Cold Spring Harbor, Long Island.*—From the data on the surface area and electrical mobilities of red blood cells in a given solution under approximately physiological conditions, the net surface charge per cell as well as the charge per unit area can be calculated by means of the modern theory of electrolytes. The lowest value of the net charge density in the series investigated was 1890 electrostatic units in the rabbit. Man and the rhesus monkey were the same, both having approximately 4500 electrostatic units of net charge per square centimeter. Amongst the mammals investigated, given here in the order of increasing charge density, were: rabbit, sloth, pig, opossum, guinea pig, man, rhesus monkey, cat, mouse, rat, dog; the dog had the highest charge density of 5600 electrostatic units. This order is completely changed if the effective number of electrons at the surface of the cell, rather than the charge density, is calculated because this depends upon the size of the cell. Man, among the animals studied, had the highest number of effective electrons at the surface, the value being equal to 15 million electrons. In cases of anemia in human beings, the abnormal cells apparently possess a mechanism which is capable of keeping the surface density of net charge constant even though comparatively large changes in surface area may occur.

24. Absolute Photoelectric Yield of Beryllium, Magnesium, and Sodium. MARVIN M. MANN AND LEE A. DUBRIDGE, *University of Rochester.*—Measurements of the photoelectric yield of these metals have been obtained for wave-lengths ranging from the threshold down to 2400A. Values of α, the probability that an electron at the surface of the metal will absorb a quantum and appear outside as a photoelectron, have been calculated for each surface from the vertical shift of the curves plotted by the Fowler method. Comparison of these values with those computed from simple theoretical considerations, assuming all the light to be absorbed by those electrons in the image field, shows that the theoretical values are greater than experimental values by a factor of approximately 100. Preliminary measurements on slightly contaminated surfaces indicate that α may vary by no more than a factor of 2 or 3 for a given metal. For different metals α may vary by as much as 100 times. The discrepancy between theoretical and observed values of α may be explained by the fact that those electrons in the image field of the surface absorb only a small portion of light incident on the surface. The value of the photoelectric work function of beryllium obtained by the Fowler method is 3.92 volts.

25. Normal Energy Distribution of Photoelectrons from Potassium Films as a Function of Temperature. C. L. HENSHAW, *Yale University.*—Using a parallel plate condenser the photoelectric normal energy distribution of thin potassium films on silver and platinum has been studied as a function of temperature for films of different thicknesses produced by the molecular ray method. Contact potential was determined by the Kelvin method to a precision of less than 0.02 volt. The results were analyzed by DuBridge's method[1] of fitting the Fowler universal curve. Some irreversible changes in the character of the surface occur such as contact potential or saturation current, but after these are eliminated there are certain deviations from the Fowler curve at the low current end which are reversible with temperature. Adequate shifts for frequency and temperature can still be obtained. The deviations seem to be affected by the temperature at which the film was originally produced. Brady[2] has found no deviations of the *total* energy distribution of potassium films on silver, hence the present observations are probably best explained by changes in the direction of emission of the photoelectrons. With optimum geometrical conditions of the apparatus satisfactory agreement with the Fowler curve was found practically to saturation current for films which were not too thin. This suggests that, to the accuracy of the logarithmic plot, previously found deviations above 50 percent saturation can be attributed mainly to imperfect geometry rather than to transmission coefficients.

[1] L. A. DuBridge, Phys. Rev. **43**, 727 (1933).
[2] J. J. Brady, Phys. Rev. **46**, 768 (1934).

26. Field Currents and Thermionic Currents from Thoriated Tungsten and Pure Tungsten. A. J. AHEARN, *Bell Telephone Laboratories, Inc.*—When the electric field applied to a cold thoriated tungsten filament is raised to a sufficiently high value, 1 to 2×10^6 volts/cm, breakdown occurs, i.e., suddenly the field current discontinuously increases by an enormous amount. This breakdown raises the field current curve to higher currents by about one million-fold. After such a breakdown has occurred, the thermionic activity of the filament is increased. However, when the filament is thoriated and dethoriated by the usual thermal treatment, the field current remains unchanged to within 15 percent. Low temperature treatments (about 1300°K) after but not before breakdown further increase the field currents. High temperature treatments (about 2600°K) erase the effects produced by the breakdown. Similar experiments with pure tungsten show the same phenomena with the following exceptions: (1) Breakdown produces no change in the thermionic emission. (2) Low temperature treatments do not further increase the field current after breakdown. These experiments indicate: (1) The increase in field current following breakdown is due to an increase in the applied field over small local areas. (2) There is sufficient local heating at breakdown to partially thoriate the filament. (3) In thoriation by thermal treatment, the points emitting field currents probably do not become thoriated.

27. Influence of Crystal Structure on Electron Emission from "218" Tungsten Wire. W. B. NOTTINGHAM, *Massachusetts Institute of Technology.*—The thermionic emission from 218 tungsten wire has been shown by Johnson and Shockley[1] to vary with crystallographic direction. Single crystals of this wire average 0.25 to 1.0 cm in length and present six strips of strong emission separated by six strips of weak emission as one explores around the filament cir-

cumference. The electron energy distribution as indicated by retarding potential measurements becomes ambiguous near "zero field" because the currents received are coming in effect from a cathode of inhomogeneous surface structure to a single collector. In the case of thoriated filaments it is thought that the actual surface exposed may be much more uniform than that found in 218 wire, thus accounting for the accurate reproducibility of the energy distribution curves. In contrast the curves observed with different samples of 218 wire have not been in exact agreement with each other and have generally shown an apparent reflection effect larger than that for thoriated tungsten. If we assume that the work function varies sinusoidally from a minimum to a maximum differing by 0.5 volt, an approximate theory gives good agreement with experiment.

[1] Phys. Rev. **49**, 436 (1936).

28. Cathode Drop in Low Pressure Discharge Tubes. T. J. KILLIAN AND R. S. PRESCOTT, *Barkon Tube Lighting Corporation, Seattle, Washington.*—The cathode drop of aluminum electrodes in low pressure high voltage gaseous discharge lamps containing carbon dioxide was studied as a function of current density and pressure for various shapes. The cathode drop of a plane disk was found to follow the Aston formula $V=A+B(I/a)^{\frac{1}{2}}/p$; where V is in volts, A and B are constants, I/a is the current density, and p is the pressure. With a cylindrical cup the relation was of the form $V=A_1+BI^k$; and was found to be practically independent of pressure in the region from 0.1 to 0.3 mm; and k was found to be in the order of 0.15. An electrode consisting of a capped cylindrical cup with a small hole pierced in the cap approximately followed the relation $V=(A_2/p)\epsilon^{-b(1/p)^c}\times(1-\epsilon^{-k_1 I})+V_{0\epsilon}{}^{-k_1 I}$. The study was made in the region between 0.05 and 0.5 mm of mercury. At 0.1 mm and 5 ma/sq. inch the voltage drop was 1700 for the disk, 550 for the cup, and 400 for the capped cup. Various mechanisms which may account for this large change in the cathode drop are discussed.

29. The Surface Tension of Water from the Velocity of Capillary Waves. V. E. EATON, *Wesleyan University.*—A ripple tank, originally designed for undergraduate instruction, has been described.[1] The following modifications have made it an instrument of precision. The waves were recorded on photographic plates and measured with a comparator. During the exposure of the plate, a method of spark recording was used to determine the frequency of the a.c. to a few thousandths of a cycle. Nine determinations of the surface tension of water gave 72.64 ± 0.03. Within the limits of experimental error the results for tap water are the same as for distilled water. The merits of this method for absolute and for comparative measurements are considered.

[1] Am. Phys. Teacher **4**, 49 (1936).

30. Energy Bands in Metallic Tungsten. MILLARD F. MANNING AND MARVIN CHODOROW, *Massachusetts Institute of Technology.*—The Wigner-Seitz-Slater cellular method as applied to the body-centered lattice has been extended to include boundary conditions for next-nearest as well as nearest neighbors. The wave-functions used are:

$$U_g=As+Bd\frac{xy}{r^2}+Cd\frac{xz}{r^2}+Dd\frac{yz}{r^2}+Ed\frac{y^2-z^2}{r^2}+Fd\frac{3x^2-r^2}{r^2}+Gg\frac{5(x^4+y^4+z^4)-3r^4}{r^4},$$

$$U_u=Hp\frac{x}{r}+Ip\frac{y}{r}+Jp\frac{z}{r}+Kf\frac{xyz}{r^3}+Lf\frac{x(5x^2-3r^2)}{r^3}+Mf\frac{y(5y^2-3r^2)}{r^3}+Nf\frac{z(5z^2-3r^2)}{r^3}.$$

Since all of the d functions are included, the method is now applicable to transition elements. To determine the relation between E and k for a general direction of propagation, it is necessary to solve a fourteenth-order determinant. For special directions of propagation a proper grouping of function breaks the determinant up into lower order determinants which can be handled. For applications to tungsten, the necessary values of the wave functions and their derivatives at the two required radii have been found by the differential analyzer, using an atomic field modified to correct for the renormalization of the valence electrons. The bands that contain electrons under ordinary conditions are: three beginning at $d_1'=0$, two at $d_2'=0$, and one at $3s_1'g_2'+2s_2'g_1'$. The concentration of electrons near the bottom of the d band accounts for the high binding energy.

31. On the Elastic Constants of an Anisotropic Solid. MILTON S. PLESSET AND RICHARD F. BAKER, *University of Rochester.*—In the most general case of an anisotropic body there are 36 elastic constants which are reduced in number by two classes of relationships. The first class, Green's relations, is usually derived from the potential energy as a quadratic function of the strains but also follow from symmetry considerations of the elastic constant tensor. The second class, Cauchy's relations, is usually based on microscopic considerations of the structure of the body, but in the present paper they are derived in a very simple way by forming three divergence functions of the stress tensor (equilibrium functions). This simple, macroscopic derivation of Cauchy's relations affords a direct way of discussing the necessary conditions for their applicability. In connection with the consideration of the elastic constants of an anisotropic body it is of interest to note that Murnaghan has given an analysis[1] of the energy of deformation of an elastic body with the following result: the assumption that the potential energy is a function of the strains alone is consistent only for an isotropic body. In the present discussion this conclusion is shown to be invalid.

[1] Murnaghan, Proc. Nat. Acad. Sci. **14**, 889 (1928).

32. Nuclear Calculation. D. R. INGLIS, *University of Pittsburgh.*—A method of calculating nuclear properties, which includes the necessary complexity and yet retains some of the analytic simplicity of single-particle representations, consists in applying perturbation theory to the representation in which protons and neutrons have the

wave functions of three-dimensional harmonic oscillators in a Cartesian coördinate system. The width of the wave functions is varied for minimum energy, as in the first-order calculation of Heisenberg. To approximate the K.E. correctly, the Hamiltonian operator is expressed in another coordinate system in which the center of gravity is at rest. In making a preliminary comparison of the accuracy of this and other methods, only the proton-neutron Majorana-type interaction $ae^{-br^2}P$ is used. The values of a (unit $Mc^2/1000$), determined for values of b from the energy of He^4 by various methods, are here tabulated:

b (unit mc^2/e^2)	1.5	2.0	2.5
Heisenberg	75	115	160
Wigner	60	90	130
Feenberg: Variation	60	91	129
Equiv. 2-body	56	84	117
This method	57	85	120
(Deuteron	51	81	122)

The convergence is rapid: The K.E. correction is greater than the second-order contribution, and contributions of quadruply excited states and of third order are almost negligible in the results given. The method is applicable to other problems, more particles and more interactions.

33. On the Electronic Structure of LiF and LiH. DOUGLAS H. EWING AND FREDERICK SEITZ, *University of Rochester.*—A solution of Hartree's equations for LiF and LiH has been concluded and from this the band structure of the electronic states has been determined using the representation theory of groups. If each atom is surrounded by a cube it is found that the total charge within these is zero for both Li and F in LiF, while in LiH, the H cube contains about 1.3 of the two valence electrons. The first result is to be modified, without question, by the Fock terms in such a direction as partly to ionize the Li cube, and a similar correction will occur in the second case.

34. The Connection Between the Kepler Problem and the Four-Dimensional Rotation Group. OTTO LAPORTE, *University of Michigan.*—In recent researches by Fock, Hulthén, and Bargmann[1] attention has been called to this connection in various ways. A simple and extremely elementary way of treating the hydrogen problem is in momentum space (Pauling-Podolsky and Hylleraas), using formulae for stereographic parameters recently developed by G. Y. Rainich and the author.[2] The wave function is seen to be a 4-dimensional hyperspherical surface harmonic divided by $(1+\xi_\rho\xi_\rho)^2$ where $\xi_i=p_i(-2mE)^{-1/2}$. The infinitesimal operators admitted by the differential equation which this function satisfies are, besides rotations (angular momentum integrals), the operators

$$\tfrac{1}{2}(1-\xi_\rho\xi_\rho)\partial/\partial\xi_i+\xi_i\xi_\rho\partial/\partial\xi_\rho+2\xi_i$$

which are identical with Runge's vector integral. It is possible in this way to obtain all eigenfunctions by differentiation in analogy with Maxwell's method of obtaining 3-dimensional solid harmonics. The evaluation of matrix elements involving radial eigenfunctions becomes simpler in momentum space using a generalization to four dimensions of Kramers' "$\xi-\eta$ method." By means of the finite transformation of the above operator a "displaced" solution is constructed which may serve as Green function or as generating function.

[1] Fock, Hulthén and Bargmann, Zeits. f. Physik, vols. 86, 98, 99.
[2] Rainich and Laporte, Trans. Am. Math. Soc. (1936).

35. The One-Dimensional Problem in the New Relativity. D. G. BOURGIN, *University of Illinois.*—A solution has been found for the one-dimensional problem of the Page-Milne relativity theories. That is to say, the motions have been determined consistent with the physically necessary postulate that equivalence of each of two observers to a third implies equivalence of all observers. The method used is that of the Lie theory of groups. With the aid of one new theorem in this discipline it is proved that $(dx^2-c^2dt^2)/F(ct-x)F(ct+x)$ is invariant. A three-parameter group generates the motions. In general the Lorentz transformations do not form a subgroup. Even when they do $[F(\ )=(\ )^n]$ it does not follow that the compound of a Lorentz transformation and one characteristic of the particular motion considered is permissible, for the two may not form a group. Page's constant acceleration case corresponds to $F(\ )=(\ )^2$. The Einstein-Lorentz velocity addition formula holds formally for the general motion though the velocities are now variable functions of distance and time.

36. Measurements of the Effect of Paraffin and Lead on the Rate of Production of Very Large Cosmic-Ray Bursts. D. HEYWORTH, *Wellesley College,* AND RALPH D. BENNETT, *Massachusetts Institute of Technology.*—Observations have been made at sea level of burst frequency and magnitude, for bursts larger than 15×10^6 ion pairs, using a model C[1] cosmic-ray intensity meter. The effects of the following on the rate of production of bursts of different magnitudes have been investigated: (a) Degree of shielding of the ionization chamber, (b) Heavy building structure above the instrument, (c) Lead placed immediately above the ionization chamber, (d) Paraffin placed immediately above the ionization chamber. We have found that: (a) In agreement with the results of Doan,[2] the burst rate is greater when the meter is partly shielded than with either full shield or no shield. (b) A heavy structure above the instrument increases the rate for the smaller bursts. (c) Lead placed above the chamber increases the rate for all sizes of bursts. (d) Paraffin placed above the chamber increases the rate for the smaller sizes more than for the larger sizes. The average burst size is increased (a) by nearly 50 percent by the addition of 23 kg of lead above the chamber, (b) by nearly 30 percent by the addition of 23 kg of paraffin above the chamber.

[1] Compton, Wollan, and Bennett, R. S. I. **5**, 415 (1934).
[2] R. L. Doan, Phys. Rev. **48**, 470 (1935).

37. A High Speed Running Film Camera for Photographic Photometry. BRIAN O'BRIEN, *Institute of Optics, University of Rochester.*—Using base and guard as in the Bausch and Lomb centrifuge microscope, a high speed camera has been constructed with a hollow duralumin

rotor open at the top and mounted directly upon the shaft of a vertical series motor. A strip of 16 mm motion picture film, 61 cm long, is mounted within the rotor, filling the circumference except for a gap of less than 0.1 mm. The film is held accurately in the focal plane by centrifugal force which reaches 15,700 times gravity at the designed speed of 200 r.p.s. A slit image 0.01 mm wide is formed on the film by a well-corrected $f:2$ objective of 50 mm focus, and two first surface mirrors. Since the focus is critical to within 0.02 mm and the rotor expands in radius approximately 0.08 mm at speed, provision is made for focusing directly upon blank film, while running, by observing through the upper mirror which is of aluminum evaporated so as to transmit about 1/10 the light for this purpose. A time resolving power of 1×10^{-7} sec. has been realized without sacrificing safety or portability, the limit being set at present by the resolving power of the photographic emulsion.

38. Slow Neutron Disintegration of Li^6 and the Disintegration Mass Scale. M. STANLEY LIVINGSTON AND J. G. HOFFMAN, *Cornell University*.—Using slow neutrons from a Rn−Be source and a shallow ionization chamber and linear amplifier the reaction $Li^6+n^1\rightarrow He^4+H^3$ has been studied and the range of the H^3 product determined to be 5.73 ± 0.05 cm at standard conditions. A direct comparison with the Po alpha-range was used and the depth of penetration into the ionization chamber determined. The total energy released is found to be 4.67 ±0.05 MEV. Grouping this reaction with the three well-determined reactions:

$$\begin{array}{lll} Li^6+H^2\rightarrow 2He^4 & +22.03\pm.06 \\ H^2+H^2\rightarrow H^3+H^1 & +\ 4.00\pm.02 \\ H^1+n^1\rightarrow H^2 & +\ 2.22\pm.06 \end{array}$$

an accurate determination of the quantity $2H^3-He^4$ can be obtained, which is 23.58 ± 0.10 MEV. This is compared with recent mass-spectroscopic values of this quantity, by Bainbridge and by Aston and is found to be midway between their values with a somewhat lower probable error. Using a mass of He^4 obtained by applying this correction to the disintegration mass scale the masses of the lighter atoms are found to be:

$n^1=1.00884$	$He^3=3.0166$
$H^1=1.00798$	$He^4=4.00355$
$H^2=2.01444$	$Li^6=6.01633$
$H^3=3.01660$	$Li^7=7.01756$

39. Experiments with Photo-Neutrons. D. P. MITCHELL, F. RASETTI, G. A. FINK AND G. B. PEGRAM, *Columbia University*.—Gamma-rays from 700 mc of radon surrounded by beryllium metal was used as the source of photo-neutrons. Surrounding the source by cylinders of water of varied size, the slow neutrons emerging were measured and the mean free path in water calculated to be about 5 cm as compared with 9 cm for Rnα–Be source. Roughly $\frac{1}{4}$ as many photo-neutrons are obtained from the Raγ–Be as from a corresponding Raα–Be source. Similar experiments were made with radon in 200 cc of D_2O instead of beryllium. Thickness of water for maximum number of emerging slow neutron $5\frac{1}{2}$ cm for Rnγ–Be compared with $8\frac{1}{2}$ for Rnα–Be, $3\frac{1}{2}$ cm for Rnγ–D compared with 7 cm for Rnα–Be.

AUTHOR INDEX TO ABSTRACTS OF THE ROCHESTER MEETING

Abramson, Harold A.—see Moyer
Ahearn, A. J.—No. 26
Anthony, R. L.—No. 8

Baker, Richard F.—see Plesset
Bennett, Ralph D.—see Heyworth
Bourgin, D. G.—No. 35

Campbell, J. S.—see Hunt
Chodorow, Marvin—see Manning
Cornell, S. D. and William W. Watson—No. 22

Dennison, D. M.—see Randall
DuBridge, Lee A.—see Mann

Eaton, V. E.—No. 29
Emberson, Richard Maury—No. 15
Evans, Robley D. and M. H. Kanner—No. 3
Ewing, Douglas H. and Frederick Seitz—No. 33

Fink, G. A.—see Mitchell
Folsom, T. R.—No. 13

Ginsburg, N.—see Randall

Hardy, T. C.—No. 9
Henshaw, C. L.—No. 25
Heyworth, D. and Ralph D. Bennett—No. 36
Hoffman, J. G.—see Livingston
Holmes, F. T.—No. 16
Hunt, M. H. M. and J. S. Campbell—No. 19

Inglis, D. R.—No. 32

Kanner, M. H.—see Evans
Kellogg, J. M. B., I. I. Rabi and J. R. Zacharias—No. 11
Killian, T. J. and R. S. Prescott—No. 28
King, Allen and W. M. Rayton—No. 1

Lang, R. J.—No. 20
Laporte, Otto—No. 34
Livingston, M. Stanley and J. G. Hoffman—No. 38
Locher, Gordon L.—No. 5

Mann, Marvin M. and Lee A. DuBridge—No. 24
Manning, Millard F. and Marvin Chodorow—No. 30
Mitchell, D. P., F. Rasetti, G. A. Fink and G. B. Pegram—No. 39
Montgomery, C. G. and D. D. Montgomery—No. 6

Montgomery, D. D.—see Montgomery, C. G.
Moyer, Laurence S. and Harold A. Abramson—No. 23

Nottingham, W. B.—No. 27

O'Brien, Brian—No. 37

Pegram, G. B.—see Mitchell
Plesset, Milton S. and Richard F. Baker—No. 31
Prescott, R. S.—see Killian

Rabi, I. I.—see Kellogg
Randall, H. M., N. Ginsburg, D. M. Dennison and R. L. Webber—No. 21
Rasetti, F.—see Mitchell
Rayton, W. M.—see King
—— **and T. R. Wilkins**—No. 2

Sabine, G. B.—No. 17
Schiff, L. I.—No. 4
Seitz, Frederick—see Ewing
Sinclair, David and Harold W. Webb—No. 18
Sixtus, K. J.—No. 10
Speh, Karl C.—No. 7
Storks, K. H.—No. 12

Townsend, Agnes—No. 14

Watson, William W.—see Cornell
Webb, Harold W.—see Sinclair
Webber, R. L.—see Randall
Wilkins, T. R.—see Rayton

Zacharias, J. R.—see Kellogg